

Aus dem Institut für Kardiovaskuläre Physiologie und Pathophysiologie,
Walter Brendel Zentrum für experimentelle Medizin
der Ludwig-Maximilians-Universität München
Kommissarischer Direktor: Prof. Dr. med. Markus Sperandio



The role of Preimplantation factor (PIF) on leukocyte recruitment *in vivo*

DISSERTATION

zum Erwerb des Doctor of Philosophy (Ph.D.)
an der Medizinischen Fakultät der
Ludwig-Maximilians-Universität München

Vorgelegt von

Roland Thomas Immler

aus

Wangen im Allgäu

am

12.Juni 2019

Mit Genehmigung der Medizinischen Fakultät
der Universität München

Supervisor: *Prof. Dr. med. Markus Sperandio*

Second expert: *PD Dr. rer. nat. Markus Moser*

Dean: *Prof. Dr. med. dent. Reinhard Hickel*

Date of oral defense: *19th of September 2019*

Für Mathis.

Abstract

Throughout pregnancy, immune cells infiltrate and colonize the placenta to ensure fetal development and successful birth. Thereby, they regulate tissue remodeling and protect the unborn from invading pathogens. At the same time, immune cells within the placenta require tight regulation in order to prevent recognition of the embryo as a 'semi-allograft'. Extra-embryonic tissue actively modulates immune cell functions by expressing growth factors and cytokines. Preimplantation factor, a 15 amino acid small peptide, is produced by trophoblast cells and continuously secreted into maternal circulation. It has been shown to interfere with immune cell functions in autoimmune disease models, but underlying molecular mechanisms remain unclear.

This work investigated the function of PIF in acute inflammatory scenarios, reflecting its role within maternal serum. Analysis of leukocyte recruitment in postcapillary venules of TNF- α stimulated cremaster muscles in the mouse revealed that (i) leukocyte rolling, (ii) leukocyte adhesion and (iii) neutrophil extravasation is impaired in the presence of PIF. With the help of several *ex vivo* and *in vitro* assays, reduced leukocyte rolling could be linked to effects of PIF on the endothelial compartment. Impaired leukocyte adhesion and reduced extravasation in turn could be attributed to a direct effect of PIF on neutrophils. PIF inhibits K⁺ efflux via the voltage gated potassium channel K_v1.3 on neutrophils, thereby reducing sustained calcium influx into the cells. Decreased intracellular Ca²⁺ concentrations impair post-arrest modification steps, namely neutrophil spreading and adhesion-strengthening, resulting in increased susceptibility to physiological shear forces and in reduced adhesion and extravasation.

Taken together, this work demonstrates that PIF modulates neutrophil function during immune responses, offering therapeutic potential beyond pregnancy to protect patients from exuberant inflammation and excess neutrophil recruitment.

Acknowledgments

First and foremost, I would like to thank *Prof. Dr. med. Markus Sperandio* for giving me the opportunity to do my PhD under his supervision. Your competent, enthusiastic, friendly and fatherly support throughout all the years and your faith in my skills and in our project have been the stimulus to put all my effort in this work.

In the same manner, I would like to thank my colleagues and friends *Myri, Angi, Kristina, Sergi, Nadine*, and all current and former members of the Sperandio lab, but especially *Moni* and *Ina*. Your help, your suggestions, and primarily the friendly atmosphere you created rarely let labor time feel like labor time.

This work benefited a lot from productive and successful collaborations. *Dr. rer. nat. Susanna Zierler, Wiebke Nadolni, Prof. Scott I Simon, Vasilios Morikis, Dr. med. Jessica Tilgner, PD Dr. med. Jochen Grommes, PD Dr. rer. nat. Hanna Mannell* and *Dr. med. Georg Hupel* contributed with important experiments and teaching of interesting and helpful techniques. In open and positive discussions, my thesis advisory committee members *Prof. Dr. Dr. med. Oliver Söhnlein* and *PD Dr. rer. nat. Markus Moser* supported to a great extent this project and expanded my scientific knowledge. Thank you all for your professional work, your ideas and your valuable time you invested into this study.

As a part of the Integrated Research Training Group 914 (IRTG914) of the SFB914, I profited a lot from offered seminars, courses and meetings. Thank you, *Verena* for having an eye on me all the time and on all the deadlines and paper work that had to be done.

I would also like to thank my personal environment, my *family, flatmates, friends*, and particularly *Linda*. Thank you for your support, your patience, respect and your understanding throughout the years. You almost never complained when I preferred to spend evenings and weekends with immune cells instead of with you. You tried to understand the problems and questions I shared with you and you allowed me to stay in my own intellectual world of immune cells and ion channels when I was not able to leave it even in after-work hours.

Fabi, thank you again for helping me with \LaTeX typesetting. Remaining deficiencies are still in my responsibility.

Contents

Abstract	v
Acknowledgments	vii
I. Thesis	1
1. Introduction	3
1.1. The feto-maternal interface	3
1.1.1. Successful pregnancy: Immune cells cooperating at the feto-maternal interface	3
1.1.2. Pro- and anti-inflammatory states during pregnancy	3
1.1.3. Immune cell populations within the feto-maternal interface	5
1.1.4. Immune cell regulation by trophoblast cells	7
1.1.5. Preimplantation factor (PIF) modulates maternal immune cell functions during pregnancy	7
1.2. Neutrophil recruitment cascade	9
1.2.1. Tethering and rolling	9
1.2.2. Slow rolling, arrest and adhesion	10
1.2.3. Post-arrest modifications, intraluminal crawling and transmigration	11
1.3. Calcium signaling in neutrophils	12
1.3.1. Store-operated Ca^{2+} entry (SOCE)	12
1.3.2. Ca^{2+} signaling during neutrophil rolling and arrest	13
1.3.3. Additional ion channels in Ca^{2+} signaling – The voltage gated potassium channel $K_v1.3$	14
1.4. Aim of the thesis	14
2. Materials	17
2.1. Animals	17
2.2. Human blood samples	17
2.3. Recombinant proteins	17
2.4. Chemicals, reagents, important items	18
2.5. Software	18
2.6. Antibodies	19
3. Methods	21
3.1. Intravital microscopy of the mouse cremaster muscle	21
3.1.1. TNF- α induced acute inflammation	21
3.1.2. Perivascular neutrophils in TNF- α induced acute inflammation	21

3.1.3.	Trauma induced acute inflammation	22
3.1.4.	CXCL1 induced leukocyte adhesion	22
3.2.	Neutrophil isolation	22
3.2.1.	Isolation of murine neutrophils	22
3.2.2.	Isolation of human neutrophils	22
3.3.	Cultivation of Jurkat cells	23
3.4.	Flow chamber assays	23
3.4.1.	Selectin-dependent leukocyte rolling <i>in vitro</i>	23
3.4.2.	Leukocyte slow rolling and adhesion <i>in vitro</i>	23
3.4.3.	Leukocyte slow rolling and adhesion <i>ex vivo</i>	23
3.4.4.	Human neutrophil rolling and slow rolling <i>in vitro</i>	24
3.4.5.	Neutrophil spreading <i>in vitro</i>	24
3.5.	Fluorescence activated cell sorting (FACS)	24
3.5.1.	Surfacemarkers	24
3.5.2.	Selectin binding	25
3.5.3.	Soluble ICAM-1 binding	25
3.5.4.	LFA-1 activation	25
3.5.5.	K _V 1.3 expression	25
3.6.	Confocal microscopy	26
3.7.	Western blot	26
3.8.	Patch clamp of isolated human neutrophils	27
3.9.	Transwell assay	27
3.10.	Electric Cell-Substrate Impedance Sensing (ECIS)	27
3.11.	Statistical analysis	28
4.	Results	29
4.1.	PIF disrupts neutrophil adhesion by reducing K _V 1.3-regulated SOCE	29
4.1.1.	PIF impairs leukocyte adhesion <i>in vivo</i> , <i>ex vivo</i> and <i>in vitro</i>	29
4.1.2.	PIF prevents leukocyte slow rolling <i>in vivo</i> , <i>ex vivo</i> and <i>in vitro</i>	30
4.1.3.	PIF does not change expression levels of adhesion relevant surface molecules on neutrophils	31
4.1.4.	PIF does not alter β ₂ integrin activation	32
4.1.5.	K _V 1.3 is expressed on human and murine neutrophils	33
4.1.6.	K _V 1.3 on human neutrophils is functional	35
4.1.7.	Genetic deletion and inhibition of K _V 1.3 impairs leukocyte adhesion <i>in vivo</i>	36
4.1.8.	Genetic deletion and inhibition of K _V 1.3 prevents leukocyte slow rolling <i>in vivo</i>	37
4.1.9.	Genetic loss of K _V 1.3 does not alter surface expression levels of adhesion relevant molecules	38
4.1.10.	PIF reduces voltage-induced K _V 1.3 currents in K _V 1.3-overexpressing HEK-293 cells	39
4.1.11.	PIF reduces voltage-induced K _V 1.3 currents in human neutrophils	39
4.1.12.	Inhibition of K _V 1.3 by PIF impairs calcium signaling in human neutrophils	40

4.1.13. PIF impairs post-arrest modifications in neutrophils	41
4.1.14. PIF increases susceptibility to shear forces <i>in vitro</i> and <i>in vivo</i>	41
4.2. PIF reduces extravasation of neutrophil into inflamed tissue	42
4.2.1. PIF reduces the number of transmigrated neutrophils in TNF- α stimulated cremaster muscles	42
4.2.2. Inhibition and genetic deletion of K _V 1.3 reduces the number of transmigrated neutrophils in TNF- α stimulated cremaster muscles	43
4.2.3. PIF impairs neutrophil recruitment in an animal model of acute lung injury (ALI) after LPS stimulation.	45
4.2.4. PIF does not change neutrophil transmigration in a transwell assay	45
4.2.5. PIF reduces vascular leakage in a model of ALI but does not alter TNF- α induced changes in the resistance of HUVEC monolayers	46
4.3. PIF alters selectin dependent leukocyte rolling	47
4.3.1. PIF alters leukocyte rolling <i>in vivo</i>	47
4.3.2. PIF does not influence the expression level of surface molecules important for neutrophil rolling	47
4.3.3. PIF does not change neutrophil binding capacity to E- and P-selectin <i>in vitro</i>	49
4.3.4. Genetic deletion or pharmacological inhibition of K _V 1.3 does not influence leukocyte rolling <i>in vivo</i>	50
4.3.5. Genetic deletion of K _V 1.3 does not alter the expression of rolling relevant surface molecules on peripheral blood neutrophils	50
4.3.6. PIF does not alter E- and P-selectin dependent leukocyte rolling <i>in vitro</i>	50
5. Discussion	55
5.1. PIF reduces selectin dependent leukocyte rolling	55
5.2. PIF disrupts leukocyte adhesion and extravasation	56
5.2.1. PIF does not affect chemokine induced inside-out β_2 integrin activation	56
5.2.2. PIF inhibits K _V 1.3 on neutrophils	57
5.2.3. K _V 1.3 on neutrophils regulates [Ca ²⁺] _i	58
5.2.4. PIF lowers the number of perivascular neutrophils	59
5.3. PIF as a potential therapeutic drug to treat inflammatory diseases	59
5.4. PIF modulates immune cells during pregnancy	61
5.5. Conclusion	62
Bibliography	63
II. Appendix	87
A. Results from collaboration partners	89
A.1. PIF reduces voltage-induced K _V 1.3 currents in K _V 1.3-overexpressing HEK-293 cells	89
A.2. Inhibition of K _V 1.3 by PIF impairs calcium signaling in human neutrophils	89
A.3. PIF increases susceptibility to shear forces <i>in vitro</i>	91

A.4. PIF impairs neutrophil recruitment in an animal model of acute lung injury after LPS stimulation	93
A.5. PIF reduces vascular leakage in a model of ALI	93
III. Curriculum vitae	97
B. Publications	101
C. Conferences	103
IV. Manuscript	105
D. Affidavit	145

List of Figures

1.1. Feto-maternal interface, 2 nd and 3 rd trimester.	4
1.2. Neutrophil recruitment cascade.	9
1.3. Different conformations of β_2 -integrins.	11
1.4. Store operated calcium entry (SOCE) in neutrophils.	13
1.5. Ca^{2+} signaling synchronizes neutrophil adhesion under flow.	15
1.6. $K_V1.3$ signaling in immune cells.	16
3.1. Detection of different LFA-1 affinity states.	26
4.1. PIF impairs leukocyte adhesion <i>in vivo</i> , <i>in vitro</i> and <i>ex vivo</i>	30
4.2. PIF prevents leukocyte slow rolling <i>in vivo</i> , <i>ex vivo</i> and <i>in vitro</i>	32
4.3. PIF does not alter expression levels of adhesion relevant surface molecules on neutrophils.	33
4.4. PIF does not alter β_2 integrin activation.	34
4.5. $K_V1.3$ is expressed on human and murine neutrophils.	35
4.6. $K_V1.3$ on human neutrophils is functional.	36
4.7. Neutrophils from $K_V1.3^{-/-}$ mice do not express $K_V1.3$	37
4.8. Genetic deletion or pharmacological inhibition of $K_V1.3$ impairs leukocyte recruitment in TNF- α stimulated mouse cremaster muscle.	37
4.9. Genetic deletion and inhibition of $K_V1.3$ prevents leukocyte slow rolling.	38
4.10. Genetic deletion of $K_V1.3$ does not alter the expression of adhesion relevant surface molecules on peripheral blood neutrophils.	39
4.11. PIF reduces voltage-induced $K_V1.3$ currents in human neutrophils.	40
4.12. PIF impairs neutrophil spreading.	42
4.13. PIF increases susceptibility to shear forces <i>in vivo</i>	43
4.14. PIF reduces the number of transmigrated neutrophils in TNF- α stimulated cremaster muscles.	44
4.15. Inhibition and genetic loss of $K_V1.3$ reduces the number of transmigrated neutrophils in TNF- α stimulated cremaster muscles.	44
4.16. PIF does not change neutrophil transmigration in a transwell assay.	45
4.17. PIF does not alter integrity of cultured HUVEC cells upon TNF- α stimulation.	46
4.18. PIF alters leukocyte rolling <i>in vivo</i>	48
4.19. PIF does not influence the expression level of surface molecules important for neutrophil rolling.	49
4.20. PIF does not change neutrophil binding capacity to E- and P-selectin under static conditions <i>in vitro</i>	50
4.21. Genetic deletion or pharmacological inhibition of $K_V1.3$ does not influence leukocyte rolling.	51

4.22. Genetic deletion of K _V 1.3 does not alter the expression of rolling relevant surface molecules on peripheral blood neutrophils.	51
4.23. PIF does not change E- and P-selectin dependent leukocyte rolling in <i>in vitro</i> microflow chambers.	52
5.1. PIF disrupts neutrophil recruitment by reducing K _V 1.3-regulated SOCE. . . .	60
A.1. PIF reduces voltage-induced K _V 1.3 currents in K _V 1.3-overexpressing HEK-293 cells.	90
A.2. K _V 1.3 is involved in CRAC channel dependent Ca ²⁺ influx in human neutrophils.	91
A.3. K _V 1.3 regulates total Ca ²⁺ flux after CXCL8 stimulation in human neutrophils.	91
A.4. K _V 1.3 regulates intracellular Ca ²⁺ concentrations under shear stress conditions.	92
A.5. PIF increases susceptibility to shear forces <i>in vitro</i>	92
A.6. PIF impairs neutrophil recruitment in an animal model of acute lung injury.	94
A.7. PIF reduces vascular leakage in a model of acute lung injury but does not alter integrity of cultured HUVEC cells upon TNF- α stimulation.	95

List of Tables

1.1. PIF serum levels of pregnant women.	8
2.1. Used recombinant proteins.	17
2.2. Used chemicals, reagents and important items.	18
2.3. Used software.	18
2.4. Used antibodies.	19
4.1. Hemodynamic parameters of WT mice treated with TNF- α	30
4.2. Number of mice, flow chambers, cells per FOV, and WBCs in <i>in vitro</i> and <i>ex vivo</i> flow chamber assays.	31
4.3. Hemodynamic parameters of WT and <i>K_v1.3^{-/-}</i> mice pre-treated as indicated prior to TNF- α stimulation.	38
4.4. Hemodynamic parameters before and after CXCL1 injection <i>in vivo</i>	43
4.5. Hemodynamic parameters of WT mice treated with TNF- α after the application of selectin blocking antibodies	48
4.6. Hemodynamic parameters of WT mice in a trauma induced inflammation model of the mouse cremaster before and after the application of P-selectin blocking antibodies.	49
4.7. Number of mice, flow chambers and cells per FOV of <i>in vitro</i> flow chamber assay.	53

Abbreviations

5-MOP	5-Methoxypsoralen
ACKR2	Atypical chemokine receptor 2
ALI	Acute lung injury
ANOVA	Analysis of variance
APC	Allophycocyanin
APS	Anti-phospholipid syndrome
ARDS	Acute respiratory distress syndrome
BAL	Broncho-alveolar lavage
BM	Basement membrane
BSA	Bovine serum albumine
BV	Brilliant violet
[Ca ²⁺] _i	intracellular Ca ²⁺ concentration
COPD	Chronic obstructive pulmonary disease
CRAC channel	Ca ²⁺ release-activated Ca ²⁺ channel
DC	Dendritic cell
DAG	Diacylglycerol
DAPI	4,6-diamidino-2-phenylindole
DMSO	Dimethyl sulfoxid
EAE	Experimental autoimmune encephalomyelitis
EDTA	Ethylenediaminetetraacetic acid
EGTA	Ethylene glycol-bis(β-aminoethyl ether)-N,N,N',N'-tetraacetic acid
ELISA	Enzyme-linked immunosorbent assay
ER	Endoplasmic reticulum
ESAM	Endothelial cell-selective adhesion molecule
ESL-1	E-selectin ligand-1
FITC	Fluorescein isothiocyanate
FCS	Fetal calf serum
FcγR	Fcγ receptor
FOV	Field of view
GAPDH	Glyceraldehyde 3-phosphate dehydrogenase
GPCR	G-protein coupled receptor
HBSS	Hanks balanced salt solution
HE	Hematoxylin and eosin
HLA-	Human leukocyte antigen
H-PIF	PIF homolog
HUVEC	Human umbilical vein endothelial cells
ICAM	Intracellular adhesion molecule

ID	Inner diameter
IL	Interleukin
i.p.	Intra peritoneal
IP ₃	Inositol-1,4,5 triphosphate
IP ₃ R	IP ₃ receptor
i.s.	Intrascrotal
IVM	Intravital microscopy
JAM	Junctional adhesion molecule
LFA-1	Leukocyte function antigen-1
LCP-1	L-plastin
LPS	Lipopolysaccharide
Mac-1	Macrophage-1 antigen
MCP-1	Monocyte chemotactic protein-1
M-CSF	Macrophage colony-stimulating factor
MFI	Mean fluorescence intensity
MMP	Matrix metalloproteinase
MS	Multiple sclerosis
MST1	Mammalian sterile 20-like kinase 1
NA	Numerical aperture
NE	Neutrophil elastase
NK cell	Natural killer cell
OD	Outer diameter
ON	Over night
PAP-1	5-(4-Phenoxybutoxy)psoralen
PB	Pacific blue
PE	Phycoerythrin
PECAM-1	Platelet endothelial cell adhesion molecule-1
PFA	Paraformaldehyde
PGF	Placental growth factor
PI3K	Phosphoinositide 3-kinase
PIF	Preimplantation factor
PIP ₂	Phosphatidylinositol 4,5 bisphosphate
PKC	Protein kinase C
PLC	Phospholipase
PM	Plasma membrane
PSGL-1	P-selectin glycoprotein ligand-1
PTX3	Pentraxin 3
PVDF	Polyvinylidenfluorid
RACK-1	Receptor for activated protein kinase C-1
RAGE	Receptor for advanced glycation end products
rh	Recombinant human
rm	Recombinant mouse
RIPA	Radioimmunoprecipitation assay
ROCE	Receptor operated calcium entry

ROS	Reactive oxygen species
RT	Room temperature
scrPIF	Scrambled PIF
SDF-1	Stromal cell-derived factor-1
SDS-PAGE	Sodium dodecyl sulfate–polyacrylamide gel electrophoresis
SEM	Standard error of mean
SFK	Src family kinase
SOCE	Store-operated calcium entry
STIM-1	Stromal interaction molecule 1
TCR	T cell receptor
TEM	Transendothelial migration
T _{CM} cell	Central memory T cell
T _{EM} cell	Effector memory T cell
TGF- β	Tissue growth factor- β
T _h cell	Helper T cell
T1DM	Type I diabetes mellitus
TLR4	Toll-like receptor 4
TNF- α	Tumor necrosis factor- α
TRAM-34	1-[(2-Chlorophenyl)diphenylmethyl]-1H-pyrazole
T _{reg} cell	Regulatory T cell
TRPC	Transient receptor potential canonical
VCAM-1	Vascular cell adhesion molecule-1
VEGF	Vascular endothelial growth factor
VLA	Very late antigen
WBC	White blood cell count
WT	Wildtype

Part I.
Thesis

1. Introduction

1.1. The feto-maternal interface

The placenta is the central structure during pregnancy of eutherian mammals. It defines the feto-maternal interface and exchange of all gas, nutrition and waste is carried out along this barrier¹. The placenta is composed of maternal decidua and extra-embryonic trophoblast. During blastocyst invasion, trophoblast cells enter decidualized endometrial epithelium and anchor into the tissue². Even prior to implantation, endometrial cells transit into decidual cells, preparing for trophoblast invasion³. Resident and infiltrating immune cells start to remodel the tissue³. Remodeling occurs in several steps until the definitive placental structure is established in transition from 1st to 2nd trimester¹ (Fig. 1.1). There, trophoblast cells, forming villous trees are bathed by maternal blood, ensuring maximum mass transfer⁴. Extravillous trophoblast cells anchor the villi into the decidua⁵. Consequently, 'semi-allogenic' embryonic cells are in direct contact with maternal decidual cells and maternal blood.

1.1.1. Successful pregnancy: Immune cells cooperating at the feto-maternal interface

Throughout pregnancy, maternal immune cells colonize the placenta and are a prerequisite for successful gestation⁶. Around 40% of the decidua is composed of maternal leukocytes¹. As outlined below, uterine immune cells are often characterized by a unique phenotype, differing from their counterparts present in other tissues⁷. In the placenta, they participate in tissue remodeling and in protection of the growing embryo/fetus from invading pathogens. Imbalance in the composition of intrauterine immune cells can cause severe complications during pregnancy, such as poor endometrial vascularization, impaired blastocyst implantation, or fetal loss⁸. For a long time, pregnancy has been seen as a state of constant local immune suppression⁹. With the findings of varying immune cell compositions in the placenta throughout gestation, the picture emerged that pro- and anti-inflammatory periods alternate during pregnancy⁶. Nowadays, it is clear that the ability of maternal immune cells to adapt to different developmental stages is a prerequisite for successful pregnancy⁹.

1.1.2. Pro- and anti-inflammatory states during pregnancy

The supportive role of immune cells for successful pregnancy starts even prior to fertilization. Endometrial immune cells permanently colonize the uterus, regulating normal menstrual cycle¹⁰. Fertilization induces leukocytes to infiltrate the endometrium at time of conception around day 23-25 of menstrual cycle, thereby taking part in pre-decidualization^{1,7}. Early steps of pregnancy, like initial blastocyst attachment to the uterus wall, trophoblast invasion

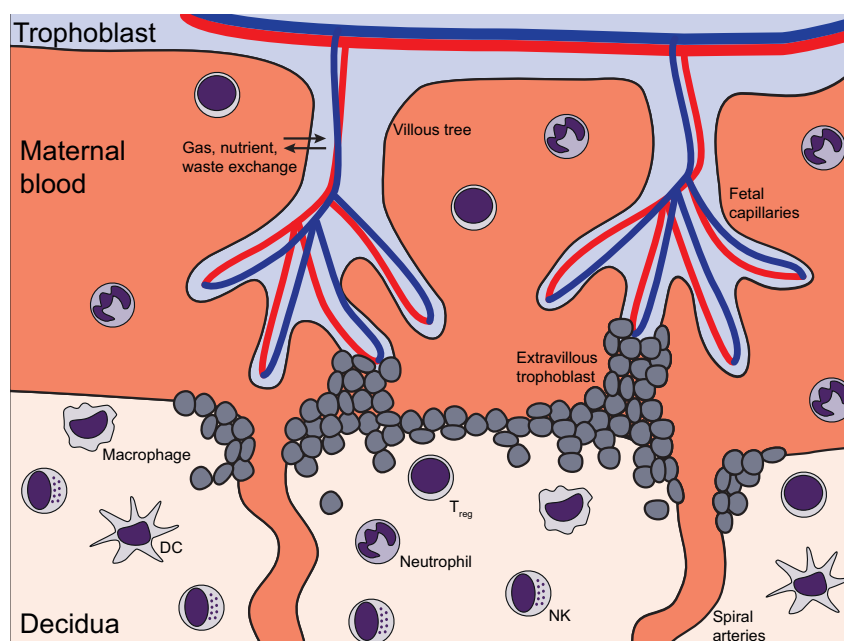


Figure 1.1.: Feto-maternal interface, 2nd and 3rd trimester. Extra-embryonic trophoblast anchors into the decidua and forms chorionic villi which get bathed with maternal blood to ensure gas, nutrient and waste exchange. Extravillous trophoblast cells link villi to the decidua. Maternal immune cells colonize the decidua and fulfill important regulatory functions without initiating immune responses against 'semi-allogenic' trophoblast cells. DC: dendritic cell, NK: natural killer cell, T_{reg}: regulatory T cell. (modified from^{1,4}).

and accompanying placentation require a pro-inflammatory milieu⁶. Endometrial stromal cells and invading immune cells produce and secrete a variety of pro-inflammatory mediators, including interleukin-6 (IL-6), IL-8 (CXC-chemokine ligand 8, CXCL8), CXCL1 (mouse), or tumor necrosis factor- α (TNF- α), important for upregulation of adhesion molecules, removal of preexisting mucin layers and further attraction of leukocytes^{6,11}. Invading immune cells additionally secrete pro-angiogenic factors like vascular endothelial growth factor (VEGF) or placental growth factor (PGF)⁷, enabling tissue remodeling and vascularization of the decidua. In animal models, deletion of different immune cell populations like dendritic cells¹² or macrophages¹³ resulted in infertility, ineffective implantation and early abortion, demonstrating the critical role of immune cells in early pregnancy. Importance of a general pro-inflammatory milieu has been highlighted by observations that local injury caused e.g. by endometrial biopsies increases receptivity and doubles the incidence of successful pregnancy¹⁴.

Implantation and placentation is followed by a period of fetal growth and development. This stage is characterized by an anti-inflammatory environment, lasting from week 13 to week 27 in humans⁶. During this period, both, immune and trophoblast cells produce primarily anti-inflammatory mediators like IL-10, IL-15 or tissue growth factor- β (TGF- β)^{6,1}, reducing cytotoxicity of immune cells and creating immune tolerance. Higher levels of pro-inflammatory mediators in this period and ensuing recruitment of leukocytes may lead to miscarriage and preterm birth¹⁵.

Parturition and its initiation is again accompanied by pro-inflammatory processes, medi-

ated in particular by NF- κ B-signaling¹⁶. In preparation of delivery, immune cells infiltrate the cervix, decidua and myometrium¹⁷, a prerequisite for uterus contractions, subsequent delivery and separation of the placenta⁶. After labor, leukocytes play an important role in postpartum tissue remission and repair^{17,18}.

1.1.3. Immune cell populations within the feto-maternal interface

A lot of different immune cell populations participate in initiation, maintenance and termination of pregnancy with different ratios and functions, depending on the gestational age¹⁹, among them natural killer (NK) cells, macrophages, dendritic cells (DCs), regulatory T (T_{reg}) cells, neutrophils, mast cells, and B lymphocytes^{1,6,7}.

NK cells:

Approximately 70% of decidual leukocytes in the 1st trimester are NK cells¹. In comparison to peripheral NK cell populations, uterine NK cells have a distinct phenotype²⁰. They exhibit lower cytotoxicity and produce a vast variety of growth factors, angiogenic factors, pro- and anti-inflammatory cytokines²¹, qualifying them as key regulators of uterine vascular remodeling²². The specific phenotype of uterine NK cells is in parts mediated by IL-15, which is secreted by intrauterine macrophages and trophoblast cells²³. The importance of NK cells in normal decidua formation has been shown in mice, where depletion of uterine NK cells resulted in fetal loss due to incomplete vascularization²⁴. In line, endometrial biopsies from women with unexplained infertility exhibited reduced numbers of NK cells compared to biopsies from fertile women²⁵.

Macrophages:

Displaying pro- and anti-inflammatory properties during different stages of pregnancy, macrophages play a pivotal role. With 20-25%, they constitute the second largest leukocyte population in 1st trimester deciduas¹. During that period, they exhibit predominantly a M2-like phenotype²⁶, secreting anti-inflammatory mediators like IL-10 and TGF- β ⁷. In early pregnancy, they further contribute to tissue remodeling and angiogenesis via release of VEGF or matrix metalloproteinase 9 (MMP9)^{27,28,29}. Additionally, decidual macrophages are implicated to have an important scavenger function by taking up apoptotic trophoblasts, thereby preventing activation of pro-inflammatory signaling pathways³⁰. Expression of surface receptors like hemoglobin scavenger receptor (CD163) or mannose receptor (CD206) further suggests that they also face a role in protecting the fetus against infections by eliminating invading pathogens³¹. Deletion of macrophages in mice resulted in implantation failure, underlining its important role especially in early pregnancy¹³. Peri-parturition, infiltrating macrophages into the uterus and cervix exhibit a more pro-inflammatory phenotype¹⁷ by participating in the degradation of the extracellular matrix through secretion of MMPs and pro-inflammatory cytokines³². In addition, intrauterine macrophages also contribute to

postpartum tissue repair³³.

T_{reg} cells:

T_{reg} cells play a central role in maintaining an anti-inflammatory environment by suppressing immune responses against paternal antigens^{34,35}. Their important role during pregnancy has been demonstrated in animal models, where depletion of Foxp3⁺ T_{reg} cells resulted in infertility, ineffective implantation and early abortion³⁶. In line, endometrial tissue of infertile women exhibit reduced amounts of Foxp3 mRNA, indicating impaired T cell differentiation into T_{reg} cells³⁷. Interestingly, these cells persist beyond parturition, decreasing the resorption rate in a second pregnancy with the same paternal background³⁸.

Dendritic cells:

Like most other leukocytes, uterine dendritic cells (DCs) exhibit a distinctive phenotype compared to circulating or tissue resident DCs from other organs⁷. Similar to NK cells and macrophages, DCs play a crucial role in early pregnancy, by promoting implantation and decidua formation, as their depletion causes impaired implantation, embryo resorption and perturbed angiogenesis¹². Supportive functions of DCs for successful pregnancy start even prior to fertilization. DCs in the vaginal lumen encounter parental antigens from male sperm directly after copulation^{39,40}. These cells do not migrate into lymph nodes, but are locally involved in the communication between T_{reg} cells and trophoblast cells⁴¹ and are able to directly activate T_{reg} cells⁴². Hence, they seem to play an important role in the generation of immune tolerance towards paternal antigens. In addition, they secrete IL-10 and soluble human leukocyte antigen-G (HLA-G), further promoting tolerance⁴³.

Neutrophils:

Neutrophils, primarily associated with pro-inflammatory functions, high cytotoxicity and accompanied tissue damage⁴⁴ need to be tightly regulated during pregnancy. Therefore, presence of neutrophils in close proximity to the fetus has been classically correlated with severe problems like pre-eclampsia or fetal loss^{18,45}. Indeed, high numbers of neutrophils are present in pre-eclamptic placentae^{46,47} and neutrophils have been shown to contribute to fertility problems in women suffering from anti-phospholipid syndrome (APS), an autoimmune disease with a high coincidence of pregnancy related complications⁴⁸. Surprisingly, Amsalem and colleagues recently described a 2nd trimester uterine neutrophil population which is characterized by pro-angiogenic and reduced cytotoxic properties, similar to the phenotype of decidual macrophages or NK cells⁴⁹, suggesting that neutrophils infiltrate the placenta as well and contribute to successful pregnancy. Similar to macrophages, neutrophils play an important role during labor¹⁷. They infiltrate the myometrium, secreting MMPs and pro-inflammatory cytokines⁵⁰ and are involved in post-partum tissue repair³³. In contrast to macrophages, neutrophils do not participate in ripening of the cervix¹⁷.

Taken together, maternal leukocytes surrounding the fetus during pregnancy fulfill important functions in placentation and immune surveillance. Alterations in their quantity and quality can cause severe perturbations, leading to impaired embryonic development and eventually fetal death. Therefore, these cells need to be tightly regulated in order to prevent recognizing the unborn as a 'semi-allogenic transplant' and to not initiate immune responses against fetal tissue. Immune cells generally seem to shift towards a regulatory and less cytotoxic phenotype within the placenta, arguing for tissue-induced tolerance.

1.1.4. Immune cell regulation by trophoblast cells

Trophoblast cells actively shape maternal immune cell functions by expressing a variety of growth factors and cytokines^{6,51}. Constitutive secretion of CXCL12 (stromal cell-derived factor-1, SDF-1), CXCL8 and CCL2 (monocyte chemotactic protein-1, MCP-1)^{6,52} for example attracts lymphocytes, neutrophils and monocytes. Trophoblast derived IL-15 and TGF- β shift decidual NK cells into their specific pro-angiogenic and low cytotoxic phenotype²¹. TGF- β is further important for the development of naive CD4⁺ T into Foxp3⁺ T_{reg} cells⁵². Recruited CD14⁺ monocytes to the feto-maternal interface differentiate into M2-like macrophages, induced by macrophage colony-stimulating factor (M-CSF) and IL-10^{51,53} that is secreted by trophoblast cells.

Attraction and parallel modulation of maternal immune cells at the feto-maternal interface needs to be finely tuned to maintain the protective properties of immune cells. At the same time, they need to be restricted from recognizing extra-embryonic and embryonic tissue as a 'semi-allograft' and from initializing immune responses against the unborn. Besides the mostly tolerogenic phenotype of many of the decidual leukocytes, trophoblast cells express the atypical chemokine receptor 2 (ACKR2) and internalize and scavenge pro-inflammatory chemokines, thereby reducing chemokine gradients towards fetal tissue^{54,55}. In addition, trophoblast cells do not express the classical HLA-A and -B, but HLA-C and non-classical HLA-E, -F and -G^{56,57}. Decidual NK cells bind to HLA-G via the receptor KIR2DL4⁵⁸ resulting in the suppression of cytotoxic properties of NK cells⁵⁹. Also other immune cells like macrophages⁶⁰, T cells⁶¹ and B cells⁶² bind to HLA-G via the receptors ILT2, ILT4⁶³, resulting in modulation of their functions.

1.1.5. Preimplantation factor (PIF) modulates maternal immune cell functions during pregnancy

Another factor which is expressed by trophoblast cells of many mammalian species and which is thought to contribute to feto-maternal crosstalk, is Preimplantation factor (PIF), a 15 amino acid small peptide^{64,65,66,67}. PIF is already secreted at very early gestational stages, even prior to implantation⁶⁸ and can be detected in the maternal circulation throughout pregnancy (Tab. 1.1⁶⁹). Sufficient PIF serum levels are required for embryonic development⁶⁸ and positively correlate with successful birth⁶⁶. PIF changes the expression pattern of endometrial stromal cells and 1st trimester decidua cells towards a pro-receptive milieu⁷⁰,

thereby promoting trophoblast invasion^{67,71,72}. *In vitro*, PIF enhances the expression of protolerogenic HLA molecules in trophoblast cells⁷³. Until now, the gene encoding for PIF has not been discovered and its exact origin is still controversial.

Table 1.1.: PIF serum levels of pregnant women. Mean±SEM, from⁶⁹

Trimester	PIF levels [nM]
1 st	50.1±4.8
2 nd	60.7±7.3
3 rd	58.8±6.4

PIF was shown to interact with immune cells^{64,65,74} and therefore suggested to modulate maternal immune cell function during pregnancy^{64,75}. In a murine model of LPS induced fetal loss, PIF administration increased fetal survival and changed placental and serum cytokine profiles⁷⁶. Interestingly, trophoblast PIF expression increased upon LPS stimulation. Further, PIF reduces the expression of the endometrial inflammatory marker prostaglandin F_{2α}⁷⁷.

PIF's properties to modulate immune cell function have been also assessed outside the context of pregnancy, in animal models for autoimmune diseases. In a model for type I diabetes mellitus (T1DM), continuous PIF administration lowered the number of invading immune cells into the mouse pancreas, thereby preserving insulin production and overall architecture of the islets of Langerhans⁷⁸. Similar, in a model for experimental autoimmune encephalomyelitis (EAE), PIF treatment lowered immune cell infiltration into the central nervous system and attenuated the progression of the disease⁷⁹. Mueller and colleagues demonstrated in a newborn rat hypoxic-ischemic brain injury model that PIF administration has neuro-protective properties by reducing *let7* mRNA expression in a toll-like receptor 4 (TLR4) dependent manner⁸⁰. In a follow-up study they were able to decipher that PIF, via TLR4, PI3K/Akt and *let7* signaling, upregulates anti-inflammatory IL-10 expression⁸¹. Further, PIF reduced graft-versus host disease after bone marrow transplantation in mice⁸² and had positive effects in non-human primates following ovarian tissue transplantation⁸³. In a mouse model of atherosclerosis, PIF administration reduced sclerotic lesions and lowered the number of infiltrated immune cells⁸⁴.

Although, effects of PIF on immune cell function have been proven in several disease models, molecular mechanisms how PIF interferes with immune cells are not clear. Especially its role in the maternal circulation is completely unknown. Therefore, immune modulatory properties of PIF in acute, primarily neutrophil driven, inflammatory scenarios outside the context of pregnancy were investigated in this study to better understand PIF's serum function and to reveal underlying molecular mechanisms of PIF dependent immune modulation.

1.2. Neutrophil recruitment cascade

Neutrophils are the most abundant white blood cells in the circulation of humans⁸⁵ and the first cells to arrive at sites of inflammation⁴⁴. They belong to the innate arm of the immune system and exert important functions during immune responses by fighting invading pathogens and recruiting other immune cells⁸⁶.

Recruitment of neutrophils from postcapillary venules to sites of inflammation follows a distinct and tightly regulated multi-step cascade of receptor–ligand interactions and subsequent signaling events⁸⁷, including initial tethering and rolling, adhesion and intraluminal crawling, followed by transmigration and interstitial migration⁸⁸ (Fig. 1.2).

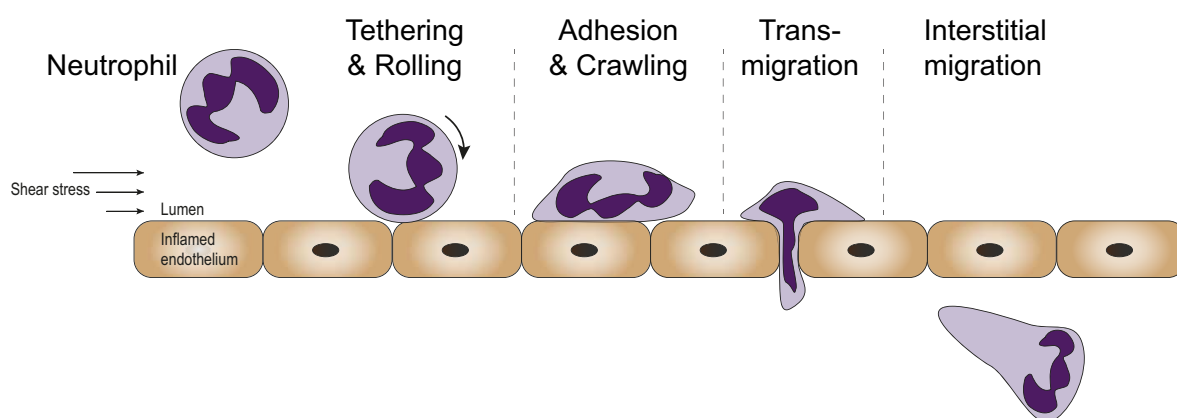


Figure 1.2.: Neutrophil recruitment cascade. To sites of inflammation, neutrophils follow a well defined cascade of events including tethering, rolling, adhesion, intraluminal crawling, transmigration and interstitial migration.

1.2.1. Tethering and rolling

The initial steps of neutrophil recruitment, tethering and subsequent rolling are mediated by interaction of selectins, expressed on inflamed endothelial cells and neutrophils with their respective ligands^{89,90}. Selectins are a family of three type I transmembrane glycoproteins which bind to fucosylated and sialylated glycoprotein ligands via their calcium-dependent C-type lectin domain^{91,92}. P-selectin (CD62P) is expressed by megakaryocytes/platelets and endothelial cells⁹³, where it is pre-stored in α -granules or Weibel-Palade bodies, respectively⁹¹. P-selectin is translocated to the cell surface within minutes upon stimulation by mediators such as thrombin or histamine⁹². P-selectin interacts with its predominant ligand P-Selectin Glycoprotein Ligand-1 (PSGL-1, CD162) and CD24 on leukocytes⁹⁴. Activation with TNF- α , IL-1 β or lipopolysaccharide (LPS) further induces transcriptional upregulation of P-selectin in mice but not in humans^{95,96}. E-selectin (CD62E) is not pre-stored in vesicles and needs to be *de novo* synthesized by endothelial cells upon stimulation⁹⁰. Bone marrow and skin endothelial cells constitutively express E-selectin⁹². On the surface, it interacts with PSGL-1 and additionally with CD44 and E-selectin ligand-1 (ESL-1)⁹⁷. L-selectin (CD62L) is constitutively expressed on leukocytes where it plays a crucial role in lymphocyte homing⁹⁸. During recruitment, adherent leukocytes are able to capture free floating leukocytes via L-selectin–PSGL-1 interaction, a process called secondary tethering^{99,100}. In addition, human

but not murine L-selectin is able to bind to E-selectin^{101,102}, thereby contributing to leukocyte rolling.

Selectin bonds with their ligands are characterized as catch bonds, interactions which require certain tensile forces^{103,104} and which are enhanced by increasing mechanical tension on the bonds¹⁰⁵. High on- and off-rates of selectin–selectin ligand bonds result in leukocyte rolling¹⁰⁶ along inflamed endothelium and determine characteristic E- and P-selectin-dependent rolling velocities^{107,108,109}. To roll even at high shear forces, neutrophils form tethers and slings, subcellular elongations of the cell membrane¹¹⁰.

1.2.2. Slow rolling, arrest and adhesion

Integrins expressed on neutrophils contribute to rolling, arrest and adhesion to inflamed endothelium. Integrins are heterodimeric transmembrane proteins and consist of an α - and a β -subunit¹¹¹ with 18 different α - and 8 β -subunits known to be genetically encoded in mice and humans⁸⁷. Neutrophil rolling, adhesion and subsequent crawling is mainly mediated by members of β_2 -integrins, namely lymphocyte function antigen-1 (LFA-1, $\alpha_L\beta_2$, CD11a/CD18) and macrophage-1 antigen (Mac-1, $\alpha_M\beta_2$, CD11b/CD18)¹¹². Intracellular adhesion molecule-1 (ICAM-1) which is constitutively expressed on endothelial cells is the major ligand for β_2 -integrins during neutrophil recruitment⁸⁸, but also other adhesion molecules like ICAM-2¹¹³ or receptor for advanced glycation end products (RAGE)¹¹⁴ are important β_2 -integrin ligands in the context of neutrophil recruitment. Upon activation, integrins change their conformation from a bent, low affinity (low affinity αI domain) to an extended, intermediate (low/intermediate affinity αI domain) or extended fully activated conformation (high affinity αI domain, Fig. 1.3-A), thereby increasing the affinity to their binding partners¹¹⁵. Fan and colleagues¹¹⁶ described a fourth, anti-inflammatory high-affinity, bent conformation. This state allows integrins to bind to ICAM-1 expressed on neutrophils, thereby preventing intercellular integrin interactions (Fig. 1.3-B). Recently, L-plastin (LCP-1) which is expressed in leukocytes, was shown to bind to bent Mac-1, thereby attenuating leukocyte adhesion¹¹⁷. Rolling along inflamed endothelium allows neutrophils to recognize pro-inflammatory chemokines and other chemoattractants immobilized on the luminal surface⁴⁴. Recognition of chemokines by G-protein coupled receptors (GPCRs) leads to changes in the conformation of β_2 -integrins (chemokine induced inside-out signaling) and concomitant deceleration of rolling neutrophils up to full arrest⁸⁸. Additional to GPCR-mediated β_2 -integrin activation, E-selectin–PSGL-1 engagement activates β_2 -integrins either directly via intracellular downstream signaling^{118,119}, or by the release of S100A8/A9 and autocrine activation via TLR4 downstream signaling¹²⁰. In humans, E-selectin–L-selectin interactions are able to induce release of S100A8/A9 as well¹⁰².

Talin-1 and kindlin-3 are critical intracellular co-activators of β_2 -integrins during inside-out signaling^{111,121} with distinct roles in integrin activation^{115,122}. Both molecules bind directly to the intracellular tail of the β_2 -subunit, thereby shifting integrins into activated states^{112,123}. Whereas talin-1 is required for both, intermediate and fully activated LFA-1, kindlin-3 is indispensable only for high-affinity conformation¹²⁴.

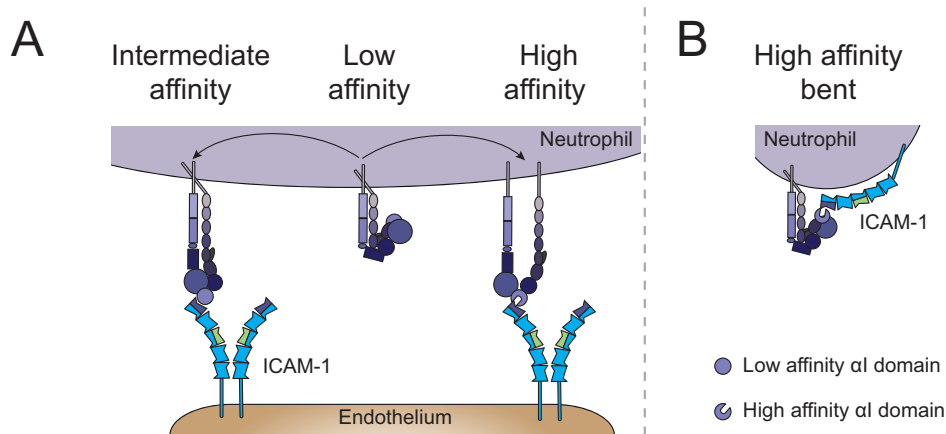


Figure 1.3: Different conformations of β_2 -integrins. (A) Integrins change their conformational state upon activation, thereby influencing the binding affinity to ligands such as ICAM-1. (B) In the high affinity-bent conformation, β_2 -integrins bind to ICAM-1 expressed on neutrophils (modified from¹¹¹).

1.2.3. Post-arrest modifications, intraluminal crawling and transmigration

To withstand shear forces, neutrophils need to undergo post-arrest modifications, including adhesion strengthening and spreading, mediated by signaling events downstream of activated and ligand bound β_2 -integrins (integrin outside-in signaling)^{125,126}. LFA-1-ICAM-1 engagement activates Src family kinases (SFKs), which among others phosphorylate and activate Vav-family molecules and phospholipase C γ (PLC γ) via spleen tyrosine kinase (Syk)¹²⁷. Downstream signaling via Vav leads to activation of the Rho GTPase family members Cdc42, Rac and RhoA¹²⁸, key molecules for cytoskeletal rearrangement. Firm adhesion requires linkage of the actin cytoskeleton to adhesion spots, consisting of clustered β_2 -integrins bound to their endothelial ligands. Talin-1, composed of a head and a rod domain, has multiple binding sites for the F actin-binding protein vinculin¹²¹ and is able to directly bind to F actin¹²⁹, therefore linking the actin cytoskeleton to the adhesion complex¹³⁰. Besides talin-1 and kindlin-3, a huge variety of molecules gets recruited to focal adhesion sites during inside-out and outside-in integrin activation^{131,132,133}, promoting integrin clustering, cytoskeletal rearrangement and firm adhesion.

Before neutrophils exit the blood vessel into the interstitial tissue, they crawl along the vessel wall to find appropriate spots for transmigration¹³⁴. Multiple chemoattractants, immobilized on the endothelial surface, guide their way towards transmigration loci^{135,136}. In addition, adherent platelets at the inflamed vessel wall contribute in directing neutrophil extravasation¹³⁷. Whereas LFA-1 is the major β_2 integrin during neutrophil adhesion, intraluminal crawling is predominantly dependent on interactions of activated Mac-1 with endothelial expressed ICAM-1, ICAM-2 and vascular cell adhesion molecule-1 (VCAM-1, CD106)^{113,134}. At the exit site, neutrophils first have to pass the endothelial layer, before overcoming the underlying basement membrane (BM) and the discontinuous layer of pericytes¹³⁴. Transendothelial migration (TEM) of neutrophils usually occurs via the paracellular route and to a minor extent directly through endothelial cell bodies, via the transcellular route¹³⁸. TEM requires many ligand-receptor interactions, inducing downstream signaling in both, neutrophils and endothelial cells¹³⁹. Engagement of LFA-1 and very late antigen-4 (VLA-4, CD49c/CD29,

$\alpha_4\beta_1$ integrin) on neutrophils with endothelial expressed ICAM-1 and VCAM-1, respectively lead to clustering of ICAM-1 and VCAM-1 at EC junctions and to intracellular signaling in endothelial cells^{140,141}. As a consequence, intracellular VE-cadherin tails get dephosphorylated¹⁴², resulting in the retraction of VE-cadherin adherens junctions¹⁴³. Tight junction molecules from the junctional adhesion molecule (JAM) family, JAM-A¹⁴⁴, JAM-B, JAM-C¹⁴⁵, endothelial cell-selective adhesion molecule (ESAM)¹⁴⁶, as well as platelet endothelial cell adhesion molecule-1 (PECAM-1, CD31)¹⁴⁷ and CD99¹⁴⁸ are all located in and around endothelial junctions and help guiding neutrophils through the endothelial layer¹³⁴.

The underlying BM is a highly crosslinked network, mainly composed of laminins and type IV collagen and incorporated pericytes¹⁴⁹. To overcome this barrier, neutrophils use 'low expression regions', characterized by a less dense meshwork of matrix proteins¹³⁸. Neutrophil-endothelial cell engagement induces MST-1 dependent release of vesicle-stored VLA-3 ($\alpha_3\beta_1$) and VLA-6 ($\alpha_6\beta_1$) and neutrophil elastase (NE)¹⁵⁰, a pre-requisite for BM penetration¹⁵¹. Following BM penetration the cells crawl along pericytes in a ICAM-1- β_2 integrin dependent manner¹⁵². Within the interstitium, neutrophils migrate to the site of insult, in a largely β_2 integrin independent manner¹⁵³, involving MMPs¹⁵⁴.

1.3. Calcium signaling in neutrophils

Calcium is an evolutionary highly conserved signaling molecule¹⁵⁵ which regulates a huge spectrum of biological processes ranging from signal transduction in neurons to muscle contractions. Also functions of immune cells¹⁵⁶, including neutrophils¹⁵⁷ depend on Ca^{2+} signaling. Thereby, changes in intracellular Ca^{2+} concentrations ($[\text{Ca}^{2+}]_i$) are a hallmark in neutrophil activation and many functions during neutrophil recruitment depend on Ca^{2+} signaling¹⁵⁸.

1.3.1. Store-operated Ca^{2+} entry (SOCE)

The predominant mechanism to increase $[\text{Ca}^{2+}]_i$ in neutrophils is store-operated calcium entry (SOCE) via Ca^{2+} release-activated Ca^{2+} (CRAC) channels¹⁵⁹ (Fig. 1.4). Under baseline conditions, extracellular Ca^{2+} concentrations are 10 000-fold higher compared to cytosolic levels¹⁶⁰, creating a high electrochemical driving force for Ca^{2+} to enter the cell. In neutrophils, SOCE can be initiated via engagement of numerous receptors with their ligands, namely by GPCRs¹⁶¹, Fc γ receptors (Fc γ R)¹⁶², activated β_2 -integrins^{163,164} and PSGL-1/L-selectin-E-selectin interaction^{119,165,166}. Fc γ receptors, β_2 -integrins, PSGL-1, and L-selectin activate members of the PLC- γ subfamily, PLC γ 1 and PLC γ 2 via Syk^{119,167}. Activation of GPCRs dissociates G protein subunits α from $\beta\gamma$, resulting in activation of PLC β 2 and PLC β 3¹⁶⁷. PLCs convert membrane-bound phosphatidylinositol 4,5 biphosphate (PIP₂) into diacylglycerol (DAG) and inositol-1,4,5 triphosphate (IP₃)¹⁵⁵. IP₃ opens IP₃ receptors (IP₃R) in the membrane of the endoplasmic reticulum (ER), triggering the release of Ca^{2+} out of the ER into the cytoplasm¹⁵⁶. Stromal interaction molecule 1 (STIM1) senses the Ca^{2+} concentration in the ER¹⁶⁸ and translocates to ER regions of close proximity to the plasma membrane (PM) upon ER Ca^{2+} store depletion, where it binds to Orai1¹⁶⁹, the predominant CRAC channel in neutrophils¹⁶⁶. STIM1-Orai1 engagement in turn opens the Orai1 channel,

resulting in influx of extracellular Ca^{2+} into the cell¹⁵⁸.

An alternative mechanism of Ca^{2+} influx besides SOCE is receptor operated calcium entry (ROCE)¹⁷⁰. Transient receptor potential canonical (TRPC) channel 6 and TRPC3, two non-selective Ca^{2+} and Na^{+} channels which are also expressed on neutrophils¹⁷¹ are activated directly by DAG¹⁷², the complementary cleavage product of PIP_2 conversion.

Many innate immune defense processes in neutrophils depend on an increase in $[\text{Ca}^{2+}]_i$, among them β_2 -integrin activation¹⁶⁵, cytoskeletal rearrangement¹⁷³, migration¹⁷⁴, degranulation, phagocytosis, or reactive oxygen species (ROS) production¹⁷⁵.

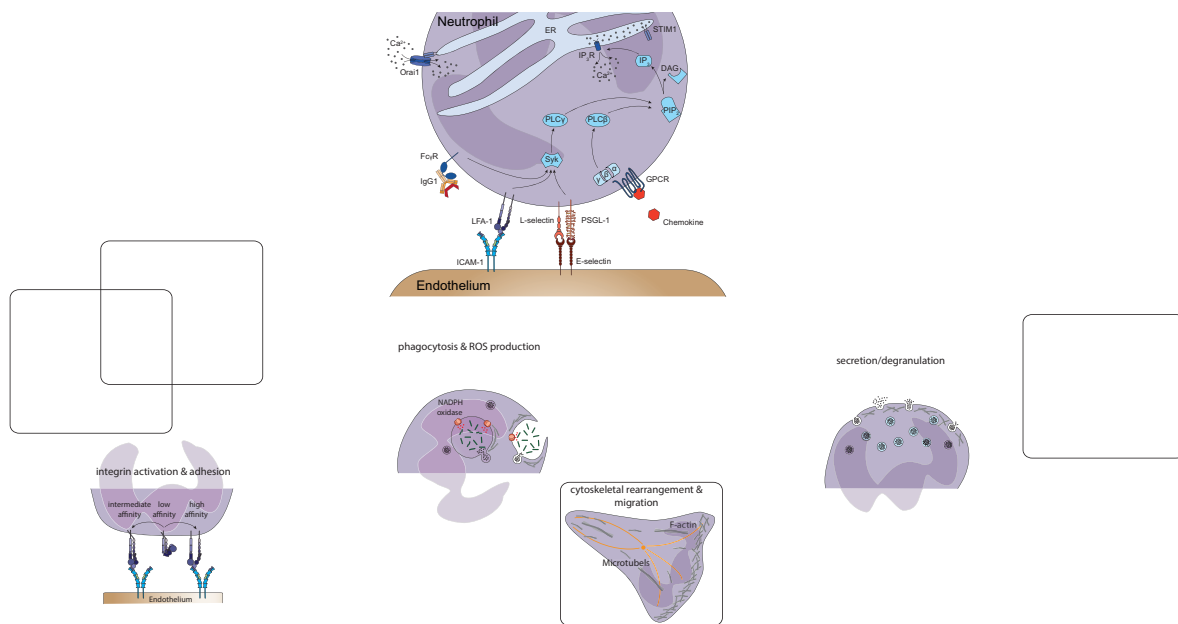


Figure 1.4.: Store operated calcium entry (SOCE) in neutrophils. Various receptor–ligand interactions induce calcium signaling in neutrophils. While $\text{Fc}\gamma$ receptors, LFA-1, L-selectin and PSGL-1 signal via Syk and $\text{PLC}\gamma$, activation of GPCRs results in the dissociation of G protein subunits α from $\beta\gamma$ and activation of $\text{PLC}\beta$. Both PLCs convert PIP_2 into DAG and IP_3 , resulting in IP_3R activation and subsequent Ca^{2+} flux out of the endoplasmic reticulum (ER). Ca^{2+} store depletion induces translocation of the Ca^{2+} sensor STIM1 and subsequent activation of Orail, leading to influx of extracellular Ca^{2+} (modified from¹⁵⁸).

1.3.2. Ca^{2+} signaling during neutrophil rolling and arrest

Ca^{2+} flux is a key-regulator of adhesion strengthening, neutrophil polarization and of transition from a rolling and adherent to a migratory phenotype¹⁵⁹. Shear stress acting on rolling and adherent neutrophils plays an important role in synchronizing and enhancing Ca^{2+} signaling during recruitment of neutrophils¹⁷⁶. Neutrophil rolling on E-selectin induces release of Ca^{2+} stored in the ER via engagement with PSGL-1 and L-selectin (human) and downstream activation of the $\text{PLC}\gamma/\text{PIP}_2/\text{IP}_3\text{R}$ axis^{119,165} (Fig. 1.5-A). This increase in $[\text{Ca}^{2+}]_i$ is amplified by mechanical shear forces, acting on selectin–selectin ligand bonds and results in a shift from low affinity to intermediate affinity LFA-1^{165,176}. Interaction of intermediate affinity LFA-1 with ICAM-1 decelerates rolling neutrophils. Chemokine recognition by GPCRs and subsequent downstream signaling further increase $[\text{Ca}^{2+}]_i$ ^{165,177} (Fig. 1.5-B). In

addition, DAG activates β_2 -integrins via protein kinase C (PKC)¹⁷⁸. Outside-in signaling mediated by LFA-1 and ICAM-1 contributes to the increase of $[Ca^{2+}]_i$, again in a shear force dependent manner^{158,176}.

All these inside-out and outside-in signaling events, amplified by mechano-transduction lead to ER Ca^{2+} -store depletion and CRAC channel dependent Ca^{2+} influx. Tensile forces, acting on LFA-1 bonds enhance binding of kindlin-3 to β_2 -integrin tails and concomitant recruitment of Orai1 to adhesion spots^{179,180}. Clustering of LFA-1, kindlin-3 and Orai1 locally increases $[Ca^{2+}]_i$, facilitating the recruitment of talin-1, thereby linking the cytoskeleton to the focal adhesion spots and mediating adhesion strengthening and neutrophil polarization (Fig. 1.5-C).

1.3.3. Additional ion channels in Ca^{2+} signaling – The voltage gated potassium channel $K_V1.3$

Although Orai1 is the predominant Ca^{2+} channel mediating Ca^{2+} influx into activated neutrophils, numerous additional ion channels have been shown to be involved in the regulation of $[Ca^{2+}]_i$ in immune cells^{156,158}, among them the voltage gated potassium channel $K_V1.3$ ¹⁸¹. $K_V1.3$ channels are tetramers, consisting of 6 transmembrane helices which are expressed in immune cells, vascular smooth muscle cells and cells of the nervous system¹⁸². The role of $K_V1.3$ in immune cells has mainly been addressed in T lymphocytes¹⁸³, where it regulates Ca^{2+} influx via K^+ efflux¹⁵⁶. Activation of T lymphocytes by T cell receptors (TCR) or GPCRs activates $PLC\gamma$ or $PLC\beta$, respectively, which convert PIP_2 into DAG and IP_3 ¹⁸⁴ (Fig. 1.6). IP_3 - IP_3R interaction initiates the release of ER stored Ca^{2+} and STIM1 mediated activation of CRAC channels. Both, ER Ca^{2+} store depletion and influx of extracellular Ca^{2+} depolarize the PM and open the voltage sensitive K^+ channel $K_V1.3$ ¹⁸³. K^+ efflux hyperpolarizes the PM and maintains a high electrical gradient for cations to enter the cell, thereby sustaining Ca^{2+} influx through CRAC channels¹⁸¹.

$K_V1.3$ is also expressed on B lymphocytes¹⁸⁵, NK cells¹⁸⁶, macrophages¹⁸⁷, megakaryocytes/platelets¹⁸⁸, and DCs¹⁸⁹. There is one controversial report about $K_V1.3$ in neutrophils¹⁹⁰, however, data about its function in this cell type do so far not exist.

1.4. Aim of the thesis

Throughout pregnancy, immune cells colonize the placenta and fulfill important functions, necessary for successful embryonic development. Different mechanisms have evolved that ensure immune cell functions in close proximity to the fetus without initialization of immune responses against the unborn. Nevertheless, immune cell regulation during pregnancy is still incomplete understood.

Preimplantation factor (PIF) is a small peptide secreted by trophoblast cells and detectable in maternal circulation during pregnancy. PIF has been shown to modulate immune cell function in animal models of autoimmune diseases, but the underlying mechanisms how PIF interferes with immune cells are not known. Therefore, this study aimed to investigate how

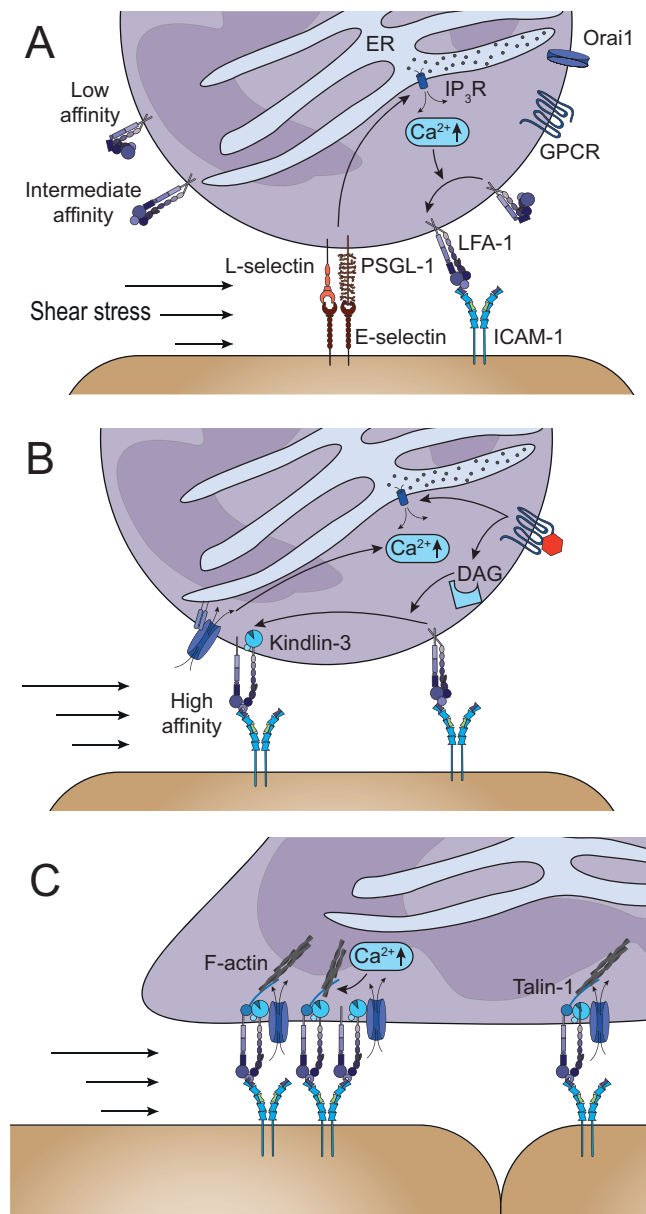


Figure 1.5.: Ca^{2+} signaling synchronizes neutrophil adhesion under flow. (A) E-selectin dependent neutrophil rolling induces release of ER stored Ca^{2+} by downstream signaling of E-selectin ligands PSGL-1 and L-selectin (humans), amplified by shear forces acting on selectin–selectin ligand bonds. Increase in $[Ca^{2+}]_i$ shifts bent, low affinity LFA-1 integrins to the intermediate state, allowing interaction with endothelial expressed ICAM-1, followed by deceleration of rolling neutrophils. (B) Activation of GPCRs support ER Ca^{2+} store depletion and CRAC channel mediated influx of extracellular Ca^{2+} . Increase in $[Ca^{2+}]_i$ together with DAG signaling fully activate LFA-1 integrins, leading to full arrest of the cells. Tensile forces acting on LFA-1–ICAM-1 bonds recruit kindlin-3, which in turn recruits Orai1, resulting in formation of a complex that ensures high Ca^{2+} concentrations directly at adhesion spots. (C) Talin-1 gets recruited in a Ca^{2+} dependent manner, linking the adhesion sites to the cytoskeleton, thereby enabling neutrophil spreading and polarization (modified from¹⁵⁸).

PIF interferes with innate immune cells during acute inflammatory processes outside the context of pregnancy, thereby altering neutrophil recruitment to sites of inflammation. The

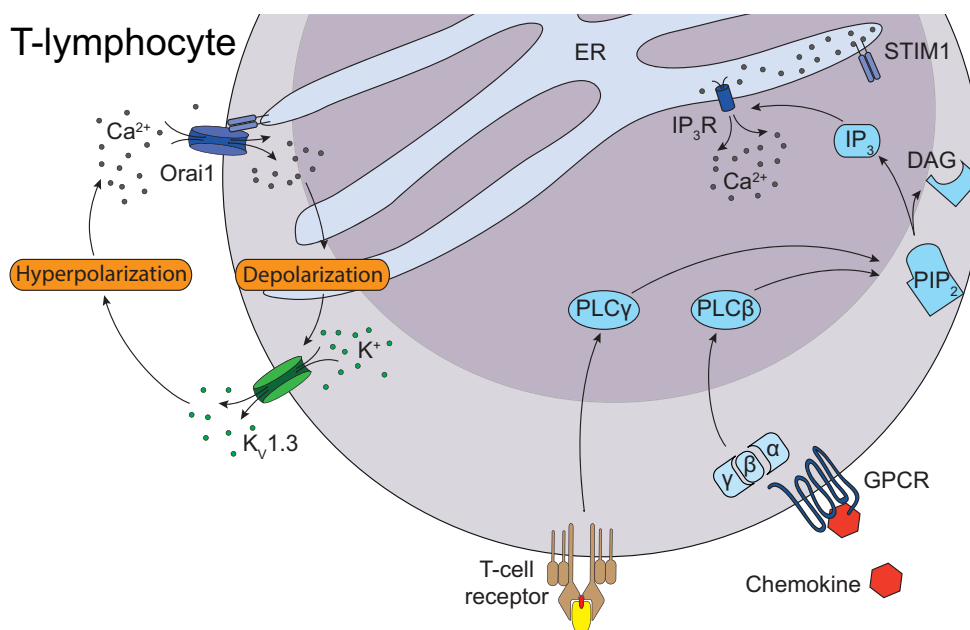


Figure 1.6.: $K_v1.3$ signaling in immune cells. Activation of T-lymphocytes via T-cell receptors or GPCRs results in the release of ER stored- Ca^{2+} and subsequent Ca^{2+} influx via CRAC channels. Increase of $[Ca^{2+}]_i$ depolarizes the cell membrane and opens the voltage gated potassium channel $K_v1.3$. K^+ efflux leads to a hyperpolarization and allows further Ca^{2+} influx, thereby maintaining high $[Ca^{2+}]_i$.

work wanted to elucidate underlying molecular mechanism, helping to better understand its biological function in maternal serum and in the placenta and highlighting its potential as an anti-inflammatory drug in diverse inflammatory disorders.

Therefore, the aims of this work include:

- to investigate which steps of the neutrophil recruitment cascade are affected by PIF
- to uncover which cellular compartment (neutrophils and/or endothelium) is the target of PIF
- to identify the cellular interaction partner of PIF on neutrophils
- to elucidate downstream signaling events of PIF- $K_v1.3$ engagement.

2. Materials

2.1. Animals

C57BL/6 wildtype (WT) mice were purchased from Charles River Laboratories (Sulzfeld, Germany) and Janvier Labs (Saint Berthevin, France), *Kcna3^{tm1Lys}* (*Kv1.3^{-/-}*) mice¹⁹¹ were obtained from Jackson Laboratories. All mice were maintained at the Walter Brendel Center for Experimental Medicine, LMU, Munich, or at the Biomedical Center, LMU, Planegg-Martinsried. *Kv1.3^{-/-}* mice were back-crossed inhouse into C57BL/6 background. 8-25 weeks old female and male mice were used for experiments. The conducted experiments were approved by the government of Oberbayern, Germany, AZ 55.2-1-54-2531-122/12, -229/15 and ROB-55.2-2532.Vet_02-18-22.

2.2. Human blood samples

Human blood samples were taken from healthy male and female volunteers. Blood sampling was approved by the ethical committee from the Ludwig-Maximilians-Universität München, Munich, Germany (Az.611-15).

2.3. Recombinant proteins

Table 2.1.: Used recombinant proteins. rm: recombinant mouse, Fc: linked human Fc part at the N-terminus, rh: recombinant human.

Name	Supplier
PIF	BioIncept LLC.
scrambledPIF (scrPIF)	BioIncept LLC.
PIF homolog (H-PIF)	Bachem
rmTNF- α	R&D Systems
rmCXCL1	Peprtech
rmP-selectin/Fc	R&D Systems
rmE-selectin/Fc	R&D Systems
rmICAM-1/Fc	R&D Systems
rhE-selectin/Fc	R&D Systems
rhICAM-1	R&D Systems
rhCXCL8	Peprtech

2.4. Chemicals, reagents, important items

Table 2.2.: Used chemicals, reagents and important items. m: murine, h: human

Name	Supplier	Name	Supplier
Ketamine	Pharmacia GmbH	Glass capillaries (0.04x0.4)	CM Scientific
Xylazine	Bayer	Glass capillaries (0.2x2.0)	CM Scientific
Catheter tube	Smith medical	Lysing solution	BD
DMSO	Sigma-Aldrich	EDTA	Merck
Transwells	Corning	Object slides (removable)	Ibidi
Paraformaldehyde	Applichem	Poly-L-lysine	Sigma-Aldrich
Giemsa	Merck	DAPI	Invitrogen
Eukitt	Sigma-Aldrich	ProLong Antifade	Thermo Fisher
EGTA	Carl Roth	Triton X-100	Applichem
Percoll	Sigma-Aldrich	Sodium deoxycholate	Sigma-Aldrich
BSA	Capricorn Scientific	Tris-HCL	Merck
Hepes	Sigma-Aldrich	Protease inhibitors	Sigma-Aldrich
PMN enrichment kit (m&h)	Stemcell	Phosphatase inhibitors	Roche
Polymorphprep	Axi-Shield PoC	PVDF membrane	Immobilon
RPMI 1640	Sigma-Aldrich	Blocking solution	LI-COR
Penicillin	Invitrogen	Patch pipettes	Science Products
Streptomycine	Invitrogen	PAP-1	Sigma-Aldrich
FCS	Invitrogen	TRAM-34	abcam
Casein	Sigma-Aldrich	Flow-Count Fluospheres	Beckman Coulter

2.5. Software

Table 2.3.: Used software.

Name	Distributor
VirtualDub (1.9.11)	GNU General Public License
ImageJ ¹⁹²	National Institute of Health
MtrackJ ¹⁹³ (ImageJ plugin)	Eric Meijering
Kaluza (1.5)	Beckman Coulter
FlowJo (10.4)	Treestar
Leica Application Suites	Leica
IgorPro6	WaveMetrics
Patchmaster	HEKA Elektronik
GraphPad Prism 7	Graphpad software
Adobe Illustrator (CS6)	Adobe

2.6. Antibodies

Table 2.4.: Used antibodies. FITC: fluorescein isothiocyanate, APC: allophycocyanin, BV: brilliant violet, PE: phycoerythrin, PB: pacific blue.

Antigen	Dye	Reactivity	Clone	Supplier
E-selectin (CD62E)	-	rat α -mouse	9A9	Invivo
P-selectin (CD62P)	-	rat α -mouse	RB40.34	Invivo
β_2 (CD18)	FITC	rat α -mouse	C71/16	Pharmlingen
LFA-1 (CD11a)	APC	rat α -mouse	M17/4	eBioscience
Mac-1 (CD11b)	BV570	rat α -mouse	M1/70	BioLegend
PSGL-1 (CD162)	PE	rat α -mouse	2PH1	Pharmlingen
CD44	BV570	rat α -mouse	IM7	Biolegend
L-selectin (CD62L)	FITC	rat α -mouse	MEL-14	BioLegend
CXCR2 (CD182)	APC	rat α -mouse	242216	R&D Systems
Ly6G	PB	rat α -mouse	1A8	BioLegend
Fc block CD16/CD32	-	rat α -mouse	93	BioLegend
Fc γ	biotin	goat α -human	polyclonal	eBioscience
Streptavidin	PerCP-Cy5.5	-	-	eBioscience
β_2 (CD18)	-	mouse α -human	KIM127	Invivo
β_2 (CD18)	-	mouse α -human	mAb24	Hycult biotech
LFA-1 (CD11a)	-	mouse α -human	HI111	BioLegend
Mac-1 (CD11b)	-	mouse α -human	ICRF44	BioLegend
CD15	FITC	mouse α -human	HI98	BioLegend
CD66b	PB	mouse α -human	G10F5	BioLegend
K γ 1.3	-	rabbit α -	polyclonal	Alomone labs
GAPDH	-	mouse α -	6C5	Calbiochem
Secondary	PE	goat α -mouse	-	Pharmlingen
Secondary	Alexa488	donkey α -rabbit	-	Invitrogen
Secondary	IRDye800CW	goat α -rabbit	-	LI-COR
Secondary	IRDye680RD	goat α -mouse	-	LI-COR
IgG _{2a} -isotype	FITC	rat α -mouse	-	eBioscience
IgG _{2a} -isotype	APC	rat α -mouse	RTK2758	BioLegend
IgG _{2b} -isotype	BV570	rat α -mouse	RTK5430	BioLegend
IgG _{1b} -isotype	PE	rat α -mouse	-	life technologies
IgG ₁ -isotype	-	mouse α -human	11711	R&D Systems

3. Methods

3.1. Intravital microscopy of the mouse cremaster muscle

Intravital microscopy (IVM) of the mouse cremaster muscle was performed as previously described¹⁵⁰. Briefly, male mice were anesthetized by an intraperitoneal (i.p.) injection of ketamine/xylazine (125 mg/kg body weight ketamine and 12.5 mg/kg body weight xylazine in a volume of 0.1 ml/8 g body weight). The trachea was cannulated to ensure sufficient breathing during image acquisition. The right carotid artery was cannulated using a plastic tube (outer and inner tube diameter: OD: 0.61 mm, ID: 0.28 mm) as well for later blood sampling (using a ProCyte Dx; IDEXX Laboratories) or antibody administration. The cremaster muscle was dissected, mounted and constantly superfused with a thermo-controlled bicarbonate buffer^{194,195} throughout the entire experiment. IVM was carried out on an Olympus BX51 WI microscope, equipped with a 40x objective (Olympus, 0.8NA, water immersion objective) and a CCD camera (KAPPA CF 8 HS). Postcapillary venules were recorded using VirtualDub and blood flow velocity of each venule was determined with the help of a dual photodiode (Circusoft Instrumentation). Movie sequences were analyzed off-line with ImageJ software^{192,193}. Different approaches were used to study leukocyte recruitment *in vivo* in the mouse cremaster muscle, reflecting different inflammatory scenarios.

3.1.1. TNF- α induced acute inflammation

Injection of TNF- α leads to strong inflammation, accompanied by transcriptional upregulation of many important adhesion molecules, among them E-selectin and ICAM-1⁹⁵. 1 h prior to induction of inflammation by intrascrotal injection (i.s.) of TNF- α (500 ng), WT or *Kv1.3*^{-/-} mice were i.s. injected with either 1 μ g PIF, a scrambled version of the peptide (scrPIF), a PIF homolog (H-PIF), 30 μ g PAP-1¹⁹⁶, a combination of PIF and PAP-1, carrier substance (Ctrl, 0.25% DMSO/PBS), or left untreated, respectively. 2 h after TNF- α stimulation, IVM was carried out. To study the different contributions of P- and E-selectin during leukocyte rolling in TNF- α inflamed cremaster muscles, selectin-blocking antibodies were applied via the carotid artery catheter during the experiments (α -E-selectin: clone: 9A9, 30 μ g; α -P-selectin: clone: RB40.34, 30 μ g).

3.1.2. Perivascular neutrophils in TNF- α induced acute inflammation

After IVM, cremaster muscles were removed and fixed with 4% paraformaldehyde (PFA), stained with Giemsa and mounted (Eukitt) to investigate leukocyte extravasation. Analysis was conducted at the core facility Bioimaging of the Biomedical Center with a Leica DM2500

microscope, equipped with a 100x objective (Leica, 1.4NA, oil immersion) and a Leica DMC2900 CMOS camera.

3.1.3. Trauma induced acute inflammation

Surgical preparation of the cremaster muscle alone results in a rapid release of P-selectin out of Weibel-Palade bodies and subsequent P-selectin dependent leukocyte rolling along postcapillary venules⁹¹. To study the effects of PIF in this mild, trauma induced acute inflammatory setting, WT mice received either 1 µg PIF or scrPIF i.s. 2 h prior to IVM. During the experiment, P-selectin-blocking antibodies (30 µg) were applied via the carotid artery catheter to fully abrogate leukocyte rolling.

3.1.4. CXCL1 induced leukocyte adhesion

To analyze CXCL1 induced LFA-1 activation *in vivo*, either 1 µg PIF or scrPIF was applied to WT mice i.s. 2 h prior to IVM. Leukocyte adhesion was quantified before and after the administration of 600 ng CXCL1 via the carotid artery catheter in the same postcapillary venule.

3.2. Neutrophil isolation

3.2.1. Isolation of murine neutrophils

Femurs and tibiae of male and female mice were flushed with PBS through a cell strainer (grid size: 40 µm). Two different approaches were used to isolate neutrophils. For Percoll density gradient centrifugation, two percoll solutions with different densities (1.11 and 1.08 g/ml) were layered and the flushed bone marrow derived cells were added on top. After centrifugation at 1000 g for 30 min at room temperature (RT) without brakes, the neutrophil-containing cell layer was carefully taken and resuspended in Hanks Balanced Salt Solution (HBSS, containing 0.1% Glucose, 1 mM CaCl₂ and MgCl₂, 0.25% BSA and 10 mM Hepes, pH 7.4). As a second approach, neutrophils were isolated using EasySep neutrophil negative isolation kit according to the manufacturers protocol.

3.2.2. Isolation of human neutrophils

Blood was withdrawn from human healthy volunteer donors to isolate human neutrophils. Therefore, two different approaches were used. For density centrifugation, whole blood was added on a layer of Polymorphprep, centrifuged at 500 g for 30 min at RT without brakes and the neutrophil-containing cell layer was taken and resuspended in HBSS. Again, an EasySep neutrophil negative selection kit was used as an additional approach according to the manufacturers protocol.

3.3. Cultivation of Jurkat cells

Immortalized human T lymphocyte Jurkat cells were cultured in RPMI 1640 growth medium, supplemented with 10% FCS, penicillin and streptomycin (both 100 U/ml) at 37 °C in 5% CO₂. Cells were a kind gift from Dr. Susanna Zierler (Walther-Straub-Institute, LMU, Munich).

3.4. Flow chamber assays

To study the different steps of leukocyte recruitment in a more simplified scenario, small rectangular borosilicate glass capillaries were coated with different combinations of adhesion molecules to mimic the inflamed endothelium as previously described¹²⁰. Adhesion molecules were coated for 3 h at room temperature (RT) and blocked with 5% Casein/PBS over night (ON). Experiments were carried out on an OlympusBX51 WI microscope, equipped with a 20x objective (Olympus, 0.95NA, water immersion objective) and a CCD camera (KAPPA CF 8 HS). Leukocyte rolling, leukocyte adhesion and leukocyte rolling velocities were analyzed on the basis of the recorded movie sequences using ImageJ.

3.4.1. Selectin-dependent leukocyte rolling *in vitro*

Selectin-dependent leukocyte rolling was studied using E-selectin or P-selectin (both 20 µg/ml) coated flow chambers (0.04 x 0.4 mm). Whole blood of male and female WT mice was collected via the carotid artery catheter into heparinized tubes and incubated with 300 nM PIF, scrPIF or vehicle control (Ctrl) for 10 min at RT. Flow chambers were perfused with the pre-treated whole blood at a constant shear stress level of 2 dyne/cm² using a high precision syringe pump (Harvard Apparatus).

3.4.2. Leukocyte slow rolling and adhesion *in vitro*

To study leukocyte slow rolling velocities and adhesion *in vitro*, glass capillaries (0.04 x 0.4 mm) were coated with E-selectin (20 µg/ml), ICAM-1 (15 µg/ml) and CXCL1 (15 µg/ml). Whole blood from WT mice was again withdrawn via the carotid artery catheter into heparinized tubes, incubated with 300 nM PIF or vehicle control (Ctrl) and perfused through the flow chambers at a constant shear stress level of 2 dyne/cm² again using a high precision syringe pump.

3.4.3. Leukocyte slow rolling and adhesion *ex vivo*

Leukocyte adhesion and slow rolling was further investigated using *ex vivo* flow chambers. Therefore, capillaries (0.04 x 0.4 mm) were coated either with E-selectin, ICAM-1 and CXCL1, or with E-selectin and ICAM-1. Male WT mice pre-treated with an i.s. injection of either 1 µg

PIF or scrPIF were directly connected via the carotid artery catheter to the flow chamber.

3.4.4. Human neutrophil rolling and slow rolling *in vitro*

To study rolling and slow rolling in human neutrophils, glass capillaries (0.2 x 2.0 mm) were coated with E-selectin (5 µg/ml) alone or with a combination of E-selectin (5 µg/ml) and ICAM-1 (4 µg/ml). Human neutrophils were isolated using density centrifugation and incubated with either 100 nM PIF or scrPIF for 10 min at RT in HBSS and perfused through the microflow devices (10⁶/ml) at a constant shear stress level of 2 dyne/cm² using a high precision syringe pump. Movie sequences were recorded with a Zeiss Axioskop2 (provided with a 20x water objective, 0.5NA and a Hitachi KP-M1AP camera) and analyzed using ImageJ.

3.4.5. Neutrophil spreading *in vitro*

Spreading of human neutrophils was investigated in glass capillaries (0.2 x 2.0 mm) coated with E-selectin (5 µg/ml), ICAM-1 (4 µg/ml) and CXCL8 (10 µg/ml). Human neutrophils were isolated using density centrifugation and pre-treated with either 300 nM PIF, 10 nM PAP-1 or vehicle control (Ctrl) for 10 min at RT in HBSS. Cells (10⁶/ml) were then introduced into the chambers with a constant shear stress level of 1 dyne/cm² and changes in cell shape were recorded with a Zeiss Axioskop2 (provided with a 20x water objective, 0.5NA and a Hitachi KP-M1AP camera). Cell perimeter, circularity (defined as $4\pi \frac{[Area]}{[Perimeter]^2}$) and solidity (defined as $\frac{[Area]}{[ConvexArea]}$) were quantified using ImageJ.

3.5. Fluorescence activated cell sorting (FACS)

3.5.1. Surfacemarkers

Expression levels of surface molecules which are important for neutrophil rolling and adhesion were analyzed by flow cytometry¹⁵⁰. To do this, WT mice received an i.s. injection of 1 µg PIF or vehicle 2 h prior to exsanguination by retro-orbital puncture. In another set of experiments WT and *Kv1.3*^{-/-} mice were exsanguinated without prior injection. Whole blood was stained with antibodies against CD18 (β₂, clone C71/16), CD11a (LFA-1, clone M17/4), CD11b (Mac-1, clone M1/70), PSGL-1 (CD162, clone 2PH1), CD44 (clone IM7), L-selectin (CD62L, clone MEL-14), and CXCR2 (CD182, clone 242216; all 5 µg/µl) for 15 min at RT. α-Ly6G was used to define the neutrophil population (5 µg/µl, clone 1A8). Erythrocytes were lysed and cells were fixed using FACS lysing solution. Samples were analyzed with a Beckman Coulter Gallios flow cytometer and Kaluza Flow analysis Software.

3.5.2. Selectin binding

P- and E-selectin binding to neutrophils was performed as previously described¹⁹⁷. Briefly, WT mice received an i.s. injection of 1 µg PIF or scrPIF 2 h prior to exsanguination by retro-orbital puncture. Whole blood was incubated with a Fc-blocking antibody (α -CD16/CD32) for 15 min at 4 °C and rm selectin chimeras (recombinant peptide with a human IgG₁ part, 3.6 µg/sample) were pre-complexed for 10 min at RT with α -human Fc gamma-biotin. Cells were then incubated with pre-complexed selectins for 50 min at 4 °C, fixed with FACS lysing solution and further stained with fluorescent labeled streptavidin. As control, incubation was carried out in the presence of EDTA (10 mM) to chelate Ca²⁺ which is required for selectin-selectin ligand interaction. α -Ly6G was used to define the neutrophil population. Samples were analyzed with a Beckman Coulter Gallios flow cytometer and Kaluza Flow analysis Software.

3.5.3. Soluble ICAM-1 binding

Binding of soluble ICAM-1 to activated neutrophils was carried out as described recently¹²⁴. Bone marrow derived neutrophils from WT mice were isolated using Percoll density gradient centrifugation and resuspended in HBSS buffer and incubated with 300 nM PIF or scrPIF for 10 min at RT. ICAM-1 (40 µg/ml, with a human IgG₁ part) was pre-complexed for 10 min at RT with α -human Fc gamma-biotin and fluorescent labeled streptavidin and added to the cells (1.5x10⁶/sample) for 3 min at 37 °C together with CXCL1 (10 nM). Stimulation was stopped by adding ice-cold FACS lysing solution to the cells. α -Ly6G was used to define the neutrophil population. Samples were analyzed with a Beckman Coulter Gallios flow cytometer and Kaluza Flow analysis Software.

3.5.4. LFA-1 activation

LFA-1 activation assay was performed as previously described¹²⁰. Human neutrophils were isolated using Polymorphprep and incubated with 100 nM PIF or scrPIF for 10 min at RT. Cells (5x10⁵/sample) were activated with CXCL8 (10 nM) in the presence of either KIM127- or mAb24-antibody for 5 min at 37 °C, both detecting intermediate and high affinity (KIM127, 10 µg/µl) or high affinity LFA-1 only (mAb24, 10 µg/µl)¹¹² (Fig. 3.1). Stimulation was stopped by adding ice-cold FACS lysing solution to the cells. α -CD15 (clone W6D3, 5 µg/µl) and α -CD66b (clone G10M5, 5 µg/µl) was used to define human neutrophil population. Samples were analyzed with a Beckman Coulter Gallios flow cytometer and Kaluza Flow analysis Software.

3.5.5. K_v1.3 expression

Human and murine neutrophils were isolated using density centrifugation (Polymorphprep and Percoll respectively) and stained for 30 min with an α -K_v1.3 antibody (polyclonal, 10 µg/µl). Secondary antibody (donkey α -rabbit-Alexa488, 5 µg/µl) was added for 15 min

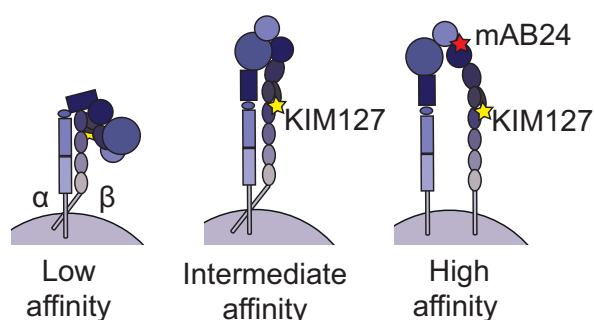


Figure 3.1.: Detection of different LFA-1 affinity states. KIM127 and mAB24 bind to distinct epitopes on the β_2 integrin subunit, serving as markers for integrin activation (α : α -subunit, β : β -subunit)¹¹².

at RT. Jurkat cells were used as control. Samples were analyzed with a Beckman Coulter Gallios flow cytometer and Kaluza Flow analysis Software. Neutrophils were assigned to Ly6G-positive and CD15-, CD66b-double-positive populations, respectively.

3.6. Confocal microscopy

Murine and human neutrophils were isolated using density gradient centrifugation and allowed to attach on poly-L-lysine (0.1%) coated object slides for 15 min. After fixation with 2% PFA for 10 min and blocking with 2% BSA for 1 h at RT, cells were stained ON at 4 °C using α -K_v1.3 antibody (polyclonal, rabbit, 5 μ g/ μ l). Alexa488 coupled donkey α -rabbit (5 μ g/ μ l) was added for 1 h at RT before cell nuclei were stained with DAPI for 5 min at RT. Samples were embedded in ProLong Diamond antifade mounting medium and imaged at the Core facility Bioimaging of the Biomedical Center with a Leica SP8X WLL microscope, equipped with a HC PL APO 40x/1.30NA oil immersion objective. Images were processed (including removal of outliers and background subtraction in the 488 channel) using ImageJ.

3.7. Western blot

Murine and human neutrophils were isolated using the respective neutrophil enrichment kit, lysed (10⁶ cells/100 μ l), homogenized with modified RIPA lysis buffer (150 mM NaCl, 1% Triton X-100, 0.5% Sodium deoxycholate, 50 mM Tris-HCl pH 7.3, 2 mM EDTA, supplemented with protease and phosphatase inhibitors and 1xLaemmli sample buffer) and boiled for 5 min at 95 °C. Jurkat cells were used as positive control. Proteins were resolved by 12% SDS-PAGE and electrophoretically transferred onto PVDF membranes. After blocking, membranes were incubated with rabbit α -K_v1.3 (3 μ g/ μ l) and mouse α -GAPDH (clone 6C5, 1.5 μ g/ μ l) at 4 °C ON. Secondary antibodies (goat α -rabbit-IRDye 800CW and goat α -mouse-IRDye 680RD) were added for 1 h at RT. An Odyssey CLx (LI-COR Bioscience) was used for detection.

3.8. Patch clamp of isolated human neutrophils

Human neutrophils were isolated using neutrophil negative selection kit and resuspended in HBSS. For patch clamp experiments in whole-cell configuration, neutrophils were seeded on poly-D-lysine coated cover slips in standard extracellular solution (containing 140 mM NaCl, 2.8 mM KCl, 2 mM MgCl₂, 1 mM CaCl₂, 10 mM HEPES, 11 mM glucose, pH7.2, 300 mOsm). Borosilicate glass patch pipettes with a resistance of 2–3.5 MΩ were filled with intracellular solution (containing: 134 mM KF, 2 mM MgCl₂, 1 mM CaCl₂, 10 mM HEPES, 10 mM EGTA, pH7.2, 300 mOsm). Solutions were adjusted to 300 mOsm using a Vapro 5520 osmometer (Wescor Inc). Cells were clamped at holding potentials of –80 mV intermitted by repeated 200 ms voltage steps from –80 mV to +40 mV using a 10 mV interval applied every 30 s. Current maxima at +40 mV were used for the calculation of K_V1.3 current amplitudes. Currents were normalized to cell size as current densities in pA/pF. Capacitance was measured using the automated capacitance cancellation function of the EPC-10 (HEKA, Harvard Bioscience). 300 nM PIF, 10 nM PAP-1, 1 μM TRAM-34 or carrier substance (Ctrl) were either added to the bath solution at least 15 min prior to electrophysiological recordings or directly applied via an application pipette using constant pressure. Experiments were analyzed using IgorPro6 software.

3.9. Transwell assay

Bone marrow derived murine neutrophils were isolated using EasySep neutrophil enrichment kit and resuspended in HBSS. Cells were incubated with 300 nM PIF or scrPIF or carrier substance for 10 min at RT. 3x10⁵ cells in 100 μl HBSS were added into the upper compartment and transmigration through the transwells (pore size 5 μm) was induced by adding CXCL1 (in HBSS, 1 ng/ml or 10 ng/ml) into the lower compartment. Cells were allowed to migrate for 45 min at 37 °C. Cells in the lower compartment were collected and quantified with a Beckman Coulter Gallios flow cytometer and Kaluza Flow analysis Software. α-Ly6G was again used to define the neutrophil population and Flow-Count Fluorospheres were used to count the cells.

3.10. Electric Cell-Substrate Impedance Sensing (ECIS)

Endothelial electric resistance was measured using a electrical impedance system (ECIS 1600R; Applied BioPhysics). Human umbilical vein endothelial cells (HUVECs) from passage 1 or 2 were grown to confluence on coated (Ibidi-treat) gold microelectrodes. Cells were stimulated with 10 ng/μl TNF-α in the presence of either 300 nM PIF or carrier substance and electric resistance of the cell monolayer was measured over time. A control group was left untreated (w/o).

3.11. Statistical analysis

All data were analyzed and edited using GraphPad Prism 7 software and are depicted as either mean \pm SEM, cumulative frequencies, mean or representative images/traces. Statistical tests were carried out according to the number of groups being compared. For pairwise comparison, unpaired or paired student's t-test was used. For more than two groups, a 1-way or 2-way analysis of variance (ANOVA) with either Dunnett's (to compare experimental groups against control) or Turkey's (to compare all groups with each other) post-hoc test was carried out. P-values <0.05 were considered statistically significant and marked as follows: *: <0.05; **: <0.01; ***: <0.001.

4. Results

This project has emanated from my master's thesis (title: '*Analysis of potential immunomodulatory effects of PreImplantation factor (PIF) on leukocyte recruitment*' at the faculty of Biology, LMU Munich, 2013). Results in Fig. 4.1-A, Fig. 4.2-A, Fig. 4.14-B, Fig. 4.18, and in Fig. 4.20-B are based on experiments carried out during this period.

Major part of the present work has been assembled to a manuscript (see part IV) which will be submitted soon to *Science Immunology* for peer review.

4.1. PIF disrupts neutrophil adhesion by reducing K_v1.3-regulated SOCE

4.1.1. PIF impairs leukocyte adhesion *in vivo*, *ex vivo* and *in vitro*

To investigate the influence of PIF on leukocyte adhesion in an acute inflammatory, predominantly neutrophil driven¹⁹⁸ setting, WT mice were i.s. injected with 1 µg PIF 1 h prior to stimulation with TNF-α. 2 h after injection of TNF-α, IVM of the mouse cremaster muscle was performed. As controls, either the carrier substance (Ctrl) or 1 µg of a scrambled version of the peptide (scrPIF) was applied. In addition, another experimental group received 1 µg of PIF obtained from a different manufacturer (homologous-PIF; H-PIF). Both, administration of PIF and H-PIF resulted in significantly reduced numbers of adherent leukocytes to inflamed postcapillary venules (Fig. 4.1-A). Importantly, administration of PIF or H-PIF did not alter systemic white blood cell counts (WBC) compared to controls (Tab. 4.1).

To discriminate between the contribution of the endothelial and the hematopoietic compartment to the observed phenotype *in vivo*, *in vitro* flow chamber assays were carried out. To do this, small glass capillaries were coated with E-selectin, ICAM-1 and CXCL1 to mimic inflamed endothelium. Whole blood from WT mice was incubated with 300 nM PIF or carrier substance (Ctrl) and perfused through the microfluidic devices at a constant shear stress level of 2 dyne/cm². Numbers of adherent leukocytes on the coated glass surface were significantly decreased in the presence of PIF compared to control (Fig. 4.1-B), indicating that the observed reduction of leukocyte adhesion *in vivo* is predominantly mediated by a direct effect of PIF on leukocytes.

To further validate this assumption, WT mice were i.s. injected with 1 µg PIF or scrPIF and 2 h later directly connected to E-selectin, ICAM-1 and CXCL1 coated flow chambers via the carotid artery catheter. Indeed, i.s. application of PIF reduced number of adherent leukocytes in *ex vivo* flow chambers to a similar extent as *in vivo* and *in vitro* (Fig. 4.1-C). Of note, reduced leukocyte adhesion *in vitro* and *ex vivo* could not be attributed to differences in number of overall WBCs or cells per field of view (FOV) (Tab. 4.2). Taken together, PIF

4. Results

reduces leukocyte adhesion *in vivo* in TNF- α induced acute inflammation, an effect which may be primarily related to a direct impact of PIF on leukocytes, because the same reduction could be observed in *in vitro* and *ex vivo* flow chamber assays.

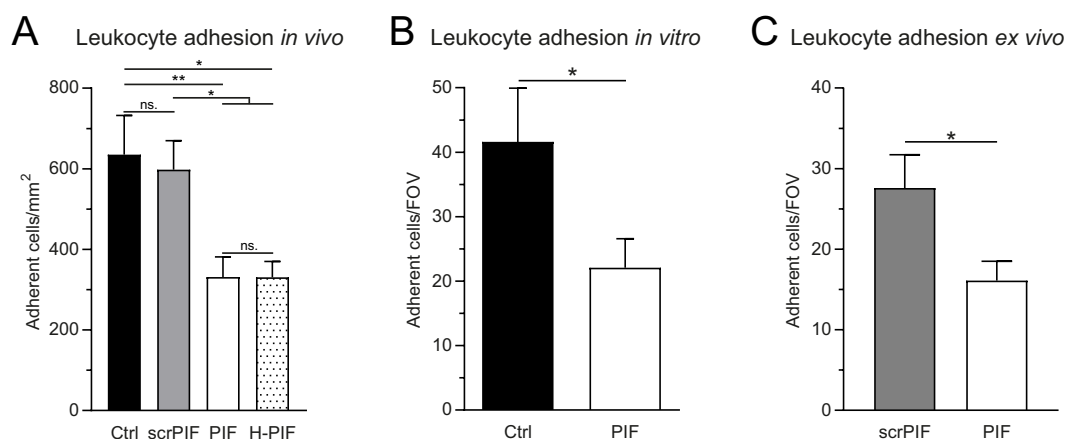


Figure 4.1.: PIF impairs leukocyte adhesion *in vivo*, *in vitro* and *ex vivo*. (A) Number of adherent leukocytes in TNF- α stimulated cremaster postcapillary venules of WT mice pre-treated with either vehicle control (Ctrl), scrPIF, PIF or H-PIF, respectively (mean \pm SEM, n=8-10 mice per group, 1-way ANOVA, Tukey's multiple comparison, ns.: not significant). (B) Number of adherent leukocytes in E-selectin, ICAM-1 and CXCL1 coated flow chambers perfused with whole blood from WT mice pre-incubated with either vehicle control (Ctrl) or PIF (mean \pm SEM, n=5 mice per group, unpaired student's t-test). (C) Number of adherent leukocytes in E-selectin, ICAM-1 and CXCL1 coated flow chambers auto-perfused with whole blood from WT mice pre-treated i.s. with either scrPIF or PIF (mean \pm SEM, n=5-6 mice per group, unpaired student's t-test).

Table 4.1.: Hemodynamic parameters of WT mice treated with TNF- α . Ven.: venules, \emptyset : vessel diameter, Syst. count: systemic white blood cell count (WBC). ns.: not significant (mean \pm SEM, 1-way ANOVA, Tukey's multiple comparison).

Treatment	Mice <i>n</i>	Ven. <i>n</i>	\emptyset [μ m]	Centerline velocity [μ m/s]	Shear rate [s ⁻¹]	Syst. count [cells/ μ l]
Ctrl	8	23	33 \pm 1	1565 \pm 115	1171 \pm 81	4033 \pm 364
scrPIF	8	24	33 \pm 1	1621 \pm 134	1199 \pm 85	4095 \pm 508
PIF	10	33	32 \pm 1	1652 \pm 142	1296 \pm 116	3969 \pm 339
H-PIF	8	23	31 \pm 1	1674 \pm 145	1326 \pm 121	3889 \pm 223
			ns. p=0.8872	ns. p=0.9556	ns. p=0.7081	ns. p=0.9832

4.1.2. PIF prevents leukocyte slow rolling *in vivo*, *ex vivo* and *in vitro*

Neutrophil adhesion in TNF- α stimulated post-capillary venules of the mouse cremaster muscle is predominantly mediated by the activated β_2 integrin LFA-1 on neutrophils and endothelium expressed ICAM-1¹⁹⁹. β_2 integrins further contribute to the deceleration of rolling leukocytes during their recruitment⁸⁷. To check whether reduced leukocyte adhesion is caused by altered β_2 integrin activation on leukocytes, leukocyte rolling velocities in

Table 4.2.: Number of mice, flow chambers, cells per FOV, and WBCs in *in vitro* and *ex vivo* flow chamber assays. WBC: white blood cell count, ns.: not significant (mean \pm SEM, unpaired student's t-test).

	Treatment	Mice <i>n</i>	Flow chambers <i>n</i>	WBC [cells/ μ l]	Cells FOV ⁻¹
<i>in vitro</i>	Ctrl	5	8	-	74 \pm 11
	PIF	5	10	-	88 \pm 21
					ns. p=0.6038
<i>ex vivo</i>	scrPIF	6	12	5608 \pm 632	34 \pm 5
	PIF	5	10	5125 \pm 362	25 \pm 4
					ns. ns. p=0.5375 p=0.1722

TNF- α stimulated venules of cremaster muscles were analyzed. Injection of PIF and H-PIF 1 h prior to induction of inflammation resulted in increased rolling velocities along the inflamed endothelium compared to controls (Fig. 4.2-A).

To demonstrate that increased slow rolling velocities are a consequence of direct interaction of PIF with leukocytes, flow chamber assays were performed to measure leukocyte slow rolling velocities *in vitro*. Incubation of murine whole blood with 300 nM PIF significantly increased rolling velocities in E-selectin, ICAM-1 and CXCL1 coated flow chambers compared to control treatment (Fig. 4.2-B). In line, *i.s.* injection of 1 μ g PIF 2 h prior to investigation significantly increased rolling velocities of leukocytes in E-selectin and ICAM-1 as well as in E-selectin, ICAM-1 and CXCL1 coated autoperfused flow chambers compared to control (Fig. 4.2,-C,-D). Additionally, rolling velocities of isolated human neutrophils were investigated in E-selectin and in E-selectin and ICAM-1 coated microfluidic devices. As expected, rolling velocities of control cells were significantly slower in E-selectin and ICAM-1 coated flow chambers compared to E-selectin coated chambers (Fig. 4.2-E). Incubation with 100 nM PIF in turn prevented neutrophil slow rolling on E-selectin and ICAM-1 substrate, whereas E-selectin dependent rolling velocities were not altered. In summary, analyses of leukocyte rolling velocities *in vivo*, *in vitro* and *ex vivo* revealed that leukocyte slow rolling is disturbed in the presence of PIF, suggesting altered β_2 integrin activity.

4.1.3. PIF does not change expression levels of adhesion relevant surface molecules on neutrophils

To exclude that different levels of adhesion relevant molecules on neutrophils are the reason for observed alterations in leukocyte interaction with inflamed endothelium, surface expression of CD18 (β_2 integrin subunit), CD11a (LFA-1), CD11b (Mac-1) and the GPCR CXCR2 were analyzed on peripheral blood neutrophils with or without pre-treatment with PIF. WT mice were *i.p.* injected with 1 μ g PIF or carrier substance (Ctrl) 2 h prior to retro-orbital exsanguination and subsequently analyzed by flow cytometry. Administration of PIF did not alter expression levels of investigated surface molecules compared to control (Fig. 4.3), demonstrating that the observed differences in adhesion and slow rolling cannot

4. Results

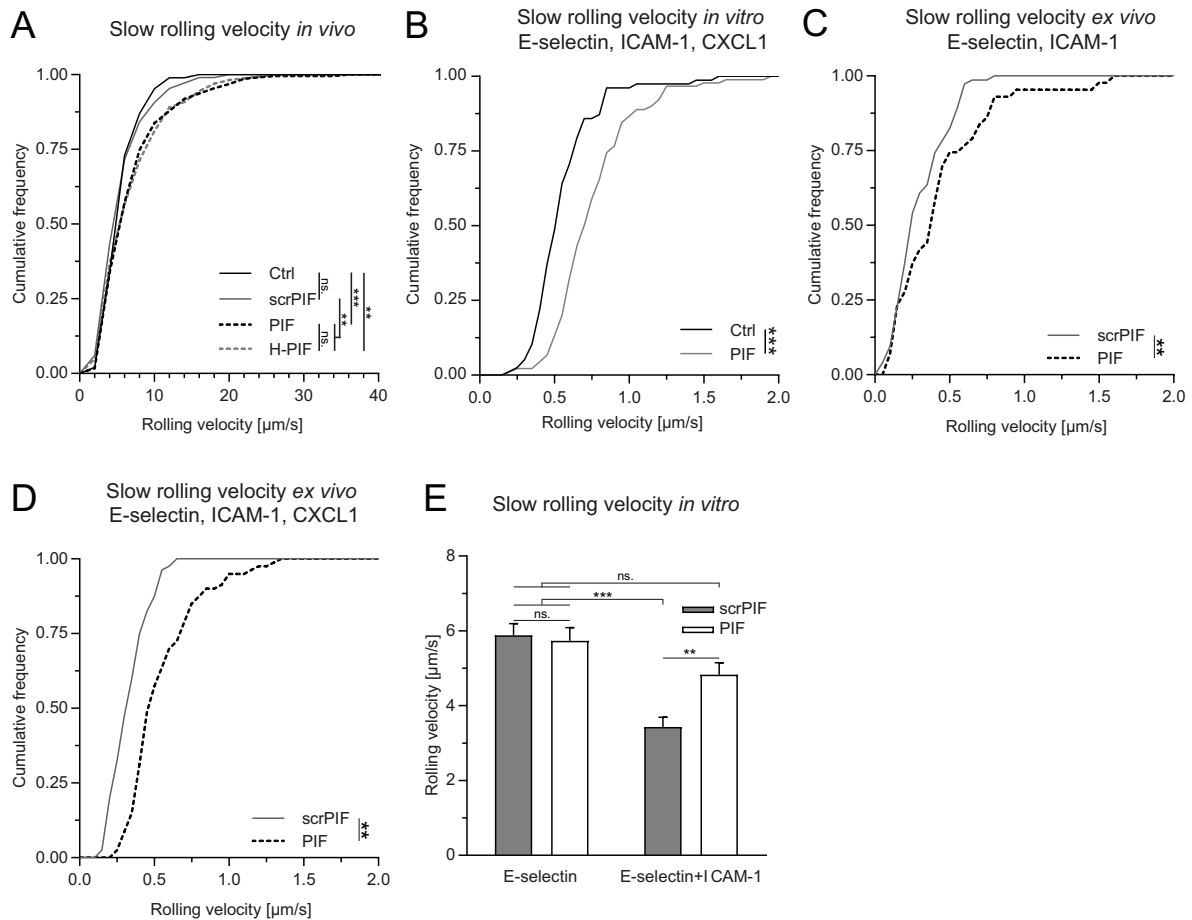


Figure 4.2.: PIF prevents leukocyte slow rolling *in vivo*, *ex vivo* and *in vitro*. (A) Leukocyte rolling velocities in postcapillary venules of TNF- α treated mouse cremaster muscles, injected i.s. with either PIF, H-PIF, scrPIF or carrier substance (Ctrl) 1 h prior to induction of inflammation (cumulative frequency, n= 192 (Ctrl), 215 (scrPIF), 222 (PIF), 164 (H-PIF) cells of 8-10 mice, 1-way ANOVA, Tukey's multiple comparison, ns.: not significant). (B) Leukocyte rolling velocities in E-selectin, ICAM-1 and CXCL1 coated flow chambers perfused with murine whole blood, pre-incubated with PIF or vehicle (Ctrl, cumulative frequency, n= 78 (Ctrl), 90 (PIF) cells of 5 mice per group, unpaired student's t-test). WT mice were i.s. injected with PIF or scrPIF and directly connected to microflow chambers 2 h after injection. Leukocyte rolling velocities were analyzed in (C) E-selectin and ICAM-1 (cumulative frequency, n= 80 (scrPIF), 80 (PIF) cells of 5-7 mice, unpaired student's t-test) and in (D) E-selectin, ICAM-1 and CXCL1 coated flow chambers (cumulative frequency, n= 74 (scrPIF), 43 (PIF) cells of 5-6 mice, unpaired student's t-test). (E) Rolling velocities of isolated human neutrophils on E-selectin and E-selectin and ICAM-1 coated flow chambers (mean \pm SEM, E-selectin: n= 50 (scrPIF), 50 (PIF) of 4-5 donors, E-selectin, ICAM-1: n= 60 (scrPIF), 60 (PIF) of 4 donors, 2-way ANOVA, Sidak's multiple comparison).

be attributed to altered expression of β_2 integrins or to different levels of CXCR2.

4.1.4. PIF does not alter β_2 integrin activation

Next, the influence of PIF on β_2 integrin activation was investigated by an ICAM-1 binding assay. For this, bone marrow derived murine neutrophils were stimulated with CXCL1 to induce GPCR mediated inside-out integrin activation and subsequent binding of integrins

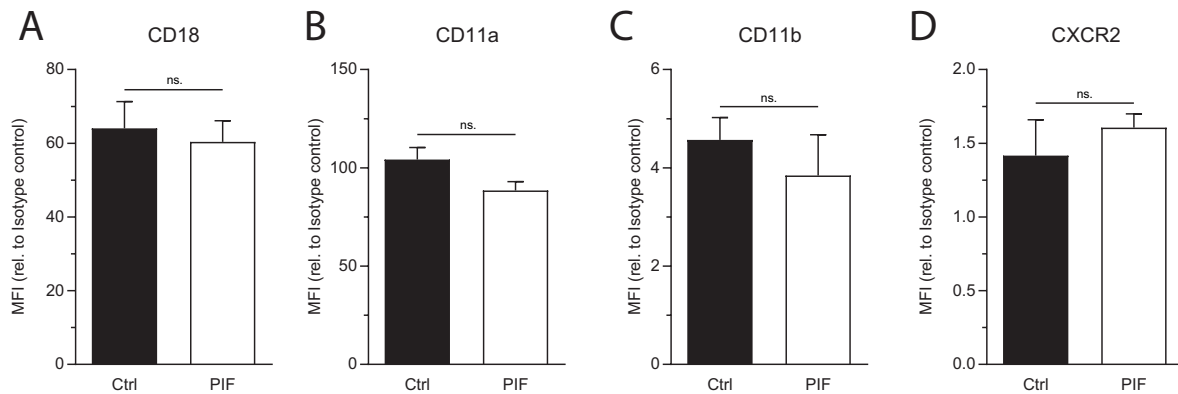


Figure 4.3.: PIF does not alter expression levels of adhesion relevant surface molecules on neutrophils. Surface expression levels of (A) CD18, (B) CD11a, (C) CD11b and (D) CXCR2 on peripheral blood neutrophils of WT mice injected i.p. with PIF or vehicle (Ctrl) (MFI= Mean fluorescence intensity, mean \pm SEM, n=3 mice per group, unpaired student's t-test, ns.: not significant).

to soluble ICAM-1. In this assay, binding of activated neutrophils to ICAM-1 is mainly mediated by LFA-1¹²⁴. Activation with CXCL1 increased the binding capacity of LFA-1 on control neutrophils to ICAM-1 (Fig. 4.4-A). Pre-incubation with 300 nM PIF did not significantly change this affinity, demonstrating that CXCL1 induced LFA-1 integrin activation is not affected by the presence of PIF.

In a second set of experiments, human neutrophils were used in order to study the different affinity states of LFA-1, the predominant β_2 integrin mediating neutrophil adhesion¹⁹⁹, in more detail. Isolated human neutrophils were incubated with 100 nM PIF or scrPIF and stimulated with CXCL8 in the presence of the LFA-1 binding antibodies KIM127 (recognizing the intermediate and fully activated β_2 integrin conformation) or mAB24 (recognizing exclusively the fully activated β_2 integrin conformation, see Fig. 3.1). Application of CXCL8 increased binding of KIM127 and mAB24 to control neutrophils, reflecting LFA-1 activation (Fig. 4.4-B,-C). No differences could be detected in PIF treated cells compared to control. In addition, overall LFA-1 and Mac-1 surface expression before and after CXCL8 incubation were monitored. In line with the previous experiments (Fig. 4.3), PIF did not change surface levels of LFA-1 and Mac-1 on human neutrophils (Fig. 4.4-D,-E). These results indicate that GPCR mediated inside-out signaling, leading to β_2 integrin activation in neutrophils, is not affected under static conditions by PIF.

4.1.5. $K_V1.3$ is expressed on human and murine neutrophils

Conducted experiments revealed that impaired leukocyte adhesion in the presence of PIF cannot be explained by an interference of PIF with β_2 integrin activation. Therefore, alternative pathways important for leukocyte adhesion were studied. Mass spectrometry analysis of decidua cells revealed a multitude of potential binding partners of PIF⁷⁰, but their functional relevance has not been addressed so far. One putative candidate PIF is proposed to interfere with, is the voltage gated potassium channel $K_V1.3$. $K_V1.3$ is expressed in vascular smooth muscle cells, in various cell types of the nervous system and in several immune cell sub-

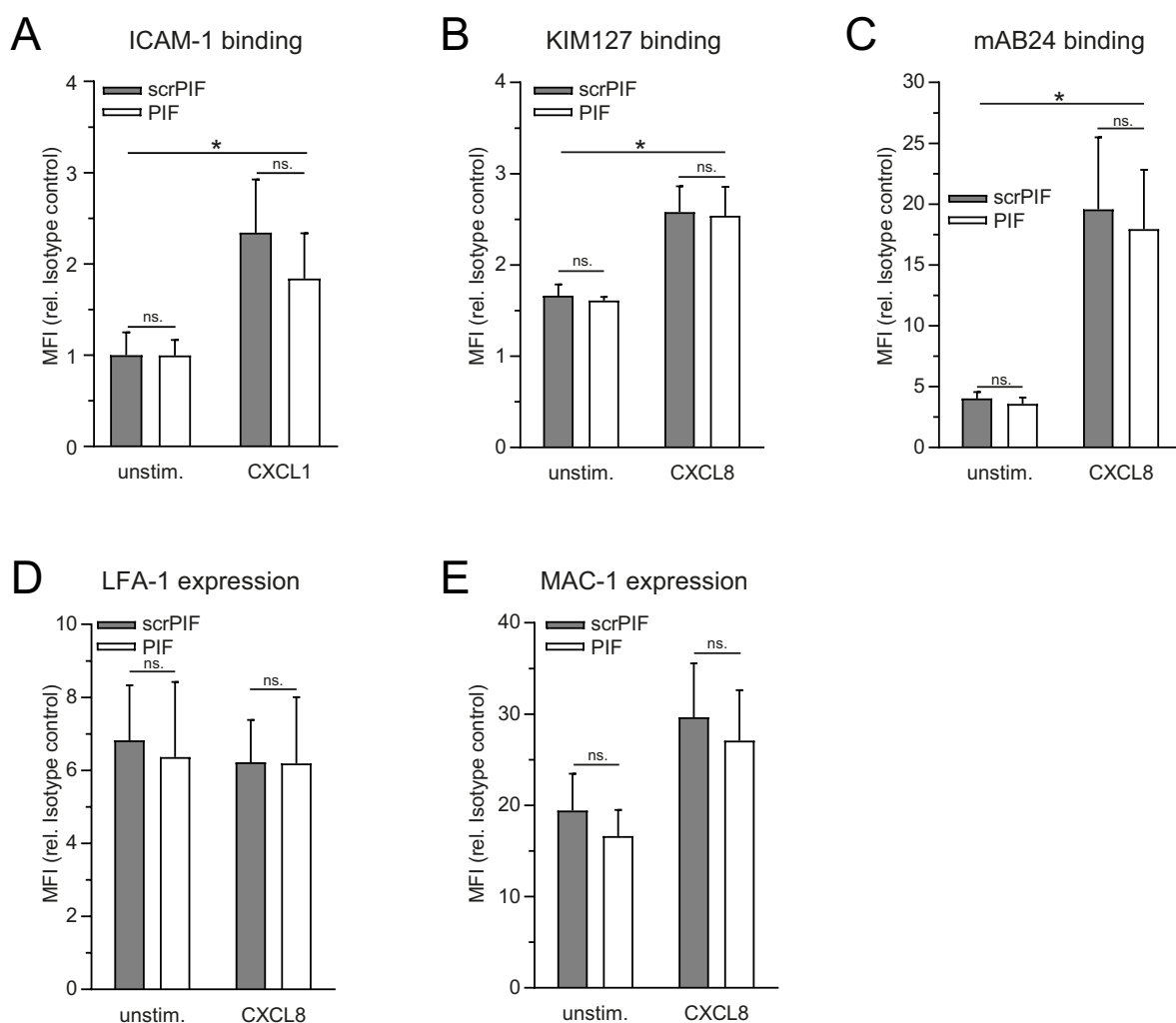


Figure 4.4.: PIF does not alter β_2 integrin activation. (A) CXCL1 induced binding capacity of bone marrow derived murine neutrophils pre-incubated with PIF or scrPIF to ICAM-1 (MFI= Mean fluorescence intensity, mean \pm SEM, n=4 mice per group, 2-way repeated measurements ANOVA, repeated Sidak's multiple comparison). (B) KIM127 and (C) mAB24 binding to human neutrophils pre-treated with PIF or scrPIF and stimulated with CXCL8. (D) Total LFA-1 and (E) total Mac-1 expression of human neutrophils before and after stimulation with CXCL8 (mean \pm SEM, n=3, 2-way repeated measurements ANOVA, repeated Sidak's multiple comparison, ns.: not significant).

sets¹⁸². In lymphocytes, it was shown to interfere with β_1 integrin function²⁰⁰. Expression of $K_V1.3$ on neutrophils is controversial, since only one publication reported the presence of the K^+ channel on human neutrophils¹⁹⁰ and functional data is lacking completely.

$K_V1.3$ expression on neutrophils was assessed by western blot (Fig. 4.5-A), revealing expression on both, human and murine neutrophils. Jurkat cells, which are known to express $K_V1.3$ ²⁰¹, were used as a positive control. Immune fluorescence stainings analyzed by confocal microscopy and flow cytometry demonstrated surface location of $K_V1.3$ on human and murine neutrophils (Fig. 4.5-B and 4.5-C).

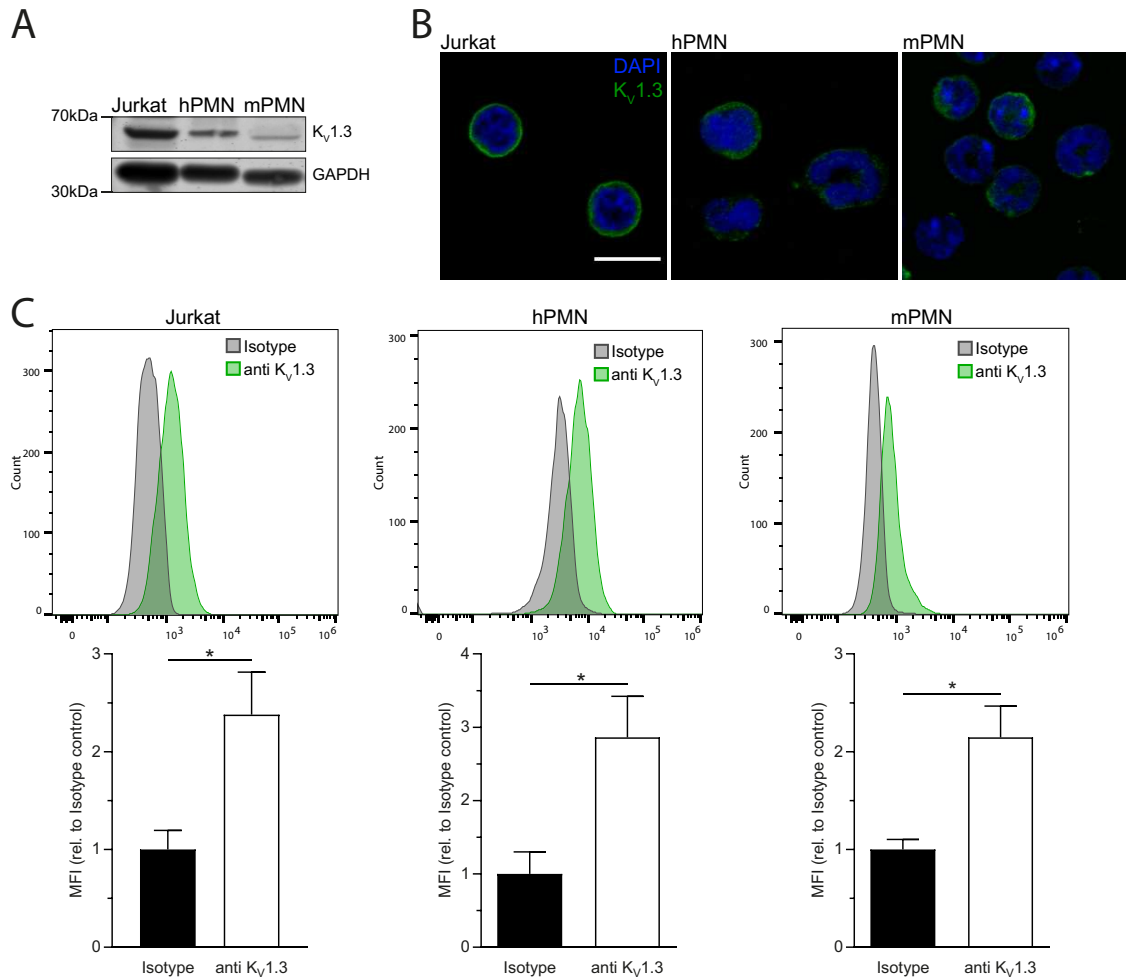


Figure 4.5: $K_V1.3$ is expressed on human and murine neutrophils. (A) Total $K_V1.3$ and GAPDH (loading control) protein levels of human (hPMN) and murine neutrophils (mPMN). Jurkat cell lysates served as positive control (representative blot; $n=3$). (B) Representative confocal micrographs of Jurkat cells, hPMNs and mPMNs stained for $K_V1.3$ (scale bar: 10 μm ; $n=3$ independent experiments). (C) Surface expression of $K_V1.3$ analyzed by flow cytometry (representative overlays (upper panel) and quantification (lower panel); MFI= Mean fluorescence intensity; mean \pm SEM, $n=3-4$, unpaired student's t-test).

4.1.6. $K_V1.3$ on human neutrophils is functional

Whole cell patch clamp technique was used to validate the electrophysiological functionality of $K_V1.3$ on neutrophils. Isolated human neutrophils seeded on poly-D-lysine coated cover slips were activated with a 10 mV step protocol ranging from -80 mV to $+40$ mV at a holding potential of -80 mV with 30 s intervals²⁰² to induce voltage activated potassium currents. Control cells exhibited a typical voltage dependent increase of currents²⁰³, (Fig. 4.6-A) which was reduced by pre-incubation of the cells with the $K_V1.3$ -specific inhibitor 5-(4-Phenoxybutoxy)psoralen (PAP-1, 10 nM)¹⁹⁶ (Fig. 4.6-B). In addition, $K_V1.3$ -currents were activated with a single voltage-step up to $+40$ mV before and after direct and local application of PAP-1. Again, PAP-1 reduced potassium currents (Fig. 4.6-C), demonstrating

expression of functional $K_V1.3$ on primary human neutrophils.

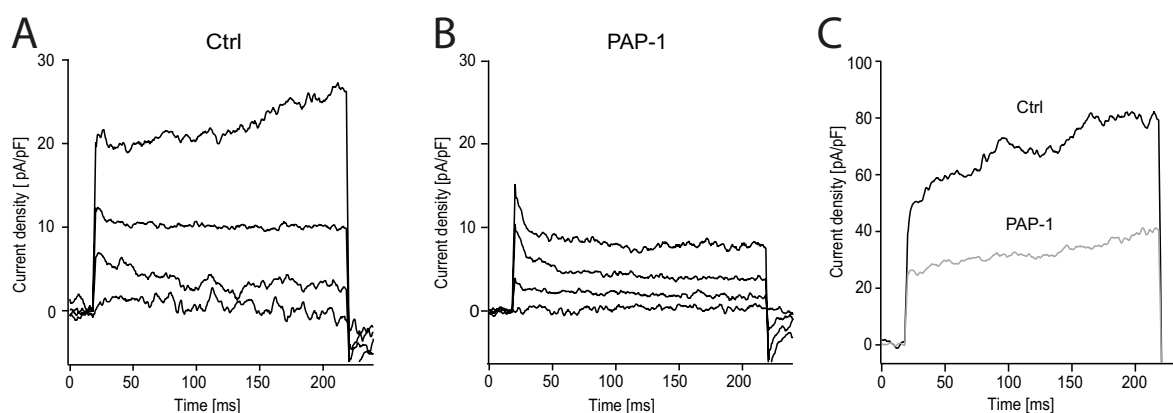


Figure 4.6.: $K_V1.3$ on human neutrophils is functional. Voltage-activated potassium currents induced by application of consecutive 10 mV steps from -80 mV to $+40$ mV in (A) control and in (B) PAP-1 pre-treated neutrophils (representative traces no. 1, 4, 8, 13; $n=10$ cells per group). (C) Potassium currents in human neutrophils before (black) and after direct application of PAP-1 (grey) after current activation with a single voltage-step from the holding-potential of -80 mV to $+40$ mV (representative traces; $n=4$ cells).

4.1.7. Genetic deletion and inhibition of $K_V1.3$ impairs leukocyte adhesion *in vivo*

To elucidate whether genetic deletion or pharmacological inhibition of $K_V1.3$ affects leukocyte adhesion *in vivo* similar to PIF treatment, $K_V1.3^{-/-}$ mice¹⁹¹ were i.s. injected with $TNF-\alpha$ 2 h prior to IVM and numbers of adherent leukocytes to inflamed postcapillary venules in the mouse cremaster were analyzed. Western blot and immune fluorescence staining were carried out to prove absence of $K_V1.3$ on protein level in knockout neutrophils (Fig. 4.7). Genetic loss of $K_V1.3$ resulted in decreased numbers of adherent cells to inflamed endothelium compared to control (Fig. 4.8-A). Of note, this decrease was equivalent to the reduction in PIF treated WT mice (Fig. 4.1-A). To demonstrate that PIF exerts its inhibitory effect on leukocyte adhesion predominantly via interference with $K_V1.3$, PIF was i.s. injected into $K_V1.3^{-/-}$ mice 1 h prior to induction of inflammation. Application of PIF did not further lower leukocyte adhesion, indicating no additive effects of PIF in $K_V1.3^{-/-}$ mice. In line, WT mice i.s. injected with $30 \mu\text{g}$ PAP-1 1 h prior to $TNF-\alpha$ stimulation displayed a significant reduced number of adherent leukocytes in postcapillary vessels of the cremaster muscle compared to vehicle treated control mice (Fig. 4.8-B). Again, a combination of PIF and PAP-1 resulted in the same phenotype. No differences in the overall WBCs could be detected among all experimental groups in both settings (Tab. 4.3). Taken together, these results demonstrate that $K_V1.3$ is crucial for leukocyte adhesion *in vivo*. Lack or inhibition of $K_V1.3$ leads to reduced number of adherent leukocytes comparably to PIF treatment, suggesting that PIF might influence leukocyte adhesion by interfering with $K_V1.3$ activity.

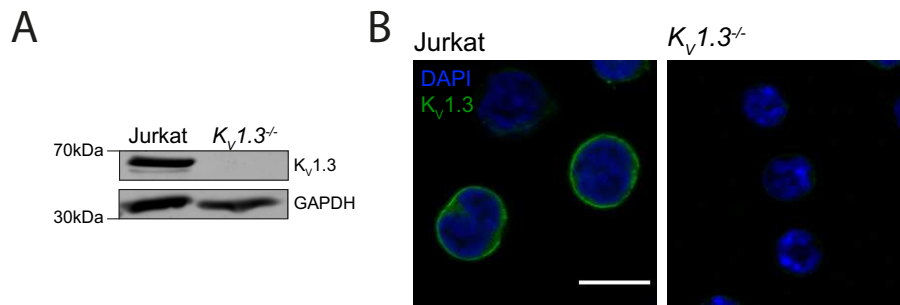


Figure 4.7: Neutrophils from $K_V1.3^{-/-}$ mice do not express $K_V1.3$. (A) Total $K_V1.3$ protein levels of Jurkat cells (positive control) and of $K_V1.3^{-/-}$ neutrophils. GAPDH served as loading control (representative blot; $n=3$ independent experiments). (B) Representative confocal micrographs of Jurkat cells and $K_V1.3^{-/-}$ neutrophils (scale bar: 10 μm ; $n=3$ independent experiments).

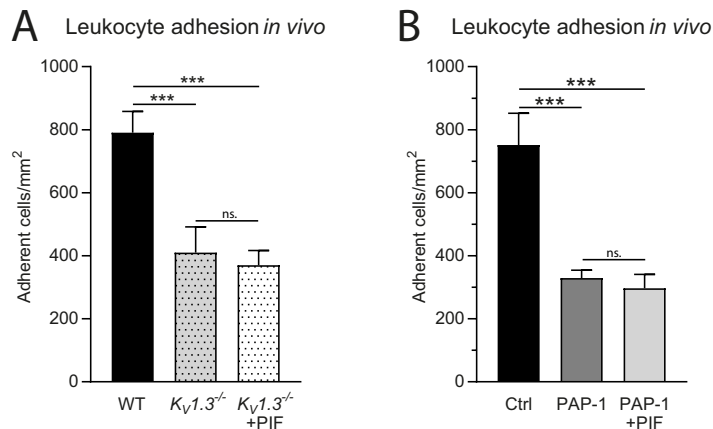


Figure 4.8: Genetic deletion or pharmacological inhibition of $K_V1.3$ impairs leukocyte recruitment in $\text{TNF-}\alpha$ stimulated mouse cremaster muscle. (A) Leukocyte adhesion was analyzed in $\text{TNF-}\alpha$ stimulated mouse cremaster muscles venules of WT and $K_V1.3^{-/-}$ mice and of $K_V1.3^{-/-}$ mice pre-treated with PIF (mean \pm SEM, $n=5$ mice per group, 1-way ANOVA, Tukey's multiple comparison, ns.: not significant). (B) Additionally, WT mice received an i.s. injection of either vehicle (Ctrl), PAP-1 or PAP-1 plus PIF 1 h prior to $\text{TNF-}\alpha$ stimulation and leukocyte adhesion was quantified (mean \pm SEM, $n=4$ mice per group, 1-way ANOVA, Tukey's multiple comparison).

4.1.8. Genetic deletion and inhibition of $K_V1.3$ prevents leukocyte slow rolling *in vivo*

Leukocyte rolling velocities were analyzed to investigate whether genetic loss or pharmacological inhibition of $K_V1.3$ interferes with leukocyte slow rolling *in vivo* similar to PIF treatment. WT, $K_V1.3^{-/-}$ and $K_V1.3^{-/-}$ mice pre-treated i.s. with 1 μg PIF, were stimulated i.s. with $\text{TNF-}\alpha$ 2 h prior to IVM of the cremaster muscle and rolling velocities were analyzed. $K_V1.3^{-/-}$ leukocytes rolled significantly faster along inflamed postcapillary venules compared to WT cells and additional PIF application did not further increase leukocyte slow rolling velocities (Fig. 4.9-A). In addition, leukocyte rolling velocities in WT mice i.s. injected with 30 μg PAP-1 prior to $\text{TNF-}\alpha$ were significantly faster compared to control cells. A combination of PAP-1 and PIF did not further affect leukocyte slow rolling velocities, suggesting

4. Results

Table 4.3.: Hemodynamic parameters of WT and $K_V1.3^{-/-}$ mice pre-treated as indicated prior to TNF- α stimulation. Ven.: venules, \emptyset : vessel diameter, **Syst. count:** systemic white blood cell count (WBC). **ns.:** not significant (mean \pm SEM, 1-way ANOVA, Tukey's multiple comparison).

	Mice <i>n</i>	Ven. <i>n</i>	\emptyset [μ m]	Centerline velocity [μ m/s]	Shear rate [s^{-1}]	Syst. count [cells/ μ l]
WT	5	19	31 \pm 1	1737 \pm 151	1381 \pm 122	2064 \pm 234
$K_V1.3^{-/-}$	5	19	29 \pm 1	1742 \pm 150	1465 \pm 126	2516 \pm 456
$K_V1.3^{-/-}$+PIF	5	19	31 \pm 1	1900 \pm 106	1541 \pm 106	2956 \pm 347
			ns. p=0.2633	ns. p=0.6358	ns. p=0.6350	ns. p=0.2509
Ctrl	4	17	30 \pm 1	1753 \pm 172	1448 \pm 154	3818 \pm 189
PAP-1	4	15	30 \pm 1	2047 \pm 294	1677 \pm 230	4085 \pm 406
PAP-1+PIF	4	15	29 \pm 1	1513 \pm 157	1283 \pm 116	3393 \pm 495
			ns. p=0.4690	ns. p=0.3543	ns. p=0.4324	ns. p=0.2649

that genetic loss and pharmacological inhibition of $K_V1.3$ impairs leukocytes to decelerate during rolling along inflamed vessels in acute inflammations to a comparable extent as PIF treatment.

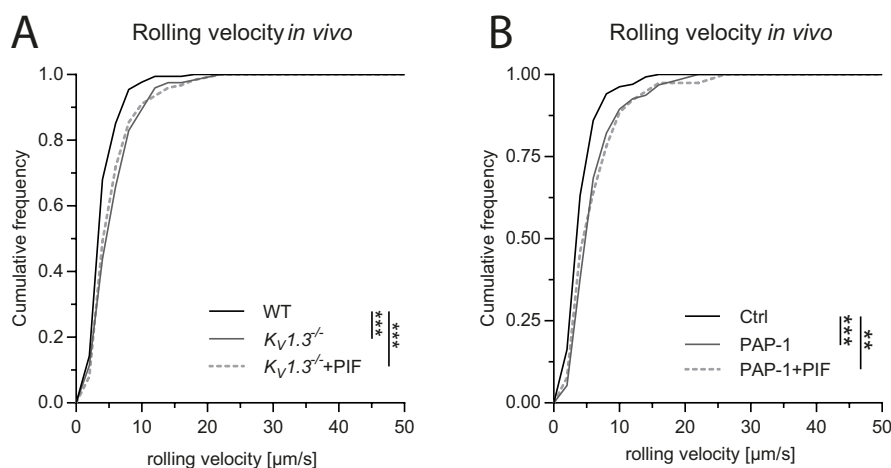


Figure 4.9.: Genetic deletion and inhibition of $K_V1.3$ prevents leukocyte slow rolling. Leukocyte rolling velocities were analyzed in TNF- α stimulated (A) WT, $K_V1.3^{-/-}$ and $K_V1.3^{-/-}$ mice pre-treated with PIF (cumulative frequency, $n=175$ (WT), 123 ($K_V1.3^{-/-}$) 124 ($K_V1.3^{-/-}$ +PIF) cells of 5 mice per group, 1-way ANOVA, Tukey's multiple comparison) and in (B) WT mice pre-treated with PAP-1, PAP-1 plus PIF or carrier substance (Ctrl, cumulative frequency, $n=136$ (Ctrl), 105 (PAP-1), 82 (PAP-1+PIF) cells of 4 mice per group, 1-way ANOVA, Tukey's multiple comparison).

4.1.9. Genetic loss of $K_V1.3$ does not alter surface expression levels of adhesion relevant molecules

Expression levels of β_2 integrins and the GPCR CXCR2 were also determined in peripheral blood neutrophils from $K_V1.3^{-/-}$ mice to exclude alterations in surface molecule composition

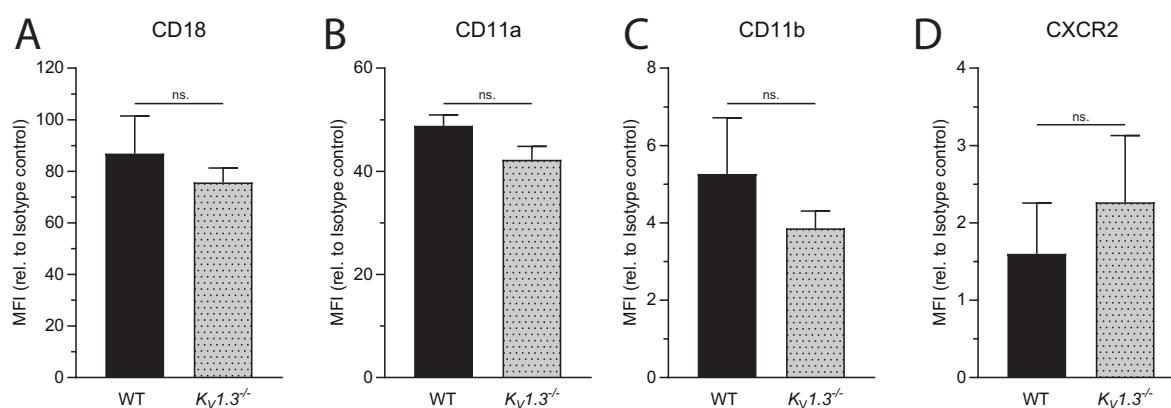


Figure 4.10.: Genetic deletion of $K_V1.3$ does not alter the expression of adhesion relevant surface molecules on peripheral blood neutrophils. Expression levels of (A) CD18, (B) CD11a, (C) CD11b, and (D) CXCR2 were measured by flow cytometry (MFI: mean fluorescence intensity; mean \pm SEM, n=3 mice per group, unpaired student's t-test, ns.: not significant).

as a reason for the observed adhesion defect in knockout mice. Indeed, no differences in CD18, CD11a, CD11b and CXCR2 surface expression could be detected in knockout cells compared to WT control (Fig. 4.10).

4.1.10. PIF reduces voltage-induced $K_V1.3$ currents in $K_V1.3$ -overexpressing HEK-293 cells

To test whether PIF modifies neutrophil function by inhibition of $K_V1.3$, whole cell patch clamp experiments were conducted using $K_V1.3$ -overexpressing HEK-293 cells (h $K_V1.3$ -HEK-293). Experiments were carried out in collaboration with Susanna Zierler and Wiebke Nadolni from the Walther-Straub-Institut, LMU, Munich, Germany (see Fig. A.1 in A.1), demonstrating that PIF inhibits $K_V1.3$ in a dose dependent manner with an IC_{50} of 10.2 ± 5 nM.

4.1.11. PIF reduces voltage-induced $K_V1.3$ currents in human neutrophils

Whole cell patch clamp experiments were repeated with isolated human neutrophils to verify PIF's inhibitory properties on $K_V1.3$ in these cells. The same consecutive step protocol was applied to induce $K_V1.3$ -specific currents in neutrophils incubated with either 300 nM PIF, 10 nM PAP-1, or carrier substance (Ctrl). In addition, neutrophils were treated with 1 μ M 1-[(2-Chlorophenyl)diphenylmethyl]-1H-pyrazole (TRAM-34), a specific inhibitor for $K_{Ca}3.1$ ²⁰⁴, a K^+ channel also expressed on neutrophils²⁰⁵. Control cells developed voltage-dependent currents upon activation (Fig. 4.11-A). Pre-incubation with PIF in turn significantly inhibited voltage induced currents, comparably to inhibition using PAP-1 (Fig. 4.11-B, -C and -E). Application of TRAM-34 to the cells did not significantly lower currents (Fig. 4.11-D). These results show that PIF inhibits $K_V1.3$ in human neutrophils, similar to the known $K_V1.3$ inhibitor PAP-1.

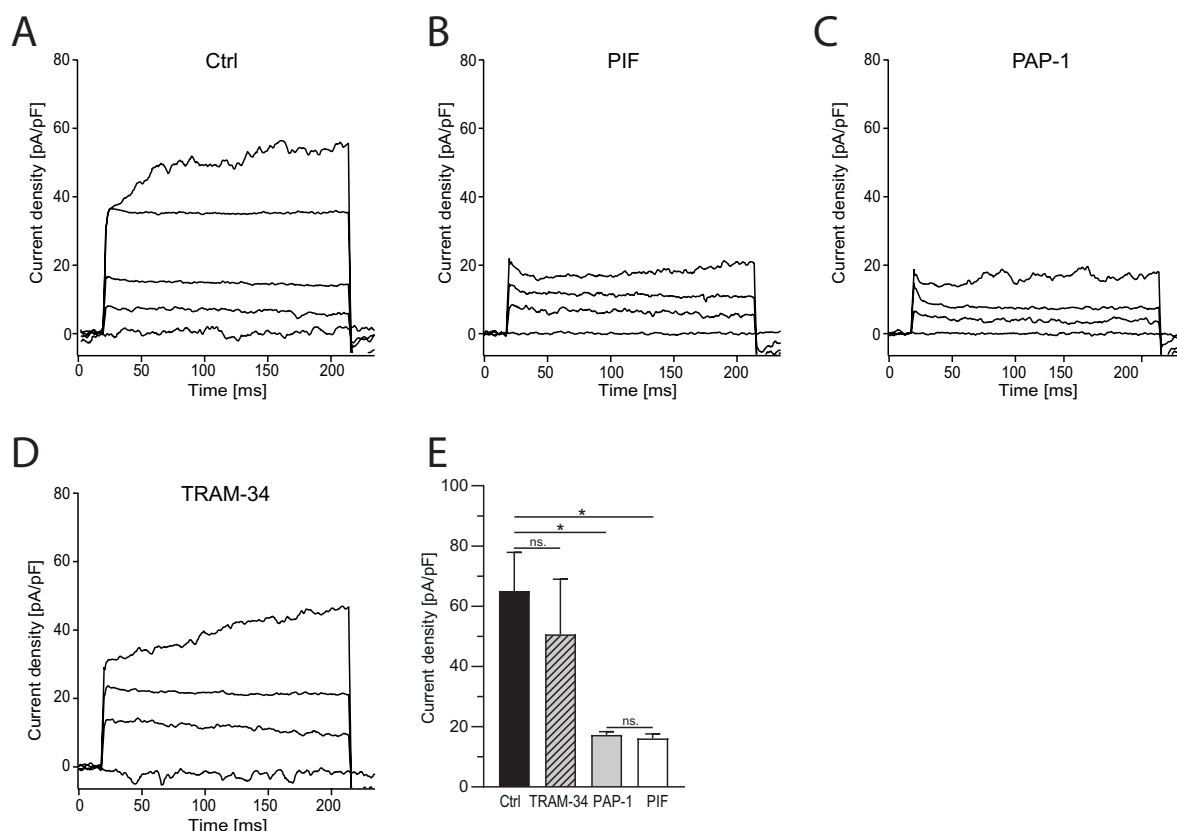


Figure 4.11.: PIF reduces voltage-induced $K_V1.3$ currents in human neutrophils. Voltage-dependent $K_V1.3$ currents in human neutrophils, triggered by the application of 13 consecutive 10 mV voltage steps from -80 mV to $+40$ mV after incubation with (A) carrier substance (Ctrl, representative traces no. 1, 4, 8, 10, 13, of $n=15$ cells), (B) PIF (representative traces no. 1, 4, 8, 13 of $n=8$ cells), (C) PAP-1 (representative traces no. 1, 4, 8, 13, of $n=10$ cells), or (D) TRAM-34 (representative traces no. 1, 4, 8, 12, of $n=13$ cells). (E) Quantification of current densities extracted at 100 ms (mean \pm SEM, 1-way ANOVA, Tukey's multiple comparison, ns.: not significant).

4.1.12. Inhibition of $K_V1.3$ by PIF impairs calcium signaling in human neutrophils

In lymphocytes, $K_V1.3$ was shown to be involved in the regulation of Ca^{2+} signaling by sustaining Ca^{2+} influx via store-operated Ca^{2+} entry (SOCE)¹⁵⁶. K^+ efflux via $K_V1.3$ maintains an electrical gradient over the cell membrane, enabling continuous Ca^{2+} influx into the cells¹⁸³. To elucidate the role of $K_V1.3$ in Ca^{2+} signaling in human neutrophils, Scott I. Simon and Vasilios Morikis from the University of California, Davis, USA investigated in a collaboration changes in $[Ca^{2+}]_i$ in isolated human neutrophils in the presence of PIF and PAP-1. Their experiments demonstrated that inhibition of $K_V1.3$ in neutrophils using PIF and PAP-1 significantly reduces $[Ca^{2+}]_i$ both, under static and under flow conditions, thereby revealing a substantial contribution of $K_V1.3$ to regulation of SOCE in neutrophils. (see Fig. A.2, Fig. A.3 and Fig. A.4 in A.2).

4.1.13. PIF impairs post-arrest modifications in neutrophils

High $[Ca^{2+}]_i$ in neutrophils during arrest is essential for the cells to polarize and to initialize a migratory phenotype^{165,166}. To study how reduced $[Ca^{2+}]_i$ upon $K_V1.3$ inhibition via PIF influences post-arrest modifications under shear, neutrophil spreading was observed. Flow chambers were coated with E-selectin, ICAM-1 and CXCL8 and isolated human neutrophils pre-incubated with either 300 nM PIF, 10 nM PAP-1 or vehicle (Ctrl). Neutrophils were then introduced into the chambers to monitor changes in cell shape over time at a constant shear stress level of 1 dyne/cm² (Fig. 4.12-A). Analysis of cell perimeter, cell circularity (reflecting the roundness of a cell) and cell solidity (reflecting the number of extensions and protrusions of a cell) revealed that neutrophils incubated with PIF or PAP-1 remained smaller (Fig. 4.12-B), rounder (Fig. 4.12-C) and displayed fewer protrusions (Fig. 4.12-D) over time. These results demonstrate that inhibition of $K_V1.3$ with PIF or PAP-1 reduces the ability of neutrophils to spread properly and to polarize under physiological shear stress conditions.

4.1.14. PIF increases susceptibility to shear forces *in vitro* and *in vivo*

To evaluate whether the disability of neutrophils to polarize and to switch to a migratory phenotype in the presence of PIF has implications on the resistance to shear forces, a detachment-assay was carried out by Anna Yevtushenko in the course of a Bachelor's thesis (title: '*The role of PreImplantation Factor (PIF) in leukocyte recruitment*' at the faculty for Chemistry and Pharmacy, LMU Munich, 2017), co-supervised by me. In this assay, incubation with PIF or PAP-1 resulted in an higher susceptibility to increasing shear forces (see Fig. A.5 in A.3).

To validate these findings in an *in vivo* setting, WT mice were injected i.s. with 1 μ g PIF or scrPIF 2 h prior to dissection of the cremaster muscle and subsequent IVM. One postcapillary venule was recorded before and after application of 600 ng CXCL1 via the carotid catheter and number of adherent leukocytes was assessed. Injection of CXCL1 induced a strong increase in adherent leukocytes 1 min after injection in scrPIF controls compared to before and number of adherent leukocytes did not change after 5 min (Fig. 4.13). An initial increase in number of adherent cells 1 min after CXCL1 application could be observed in PIF treated animals as well. In contrast to control treatment, number of adherent cells already decreased 5 min after *in vivo* stimulation, suggesting that in PIF treated animals, CXCL1 injection is able to initially increase leukocytes adhesion, but activated and arrested cells are not able to efficiently adhere under *in vivo* flow conditions. Of note, hemodynamic parameters did not differ among the groups (Tab. 4.4).

Summarizing, PIF reduces leukocyte adhesion and prevents leukocyte slow rolling *in vivo* in a mouse model of TNF- α induced acute inflammation. *In vitro* and *ex vivo* flow chambers and functional assays revealed that this phenotype is due to a direct effect of PIF on leukocytes, but not mediated by an interference of PIF with β_2 integrin surface expression or activation. In turn, PIF inhibits $K_V1.3$ on neutrophils, thereby reducing β_2 integrin and GPCR mediated increase in $[Ca^{2+}]_i$. Reduced $[Ca^{2+}]_i$ leads to impaired neutrophil spreading and adhesion strengthening, resulting in increased susceptibility to physiological shear forces.

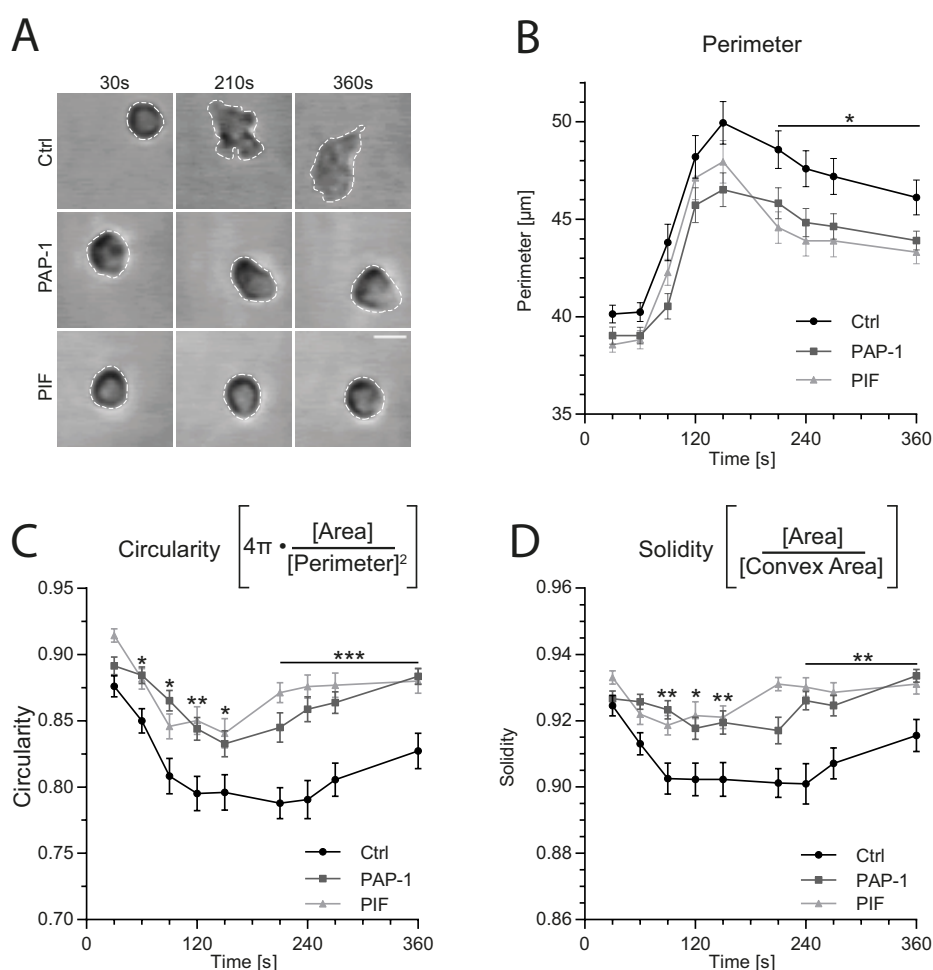


Figure 4.12.: PIF impairs neutrophil spreading. Isolated human neutrophils were incubated with either PIF, PAP-1 or vehicle (Ctrl) and introduced into E-selectin, ICAM-1 and CXCL8 coated flow chambers. (A) Changes in cell shape was investigated over time and (B) cell perimeter, (C) cell circularity and (D) cell solidity were analyzed (mean±SEM, n=49 (Ctrl), 60 (PAP-1) and 42 (PIF) cells from n=5 independent experiments, 1-way ANOVA, Dunnett's multiple comparison).

4.2. PIF reduces extravasation of neutrophil into inflamed tissue

4.2.1. PIF reduces the number of transmigrated neutrophils in TNF- α stimulated cremaster muscles

To exert its functions during acute inflammatory processes, neutrophils need to exit the vascular compartment and enter the surrounding tissue⁸⁶. To see whether PIF treatment also influences the number of perivascular leukocytes in acute inflammation, neutrophil extravasation was assessed in TNF- α stimulated cremaster muscles. Therefore, 1 μ g PIF was injected i.s. into WT mice 1 h prior to TNF- α stimulation. 2 h later cremaster muscles were removed, fixed, stained with Giemsa and number of transmigrated leukocytes was analyzed. As controls, mice received either an i.s. injection of 1 μ g scrPIF or carrier substance (Ctrl) (Fig. 4.14-A). PIF treated animals exhibited significantly reduced numbers of perivascular

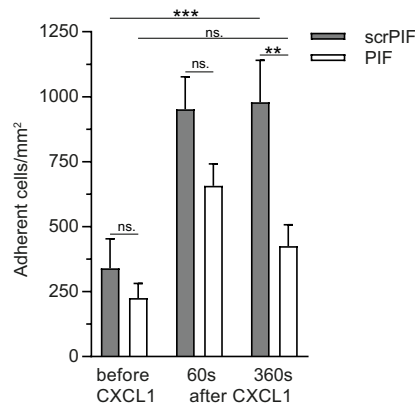


Figure 4.13.: PIF increases susceptibility to shear forces *in vivo*. WT mice were i.s. injected with PIF or scrPIF 2h prior to IVM of the mouse cremaster muscle. Number of adherent leukocyte were analyzed before and after application of CXCL1 via the carotid catheter (n=4-5 mice, repeated 2-way ANOVA, Sidak's and Tukey's multiple comparison, ns.: not significant).

Table 4.4.: Hemodynamic parameters before and after CXCL1 injection *in vivo*. Ø: vessel diameter, WBC: white blood cell count, ns.: not significant (mean±SEM, unpaired student's t-test).

Time	Treatment	Ø [µm]	Centerline velocity [µm/s]	Shear rate [s ⁻¹]	WBC [cells/µl]
before	scrPIF	32±1	1900±430	1449±322	5983±651
	PIF	30±2	2260±340	1861±335	7250±751
		ns. p=0.4634	ns. p=0.5262	ns. p=0.4122	ns. p=0.2565
60s	scrPIF	-	2100±567	1622±446	-
	PIF	-	2240±470	1873±448	-
		-	ns. p=0.8532	ns. p=0.7074	-
360s	scrPIF	-	1675±496	1290±380	3683±342
	PIF	-	2280±445	1903±430	4618±553
		-	ns. p=0.3944	ns. p=0.3341	ns. p=0.2204

neutrophils in stimulated cremaster muscles compared to both controls, whereas number of perivascular eosinophils and other leukocyte subsets was not altered (Fig. 4.14-B).

4.2.2. Inhibition and genetic deletion of K_v1.3 reduces the number of transmigrated neutrophils in TNF-α stimulated cremaster muscles

Neutrophil migration and cytoskeletal rearrangement are highly dependent on changes in [Ca²⁺]_i¹⁵⁸. Since K_v1.3 regulates Ca²⁺ influx via SOCE in neutrophils, K_v1.3^{-/-} mice and PAP-1 treatment were used to investigate neutrophil extravasation as a function of K_v1.3 activity. Cremaster muscles from untreated WT and K_v1.3^{-/-} mice and from WT mice i.s. injected with 30 µg PAP-1 were stimulated with TNF-α, fixed and stained to analyze the number

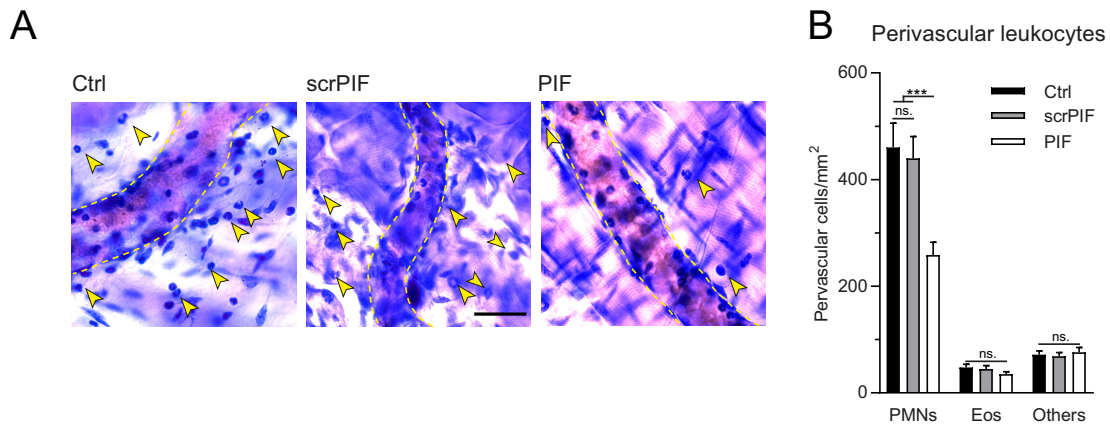


Figure 4.14.: PIF reduces the number of transmigrated neutrophils in TNF- α stimulated cremaster muscles. (A) Giemsa stained cremaster muscles from WT mice pre-treated with either PIF, scrPIF or carrier substance (Ctrl) 1 h prior to TNF- α stimulation were analyzed (representative micrographs, scale bar: 30 μ m) and (B) the number of extravasated leukocytes was analyzed (Eos: eosinophils, mean \pm SEM, n=3 mice per group, 1-way ANOVA, Tukey's multiple comparison, ns.: not significant).

of extravasated leukocytes (Fig. 4.15-A). Both, inhibition and genetic deletion of $K_V1.3$ significantly lowered the number of transmigrated neutrophils into inflamed tissue compared to WT (Fig. 4.15-B), not affecting the number of perivascular eosinophils and other leukocyte subsets. These observations suggest that reduced numbers of perivascular neutrophils in PIF treated animals are a consequence of $K_V1.3$ inhibition. Whether this phenotype is a direct consequence of reduced leukocyte adhesion, or whether PIF additionally affects neutrophil transmigration steps independent of adhesion, requires further investigation.

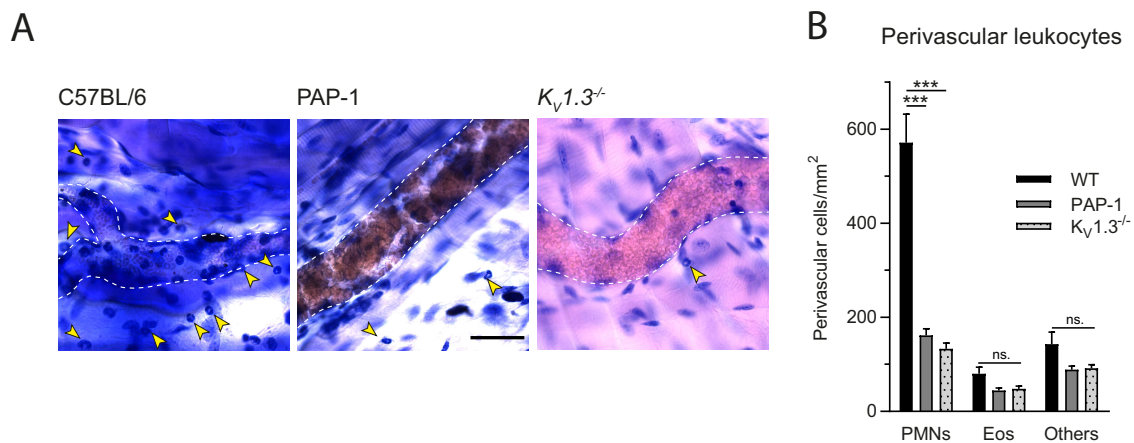


Figure 4.15.: Inhibition and genetic loss of $K_V1.3$ reduces the number of transmigrated neutrophils in TNF- α stimulated cremaster muscles. (A) TNF- α stimulated cremaster muscles from WT and $K_V1.3^{-/-}$ -mice and from WT mice pre-treated with PAP-1 were stained with Giemsa (representative micrographs, scale bar: 30 μ m) and (B) the number of extravasated leukocytes was quantified (Eos: eosinophils, mean \pm SEM, n=3 mice per group, 1-way ANOVA, Tukey's multiple comparison, ns.: not significant).

4.2.3. PIF impairs neutrophil recruitment in an animal model of acute lung injury (ALI) after LPS stimulation.

Many severe airway diseases such as bronchitis, cystic fibrosis, chronic obstructive pulmonary disease (COPD) or acute lung injury (ALI) are characterized by substantial neutrophil infiltration^{206,207}. To investigate whether inhibition of $K_V1.3$ by PIF might be a suitable therapeutic approach to treat overgrowing neutrophil infiltration in a clinically relevant setting, an ALI-mouse model after LPS inhalation²⁰⁸ was carried out in collaboration with Oliver Söhnlein, Institute for Cardiovascular Prevention (IPEK), LMU Munich, Munich, Germany, Jochen Grommes and Jessica Tilgner, RWTH Aachen, Aachen, Germany. In line with the TNF- α cremaster muscle model, they could show that PIF treatment significantly reduced neutrophil infiltration into LPS stimulated lung tissue (Fig. A.6 in A.4).

4.2.4. PIF does not change neutrophil transmigration in a transwell assay

Next, a transwell assay was carried out to delineate whether PIF treatment directly influences the ability of neutrophils to sense chemokines, thereby altering transmigration. Bone marrow derived murine neutrophils were incubated with 300 nM PIF, scrPIF or vehicle (Ctrl) and allowed to transmigrate through transwells towards different concentrations of CXCL1 (0.1, 1, 10 nM) for 45 min. CXCL1 in the lower compartment caused the cells to transmigrate through the pores in a dose-dependent manner compared to unstimulated conditions, with no differences in PIF treated cells compared to controls (Fig. 4.16). These results indicate that PIF does not alter the sensing of a chemokine gradient.

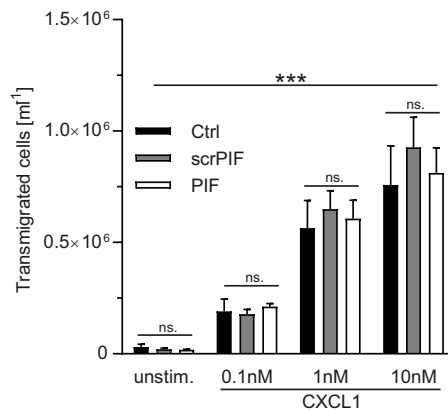


Figure 4.16.: PIF does not change neutrophil transmigration in a transwell assay. Isolated murine neutrophils were incubated with either PIF, scrPIF or vehicle (Ctrl) and transmigration was induced by different concentrations of CXCL1 (mean \pm SEM, n=4 mice per group, repeated 1-way ANOVA, repeated Tukey's multiple comparison, ns.: not significant).

4.2.5. PIF reduces vascular leakage in a model of ALI but does not alter TNF- α induced changes in the resistance of HUVEC monolayers

Massive infiltration of neutrophils into inflamed lungs is accompanied by an increase in permeability and by elevated protein content in the BAL, due to endothelial and epithelial injury²⁰⁷. Hence, in addition to the assessment of neutrophil recruitment to inflamed lungs in the ALI model, LPS induced vascular leakage was determined²⁰⁸ by Oliver Söhnlein, Jochen Grommes and Jessica Tilgner, showing that PIF pre-treatment prior to LPS inhalation significantly reduced vascular leakage (Fig. A.7 in A.5).

To find indications if PIF directly affects the integrity of stimulated endothelial cells, ECiS measurements were carried out. HUVEC cells were grown to confluence, 300 nM PIF or vehicle (Ctrl) was added together with 10 $\mu\text{g}/\text{ml}$ TNF- α and impedance was measured over time. Application of TNF- α reduced resistance of a HUVEC monolayer compared to non-stimulated cells (w/o) and no differences could be observed in HUVEC cells treated with PIF, indicating no effect of PIF on the integrity of endothelial cells in a static *in vitro* model.

Taken together, besides impaired leukocyte adhesion, PIF treatment reduces numbers of perivascular neutrophils *in vivo* in two animal models of acute inflammation. Lower numbers of transmigrated neutrophils could be attributed to the inhibitory effect of PIF on K_V1.3. Further, PIF does not alter neutrophil sensing of the chemokine CXCL1 in an tanswell assay. In an acute lung injury model after LPS inhalation, PIF treatment kept endothelial permeability on basal levels, but impedance measurements of TNF- α stimulated HUVEC cells did not reveal any changes in endothelial integrity upon PIF stimulation.

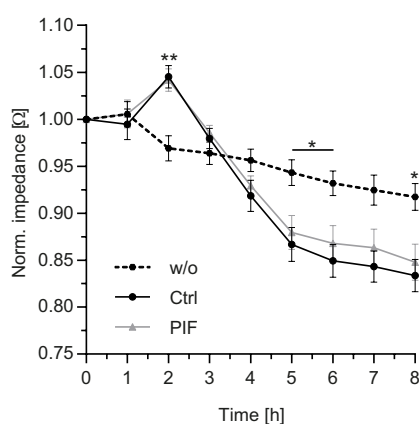


Figure 4.17.: PIF does not alter integrity of cultured HUVEC cells upon TNF- α stimulation. In ECiS experiments, resistance of HUVEC monolayers treated with PIF or vehicle (Ctrl) was measured after TNF- α stimulation. As control HUVEC cells were left untreated (w/o, mean \pm SEM, n=5 independent experiments, repeated 1-way ANOVAs, Tukey's multiple comparison).

4.3. PIF alters selectin dependent leukocyte rolling

4.3.1. PIF alters leukocyte rolling *in vivo*

Here, the influence of PIF on leukocyte rolling was investigated. For that purpose, WT mice were i.s. injected with either 1 µg of PIF, scrPIF, H-PIF or carrier substance (Ctrl), respectively 1 h prior to i.s. stimulation with TNF-α. 2 h later leukocyte rolling in postcapillary venules of the cremaster muscle was assessed using IVM. Administration of PIF and H-PIF resulted in reduced rolling flux fraction (number of rolling leukocytes, normalized to vessel size, blood flow velocity and WBC¹⁹⁸) compared to both controls (Fig. 4.18-A, (none)). To investigate the different contributions of endothelial expressed selectins on leukocyte rolling, selective antibodies against E- and P-selectin were injected into the mice during the experiments via the carotid artery catheter. P-selectin dependent rolling after administration of E-selectin blocking antibodies was significantly reduced in PIF and H-PIF pre-treated animals compared to controls (Fig. 4.18-A, (anti-E)) whereas E-selectin dependent rolling after administration of P-selectin blocking antibodies was not significantly different among all groups (Fig. 4.18-A, (anti-P)). Blockade of both, E- and P-selectin almost completely abolished leukocyte rolling in all treatment groups, demonstrating that leukocyte rolling in post-capillary venules of TNF-α stimulated mouse cremaster muscles is predominantly mediated by these two selectins. Of note, hemodynamic parameters did not differ among experimental groups (Tab. 4.1 and Tab. 4.5).

In addition to TNF-α induced inflammation, leukocyte rolling was also assessed in a trauma induced acute inflammatory scenario. Here, surgical preparation of the cremaster muscle alone leads to a rapid release of P-selectin out of Weibel-Palade bodies and subsequent P-selectin dependent rolling⁹¹. WT mice were i.s. injected with 1 µg PIF or scrPIF and IVM was carried out 2 h later. Analysis revealed that the number of rolling leukocytes was significantly decreased compared to control (Fig. 4.18-B). Application of P-selectin antibodies via the carotid artery catheter completely abolished leukocyte rolling, demonstrating that rolling is exclusively P-selectin mediated in the trauma induced acute inflammation. P-selectin-dependent leukocyte rolling velocities were measured as well, revealing increased rolling velocities in PIF treated animals compared to control (Fig. 4.18-C). Application of PIF did not change the WBC (Tab. 4.6). In summary, PIF affects P-selectin dependent leukocyte rolling in TNF-α and trauma induced inflammation, suggesting that P-selectin dependent rolling is controlled by PIF.

4.3.2. PIF does not influence the expression level of surface molecules important for neutrophil rolling

PSGL-1 is the major selectin ligand on neutrophils^{100,209}, but also CD44 and L-selectin contribute to leukocyte rolling^{97,108}. Therefore, expression levels of these surface molecules were determined by flow cytometry. I.p. injection of 1 µg PIF 2 h prior to retro-orbital exsanguination did not alter the expression of PSGL-1, CD44 or L-selectin compared to application of carrier substance (Ctrl, Fig. 4.19), displaying that alteration in surface expression of selectin ligands on peripheral blood neutrophils cannot be the reason for differences in

4. Results

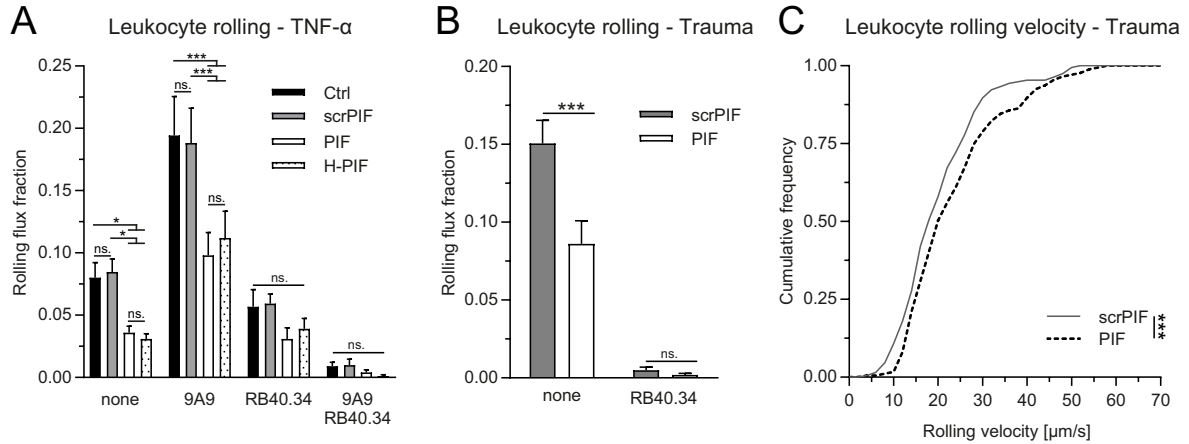


Figure 4.18.: PIF alters leukocyte rolling *in vivo*. (A) IVM was carried out in TNF- α stimulated WT mice pre-treated with either PIF, scrPIF, H-PIF or carrier substance (Ctrl) to analyze leukocyte rolling before (none) and after administration of selectin blocking antibodies (9A9: E-selectin blocking antibody, RB40.34: P-selectin blocking antibody, mean \pm SEM, n=8-10 mice per group, 1-way ANOVA, Tukey's multiple comparison, ns.: not significant). WT mice were injected with PIF or scrPIF 2 h prior to IVM to quantify (B) leukocyte rolling (mean \pm SEM, n=7 mice per group, 2-way ANOVA, Sidak's multiple comparison) and (C) leukocyte rolling velocity in trauma induced acute inflammation (cumulative frequency, n=258 (scrPIF), 234 (PIF) of 7 mice per group, unpaired student's t-test).

Table 4.5.: Hemodynamic parameters of WT mice treated with TNF- α after the application of selectin blocking antibodies 9A9: E-selectin blocking antibody, RB40.34: P-selectin blocking antibody, Ven.: venules, \emptyset : vessel diameter, Syst. count: systemic white blood cell count (WBC). ns.: not significant (mean \pm SEM, 1-way ANOVA, Tukey's multiple comparison).

		Mice <i>n</i>	Ven. <i>n</i>	\emptyset [μ m]	Centerline velocity [μ m/s]	Shear rate [s ⁻¹]	Syst. count [cells/ μ l]
9A9	Ctrl	5	14	35 \pm 1	1529 \pm 288	1089 \pm 211	4250 \pm 369
	scrPIF	5	16	32 \pm 1	1638 \pm 198	1229 \pm 137	4190 \pm 735
	PIF	5	20	32 \pm 1	1605 \pm 142	1226 \pm 107	5054 \pm 846
	H-PIF	5	15	32 \pm 1	1987 \pm 157	1549 \pm 115	5364 \pm 770
				ns. p=0.1503	ns. p=0.3899	ns. p=0.1680	ns. p=0.5711
RB40.34	Ctrl	3	12	33 \pm 2	1808 \pm 234	1393 \pm 218	3803 \pm 466
	scrPIF	3	12	32 \pm 1	1883 \pm 304	1477 \pm 255	5763 \pm 537
	PIF	3	10	31 \pm 1	1940 \pm 298	1578 \pm 266	5337 \pm 289
	H-PIF	3	11	33 \pm 2	1855 \pm 234	1370 \pm 159	4950 \pm 391
				ns. p=0.6957	ns. p=0.9889	ns. p=0.9222	ns. p=0.0574
9A9 & RB40.34	Ctrl	4	9	34 \pm 1	1189 \pm 70	862 \pm 52	4885 \pm 696
	scrPIF	3	8	31 \pm 1	1900 \pm 253	1490 \pm 163	8080 \pm 812
	PIF	3	10	32 \pm 1	1650 \pm 243	1399 \pm 202	7143 \pm 797
	H-PIF	3	9	33 \pm 1	1900 \pm 242	1425 \pm 184	6543 \pm 1489
				ns. p=0.2328	ns. p=0.0897	ns. p=0.0504	ns. p=0.1654

Table 4.6.: Hemodynamic parameters of WT mice in a trauma induced inflammation model of the mouse cremaster before and after the application of P-selectin blocking antibodies. RB40.34: P-selectin blocking antibody, Ven.: venules, Ø: vessel diameter, Syst. count: systemic white blood cell count (WBC). ns.: not significant (mean±SEM, unpaired student's t-test).

		Mice <i>n</i>	Ven. <i>n</i>	Ø [µm]	Centerline velocity [µm/s]	Shear rate [s ⁻¹]	Syst. count [cells/µl]
	scrPIF	7	26	32±1	1585±128	1227±98	6620±535
	PIF	7	26	32±1	1665±126	1291±93	6710±595
				ns. p=0.7141	ns. p=0.6555	ns. p=0.6387	ns. p=0.9123
RB40.34	scrPIF	4	12	31±1	1550±179	1228±148	5813±741
	PIF	4	14	31±1	1940±298	1550±163	5950±479
				ns. p=0.7609	ns. p=0.1639	ns. p=0.1625	ns. p=0.8813

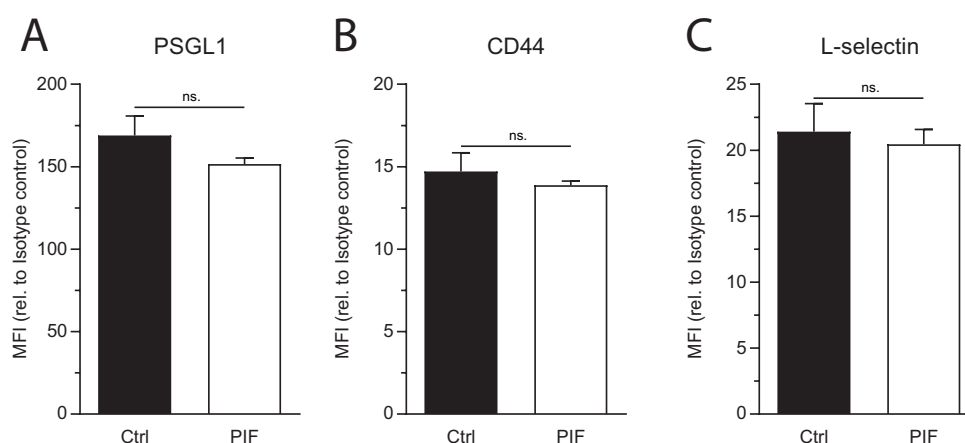


Figure 4.19.: PIF does not influence the expression level of surface molecules important for neutrophil rolling. PIF or carrier substance (Ctrl) was injected into WT mice 2 h prior to exsanguination and surface expression of (A) PSGL-1, (B) CD44 and (C) L-selectin was measured by flow cytometry (MFI: mean fluorescence intensity, mean±SEM, n=3 mice per group, unpaired student's t-test, ns.: not significant).

leukocyte rolling.

4.3.3. PIF does not change neutrophil binding capacity to E- and P-selectin *in vitro*

Next, binding capacity of murine peripheral blood neutrophils to E- and P-selectin was assessed by flow cytometry. WT mice were i.s. injected with 1 µg PIF, scrPIF or carrier substance (Ctrl) 2 h prior to retro-orbital exsanguination and whole blood was incubated with either E- or P-selectin. As a negative control whole blood was incubated with selectins in the presence of EDTA to chelate divalent ions which are necessary for selectin–PSGL-1 interaction⁹¹. Neutrophils from PIF pre-treated animals did not exhibit altered binding to neither E-, nor P-selectin (Fig. 4.20), suggesting that selectin–selectin ligand interaction is not affected by PIF under static conditions *in vitro*.

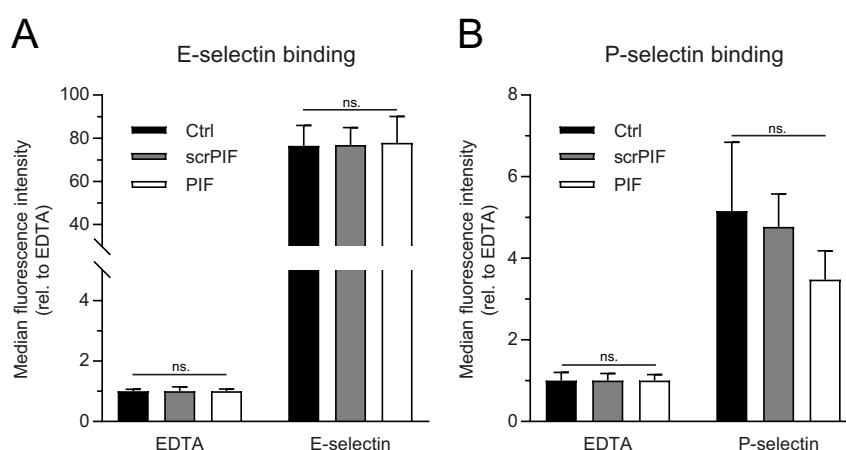


Figure 4.20.: PIF does not change neutrophil binding capacity to E- and P-selectin under static conditions *in vitro*. Binding capacity of peripheral blood neutrophils from WT mice pre-treated with either PIF, scrPIF or carrier substance (Ctrl) to (A) E-selectin (mean±SEM, n=6 mice per group, 2-way repeated measurements ANOVA, Tukey's multiple comparison) and (B) P-selectin (mean±SEM, n=4 mice per group, 2-way repeated measurements ANOVA, Tukey's multiple comparison, ns.: not significant) was measured by flow cytometry.

4.3.4. Genetic deletion or pharmacological inhibition of $K_V1.3$ does not influence leukocyte rolling *in vivo*

PIF inhibits $K_V1.3$ on neutrophils, thereby reducing the ability of the cells to adhere and to withstand shear forces. To investigate whether interference of PIF with $K_V1.3$ activity results also in reduced leukocyte rolling *in vivo*, IVM of TNF- α stimulated cremaster muscle venules of $K_V1.3^{-/-}$ mice was performed. Surprisingly, lack of $K_V1.3$ did not change the number of rolling cells compared to WT controls, but i.s. injection of 1 μ g PIF 1 h prior to onset of inflammation significantly reduced leukocyte rolling in knock-out animals (Fig. 4.21-A). In addition, WT mice were pre-treated with 30 μ g PAP-1 or carrier substance (Ctrl) 1 h prior to TNF- α stimulation. In line with the experiments using $K_V1.3^{-/-}$ animals, pharmacological inhibition of $K_V1.3$ did not alter leukocyte rolling compared to control, but a combination of PAP-1 and 1 μ g PIF together significantly reduced number of rolling leukocytes (Fig. 4.21-B). These results clearly demonstrate that PIF interferes with leukocyte rolling independent of its inhibitory capacity on $K_V1.3$.

4.3.5. Genetic deletion of $K_V1.3$ does not alter the expression of rolling relevant surface molecules on peripheral blood neutrophils

Next, surface expression of molecules important for neutrophil rolling was determined in WT and $K_V1.3^{-/-}$ peripheral blood neutrophils. As expected, surface expression of PSGL-1, CD44 and L-selectin were not found to be different on knockout neutrophils compared to WT control (Fig. 4.22).

4.3.6. PIF does not alter E- and P-selectin dependent leukocyte rolling *in vitro*.

As a last step, leukocyte rolling was analyzed in E- and P-selectin coated flow chambers *in vitro*. Whole blood from WT mice was incubated with 300 nM PIF, scrPIF or vehicle

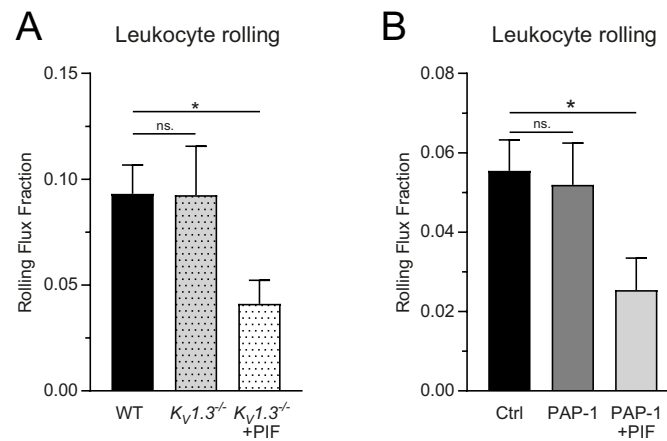


Figure 4.21.: Genetic deletion or pharmacological inhibition of $K_V1.3$ does not influence leukocyte rolling. (A) WT, $K_V1.3^{-/-}$ and $K_V1.3^{-/-}$ -mice pre-treated with PIF were i.s. stimulated with TNF- α and number of rolling leukocytes in postcapillary venules of the cremaster muscle was analyzed by IVM (mean \pm SEM, n=5 mice per group, 1-way ANOVA, Tukey's multiple comparison). (B) WT mice were injected with PAP-1, a combination of PAP-1 and PIF, or carrier substance (Ctrl) and leukocyte rolling was assessed by IVM (mean \pm SEM, n=4 mice per group, 1-way ANOVA, Tukey's multiple comparison, ns.: not significant).

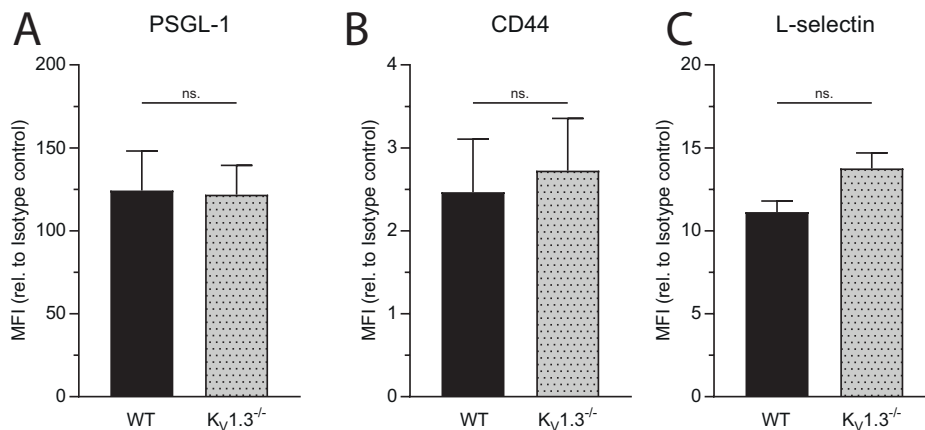


Figure 4.22.: Genetic deletion of $K_V1.3$ does not alter the expression of rolling relevant surface molecules on peripheral blood neutrophils. Expression levels of (A) PSGL-1, (B) CD44 and (C) L-selectin were measured by flow cytometry on $K_V1.3^{-/-}$ and WT neutrophils. (MFI: mean fluorescence intensity; n=3 mice per group, unpaired student's t-test, ns.: not significant).

(Ctrl) and perfused through microfluidic devices coated with either E-selectin or P-selectin, respectively at a defined shear stress level of 2 dyne/cm² (Tab. 4.7). Incubation of murine whole blood with PIF did neither change the number of rolling cells, nor rolling velocities in E-selectin and in P-selectin coated flow chambers compared to controls (Fig. 4.23). Taken together, PIF reduces P-selectin dependent leukocyte rolling in TNF- α induced inflammation *in vivo*. This reduction is independent of PIF mediated inhibition of $K_V1.3$. Neither the expression of rolling relevant surface molecules, nor selectin binding capacity is affected

by the presence of PIF. *In vitro* flow chamber assays demonstrated that changes in selectin dependent rolling *in vivo* are not due to a direct effect of PIF selectins or selectin ligands, but are rather a consequence of an effect of PIF on other rolling relevant molecules.

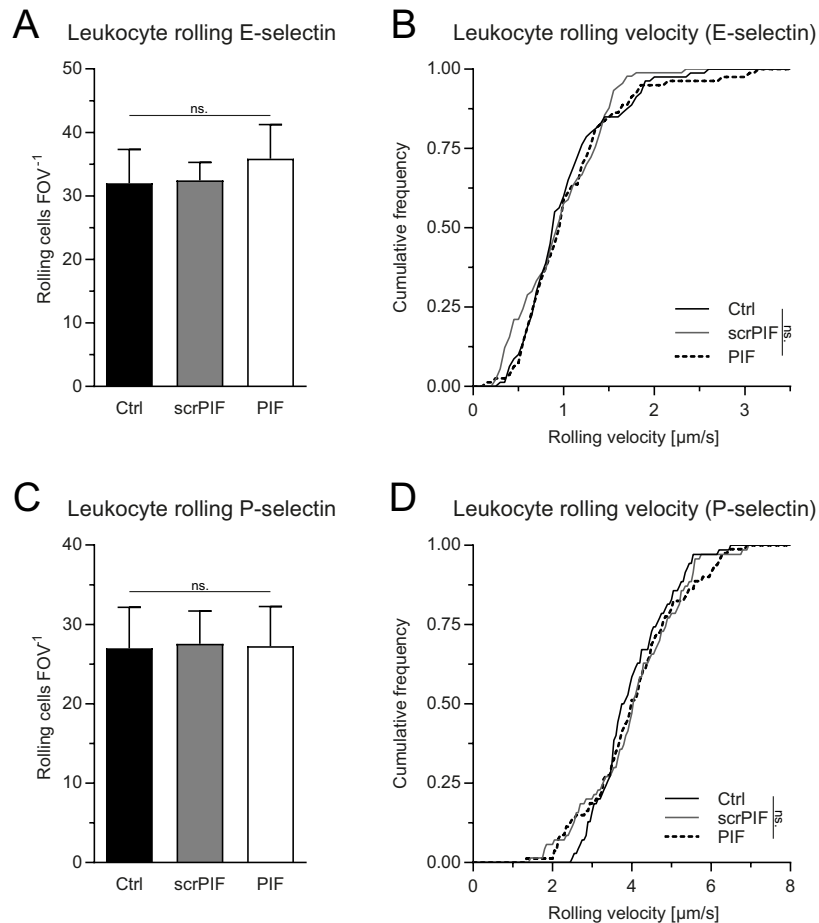


Figure 4.23.: PIF does not change E- and P-selectin dependent leukocyte rolling in *in vitro* microflow chambers. Murine whole blood was incubated with PIF, scrPIF or vehicle (Ctrl) and perfused through E-selectin coated flow chambers to assess (A) E-selectin-dependent leukocyte rolling (mean±SEM, n=5 mice per group, 1-way ANOVA, Tukey's multiple comparison, ns.: not significant) and (B) E-selectin-dependent leukocyte rolling velocity (cumulative frequency, n=80 (Ctrl), 90 (scrPIF), 80 (PIF) cells of 5 mice per group, 1-way ANOVA, Tukey's multiple comparison). Additionally, P-selectin coated flow chambers were perfused as well and (C) P-selectin-dependent leukocyte rolling (mean±SEM, n=4-5 mice per group, 1-way ANOVA, Tukey's multiple comparison) and (D) P-selectin dependent rolling velocities were analyzed (cumulative frequency, n=70 (Ctrl), 70 (scrPIF), 80 (PIF) cells of 4-5 mice per group, 1-way ANOVA, Tukey's multiple comparison).

Table 4.7.: Number of mice, flow chambers and cells per FOV of *in vitro* flow chamber assay. Mean±SEM, unpaired student's t-test

		Mice <i>n</i>	Flow chambers <i>n</i>	WBC [cells/ μ l]	Cells FOV ⁻¹
E-selectin	Ctrl	5	8	6964±351	49±10
	scrPIF	5	9	6659±409	52±6
	PIF	5	8	6843±432	47±4
				ns. p=0.8612	ns. p=0.8797
P-selectin	Ctrl	4	7	5747±566	33±5
	scrPIF	5	7	5596±556	36±6
	PIF	5	8	5536±498	33±5
				ns. p=0.9506	ns. p=0.9255

5. Discussion

During pregnancy, the maternal immune system fulfills a double function. Locally, in close proximity to the fetus, it requires to be desensitized to embryonic tissue in order not to recognize it as a 'semi-allogenic transplant'. Globally, it needs to efficiently protect the organism from viral and bacterial infections. A closer look however reveals that pregnant women are more susceptible to infections^{210,211,212} and that the course of pre-existing autoimmune diseases often appears attenuated^{213,214}. After parturition, the immune system reverts to its non-pregnant state and autoimmune diseases often relapse. These observations argue for pregnancy specific factors, which are able to systemically modulate maternal immune cell functions.

The 15 amino acid small peptide Preimplantation factor (PIF) is expressed by trophoblast cells⁷⁵ and present in maternal serum throughout pregnancy (see Tab. 1.1)⁶⁹. It was shown to modulate immune cell functions in autoimmune disease models outside the context of pregnancy, but the molecular mechanisms, how PIF interferes with immune cells are still elusive. This work examined potential effects of PIF on neutrophil recruitment in acute inflammatory scenarios, reflecting its role in maternal circulation during pregnancy. Conducted experiments revealed that PIF interferes with neutrophil recruitment at several steps by influencing the hematopoietic as well as the endothelial compartment.

5.1. PIF reduces selectin dependent leukocyte rolling

Recruitment of neutrophils to sites of inflammation is initialized by endothelium expressed selectins⁸⁸. Interaction of E- or P-selectin with their ligands PSGL-1, CD44 and ESL-1 on immune cells results in tethering and rolling along inflamed vessels⁸⁷. Administration of PIF in a mouse model of TNF- α induced acute inflammation reduced leukocyte rolling (Fig. 4.18) in cremaster muscle postcapillary venules. Unchanged expression levels of PSGL-1, CD44 and L-selectin in the presence of PIF (Fig. 4.19) and similar rolling behavior in E- or P-selectin coated flow chambers (Fig. 4.23) indicate that altered neutrophil rolling *in vivo* is predominantly caused by PIF affecting the endothelial compartment. Equal E- and P-selectin binding *in vitro* further suggests that PIF unlikely alters glycosylation of selectin ligands, an important prerequisite for selectin-selectin ligand interactions²¹⁵. Reduction of leukocyte rolling *in vivo* by approximately 50% was still observable after blockade of E- or P-selectin dependent rolling, respectively, suggesting that PIF might alter selectin expression in endothelial cells. Cytokines like TNF- α or IL-1 β induce transcriptional upregulation of E- and P-selectin⁹⁴. PIF was shown to reduce serum levels of pro-inflammatory cytokines in LPS induced placental inflammation⁷⁶ and lowers expression of endothelium adhesion molecules in atherosclerotic *ApoE*^{-/-} mice⁸⁴. These observations suggest that PIF treatment might affect selectin expression in TNF- α stimulated endothelial cells, either directly by interfering with

transcription, expression or stability on the surface, or indirectly by changing the cytokine profile. Indeed, Weiss et al. observed reduced transcription of P-selectin in spinal cord tissue of PIF treated animals in an EAE model⁷⁹. Further, this study demonstrated that PIF treatment reduces IL-6 and IL-17 secretion of activated splenocytes, both pro-inflammatory cytokines, influencing expression of adhesion molecules. Whereas IL-6 directly induces E-selectin expression in HUVEC cells *in vitro*²¹⁶, monocytes and macrophages produce TNF- α in response to IL-17²¹⁷, which in turn induces transcriptional upregulation of E-selectin⁹⁴. In contrast to E-selectin, P-selectin is pre-stored in Weibel-Palade bodies and transferred to the luminal surface of endothelial cells within minutes upon stimulation^{218,219}. In trauma induced inflammation, surgical preparation of the mouse cremaster leads to the rapid release of P-selectin and subsequent P-selectin dependent leukocyte rolling⁹¹. Also in this model, PIF treatment reduced leukocyte rolling and at the same time increased rolling velocities (Fig. 4.18). These results suggest that in addition to selectin transcription, mobilization or turn-over rate of P-selectin may be affected by PIF. Besides P-selectin, the tetraspanin CD63 is stored in Weibel-Palade bodies and integrated into the luminal site of the PM of activated endothelial cells as well²²⁰. There, CD63 stabilizes expressed P-selectin and reduces its internalization rate, thereby contributing to P-selectin dependent leukocyte rolling and recruitment²²¹. Loss of CD63 results in reduced leukocyte rolling in mouse cremaster venules. One explanation might therefore be that PIF also affects P-selectin stabilization on the endothelial surface via or similar to CD63. Another molecule regulating neutrophil recruitment by interfering with P-selectin activity is pentraxin 3 (PTX3)²²². Produced and secreted by macrophages²²³, DCs²²⁴ and neutrophils²²⁵, PTX3 binds to P-selectin and competes with PSGL-1 binding, thereby affecting neutrophil-endothelium interaction²²². However, whether PIF regulates expression or activity of either CD63 or PTX3 to modulate P-selectin dependent rolling, requires further investigation.

5.2. PIF disrupts leukocyte adhesion and extravasation

5.2.1. PIF does not affect chemokine induced inside-out β_2 integrin activation

During recruitment, rolling along inflamed endothelium leads to deceleration of neutrophils up to total arrest⁴⁴. In a model of TNF- α induced acute inflammation, mice that were pre-treated with PIF exhibited reduced numbers of adherent leukocyte in postcapillary venules of stimulated cremaster muscles (Fig. 4.1), accompanied by increased slow rolling velocities (Fig. 4.2). In contrast to the decrease in number of rolling cells, reduced leukocyte adhesion and increased rolling velocities could be attributed to a direct effect of PIF on the immune cells, as the same phenotype could be observed in E-selectin, ICAM-1 and CXCL1 coated flow chambers *ex vivo* and *in vitro*. Neutrophil slow rolling and adhesion is mainly mediated by activated LFA-1 integrin binding to its endothelial counterpart ICAM-1¹⁹⁹. GPCR- or TLR4-downstream signaling induces LFA-1 activation, resulting in reduced neutrophil rolling velocities until complete arrest^{120,167}. A crucial intracellular co-factor during β_2 integrin activation is talin-1¹¹¹. Neutrophils lacking talin-1 exhibit disturbed slow rolling and impaired adhesion in TNF- α stimulated cremaster muscle postcapillary

venules¹²⁴. Interestingly, mass spectrometry analysis of human CD14⁺ cell lysates identified talin-1 as a potential interaction partner of PIF⁷⁴, a possible explanation for the observed effects *in vivo*, *ex vivo* and *in vitro*. Surprisingly, PIF did not alter CXCL1 induced binding of LFA-1 to soluble ICAM-1 in murine neutrophils and analysis of human neutrophils revealed no effect of PIF on CXCL8 induced LFA-1 activation (Fig. 4.4). In addition, preliminary pull-down experiments in collaboration with Markus Moser from the Max-Planck Institute of Biochemistry, Martinsried, Germany, could not confirm previously published mass spectrometry data (results not shown). This indicates that GPCR-mediated inside-out LFA-1 activation is not influenced by PIF. Similar surface levels of β_2 integrins and the GPCR CXCR2 (Fig. 4.3) further suggest that different mechanisms cause the adhesion defect in PIF treated animals.

5.2.2. PIF inhibits K_V1.3 on neutrophils

Another study, aiming to reveal interaction partners of PIF using mass spectrometry of human decidual cell lysates and proteome arrays, found a broad spectrum of putative molecules binding to PIF, among them the voltage gated potassium channel K_V1.3⁷⁰. Depolarization of the PM opens this voltage gated ion channel and allows K⁺ to efflux¹⁸¹. K_V1.3 is expressed on vascular smooth muscle cells, cells of the nervous system and on several immune cell subsets¹⁸², namely T lymphocytes²²⁶, B lymphocytes¹⁸⁵, NK cells¹⁸⁶, macrophages¹⁸⁷, DCs¹⁸⁹, and megakaryocytes/platelets¹⁸⁸. Presence of K_V1.3 on neutrophils has never been convincingly described. Already in the early 90s, Krause and Welsh²²⁷ detected a voltage dependent K⁺ current in activated human neutrophils, but they could not attribute it to a specific channel. In a study investigating neutrophils in weak electric fields, K_V1.3 was reported to be expressed in neutrophils¹⁹⁰, but it has not been characterized in regard to neutrophil function, although K_V1.3^{-/-} mice are available since 2003¹⁹¹. Using western blotting, flow cytometry, confocal microscopy (Fig. 4.5) and electrophysiological experiments (Fig. 4.6), the work presented here revealed the definitive existence and functionality of K_V1.3 on human and murine neutrophils. Reduced leukocyte adhesion and accompanied increased slow rolling velocities in TNF- α stimulated cremaster muscle postcapillary venules of K_V1.3^{-/-} mice (Fig. 4.8 and Fig. 4.9) demonstrate an important role of K_V1.3 during leukocyte recruitment. Pre-treatment of WT mice with the specific and well established K_V1.3 inhibitor PAP-1^{196,228} confirmed a significant contribution of K_V1.3 to leukocyte function. Of note, rolling was not affected in these mice (Fig. 4.21), strengthening the hypothesis that PIF affects leukocyte rolling independent of K_V1.3 inhibition on leukocytes, but rather by altering endothelial response to inflammatory cytokines.

With 40 members encoded in the genome, K_V channels form the largest group of K⁺-selective channels in humans²²⁹. Diversity is further increased by formation of heteromers among K_V1 family members. In macrophages for example, K_V1.3 forms heterotetramers with K_V1.5, thereby changing its sensitivity and function²³⁰. Patch clamp experiments demonstrated the voltage dependency of K_V1.3²⁰³, meaning the stronger the membrane depolarization is, the more outward current can be detected. Using this technique in K_V1.3-overexpressing HEK cells, Susanna Zierler and Wiebke Nadolni from Walther-Straub Institute LMU Munich, Munich, Germany, illustrated in collaboration that PIF specifically inhibits K_V1.3 mediated outward currents in a dose-dependent manner with an IC₅₀ of 10.2 \pm 5 nM (Fig. A.1). Patch

clamp with human neutrophils instead of $K_V1.3$ -overexpressing HEK cells further demonstrated that PIF reduces $K_V1.3$ dependent currents also in this cell type to a similar extent as PAP-1 (Fig. 4.11).

These findings reveal that PIF reduces K^+ outward currents in neutrophils by inhibiting $K_V1.3$. $K_V1.3$ may have an important role during leukocyte recruitment as shown by the use of the pharmacological $K_V1.3$ inhibitor PAP-1 *in vivo* and by $K_V1.3^{-/-}$ mice.

5.2.3. $K_V1.3$ on neutrophils regulates $[Ca^{2+}]_i$

In T lymphocytes, K^+ efflux via $K_V1.3$ regulates sustained Ca^{2+} entry through Ca^{2+} release-activated Ca^{2+} (CRAC) channels by maintaining an electrochemical gradient over the PM (Fig. 1.6)¹⁵⁶. Measuring $[Ca^{2+}]_i$ in human neutrophils under static and flow conditions, Scott I Simon and Vasilios Morikis from the University of California, Davies, USA were able to demonstrate that inhibition of $K_V1.3$ with PIF reduces SOCE via CRAC channels (Fig. A.2), affecting overall changes in $[Ca^{2+}]_i$ (Fig. A.3). In neutrophils, LFA-1 outside-in signaling under shear stress conditions leads to Ca^{2+} influx via CRAC channels¹⁵⁹. Using microfluidic devices coated with ICAM-1 and LFA-1 high affinity inducing antibodies, they could further unravel a contribution of $K_V1.3$ in mechanotransduced Ca^{2+} signaling (Fig. A.4).

In neutrophils, many functions depend on changes in $[Ca^{2+}]_i$ ¹⁵⁸ and impaired calcium signaling can lead to severe dysregulation of immune responses^{231,232,233}. Patients with mutations in Orai1 or STIM1 for example suffer from immunodeficiency-like disorders which are often accompanied by neutropenia and increased susceptibility to infections or sepsis²³⁴. During recruitment, high $[Ca^{2+}]_i$ is a prerequisite for neutrophils to firmly adhere and to switch to a migratory phenotype¹⁸⁰. Impaired calcium signaling results in disturbed deceleration, arrest and polarization^{165,166}. Under shear, tensile forces acting on LFA-1-ICAM-1 bonds recruit kindlin-3 to intracellular β_2 integrin tails (Fig. 1.5)¹⁸⁰. Kindlin-3 in turn links Orai1 to this complex^{166,180}, ensuring local increase of $[Ca^{2+}]_i$ ¹⁷⁶. High concentrations of Ca^{2+} at focal adhesion sites are required for recruitment of talin-1 and subsequent linkage of adhesion spots to the actin cytoskeleton¹⁸⁰. Thereby, receptor for activated protein kinase C-1 (RACK-1) was shown to be an important co-factor, as it is able to interact with kindlin-3, LFA-1²³⁵ and Orai1²³⁶. This has led to the hypothesis that kindlin-3/Orai1/LFA-1 focal clusters develop upon integrin outside-in mechanosignaling, resulting in Ca^{2+} -rich microdomains. High local Ca^{2+} concentrations enable linkage of focal adhesion sites to the actin cytoskeleton and ensuing fast and efficient cytoskeletal reorganization. This hypothesis is supported by observations that Ca^{2+} -rich microdomains are located in uropods of human neutrophils²³⁷, overlapping with clustered LFA-1^{150,238}. This work now adds evidence that K^+ efflux via $K_V1.3$ is involved in establishing multi-molecule platforms around activated and ICAM-1 bound LFA-1, as inhibition of $K_V1.3$ resulted in reduced $[Ca^{2+}]_i$ and subsequent impaired cytoskeletal rearrangement. In line with these findings, ion channels, especially K^+ channels have been shown to interact with integrins in other cell types, regulating integrin affinity and downstream signaling²³⁹. In melanoma cells²⁴⁰ and T lymphocytes²⁰⁰, $K_V1.3$ physically interacts with β_1 integrins and its inhibition disrupts $K_V1.3$ - β_1 integrin interaction²⁴⁰, indicating that physical interaction depends on channel activity. Impaired neutrophil spreading resulted in increased susceptibility to physiological shear rates *in vitro*

(Fig. A.5) and *in vivo* (Fig. 4.13). Application of soluble CXCL1 *in vivo* resulted in a rapid increase of adherent leukocytes also in PIF pre-treated animals, confirming the hypothesis that chemokine mediated inside-out LFA-1 activation is not affected by PIF (4.1.4). 6 minutes after CXCL1 administration in turn, PIF mediated inhibition of $K_V1.3$ impaired outside-in mechanosignaling via activated LFA-1, thereby reducing the ability of neutrophils to sustain adhesion to vessel walls.

5.2.4. PIF lowers the number of perivascular neutrophils

PIF treatment resulted in reduced numbers of extravasated neutrophils into TNF- α inflamed cremaster muscle tissue (Fig. 4.14). This effect could be attributed to its inhibitory properties on $K_V1.3$, since both $K_V1.3^{-/-}$ mice and PAP-1 treated WT mice exhibited a reduction of perivascular neutrophils (Fig. 4.15). The question remains whether impaired transmigration upon inhibition of $K_V1.3$ is simply a consequence of disrupted neutrophil adhesion, or whether $K_V1.3$ also regulates neutrophil functions important for diapedesis. Not only cytoskeletal rearrangement during adhesion strengthening, but neutrophil migration in general is highly dependent on Ca^{2+} signaling¹⁷⁴. Besides Orai1¹⁶⁶, additional calcium channels like TRPC1²⁴¹ or TRPC6¹⁷⁰ have been implicated to be involved in neutrophil migration. Also potassium efflux regulates neutrophil migration and chemotaxis, as genetic loss or pharmacological inhibition of the Ca^{2+} activated potassium channel $K_{Ca}3.1$ leads to reduced chemotactic behavior²⁰⁵. Hence, it is conceivable that $K_V1.3$ also mediates migration, chemotaxis and transmigration in neutrophils. Evidence comes from other cell types. In microglia cells, reduced expression of $K_V1.3$ goes along with reduced motility and lower β_1 integrin expression²⁴² Further, effector memory T (T_{EM}) cells²⁴³ and macrophages^{201,244} exhibit a reduced migratory phenotype in response to $K_V1.3$ inhibitors. However, sensing of a CXCL1 chemokine gradient in a transwell assay was not affected by PIF (Fig. 4.16). Experiments investigating the precise role of PIF and $K_V1.3$ in neutrophil migration, chemotaxis and transmigration are currently ongoing and part of a medical doctoral thesis under my co-supervision.

Summarizing the findings, inhibition of $K_V1.3$ on neutrophils by PIF disrupts sustained Ca^{2+} influx and thereby prevents neutrophil spreading and adhesion strengthening (Fig. 5.1), leading to impaired recruitment into inflamed tissue.

5.3. PIF as a potential therapeutic drug to treat inflammatory diseases

Effective host defense against invading pathogens requires fast and precisely reacting neutrophils⁴⁴. However, many diseases like rheumatoid arthritis, psoriasis, inflammatory bowel disease, COPD, or acute lung injury (ALI) are associated with massive neutrophil infiltration^{206,207,245}. Overreacting immune responses and uncontrolled neutrophil recruitment can cause tissue damage and self amplification of inflammation²⁴⁶. To investigate the therapeutic potential of PIF in treating unwanted neutrophil infiltration into inflamed tissue, Oliver

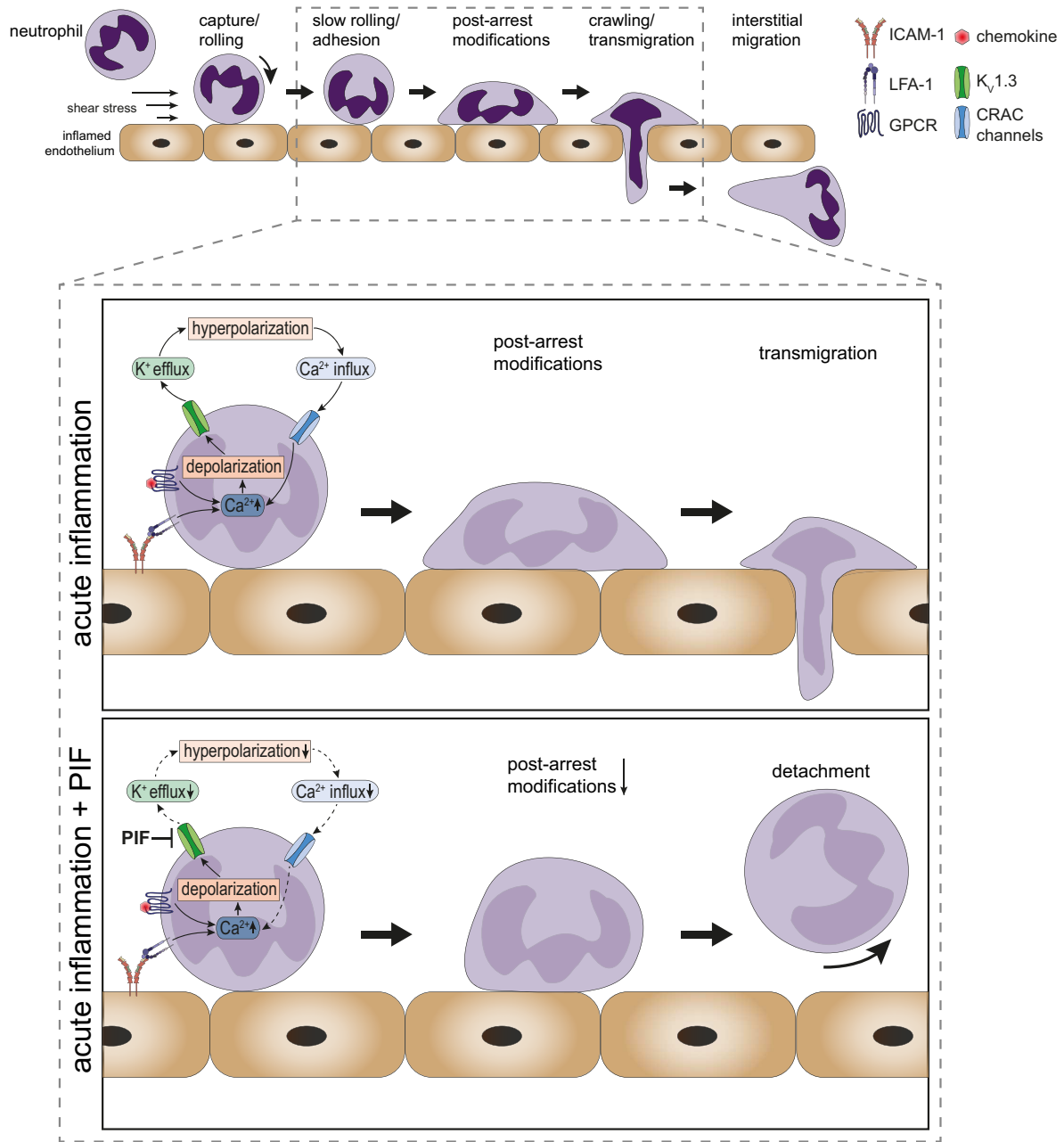


Figure 5.1.: PIF disrupts neutrophil recruitment by reducing K_v1.3-regulated SOCE. PIF inhibits the voltage-gated potassium channel K_v1.3 on neutrophils which regulates sustained Ca²⁺ via SOCE. During neutrophil recruitment, lower [Ca²⁺]_i reduces the ability of adherent neutrophils to spread and to switch to a migratory phenotype. As a consequence, cells are more susceptible to physiological shear forces and detach back into the blood stream.

Söhnlein from the Institute for Cardiovascular Prevention (IPEK), LMU Munich, Munich, Germany, Jochen Grommes and Jessica Tilgner from the RWTH Aachen, Aachen, Germany tested the small peptide in a mouse model for LPS induced ALI. In ALI as well as in acute respiratory distress syndrome (ARDS), epithelial and endothelial damage increase permeability of the alveolar-capillary barrier, leading to increased protein-rich fluid in alveoli,

accompanied by impaired gas exchange and respiratory failure²⁴⁷. Severity of ALI correlates with numbers of infiltrating neutrophils²⁴⁸. Therefore, control of neutrophil infiltration might be an interesting option to treat inflammatory diseases like ALI or ARDS. Blocking $K_V1.3$ activity with PIF reduced LPS induced neutrophil infiltration into inflamed lungs (Fig. A.6). Importantly, PIF treatment reduced vascular leakage and protein content in the BAL (Fig. A.6), revealing its potential to prevent neutrophil recruitment and accompanying tissue damage in a clinically relevant setting (Fig. 5.1).

In the last decades, many drugs have been developed to suppress inflammatory diseases by interfering with leukocyte recruitment and migration²⁴⁹. Nevertheless, there is a need to develop additional treatments, since many approaches failed during trial phases²⁵⁰. This work provides evidence that trophoblast derived PIF is able to disrupt neutrophil recruitment by blocking $K_V1.3$. In animal models for autoimmune diseases like multiples sclerosis (MS)⁷⁹, type I diabetes mellitus⁷⁸ or graft versus host disease after bone marrow transplantation⁸², PIF attenuated progression of the diseases by lowering the amount of infiltrating immune cells into affected tissue. A safety study, testing PIF in patients with immune hepatitis is currently ongoing²⁵¹.

Over the past years, $K_V1.3$ has become the subject of intensive research in T lymphocyte biology¹⁸³. In quiescent naive, central memory (T_{CM}) T and T_{EM} cells, $K_V1.3$ is expressed to a similar extent (~ 250 channels per cell)²⁵². Upon activation, $K_V1.3$ gets upregulated in T_{EM} cells (~ 1500 channels per cell), but only to a minor extent in naive T and T_{CM} cells (~ 300 channels per cell). T_{EM} cells play a pivotal role in the pathogenesis of autoimmune diseases²⁵³. They are terminally differentiated T cells which rapidly enter inflamed tissues upon activation²⁵², where they contribute to disease progression by releasing pro-inflammatory cytokines¹⁸¹. Inhibiting T_{EM} cells may be therefore a suitable approach to treat autoimmune diseases and many different $K_V1.3$ inhibitors have been designed^{196,181,228} and tested in several disease models including MS^{252,254}, T1DM²⁵⁵ and psoriasis²⁵⁶. Even outside autoimmune diseases, in animal models for obesity and insulin resistance, $K_V1.3$ inhibitors have been suggested as a potential treatment strategy²⁵⁷. This study introduces a new $K_V1.3$ inhibitor, the endogenous peptide PIF, and provides evidence that PIF attenuates progression of autoimmune diseases in animal models by interfering with $K_V1.3$ activity. Showing that $K_V1.3$ is expressed on neutrophils is of further interest, since there is emerging evidence that neutrophils contribute to a large extent to the progression of classically-seen T cell driven diseases like psoriasis, MS or T1DM^{245,258}. Interestingly, psoriasis, an autoimmune disease where neutrophil infiltration plays an important role in the progression of the disease²⁵⁹ is successfully treated with 5-Methoxypsoralen (5-MOP), a $K_V1.3$ blocker¹⁸².

5.4. PIF modulates immune cells during pregnancy

$K_V1.3$ is expressed on all leukocyte subsets which can be found in the placenta during pregnancy. Consequently, it is very likely that PIF contributes to the establishment of the unique immunological milieu around the fetus by influencing immune cells to a similar extent as demonstrated in models for autoimmune diseases. Indeed, $K_V1.3^{-/-}$ Foxp3⁻ helper T (T_h) cells exhibit a unique, IL-10 expressing, regulatory phenotype in an EAE model for MS²⁶⁰, suggesting that constant inhibition or lack of $K_V1.3$ shifts T cells into an anti-

inflammatory phenotype.

The primary aim of this work was to study the role of PIF in acute inflammatory scenarios. The use of several *in vivo*, *ex vivo* and *in vitro* approaches demonstrated that PIF alters neutrophil function, by interfering with calcium signaling, leading to impaired adhesion strengthening after arrest. PIF reduces $[Ca^{2+}]_i$ by blocking $K_V1.3$ with an IC_{50} of 10.2 ± 5 nM. Many functions in neutrophils rely on changes in $[Ca^{2+}]_i$ ¹⁵⁸, among them phagocytosis and ROS production¹⁷⁵. Neutrophils from pregnant women exhibit an overall reduced phagocytic activity²⁶¹ and diminished ROS production²⁶². Diminished ROS production in pregnancy could be attributed to a factor present in the plasma of pregnant women, as plasma from pregnant women reduced ROS production in neutrophils from non-pregnant women²⁶³. In addition, serum from pregnant mice reduces T cell activation²⁶⁴ and neutrophils exhibit changes in their Ca^{2+} oscillations upon contact with trophoblast cells *in vitro*²⁶⁵. This work suggests that PIF, present in maternal circulation throughout pregnancy, may be involved in reduced phagocytic activity and diminished ROS production of peripheral neutrophils from pregnant women, thereby increasing susceptibility to infections. In addition, PIF in maternal circulation throughout pregnancy may be an explanation why pre-existing autoimmune diseases attenuate during this period. Concentration of PIF in serum from pregnant women is around 50-60 nM, depending on the gestational age⁶⁹. By showing that PIF inhibits $K_V1.3$ with an IC_{50} of 10.2 ± 5 nM, this study suggests that plasma PIF levels during pregnancy are sufficient to interfere with functions of peripheral immune cells. However, further studies are necessary to proof whether PIF indeed modulates peripheral immune responses during pregnancy, thereby increasing susceptibility to infectious diseases and attenuating autoimmune disorders.

5.5. Conclusion

In summary, the presented data demonstrate that the embryo-derived peptide Preimplantation factor (PIF) alters immune responses in acute inflammatory scenarios. It reduces selectin-dependent leukocyte rolling along inflamed vessels, most likely by altering transcription, expression or stability of selectins on inflamed endothelial cells. PIF further directly interferes with neutrophil function by blocking the voltage gated potassium channel $K_V1.3$ on neutrophils. Inhibition of $K_V1.3$ lowers sustained Ca^{2+} entry via CRAC channels, thereby impairing cytoskeletal rearrangement during leukocyte recruitment. Hence, under physiological shear stress conditions, neutrophils are not able to efficiently adhere to inflamed endothelium and to extravasate into the surrounding tissue.

These findings for the first time uncover the role of PIF in neutrophil function at the molecular level and help to better understand how maternal immune cells are modulated during pregnancy in the placenta, but also systemically by extra-embryonic derived signaling molecules. Furthermore, it demonstrates the potency of PIF as an anti-inflammatory agent in acute and chronic inflammatory diseases, through blocking $K_V1.3$ function in neutrophils. Further studies are now warranted to test whether these findings can be successfully translated into the clinical setting. Hence, PIF might turn out to be a versatile and rather safe treatment strategy in a whole variety of disorders with disturbed innate and adaptive immunity.

Bibliography

- [1] S. E. Ander, M. S. Diamond, and C. B. Coyne, "Immune responses at the maternal-fetal interface," *Science Immunology*, vol. 4, no. 31, p. eaat6114, 2019.
- [2] H. Wang, S. Zhang, H. Lin, S. Kong, S. Wang, H. Wang, and D. R. Armant, "Physiological and molecular determinants of embryo implantation," *Molecular Aspects of Medicine*, vol. 34, no. 5, pp. 939–980, 2013.
- [3] M. Mori, A. Bogdan, T. Balassa, T. Csabai, and J. Szekeres-Bartho, "The decidua—the maternal bed embracing the embryo—maintains the pregnancy," *Seminars in Immunopathology*, vol. 38, no. 6, pp. 635–649, 2016.
- [4] N. Lamond and N. Freitag, "Vertical Transmission of *Listeria monocytogenes*: Probing the Balance between Protection from Pathogens and Fetal Tolerance," *Pathogens*, vol. 7, no. 2, p. 52, 2018.
- [5] J. Pollheimer, S. Vondra, J. Baltayeva, A. G. Beristain, and M. Knöfler, "Regulation of placental extravillous trophoblasts by the maternal uterine environment," *Frontiers in Immunology*, vol. 9, no. 2507, pp. 1–18, 2018.
- [6] G. Mor, P. Aldo, and A. B. Alvero, "The unique immunological and microbial aspects of pregnancy," *Nature Reviews Immunology*, vol. 17, no. 8, pp. 469–482, 2017.
- [7] A. C. Zenclussen and G. J. Hämmerling, "Cellular regulation of the uterine microenvironment that enables embryo implantation," *Frontiers in Immunology*, vol. 6, no. 321, 2015.
- [8] H. Deshmukh and S. S. Way, "Immunological Basis for Recurrent Fetal Loss and Pregnancy Complications," *Annual Review of Pathology: Mechanisms of Disease*, vol. 14, no. 1, pp. 185–210, 2019.
- [9] G. Mor and I. Cardenas, "The Immune System in Pregnancy: A Unique Complexity," *American Journal of Reproductive Immunology*, vol. 63, no. 6, pp. 425–433, 2010.
- [10] S. Oertelt-Prigione, "Immunology and the menstrual cycle," *Autoimmunity Reviews*, vol. 11, no. 6-7, pp. A486–A492, 2012.
- [11] E. R. Norwitz, E. A. Bonney, V. V. Snegovskikh, M. A. Williams, M. Phillippe, J. S. Park, and V. M. Abrahams, "Molecular regulation of parturition: The role of the decidual clock," *Cold Spring Harbor Perspectives in Medicine*, vol. 5, no. 11, 2015.

- [12] V. Plaks, T. Birnberg, T. Berkutzki, S. Sela, A. BenYashar, V. Kalchenko, G. Mor, E. Keshet, N. Dekel, M. Neeman, and S. Jung, "Uterine DCs are crucial for decidua formation during embryo implantation in mice," *Journal of Clinical Investigation*, vol. 118, no. 12, pp. 3954–3965, 2008.
- [13] G. Schofield and S. J. Kimber, "Leukocyte Subpopulations in the Uteri of Leukemia Inhibitory Factor Knockout Mice During Early Pregnancy¹," *Biology of Reproduction*, vol. 72, no. 4, pp. 872–878, 2005.
- [14] Y. Gnainsky, I. Granot, P. Aldo, A. Barash, Y. Or, G. Mor, and N. Dekel, "Biopsy-induced inflammatory conditions improve endometrial receptivity: The mechanism of action," *Reproduction*, vol. 149, no. 1, pp. 75–85, 2015.
- [15] R. Romero, J. Espinoza, L. F. Goncalves, J. P. Kusanovic, L. F. Friel, and S. Hassan, "The role of inflammation and infection in preterm birth," *Seminars in Reproductive Medicine*, vol. 25, no. 1, pp. 21–39, 2007.
- [16] T. M. Lindström and P. R. Bennett, "The role of nuclear factor kappa B in human labour," *Reproduction*, vol. 130, no. 5, pp. 569–581, 2005.
- [17] N. Gomez-Lopez, D. StLouis, M. A. Lehr, E. N. Sanchez-Rodriguez, and M. Arenas-Hernandez, "Immune cells in term and preterm labor," *Cellular and Molecular Immunology*, vol. 11, no. 6, pp. 571–581, 2014.
- [18] S. Giaglis, M. Stoikou, F. Grimolizzi, B. Y. Subramanian, S. V. van Breda, I. Hoesli, O. Lapaire, P. Hasler, N. G. Than, and S. Hahn, "Neutrophil migration into the placenta: Good, bad or deadly?," *Cell Adhesion and Migration*, vol. 10, no. 1-2, pp. 208–225, 2016.
- [19] M. Kwan, A. Hazan, J. Zhang, R. L. Jones, L. K. Harris, W. Whittle, S. Keating, C. E. Dunk, and S. J. Lye, "Dynamic changes in maternal decidual leukocyte populations from first to second trimester gestation," *Placenta*, vol. 35, no. 12, pp. 1027–1034, 2014.
- [20] A. Moffett-King, "Natural killer cells and pregnancy," *Nature Reviews Immunology*, vol. 2, no. 9, pp. 656–663, 2002.
- [21] J. Hanna, D. Goldman-Wohl, Y. Hamani, I. Avraham, C. Greenfield, S. Natanson-Yaron, D. Prus, L. Cohen-Daniel, T. I. Arnon, I. Manaster, R. Gazit, V. Yutkin, D. Benharroch, A. Porgador, E. Keshet, S. Yagel, and O. Mandelboim, "Decidual NK cells regulate key developmental processes at the human fetal-maternal interface," *Nature Medicine*, vol. 12, no. 9, pp. 1065–1074, 2006.
- [22] A. A. Ashkar and B. A. Croy, "Functions of uterine natural killer cells are mediated by interferon gamma production during murine pregnancy," *Seminars in Immunology*, vol. 13, no. 4, pp. 235–241, 2001.
- [23] L. M. Gaynor and F. Colucci, "Uterine natural killer cells: Functional distinctions and influence on pregnancy in humans and mice," *Frontiers in Immunology*, vol. 8, no. 467, 2017.

- [24] M.-J. Guimond, J. A. Luross, B. Wang, C. Terhorst, S. Danial, and B. Anne Croy, "Absence of Natural Killer Cells during Murine Pregnancy is Associated with Reproductive Compromise in TgE26 Mice¹," *Biology of Reproduction*, vol. 56, no. 1, pp. 169–179, 1997.
- [25] L. D. Klentzeris, J. N. Bulmer, M. A. Warren, L. Morrison, T. C. Li, and I. D. Cooke, "Lymphoid tissue in the endometrium of women with unexplained infertility: Morphometric and immunohistochemical aspects," *Human Reproduction*, vol. 9, no. 4, pp. 646–652, 1994.
- [26] S. Liu, L. Diao, C. Huang, Y. Li, Y. Zeng, and J. Y. Kwak-Kim, "The role of decidual immune cells on human pregnancy," *Journal of Reproductive Immunology*, vol. 124, pp. 44–53, 2017.
- [27] C. Gustafsson, J. Mjösberg, A. Matussek, R. Geffers, L. Matthiesen, G. Berg, S. Sharma, J. Buer, and J. Ernerudh, "Gene expression profiling of human decidual macrophages: Evidence for immunosuppressive phenotype," *PLoS ONE*, vol. 3, no. 4, p. e2078, 2008.
- [28] A. D. Hazan, S. D. Smith, R. L. Jones, W. Whittle, S. J. Lye, and C. E. Dunk, "Vascular-Leukocyte Interactions. Mechanisms of Human Decidual Spiral Artery Remodeling in Vitro," *The American Journal of Pathology*, vol. 177, no. 2, pp. 1017–1030, 2010.
- [29] A. S. Care, K. R. Diener, M. J. Jasper, H. M. Brown, W. V. Ingman, and S. A. Robertson, "Macrophages regulate corpus luteum development during embryo implantation in mice," *Journal of Clinical Investigation*, vol. 123, no. 8, pp. 3472–3487, 2013.
- [30] V. M. Abrahams, Y. M. Kim, S. L. Straszewski, R. Romero, and G. Mor, "Macrophages and Apoptotic Cell Clearance During Pregnancy," *American Journal of Reproductive Immunology*, vol. 51, no. 4, pp. 275–282, 2004.
- [31] F. Ning, H. Liu, and G. E. Lash, "The Role of Decidual Macrophages During Normal and Pathological Pregnancy," *American Journal of Reproductive Immunology*, vol. 75, no. 3, pp. 298–309, 2016.
- [32] K. J. Payne, L. A. Clyde, A. J. Weldon, T.-A. Milford, and S. M. Yellon, "Residency and Activation of Myeloid Cells During Remodeling of the Prepartum Murine Cervix¹," *Biology of Reproduction*, vol. 87, no. 5, pp. 1–7, 2012.
- [33] B. Timmons, M. Akins, and M. Mahendroo, "Cervical remodeling during pregnancy and parturition," *Trends in Endocrinology and Metabolism*, vol. 21, no. 6, pp. 353–361, 2010.
- [34] A. Erlebacher, "Mechanisms of T cell tolerance towards the allogeneic fetus," *Nature Reviews Immunology*, vol. 13, no. 1, pp. 23–33, 2012.
- [35] P. Nancy and A. Erlebacher, "T cell behavior at the maternal-fetal interface," *International Journal of Developmental Biology*, vol. 58, no. 2-4, pp. 189–198, 2014.

- [36] A. Teles, A. Schumacher, M. C. Kühnle, N. Linzke, C. Thuere, P. Reichardt, C. E. Tadokoro, G. J. Hämmerling, and A. C. Zenclussen, "Control of uterine microenvironment by Foxp3+ cells facilitates embryo implantation," *Frontiers in Immunology*, vol. 4, no. 158, pp. 1–12, 2013.
- [37] M. J. Jasper, K. P. Tremellen, and S. A. Robertson, "Primary unexplained infertility is associated with reduced expression of the T-regulatory cell transcription factor Foxp3 in endometrial tissue," *Molecular Human Reproduction*, vol. 12, no. 5, pp. 301–308, 2006.
- [38] J. H. Rowe, J. M. Ertelt, L. Xin, and S. S. Way, "Pregnancy imprints regulatory memory that sustains anergy to fetal antigen," *Nature*, vol. 490, no. 7418, pp. 102–106, 2012.
- [39] M. L. Zenclussen, C. Thuere, N. Ahmad, P. O. Wafula, S. Fest, A. Teles, A. Leber, P. A. Casalis, I. Bechmann, J. Priller, H. D. Volk, and A. C. Zenclussen, "The persistence of paternal antigens in the maternal body is involved in regulatory T-cell expansion and fetal-maternal tolerance in murine pregnancy," *American Journal of Reproductive Immunology*, vol. 63, no. 3, pp. 200–208, 2010.
- [40] D. J. Sharkey, K. P. Tremellen, M. J. Jasper, K. Gemzell-Danielsson, and S. A. Robertson, "Seminal Fluid Induces Leukocyte Recruitment and Cytokine and Chemokine mRNA Expression in the Human Cervix after Coitus," *The Journal of Immunology*, vol. 188, no. 5, pp. 2445–2454, 2012.
- [41] M.-R. Du, P.-F. Guo, H.-L. Piao, S.-C. Wang, C. Sun, L.-P. Jin, Y. Tao, Y.-H. Li, D. Zhang, R. Zhu, Q. Fu, and D.-J. Li, "Embryonic Trophoblasts Induce Decidual Regulatory T Cell Differentiation and Maternal-Fetal Tolerance through Thymic Stromal Lymphopoietin Instructing Dendritic Cells," *The Journal of Immunology*, vol. 192, no. 4, pp. 1502–1511, 2014.
- [42] P. Hsu, B. Santner-Nanan, J. E. Dahlstrom, M. Fadia, A. Chandra, M. Peek, and R. Nanan, "Altered decidual DC-SIGN+ antigen-presenting cells and impaired regulatory T-cell induction in preeclampsia," *American Journal of Pathology*, vol. 181, no. 6, pp. 2149–2160, 2012.
- [43] G. Amodio, A. Mugione, A. M. Sanchez, P. Viganò, M. Candiani, E. Somigliana, M. G. Roncarolo, P. Panina-Bordignon, and S. Gregori, "HLA-G expressing DC-10 and CD4+T cells accumulate in human decidua during pregnancy," *Human Immunology*, vol. 74, no. 4, pp. 406–411, 2013.
- [44] E. Kolaczowska and P. Kubes, "Neutrophil recruitment and function in health and inflammation.," *Nature reviews. Immunology*, vol. 13, no. 3, pp. 159–175, 2013.
- [45] S. Hahn, S. Giaglis, I. Hoesli, and P. Hasler, "Neutrophil NETs in reproduction : from infertility to preeclampsia and the possibility of fetal loss," *Frontiers in Immunology*, vol. 3, no. 362, pp. 1–8, 2012.
- [46] A. K. Gupta, P. Hasler, W. Holzgreve, S. Gebhardt, and S. Hahn, "Induction of Neutrophil Extracellular DNA Lattices by Placental Microparticles and IL-8 and Their Presence in Preeclampsia," *Human Immunology*, vol. 66, no. 11, pp. 1146–1154, 2005.

- [47] A. K. Gupta, P. Hasler, W. Holzgreve, and S. Hahn, "Neutrophil NETs: A novel contributor to preeclampsia-associated placental hypoxia?," *Seminars in Immunopathology*, vol. 29, no. 2, pp. 163–167, 2007.
- [48] P. Redecha, R. Tilley, M. Tencati, J. E. Salmon, D. Kirchhofer, N. Mackman, and G. Girardi, "Tissue factor : a link between C5a and neutrophil activation in antiphospholipid antibody-induced fetal injury," *Blood*, vol. 110, no. 7, pp. 2423–2432, 2007.
- [49] H. Amsalem, M. Kwan, A. Hazan, J. Zhang, R. L. Jones, W. Whittle, J. C. P. Kingdom, B. A. Croy, S. J. Lye, and C. E. Dunk, "Identification of a Novel Neutrophil Population: Proangiogenic Granulocytes in Second-Trimester Human Decidua," *The Journal of Immunology*, vol. 193, no. 6, pp. 3070–3079, 2014.
- [50] M. Winkler, D.-C. Fischer, P. Ruck, T. Marx, E. Kaiserling, A. Operpichler, H. Tschesche, and W. Rath, "Parturition at term: parallel increases in interleukin-8 and proteinase concentrations and neutrophil count in the lower uterine segment," *Human Reproduction*, vol. 14, no. 4, pp. 1096–1100, 1999.
- [51] J. Svensson-Arvelund, R. B. Mehta, R. Lindau, E. Mirrasekhian, H. Rodriguez-Martinez, G. Berg, G. E. Lash, M. C. Jenmalm, and J. Ernerudh, "The Human Fetal Placenta Promotes Tolerance against the Semiallogeneic Fetus by Inducing Regulatory T Cells and Homeostatic M2 Macrophages," *The Journal of Immunology*, vol. 194, no. 4, pp. 1534–1544, 2015.
- [52] R. Ramhorst, L. Fraccaroli, P. Aldo, A. B. Alvero, I. Cardenas, C. P. Leirós, and G. Mor, "Modulation and recruitment of inducible regulatory T cells by first trimester trophoblast cells," *American Journal of Reproductive Immunology*, vol. 67, no. 1, pp. 17–27, 2012.
- [53] P. B. Aldo, K. Racicot, V. Craviero, S. Guller, R. Romero, and G. Mor, "Trophoblast induces monocyte differentiation into CD14+/CD16+ macrophages," *American Journal of Reproductive Immunology*, vol. 72, no. 3, pp. 270–284, 2014.
- [54] J. Madigan, D. J. Freeman, F. Menzies, S. Forrow, S. M. Nelson, A. Young, A. Sharkey, A. Moffett, G. J. Graham, I. A. Greer, A. Rot, and R. J. B. Nibbs, "Chemokine Scavenger D6 Is Expressed by Trophoblasts and Aids the Survival of Mouse Embryos Transferred into Allogeneic Recipients," *The Journal of Immunology*, vol. 184, no. 6, pp. 3202–3212, 2010.
- [55] P. J. Teoh, F. M. Menzies, C. A. H. Hansell, M. Clarke, C. Waddell, G. J. Burton, S. M. Nelson, and R. J. B. Nibbs, "Atypical Chemokine Receptor ACKR2 Mediates Chemokine Scavenging by Primary Human Trophoblasts and Can Regulate Fetal Growth, Placental Structure, and Neonatal Mortality in Mice," *The Journal of Immunology*, vol. 193, no. 10, pp. 5218–5228, 2014.
- [56] S. Kovats, E. K. Main, C. Librach, M. Stubblebine, S. J. Fisher, and R. DeMars, "A Class I Antigen, HLA-G, Expressed in Human Trophoblasts," *Science*, vol. 248, no. 4952, pp. 220–223, 1990.

- [57] T. G. Poehlmann, A. Schaumann, S. Busch, J. S. Fitzgerald, M. Aguerre-Girr, P. Le Bouteiller, E. Schleussner, and U. R. Markert, "Inhibition of term decidual NK cell cytotoxicity by soluble HLA-G1," *American Journal of Reproductive Immunology*, vol. 56, no. 5-6, pp. 275–285, 2006.
- [58] S. Rajagopalan and E. O. Long, "A Human Histocompatibility Leukocyte Antigen (HLA)-G-specific Receptor Expressed on All Natural Killer Cells," *The Journal of Experimental Medicine*, vol. 189, no. 7, pp. 1093–1100, 1999.
- [59] L. M. Ferreira, T. B. Meissner, T. Tilburgs, and J. L. Strominger, "HLA-G: At the Interface of Maternal–Fetal Tolerance," *Trends in Immunology*, vol. 38, no. 4, pp. 272–286, 2017.
- [60] C. Li, B. L. Houser, M. L. Nicotra, and J. L. Strominger, "HLA-G homodimer-induced cytokine secretion through HLA-G receptors on human decidual macrophages and natural killer cells," *Proceedings of the National Academy of Sciences*, vol. 106, no. 14, pp. 5767–5772, 2009.
- [61] D. R. Bainbridge, S. A. Ellis, and I. L. Sargent, "HLA-G suppresses proliferation of CD4+ T-lymphocytes," *Journal of Reproductive Immunology*, vol. 48, no. 1, pp. 17–26, 2000.
- [62] A. Naji, C. Menier, F. Morandi, S. Agaoglu, G. Maki, E. Ferretti, S. Bruel, V. Pistoia, E. D. Carosella, and N. Rouas-Freiss, "Binding of HLA-G to ITIM-Bearing Ig-like Transcript 2 Receptor Suppresses B Cell Responses," *The Journal of Immunology*, vol. 192, no. 4, pp. 1536–1546, 2014.
- [63] M. Shiroishi, K. Tsumoto, K. Amano, Y. Shirakihara, M. Colonna, V. M. Braud, D. S. J. Allan, A. Makadzange, S. Rowland-Jones, B. Willcox, E. Y. Jones, P. A. van der Merwe, I. Kumagai, and K. Maenaka, "Human inhibitory receptors Ig-like transcript 2 (ILT2) and ILT4 compete with CD8 for MHC class I binding and bind preferentially to HLA-G," *Proceedings of the National Academy of Sciences of the United States of America*, vol. 100, no. 15, pp. 8856–8861, 2003.
- [64] E. R. Barnea, "Applying embryo-derived immune tolerance to the treatment of immune disorders," *Annals of the New York Academy of Sciences*, vol. 1110, pp. 602–618, 2007.
- [65] E. R. Barnea, D. Kirk, S. Ramu, B. Rivnay, R. Roussev, and M. J. Paidas, "PreImplantation Factor (PIF) orchestrates systemic antiinflammatory response by immune cells: effect on peripheral blood mononuclear cells," *American Journal of Obstetrics and Gynecology*, vol. 207, no. 4, pp. 313.e1–313.e11, 2012.
- [66] S. Ramu, C. Stamatkin, L. Timms, M. Ruble, R. G. Roussev, and E. R. Barnea, "PreImplantation factor (PIF) detection in maternal circulation in early pregnancy correlates with live birth (bovine model)," *Reproductive Biology and Endocrinology*, vol. 11, no. 105, 2013.
- [67] H. Moindjie, E. D. Santos, L. Loeuillet, H. Gronier, P. de Mazancourt, E. R. Barnea, F. Vialard, and M.-N. Dieudonne, "Preimplantation Factor (PIF) Promotes Human Trophoblast Invasion," *Biology of Reproduction*, vol. 91, no. 5, pp. 1–10, 2014.

- [68] C. W. Stamatkin, R. G. Roussev, M. Stout, V. Absalon-Medina, S. Ramu, C. Goodman, C. B. Coulam, R. O. Gilbert, R. a. Godke, and E. R. Barnea, "PreImplantation Factor (PIF) correlates with early mammalian embryo development-bovine and murine models.," *Reproductive Biology and Endocrinology*, vol. 9, no. 63, pp. 1–11, 2011.
- [69] P. Tzonis, T. Moschandreu, T. Keramitsoglou, G. Perros, M. Farmakidis, M. Varla-Leftherioti, and E. Barnea, "Kinetics of circulating preimplantation factor (PIF) levels during pregnancy," *Journal of Reproductive Immunology*, vol. 86, no. 1, p. 42, 2010.
- [70] M. J. Paidas, G. Krikun, S. J. Huang, R. Jones, M. Romano, J. Annunziato, and E. R. Barnea, "A genomic and proteomic investigation of the impact of preimplantation factor on human decidual cells," *American Journal of Obstetrics and Gynecology*, vol. 202, no. 5, pp. 459.e1–459.e8, 2010.
- [71] C. M. Duzyj, E. R. Barnea, M. Li, S. J. Huang, G. Krikun, and M. J. Paidas, "Preimplantation factor promotes first trimester trophoblast invasion," *American Journal of Obstetrics and Gynecology*, vol. 203, no. 4, pp. 402.e1–402.e4, 2010.
- [72] M. Yang, Y. Yang, S. She, and S. Li, "Proteomic investigation of the effects of preimplantation factor on human embryo implantation," *Molecular Medicine Reports*, pp. 3481–3488, 2017.
- [73] M. S. Hakam, J. M. Miranda-Sayago, S. Hayrabydyan, K. Todorova, P. S. Spencer, A. Jabeen, E. R. Barnea, and N. Fernandez, "Preimplantation Factor (PIF) Promotes HLA-G,-E,-F,-C Expression in JEG-3 Choriocarcinoma Cells and Endogenous Progesterone Activity," *Cellular Physiology and Biochemistry*, vol. 43, no. 6, pp. 2277–2296, 2017.
- [74] E. R. Barnea, S. Hayrabydyan, K. Todorova, O. Almogi-Hazan, R. Or, J. Guingab, J. McElhinney, N. Fernandez, and T. Barder, "PreImplantation factor (PIF) regulates systemic immunity and targets protective regulatory and cytoskeleton proteins," *Immunobiology*, vol. 221, no. 7, pp. 778–793, 2016.
- [75] E. R. Barnea, O. Almogi-Hazan, R. Or, M. Mueller, F. Ria, L. Weiss, and M. J. Paidas, "Immune regulatory and neuroprotective properties of preimplantation factor: From newborn to adult," *Pharmacology and Therapeutics*, vol. 156, pp. 10–25, 2015.
- [76] N. D. Simone, F. D. Nicuolo, R. Marana, R. Castellani, F. Ria, M. Veglia, G. Scambia, D. Surbek, E. Barnea, and M. Mueller, "Synthetic PreImplantation Factor (PIF) prevents fetal loss by modulating LPS induced inflammatory response," *PloS one*, vol. 12, no. 7, p. e0180642, 2017.
- [77] D. M. Nash, J. Paddison, M. C. Davies Morel, and E. R. Barnea, "Preimplantation factor modulates acute inflammatory responses of equine endometrium," *Veterinary Medicine and Science*, pp. 1–6, 2018.
- [78] L. Weiss, S. Bernstein, R. Jones, R. Amunugama, D. Krizman, L. Je Bailey, O. Almogi-Hazan, O. Hazan, Z. Yekhtin, J. Yachtin, R. Shiner, I. Reibstein, E. Triche, S. Slavin, R. Or,

- and E. R. Barnea, "Preimplantation factor (PIF) analog prevents type I diabetes mellitus (T1DM) development by preserving pancreatic function in NOD mice.," *Endocrine*, vol. 40, no. 1, pp. 41–54, 2011.
- [79] L. Weiss, R. Or, R. C. Jones, R. Amunugama, L. JeBailey, S. Ramu, S. a. Bernstein, Z. Yekhtin, O. Almogi-Hazan, R. Shainer, I. Reibstein, A. O. Vortmeyer, M. J. Paidas, M. Zeira, S. Slavin, and E. R. Barnea, "Preimplantation factor (PIF*) reverses neuroinflammation while promoting neural repair in EAE model.," *Journal of the Neurological Sciences*, vol. 312, no. 1-2, pp. 146–157, 2012.
- [80] M. Mueller, J. Zhou, L. Yang, Y. Gao, F. Wu, A. Schoeberlein, D. Surbek, E. R. Barnea, M. Paidas, and Y. Huang, "PreImplantation factor promotes neuroprotection by targeting microRNA let-7.," *Proceedings of the National Academy of Sciences of the United States of America*, vol. 111, no. 38, pp. 13882–13887, 2014.
- [81] M. Mueller, A. Schoeberlein, J. Zhou, B. Oppliger, U. Reinhart, A. Bordey, D. Surbek, and E. R. Barnea, "PreImplantation Factor bolsters neuroprotection via modulating Protein Kinase A and Protein Kinase C signaling," *Cell Death and Differentiation*, vol. 22, no. 12, pp. 2078–2086, 2015.
- [82] Y. Azar, R. Shainer, O. Almogi-Hazan, R. Bringer, S. R. Compton, M. J. Paidas, E. R. Barnea, and R. Or, "PreImplantation Factor (PIF*) Reduces Graft versus Host Disease (GVHD) by Regulating Immune Response and Lowering Oxidative Stress," *Biology of Blood and Marrow Transplantation*, vol. 19, no. 4, pp. 519–528, 2013.
- [83] M. Feichtinger, E. R. Barnea, A. Nyachio, M. Brännström, and S. S. Kim, "Allogeneic ovarian transplantation using immunomodulator preimplantation factor (PIF) as monotherapy restored ovarian function in olive baboon," *Journal of Assisted Reproduction and Genetics*, pp. 1–9, 2017.
- [84] Y. C. Chen, J. Rivera, M. Fitzgerald, C. Hausding, Y.-L. Ying, X. Wang, K. Todorova, S. Hayrabedian, E. R. Barnea, and K. Peter, "PreImplantation factor prevents atherosclerosis via its immunomodulatory effects without affecting serum lipids.," *Thrombosis and haemostasis*, vol. 115, no. 5, pp. 1010–1024, 2016.
- [85] J. Mestas and C. C. W. Hughes, "Of mice and not men: differences between mouse and human immunology.," *Journal of Immunology*, vol. 172, no. 5, pp. 2731–2738, 2004.
- [86] K. Ley, H. M. Hoffman, P. Kubes, M. A. Cassatella, A. Zychlinsky, C. C. Hedrick, and S. D. Catz, "Neutrophils : New insights and open questions," *Science Immunology*, vol. 3, no. 30, p. eaat4579, 2018.
- [87] S. Schmidt, M. Moser, and M. Sperandio, "The molecular basis of leukocyte recruitment and its deficiencies.," *Molecular Immunology*, vol. 55, no. 1, pp. 49–58, 2013.
- [88] K. Ley, C. Laudanna, M. I. Cybulsky, and S. Nourshargh, "Getting to the site of inflammation: the leukocyte adhesion cascade updated.," *Nature reviews. Immunology*, vol. 7, no. 9, pp. 678–689, 2007.

-
- [89] U. Jung and K. Ley, "Mice lacking two or all three selectins demonstrate overlapping and distinct functions for each selectin.," *Journal of Immunology*, vol. 162, pp. 6755–6762, jun 1999.
- [90] K. Ley, "The role of selectins in inflammation and disease," *Trends in Molecular Medicine*, vol. 9, no. 6, pp. 263–268, 2003.
- [91] M. Sperandio and K. Ley, "The physiology and pathophysiology of P-selectin," *Modern Aspects of Immunobiology*, vol. 15, pp. 24–26, 2005.
- [92] R. P. McEver, "Selectins: Initiators of leucocyte adhesion and signalling at the vascular wall," *Cardiovascular Research*, vol. 107, no. 3, pp. 331–339, 2015.
- [93] K. D. Patel, S. L. Cuvelier, and S. Wiehler, "Selectins: critical mediators of leukocyte recruitment.," *Seminars in Immunology*, vol. 14, no. 2, pp. 73–81, 2002.
- [94] D. Vestweber and J. E. Blanks, "Mechanisms that regulate the function of the selectins and their ligands.," *Physiological reviews*, vol. 79, no. 1, pp. 181–213, 1999.
- [95] U. Jung and K. Ley, "Regulation of E-selectin, P-selectin, and intercellular adhesion molecule 1 expression in mouse cremaster muscle vasculature," *Microcirculation*, vol. 4, no. 2, pp. 311–319, 1997.
- [96] Z. Liu, J. J. Miner, T. Yago, L. Yao, F. Lupu, L. Xia, and R. P. McEver, "Differential regulation of human and murine P-selectin expression and function in vivo.," *The Journal of Experimental Medicine*, vol. 207, pp. 2975–2987, dec 2010.
- [97] A. Zarbock, K. Ley, R. P. McEver, and A. Hidalgo, "Leukocyte ligands for endothelial selectins: specialized glycoconjugates that mediate rolling and signaling under flow.," *Blood*, vol. 118, no. 26, pp. 6743–51, 2011.
- [98] M. L. Arbornés, D. C. Ord, K. Ley, H. Ratech, C. Maynard-Curry, G. Otten, D. J. Capon, and T. F. Tedder, "Lymphocyte homing and leukocyte rolling and migration are impaired in L-selectin-deficient mice," *Immunity*, vol. 1, no. 4, pp. 247–260, 1994.
- [99] E. E. Eriksson, X. Xie, J. Werr, P. Thoren, and L. Lindbom, "Importance of Primary Capture and L-Selectin-Dependent Secondary Capture in Leukocyte Accumulation in Inflammation and Atherosclerosis in Vivo," *The Journal of Experimental Medicine*, vol. 194, no. 2, pp. 205–218, 2002.
- [100] M. Sperandio, M. L. Smith, S. B. Forlow, T. S. Olson, L. Xia, R. P. McEver, and K. Ley, "P-selectin glycoprotein ligand-1 mediates L-selectin-dependent leukocyte rolling in venules.," *The Journal of Experimental Medicine*, vol. 197, no. 10, pp. 1355–1363, 2003.
- [101] O. Zöllner, M. C. Lenter, J. E. Blanks, E. Borges, M. Steegmaier, H. G. Zerwes, and D. Vestweber, "L-selectin from human, but not from mouse neutrophils binds directly to E-selectin," *Journal of Cell Biology*, vol. 136, no. 3, pp. 707–716, 1997.

- [102] V. A. Morikis, S. Chase, T. Wun, E. L. Chaikof, J. L. Magnani, and S. I. Simon, "Selectin catch-bonds mechanotransduce integrin activation and neutrophil arrest on inflamed endothelium under shear flow," *Blood*, vol. 130, no. 19, pp. 2101–2110, 2017.
- [103] E. B. Finger, K. D. Puri, R. Alon, M. B. Lawrence, U. H. von Andrian, and S. T. A. A, "Adhesion through L-selectin requires a threshold hydrodynamic shear," *Nature*, vol. 379, pp. 266–269, 1996.
- [104] M. Lawrence, G. Kansas, E. Kunkel, and K. Ley, "Threshold levels of fluid shear promote leukocyte adhesion through selectins (CD62L, P, E)," *The Journal of Cell Biology*, vol. 136, no. 3, pp. 717–727, 1997.
- [105] W. Thomas, "Catch bonds in adhesion.," *Annual review of Biomedical Engineering*, vol. 10, pp. 39–57, 2008.
- [106] R. Alón, D. Hammer, and T. Springer, "Lifetime of the P-selectin-carbohydrate bond and its response to tensile force in hydrodynamic flow," *Nature*, vol. 374, pp. 539–542, 1995.
- [107] E. J. Kunkel and K. Ley, "Distinct Phenotype of E-Selectin-Deficient Mice E-Selectin Is Required for Slow Leukocyte Rolling In Vivo," *Circulation Research*, vol. 79, no. 6, pp. 1196–1204, 1996.
- [108] A. Hidalgo, A. J. Peired, M. K. Wild, D. Vestweber, and P. S. Frenette, "Complete identification of E-selectin ligands on neutrophils reveals distinct functions of PSGL-1, ESL-1, and CD44.," *Immunity*, vol. 26, pp. 477–489, apr 2007.
- [109] E. Kunkel, U. Jung, D. Bullard, K. Norman, B. Wolitzky, D. Vestweber, A. Beaudet, and K. Ley, "Absence of trauma-induced leukocyte rolling in mice deficient in both P-selectin and intercellular adhesion molecule 1.," *The Journal of Experimental Medicine*, vol. 183, no. 1, pp. 57–65, 1996.
- [110] P. Sundd, E. Gutierrez, E. K. Koltsova, Y. Kuwano, S. Fukuda, M. K. Pospieszalska, A. Groisman, and K. Ley, "'Slings' enable neutrophil rolling at high shear.," *Nature*, vol. 488, no. 7411, pp. 399–403, 2012.
- [111] C. T. Lefort and K. Ley, "Neutrophil arrest by LFA-1 activation.," *Frontiers in Immunology*, vol. 3, no. 157, pp. 1–10, 2012.
- [112] R. Evans, I. Patzak, L. Svensson, K. De Filippo, K. Jones, A. McDowall, and N. Hogg, "Integrins in immunity.," *Journal of Cell Science*, vol. 122, no. Pt 2, pp. 215–225, 2009.
- [113] K. Halai, J. Whiteford, B. Ma, S. Nourshargh, and A. Woodfin, "ICAM-2 facilitates luminal interactions between neutrophils and endothelial cells in vivo," *Journal of Cell Science*, vol. 127, no. 3, pp. 620–629, 2014.
- [114] D. Frommhold, A. Kamphues, I. Hepper, M. Pruenster, I. K. Lukic, I. Socher, V. Zablotskaya, K. Buschmann, B. Lange-Sperandio, J. Schymeinsky, E. Ryschich, J. Poeschl, C. Kupatt, P. P. Nawroth, M. Moser, B. Walzog, A. Bierhaus, and M. Sperandio, "RAGE

- and ICAM-1 cooperate in mediating leukocyte recruitment during acute inflammation in vivo.," *Blood*, vol. 116, no. 5, pp. 841–849, 2010.
- [115] N. Hogg, I. Patzak, and F. Willenbrock, "The insider's guide to leukocyte integrin signalling and function," *Nature Reviews Immunology*, vol. 11, no. 6, pp. 416–426, 2011.
- [116] Z. Fan, S. McArdle, A. Marki, Z. Mikulski, E. Gutierrez, B. Engelhardt, U. Deutsch, M. Ginsberg, A. Groisman, and K. Ley, "Neutrophil recruitment limited by high-affinity bent $\beta 2$ integrin binding ligand in cis," *Nature Communications*, vol. 7, pp. 1–14, 2016.
- [117] H.-Y. Tseng, A. V. Samarelli, P. Kammerer, S. Scholze, T. Ziegler, R. Immler, R. Zent, M. Sperandio, C. R. Sanders, R. Fässler, and R. T. Böttcher, "LCP1 preferentially binds clasped $\alpha M\beta 2$ integrin and attenuates leukocyte adhesion under flow.," *Journal of Cell Science*, vol. 131, no. 22, p. jcs.218214, 2018.
- [118] A. Zarbock, C. L. Abram, M. Hundt, A. Altman, C. A. Lowell, and K. Ley, "PSGL-1 engagement by E-selectin signals through Src kinase Fgr and ITAM adapters DAP12 and Fc γ R to induce slow leukocyte rolling," *The Journal of Experimental Medicine*, vol. 205, no. 10, pp. 2339–2347, 2008.
- [119] H. Mueller, A. Stadtmann, H. V. Aken, E. Hirsch, D. Wang, K. Ley, W. Dc, and A. Zarbock, "Tyrosine kinase Btk regulates E-selectin-mediated integrin activation and neutrophil recruitment by controlling phospholipase C (PLC) $\gamma 2$ and PI3K γ pathways," *Blood*, vol. 115, no. 15, pp. 3118–3127, 2010.
- [120] M. Pruenster, A. R. M. Kurz, K.-J. Chung, X. Cao-Ehlker, S. Bieber, C. F. Nussbaum, S. Bierschenk, T. K. Eggersmann, I. Rohwedder, K. Heinig, R. Immler, M. Moser, U. Koedel, S. Gran, R. P. McEver, D. Vestweber, A. Verschoor, T. Leanderson, T. Chavakis, J. Roth, T. Vogl, and M. Sperandio, "Extracellular MRP8/14 is a regulator of $\beta 2$ integrin-dependent neutrophil slow rolling and adhesion," *Nature Communications*, vol. 6, p. 6915, 2015.
- [121] M. Moser, K. Legate, R. Zent, and R. Fässler, "The tail of integrins, talin, and kindlins," *Science*, vol. 324, pp. 895–899, 2009.
- [122] M. Moser, M. Bauer, S. Schmid, R. Ruppert, S. Schmidt, M. Sixt, H.-V. Wang, M. Sperandio, and R. Fässler, "Kindlin-3 is required for beta2 integrin-mediated leukocyte adhesion to endothelial cells.," *Nature medicine*, vol. 15, no. 3, pp. 300–5, 2009.
- [123] M. Moser, B. Nieswandt, S. Ussar, M. Pozgajova, and R. Fässler, "Kindlin-3 is essential for integrin activation and platelet aggregation," *Nature Medicine*, vol. 14, no. 3, pp. 325–330, 2008.
- [124] C. C. T. Lefort, J. Rossaint, M. Moser, B. G. Petrich, A. Zarbock, S. J. Monkley, D. R. Critchley, M. H. Ginsberg, R. Fässler, and K. Ley, "Distinct roles for talin-1 and kindlin-3 in LFA-1 extension and affinity regulation," *Blood*, vol. 119, no. 18, pp. 4275–4282, 2012.

- [125] A. Mócsai, B. Walzog, and C. A. Lowell, "Intracellular signalling during neutrophil recruitment," *Cardiovascular Research*, vol. 107, no. 3, pp. 373–385, 2015.
- [126] D. Begandt, S. Thome, M. Sperandio, and B. Walzog, "How neutrophils resist shear stress at blood vessel walls: molecular mechanisms, subcellular structures, and cell–cell interactions," *Journal of Leukocyte Biology*, vol. 102, no. 3, pp. 699–709, 2017.
- [127] K. Futosi and A. Mócsai, "Tyrosine kinase signaling pathways in neutrophils," *Immunological Reviews*, vol. 273, no. 1, pp. 121–139, 2016.
- [128] C. L. Abram and C. A. Lowell, "The Ins and Outs of Leukocyte Integrin Signaling.," *Annual review of immunology*, vol. 27, pp. 339–62, 2009.
- [129] S. J. Smith and R. O. McCann, "A C-terminal dimerization motif is required for focal adhesion targeting of Talin1 and the interaction of the Talin1 I/LWEQ module with F-actin," *Biochemistry*, vol. 46, no. 38, pp. 10886–10898, 2007.
- [130] G. C. K. Roberts and D. R. Critchley, "Structural and biophysical properties of the integrin-associated cytoskeletal protein talin.," *Biophysical reviews*, vol. 1, no. 2, pp. 61–69, 2009.
- [131] J. Schymeinsky, R. Gerstl, I. Mannigel, K. Niedung, D. Frommhold, K. Panthel, J. Heesemann, M. Sixt, T. Quast, W. Kolanus, A. Mocsai, J. Wienands, M. Sperandio, and B. Walzog, "A fundamental role of mAbp1 in neutrophils: Impact on beta2 integrin-mediated phagocytosis and adhesion in vivo," *Blood*, vol. 114, no. 19, pp. 4209–4220, 2009.
- [132] R. Pick, D. Begandt, T. J. Stocker, M. Salvermoser, S. Thome, R. T. Böttcher, E. Montanez, U. Harrison, I. Forné, A. G. Khandoga, R. Coletti, L. T. Weckbach, D. Brechtefeld, R. Haas, A. Imhof, S. Massberg, M. Sperandio, and B. Walzog, "Coronin 1A, a novel player in integrin biology, controls neutrophil trafficking in innate immunity," *Blood*, vol. 130, no. 7, pp. 847–858, 2017.
- [133] T. Bromberger, S. Klapproth, I. Rohwedder, L. Zhu, L. Mittmann, C. A. Reichel, M. Sperandio, J. Qin, and M. Moser, "Direct Rap1/Talin1 interaction regulates platelet and neutrophil integrin activity in mice," *Blood*, vol. 132, no. 26, pp. 2754–2762, 2018.
- [134] D. Vestweber, "How leukocytes cross the vascular endothelium," *Nature Reviews Immunology*, vol. 15, no. 11, pp. 692–704, 2015.
- [135] S. Massena, G. Christoffersson, E. Hjertström, E. Zcharia, I. Vlodaysky, N. Ausmees, C. Rolny, J.-P. Li, and M. Phillipson, "A chemotactic gradient sequestered on endothelial heparan sulfate induces directional intraluminal crawling of neutrophils.," *Blood*, vol. 116, no. 11, pp. 1924–1931, 2010.
- [136] B. McDonald, K. Pittman, G. B. Menezes, S. a. Hirota, I. Slaba, C. C. M. Waterhouse, P. L. Beck, D. a. Muruve, and P. Kubes, "Intravascular danger signals guide neutrophils to sites of sterile inflammation.," *Science*, vol. 330, no. 6002, pp. 362–366, 2010.

- [137] G. Zuchtriegel, B. Uhl, D. Pühr-Westerheide, M. Pörnbacher, K. Lauber, F. Krombach, and C. A. Reichel, "Platelets Guide Leukocytes to Their Sites of Extravasation," *PLoS Biology*, vol. 14, no. 5, pp. 1–28, 2016.
- [138] S. Nourshargh and R. Alon, "Leukocyte Migration into Inflamed Tissues," *Immunity*, vol. 41, pp. 694–707, nov 2014.
- [139] W. A. Muller, "Mechanisms of Leukocyte Transendothelial Migration," *Annual Review of Pathology: Mechanisms of Disease*, vol. 6, no. 1, pp. 323–344, 2011.
- [140] O. Barreiro, M. Yáñez-Mó, J. M. Serrador, M. C. Montoya, M. Vicente-Manzanares, R. Tejedor, H. Furthmayr, and F. Sánchez-Madrid, "Dynamic interaction of VCAM-1 and ICAM-1 with moesin and ezrin in a novel endothelial docking structure for adherent leukocytes," *Journal of Cell Biology*, vol. 157, no. 7, pp. 1233–1245, 2002.
- [141] C. V. Carman and T. A. Springer, "A transmigratory cup in leukocyte diapedesis both through individual vascular endothelial cells and between them," *Journal of Cell Biology*, vol. 167, no. 2, pp. 377–388, 2004.
- [142] F. Wessel, M. Winderlich, M. Holm, M. Frye, R. Rivera-Galdos, M. Vockel, R. Linnepe, U. Ipe, A. Stadtmann, A. Zarbock, A. F. Nottebaum, and D. Vestweber, "Leukocyte extravasation and vascular permeability are each controlled in vivo by different tyrosine residues of VE-cadherin," *Nature Immunology*, vol. 15, no. 3, pp. 223–230, 2014.
- [143] S. K. Shaw, P. S. Bamba, B. N. Perkins, and F. W. Luscinskas, "Real-Time Imaging of Vascular Endothelial-Cadherin During Leukocyte Transmigration Across Endothelium," *The Journal of Immunology*, vol. 167, no. 4, pp. 2323–2330, 2001.
- [144] A. Woodfin, C. A. Reichel, A. Khandoga, M. Corada, M.-B. Voisin, C. Scheiermann, D. O. Haskard, E. Dejana, F. Krombach, and S. Nourshargh, "JAM-A mediates neutrophil transmigration in a stimulus-specific manner in vivo: evidence for sequential roles for JAM-A and PECAM-1 in neutrophil transmigration," *Blood*, vol. 110, no. 6, pp. 1848–1856, 2007.
- [145] A. Woodfin, M. B. Voisin, M. Beyrau, B. Colom, D. Caille, F. M. Diapouli, G. B. Nash, T. Chavakis, S. M. Albelda, G. E. Rainger, P. Meda, B. A. Imhof, and S. Nourshargh, "The junctional adhesion molecule JAM-C regulates polarized transendothelial migration of neutrophils in vivo," *Nature Immunology*, vol. 12, no. 8, pp. 761–769, 2011.
- [146] F. Wegmann, B. Petri, A. G. Khandoga, C. Moser, A. Khandoga, S. Volkery, H. Li, I. Nasdala, O. Brandau, R. Fässler, S. Butz, F. Krombach, and D. Vestweber, "ESAM supports neutrophil extravasation, activation of Rho, and VEGF-induced vascular permeability," *The Journal of Experimental Medicine*, vol. 203, no. 7, pp. 1671–1677, 2006.
- [147] S. Nourshargh, F. Krombach, and E. Dejana, "The role of JAM-A and PECAM-1 in modulating leukocyte infiltration in inflamed and ischemic tissues," *Journal of Leukocyte Biology*, vol. 80, no. 4, pp. 714–718, 2006.

- [148] A. R. Schenkel, Z. Mamdouh, X. Chen, R. M. Liebman, and W. A. Muller, "CD99 plays a major role in the migration of monocytes through endothelial junctions," *Nature Immunology*, vol. 3, no. 2, pp. 143–150, 2002.
- [149] L. Sorokin, "The impact of the extracellular matrix on inflammation," *Nature Reviews Immunology*, vol. 10, no. 10, pp. 712–723, 2010.
- [150] A. R. M. Kurz, M. Pruenster, I. Rohwedder, M. Ramadass, K. Schäfer, U. Harrison, G. Gouveia, C. Nussbaum, R. Immler, J. R. Wiessner, A. Margraf, D.-s. Lim, B. Walzog, S. Dietzel, M. Moser, C. Klein, D. Vestweber, R. Haas, S. D. Catz, and M. Sperandio, "MST1-dependent vesicle trafficking regulates neutrophil transmigration through the vascular basement membrane," *Journal of Clinical Investigation*, vol. 126, no. 11, pp. 4125–4139, 2016.
- [151] A. R. M. Kurz, S. D. Catz, and M. Sperandio, "Noncanonical Hippo Signalling in the Regulation of Leukocyte Function," *Trends in Immunology*, vol. 39, no. 8, pp. 656–669, 2018.
- [152] D. Proebstl, M.-B. Voisin, A. Woodfin, J. Whiteford, F. D'Acquisto, G. E. Jones, D. Rowe, and S. Nourshargh, "Pericytes support neutrophil subendothelial cell crawling and breaching of venular walls in vivo.," *The Journal of Experimental Medicine*, vol. 209, no. 6, pp. 1219–1234, 2012.
- [153] T. Lämmermann, B. L. Bader, S. J. Monkley, T. Worbs, R. Wedlich-Söldner, K. Hirsch, M. Keller, R. Förster, D. R. Critchley, R. Fässler, and M. Sixt, "Rapid leukocyte migration by integrin-independent flowing and squeezing," *Nature*, vol. 453, no. 7191, pp. 51–55, 2008.
- [154] M. Lerchenberger, B. Uhl, K. Stark, G. Zuchtriegel, A. Eckart, M. Miller, D. Pühr-Westerheide, M. Praetner, M. Rehberg, A. G. Khandoga, K. Lauber, S. Massberg, F. Krombach, and C. A. Reichel, "Matrix metalloproteinases modulate ameboid-like migration of neutrophils through inflamed interstitial tissue," *Blood*, vol. 122, no. 5, pp. 770–780, 2013.
- [155] R. A. Clemens and C. A. Lowell, "Store-operated calcium signaling in neutrophils.," *Journal of leukocyte biology*, vol. 98, no. October, pp. 1–6, 2015.
- [156] S. Feske, H. Wulff, and E. Y. Skolnik, "Ion channels in innate and adaptive immunity.," *Annual Review of Immunology*, vol. 33, pp. 291–353, 2015.
- [157] R. A. Clemens and C. A. Lowell, "CRAC channel regulation of innate immune cells in health and disease," *Cell Calcium*, vol. 78, no. December 2018, pp. 56–65, 2019.
- [158] R. Immler, S. I. Simon, and M. Sperandio, "Calcium signalling and related ion channels in neutrophil recruitment and function," *European Journal of Clinical Investigation*, vol. 48, no. S2, p. e12964, 2018.
- [159] N. Dixit and S. I. Simon, "Chemokines, selectins and intracellular calcium flux: Temporal and spatial cues for leukocyte arrest," *Frontiers in Immunology*, vol. 3, pp. 1–9, 2012.

- [160] R. Bagur and G. Hajnóczky, "Intracellular Ca²⁺Sensing: Its Role in Calcium Homeostasis and Signaling," *Molecular Cell*, vol. 66, no. 6, pp. 780–788, 2017.
- [161] H. Jiang, Y. Kuang, Y. Wu, W. Xie, M. I. Simon, and D. Wu, "Roles of phospholipase C beta2 in chemoattractant-elicited responses.," *Proceedings of the National Academy of Sciences of the United States of America*, vol. 94, no. 15, pp. 7971–5, 1997.
- [162] R. P. Kimberly, J. W. Ahlstrom, M. E. Click, and J. C. Edberg, "The glycosyl phosphatidylinositol-linked Fcγ₃ PMN mediates transmembrane signaling events distinct from Fcγ₂," *Journal of Experimental Medicine*, vol. 171, pp. 1239–1255, 1990.
- [163] D. B. Graham, C. M. Robertson, J. Bautista, F. Mascarenhas, M. J. Diacovo, V. Montgrain, S. K. Lam, V. Cremasco, W. M. Dunne, R. Faccio, C. M. Coopersmith, and W. Swat, "Neutrophil-mediated oxidative burst and host defense are controlled by a Vav-PLCγ₂ signaling axis in mice," *The Journal of Clinical Investigation*, vol. 117, no. 11, pp. 3445–3452, 2007.
- [164] Z. Jakus, E. Simon, D. Frommhold, M. Sperandio, and A. Mócsai, "Critical role of phospholipase Cγ₂ in integrin and Fc receptor-mediated neutrophil functions and the effector phase of autoimmune arthritis," *The Journal of Experimental Medicine*, vol. 206, no. 3, pp. 577–593, 2009.
- [165] U. Y. Schaff, I. Yamayoshi, T. Tse, D. Griffin, L. Kibathi, and S. I. Simon, "Calcium flux in neutrophils synchronizes β₂ integrin adhesive and signaling events that guide inflammatory recruitment," *Annals of Biomedical Engineering*, vol. 36, no. 4, pp. 632–646, 2008.
- [166] U. Y. Schaff, N. Dixit, E. Procyk, I. Yamayoshi, T. Tse, and S. I. Simon, "Orai1 regulates intracellular calcium, arrest, and shape polarization during neutrophil recruitment in shear flow," *Blood*, vol. 115, no. 3, pp. 657–666, 2010.
- [167] K. Futosi, S. Fodor, and A. Mócsai, "Neutrophil cell surface receptors and their intracellular signal transduction pathways," *International Immunopharmacology*, vol. 17, no. 3, pp. 638–650, 2013.
- [168] N. Demaurex and P. Nunes, "The role of STIM and ORAI proteins in phagocytic immune cells," *American Journal of Physiology - Cell Physiology*, vol. 310, no. 7, pp. C496–C508, 2016.
- [169] N. Demaurex and S. Saul, "The role of STIM proteins in neutrophil functions," *The Journal of Physiology*, vol. 596, no. 14, pp. 2699–2708, 2018.
- [170] O. Lindemann, D. Umlauf, S. Frank, S. Schimmelpfennig, J. Bertrand, T. Pap, P. J. Hanley, A. Fabian, A. Dietrich, and A. Schwab, "TRPC6 Regulates CXCR2-Mediated Chemotaxis of Murine Neutrophils," *The Journal of Immunology*, vol. 190, no. 11, pp. 5496–5505, 2013.

- [171] K. Itagaki, K. B. Kannan, B. B. Singh, and C. J. Hauser, "Cytoskeletal reorganization internalizes multiple transient receptor potential channels and blocks calcium entry into human neutrophils.," *The Journal of Immunology*, vol. 172, no. 1, pp. 601–607, 2004.
- [172] T. Hofmann, A. G. Obukhov, M. Schaefer, C. Harteneck, T. Gudermann, and G. Schultz, "Direct activation of human TRPC6 and TRPC3 channels by diacylglycerol," *Nature*, vol. 397, no. 6716, pp. 259–263, 1999.
- [173] B. A. Kruskal, S. Shak, and F. R. Maxfield, "Spreading of human neutrophils is immediately preceded by a large increase in cytoplasmic free calcium.," *Proceedings of the National Academy of Sciences of the United States of America*, vol. 83, no. 9, pp. 2919–2923, 1986.
- [174] A. Schwab, A. Fabian, P. J. Hanley, and C. Stock, "Role of Ion Channels and Transporters in Cell Migration," *Physiological Reviews*, vol. 92, no. 4, pp. 1865–1913, 2012.
- [175] P. Nunes and N. Demaurex, "The role of calcium signaling in phagocytosis.," *Journal of Leukocyte Biology*, vol. 88, no. 1, pp. 57–68, 2010.
- [176] V. A. Morikis and S. I. Simon, "Neutrophil Mechanosignaling Promotes Integrin Engagement With Endothelial Cells and Motility Within Inflamed Vessels," *Frontiers in Immunology*, vol. 9, no. 2774, 2018.
- [177] W. Schorr, D. Swandulla, and H. U. Zeilhofer, "Mechanisms of IL-8-induced Ca²⁺ signaling in human neutrophil granulocytes.," *European journal of immunology*, vol. 29, no. 3, pp. 897–904, 1999.
- [178] M. P. Davies, T. J. Hallam, and J. E. Merritt, "A role for calcium and protein kinase C in agonist-stimulated adhesion of human neutrophils," *Biochemical Journal*, vol. 267, no. 1, pp. 13–16, 1990.
- [179] N. Dixit, I. Yamayoshi, A. Nazarian, and S. I. Simon, "Migrational Guidance of Neutrophils Is Mechanotransduced via High-Affinity LFA-1 and Calcium Flux," *The Journal of Immunology*, vol. 187, no. 1, pp. 472–481, 2011.
- [180] N. Dixit, M. H. Kim, J. Rossaint, I. Yamayoshi, A. Zarbock, and S. I. Simon, "Leukocyte function antigen-1, Kindlin-3, and calcium flux orchestrate neutrophil recruitment during inflammation," *Journal of Immunology*, vol. 189, no. 12, pp. 5954–5964, 2012.
- [181] K. G. Chandy, H. Wulff, C. Beeton, M. Pennington, G. A. Gutman, and M. D. Cahalan, "K⁺ channels as targets for specific immunomodulation," *Trends in Pharmacological Sciences*, vol. 25, no. 5, pp. 280–289, 2004.
- [182] M. T. Perez Garcia, P. Ciudad, and J. R. Lopez-Lopez, "The secret life of ion channels: Kv1.3 potassium channels and cell proliferation," *American Journal of Physiology - Cell Physiology*, vol. 314, no. 1, pp. C27–C42, 2018.
- [183] M. D. Cahalan and K. G. Chandy, "The functional network of ion channels in T lymphocytes," *Immunological Reviews*, vol. 231, no. 1, pp. 59–87, 2009.

- [184] F. Fenninger and W. A. Jefferies, "What's Bred in the Bone: Calcium Channels in Lymphocytes," *The Journal of Immunology*, vol. 202, no. 4, pp. 1021–1030, 2019.
- [185] H. Wulff, H.-G. Knaus, M. Pennington, and K. G. Chandy, "K⁺ Channel Expression during B Cell Differentiation: Implications for Immunomodulation and Autoimmunity," *The Journal of Immunology*, vol. 173, no. 2, pp. 776–786, 2004.
- [186] S. Koshy, D. Wu, X. Hu, R. B. Tajhya, R. Huq, F. S. Khan, M. W. Pennington, H. Wulff, P. Yotnda, and C. Beeton, "Blocking KCa_{3.1} Channels Increases Tumor Cell Killing by a Subpopulation of Human Natural Killer Lymphocytes," *PLoS ONE*, vol. 8, no. 10, pp. 1–11, 2013.
- [187] R. Vicente, A. Escalada, M. Coma, G. Fuster, E. Sánchez-Tilló, C. López-Iglesias, C. Soler, C. Solsona, A. Celada, and A. Felipe, "Differential Voltage-dependent K⁺ Channel Responses during Proliferation and Activation in Macrophages," *Journal of Biological Chemistry*, vol. 278, no. 47, pp. 46307–46320, 2003.
- [188] C. McCloskey, S. Jones, S. Amisten, R. T. Snowden, L. K. Kaczmarek, D. Erlinge, A. H. Goodall, I. D. Forsythe, and M. P. Mahaut-Smith, "Kv1.3 is the exclusive voltage-gated K⁺ channel of platelets and megakaryocytes: Roles in membrane potential, Ca²⁺ signalling and platelet count," *Journal of Physiology*, vol. 588, no. 9, pp. 1399–1406, 2010.
- [189] E. Zsiros, K. Kis-Toth, P. Hajdu, R. Gaspar, J. Bielanska, A. Felipe, E. Rajnavolgyi, and G. Panyi, "Developmental Switch of the Expression of Ion Channels in Human Dendritic Cells," *The Journal of Immunology*, vol. 183, no. 7, pp. 4483–4492, 2009.
- [190] A. L. Kindzelskii and H. R. Petty, "Ion channel clustering enhances weak electric field detection by neutrophils: Apparent roles of SKP96365-sensitive cation channels and myeloperoxidase trafficking in cellular responses," *European Biophysics Journal*, vol. 35, no. 1, pp. 1–26, 2005.
- [191] P. A. Koni, R. Khanna, M. C. Chang, M. D. Tang, L. K. Kaczmarek, L. C. Schlichter, and R. A. Flavell, "Compensatory anion currents in Kv1.3 channel-deficient thymocytes," *Journal of Biological Chemistry*, vol. 278, no. 41, pp. 39443–39451, 2003.
- [192] J. Schindelin, I. Arganda-Carreras, E. Frise, V. Kaying, M. Longhair, T. Pietzsch, S. Preibisch, C. Rueden, S. Saalfeld, B. Schmid, J. Tinevez, D. White, V. Hartenstein, K. Eliceiri, P. Tomancak, and A. Cardona, "Fiji: an open-source platform for biological-image analysis," *Nature Methods*, vol. 9, no. 7, pp. 676–682, 2012.
- [193] E. Meijering, O. Dzyubachyk, and I. Smal, "Methods for cell and particle tracking.," *Methods in Enzymology*, vol. 504, pp. 183–200, 2012.
- [194] R. Gorczynski, B. Klitzman, and B. R. Duling, "Interrelations between contracting striated muscle and precapillary microvessels," *American Journal of Physiology - Heart and Circulatory Physiology*, vol. 235, pp. H494–H504, 1978.

- [195] K. Ley and P. Gaehtgens, "Endothelial, not hemodynamic, differences are responsible for preferential leukocyte rolling in rat mesenteric venules," *Circulation Research*, vol. 69, no. 4, pp. 1034–1041, 1991.
- [196] A. Schmitz and A. Sankaranarayanan, "Design of PAP-1, a selective small molecule Kv1.3 blocker, for the suppression of effector memory T cells in autoimmune diseases," *Molecular Pharmacology*, vol. 68, no. 5, pp. 1254–1270, 2005.
- [197] L. Borsig, R. Wong, R. O. Hynes, N. M. Varki, and A. Varki, "Synergistic effects of L- and P-selectin in facilitating tumor metastasis can involve non-mucin ligands and implicate leukocytes as enhancers of metastasis," *Proceedings of the National Academy of Sciences*, vol. 99, no. 4, pp. 2193–2198, 2002.
- [198] M. Sperandio, J. Pickard, S. Unnikrishnan, S. T. Acton, and K. Ley, "Analysis of Leukocyte Rolling In Vivo and In Vitro," *Methods in Enzymology*, vol. 416, pp. 346–371, 2006.
- [199] J. L. Dunne, C. M. Ballantyne, A. L. Beaudet, and K. Ley, "Control of leukocyte rolling velocity in TNF-alpha -induced inflammation by LFA-1 and Mac-1," *Blood*, vol. 99, no. 1, pp. 336–341, 2002.
- [200] M. Levite, L. Cahalon, A. Peretz, R. Hershkovich, A. Sobko, A. Ariel, R. Desai, B. Attali, and O. Lider, "Extracellular K⁺ and Opening of Voltage-gated Potassium Channels Activate T Cell Integrin Function: Physical and Functional Association between Kv1.3 Channels and β 1 Integrins," *The Journal of Experimental Medicine*, vol. 191, no. 7, pp. 1167–1176, 2000.
- [201] N. Villalonga, M. David, J. Bielańska, T. González, D. Parra, C. Soler, N. Comes, C. Valenzuela, and A. Felipe, "Immunomodulatory effects of diclofenac in leukocytes through the targeting of Kv1.3 voltage-dependent potassium channels," *Biochemical Pharmacology*, vol. 80, no. 6, pp. 858–866, 2010.
- [202] E. M. Grossinger, L. Weiss, S. Zierler, S. Rebhandl, P. W. Krenn, E. Hinterseer, J. Schmolzer, D. Asslaber, S. Hainzl, D. Neureiter, A. Egle, J. Pinon-Hofbauer, T. N. Hartmann, R. Greil, and H. H. Kerschbaum, "Targeting proliferation of chronic lymphocytic leukemia (CLL) cells through KCa3.1 blockade," *Leukemia*, vol. 28, no. 4, pp. 954–958, 2014.
- [203] S. Grissmer, B. Dethlefst, J. J. Wasmuth, A. L. Goldin, G. A. Gutman, M. D. Cahalan, and K. G. Chandy, "Expression and chromosomal localization of a lymphocyte K⁺ channel gene," *Proceedings of the National Academy of Sciences*, vol. 87, no. December, pp. 9411–9415, 1990.
- [204] H. Wulff, M. J. Miller, W. Haensel, S. Grissmer, M. D. Cahalan, and K. G. Chandy, "Design of a potent and selective inhibitor of the intermediate-conductance Ca²⁺-activated K⁺ channel, IKCa1: A potential immunosuppressant," *Proceedings of the National Academy of Sciences*, vol. 97, no. 14, pp. 8151–8156, 2000.

- [205] C. Henríquez, T. T. Riquelme, D. Vera, F. Julio-Kalajzić, P. Ehrenfeld, J. E. Melvin, C. D. Figueroa, J. Sarmiento, and C. A. Flores, "The calcium-activated potassium channel KCa3.1 plays a central role in the chemotactic response of mammalian neutrophils," *Acta Physiologica*, vol. 216, no. 1, pp. 132–145, 2016.
- [206] A. S. Cowburn, A. M. Condliffe, N. Farahi, C. Summers, and E. R. Chilvers, "Advances in neutrophil biology: Clinical implications," *Chest*, vol. 134, no. 3, pp. 606–612, 2008.
- [207] J. Grommes and O. Soehnlein, "Contribution of neutrophils to acute lung injury.," *Molecular Medicine (Cambridge, Mass.)*, vol. 17, no. 3-4, pp. 293–307, 2011.
- [208] J. Grommes, S. Vijayan, M. Drechsler, H. Hartwig, M. Mörgelin, R. Dembinski, M. Jacobs, T. A. Koepfel, M. Binnebösel, C. Weber, and O. Soehnlein, "Simvastatin reduces endotoxin-induced acute lung injury by decreasing neutrophil recruitment and radical formation," *PLoS ONE*, vol. 7, no. 6, pp. 1–10, 2012.
- [209] B. K. E. Norman, K. L. Moore, R. P. McEver, and K. Ley, "Leukocyte Rolling In Vivo Is Mediated by P-Selectin Glycoprotein Ligand-1," *Blood*, vol. 86, no. 12, pp. 4417–4421, 1995.
- [210] K. D. Priddy, "Immunologic Adaptions During Pregnancy," *Journal of Obstetric, Gynecologic and Neonatal Nursing*, vol. 26, no. 4, pp. 388–394, 1997.
- [211] E. Sappenfield, D. J. Jamieson, and A. P. Kourtis, "Pregnancy and susceptibility to infectious diseases," *Infectious Diseases in Obstetrics and Gynecology*, vol. 2013, pp. 1–8, 2013.
- [212] A. P. Kourtis, J. S. Read, and D. J. Jamieson, "Infection and pregnancy," *The New England Journal of Medicine*, vol. 340, no. 23, pp. 2211–2218, 2014.
- [213] S. M. Gold and R. R. Voskuhl, "Pregnancy and multiple sclerosis: from molecular mechanisms to clinical application," *Seminars in Immunopathology*, vol. 38, no. 6, pp. 709–718, 2016.
- [214] A. L. Robijn, V. E. Murphy, and P. G. Gibson, "Recent developments in asthma in pregnancy," *Current Opinion in Pulmonary Medicine*, vol. 25, no. 1, pp. 11–17, 2019.
- [215] M. Sperandio, C. a. Gleissner, and K. Ley, "Glycosylation in immune cell trafficking," *Immunological Reviews*, vol. 230, no. 1, pp. 97–113, 2009.
- [216] C. Watson, S. Whittaker, N. Smith, A. J. Vora, D. C. Dumonde, and K. A. Brown, "IL-6 acts on endothelial cells to preferentially increase their adherence for lymphocytes," *Clinical and Experimental Immunology*, vol. 105, no. 1, pp. 112–119, 1996.
- [217] J. K. Kolls and A. Lindén, "Interleukin-17 family members and inflammation," *Immunity*, vol. 21, no. 4, pp. 467–476, 2004.
- [218] R. P. McEver, J. H. Beckstead, K. L. Moore, L. Marshall-Carlson, and D. F. Bainton, "GMP-140, a platelet alpha-granule membrane protein, is also synthesized by vascular endothelial cells and is localized in Weibel-Palade bodies.," *The Journal of Clinical Investigation*, vol. 84, no. 1, pp. 92–99, 1989.

- [219] K. Ley, D. C. Bullard, M. L. Arbonés, R. Bosse, D. Vestweber, T. F. Tedder, and a. L. Beaudet, "Sequential contribution of L- and P-selectin to leukocyte rolling in vivo.," *The Journal of Experimental Medicine*, vol. 181, no. 2, pp. 669–675, 1995.
- [220] U. M. Vischer and D. D. Wagner, "CD63 is a component of Weibel-Palade bodies of human endothelial cells.," *Blood*, vol. 82, no. 4, pp. 1184–91, 1993.
- [221] E. L. Doyle, V. Ridger, F. Ferraro, M. Turmaine, P. Saftig, and D. F. Cutler, "CD63 is an essential cofactor to leukocyte recruitment by endothelial P-selectin.," *Blood*, vol. 118, no. 15, pp. 4265–4273, 2011.
- [222] L. Deban, R. C. Russo, M. Sironi, F. Moalli, M. Scanziani, V. Zambelli, I. Cuccovillo, A. Bastone, M. Gobbi, S. Valentino, A. Doni, C. Garlanda, S. Danese, G. Salvatori, M. Sassano, V. Evangelista, B. Rossi, E. Zenaro, G. Constantin, C. Laudanna, B. Bottazzi, and A. Mantovani, "Regulation of leukocyte recruitment by the long pentraxin PTX3.," *Nature Immunology*, vol. 11, no. 4, pp. 328–334, 2010.
- [223] A. Doni, M. Michela, B. Bottazzi, G. Peri, S. Velentino, N. Poelntarutti, C. Garlanda, and A. Mantovani, "Regulation of PTX3, a key component of humoral innate immunity in human dendritic cells: stimulation by IL-10 and inhibition by IFN-," *Journal of Leukocyte Biology*, vol. 79, no. 4, pp. 797–802, 2006.
- [224] P. Jeannin, B. Bottazzi, M. Sironi, A. Doni, M. Rusnati, M. Presta, V. Maina, G. Magistrelli, J. F. Haeuw, G. Hoeffel, N. Thieblemont, N. Corvaia, C. Garlanda, Y. Delneste, and A. Mantovani, "Complexity and complementarity of outer membrane protein A recognition by cellular and humoral innate immunity receptors," *Immunity*, vol. 22, no. 5, pp. 551–560, 2005.
- [225] S. Jaillon, G. Peri, Y. Delneste, I. Frémaux, A. Doni, F. Moalli, C. Garlanda, L. Romani, H. Gascan, S. Bellocchio, S. Bozza, M. a. Cassatella, P. Jeannin, and A. Mantovani, "The humoral pattern recognition receptor PTX3 is stored in neutrophil granules and localizes in extracellular traps.," *The Journal of Experimental Medicine*, vol. 204, no. 4, pp. 793–804, 2007.
- [226] M. D. Cahalan, K. G. Chandy, T. E. DeCoursey, and S. Gupta, "A voltage-gated potassium channel in human T lymphocytes," *Journal of Physiology*, vol. 358, pp. 197–237, 1985.
- [227] K. H. Krause and M. J. Welsh, "Voltage-dependent and Ca²⁺-activated ion channels in human neutrophils.," *The Journal of Clinical Investigation*, vol. 85, no. 2, pp. 491–498, 1990.
- [228] K. G. Chandy and R. S. Norton, "Peptide blockers of Kv1.3 channels in T cells as therapeutics for autoimmune disease," *Current Opinion in Chemical Biology*, vol. 38, pp. 97–107, 2017.
- [229] G. A. Gutman, K. G. Chandy, S. Grissmer, M. Lazdunski, D. Mckinnon, L. A. Pardo, G. A. Robertson, B. Rudy, M. C. Sanguinetti, W. Stu, and X. Wang, "Nomenclature

- and molecular relationships of voltage-gated potassium channels.," *Pharmacological Reviews*, vol. 57, no. 4, pp. 473–508, 2005.
- [230] N. Villalonga, A. Escalada, R. Vicente, E. Sánchez-Tilló, A. Celada, C. Solsona, and A. Felipe, "Kv1.3/Kv1.5 heteromeric channels compromise pharmacological responses in macrophages," *Biochemical and Biophysical Research Communications*, vol. 352, no. 4, pp. 913–918, 2007.
- [231] H. Zhang, R. A. Clemens, F. Liu, Y. Hu, Y. Baba, P. Theodore, T. Kurosaki, and C. A. Lowell, "STIM1 calcium sensor is required for activation of the phagocyte oxidase during inflammation and host defense," *Blood*, vol. 123, no. 14, pp. 2238–2250, 2014.
- [232] G. Sogkas, T. Vögtle, E. Rau, B. Gewecke, D. Stegner, R. E. Schmidt, B. Nieswandt, and J. E. Gessner, "Orai1 controls C5a-induced neutrophil recruitment in inflammation," *European Journal of Immunology*, vol. 45, no. 7, pp. 2143–2153, 2015.
- [233] N. Steinckwich, V. Schenten, C. Melchior, S. Brechard, and E. J. Tschirhart, "An Essential Role of STIM1, Orai1, and S100A8-A9 Proteins for Ca²⁺ Signaling and Fc R-Mediated Phagosomal Oxidative Activity," *The Journal of Immunology*, vol. 186, no. 4, pp. 2182–2191, 2011.
- [234] R. S. Lacruz and S. Feske, "Diseases caused by mutations in ORAI1 and STIM1," *Annals of the New York Academy of Sciences*, vol. 1356, no. 1, pp. 45–79, 2015.
- [235] C. Feng, Y. F. Li, Y. H. Yau, H. S. Lee, X. Y. Tang, Z. H. Xue, Y. C. Zhou, W. M. Lim, T. C. Cornvik, C. Ruedl, S. G. Shochat, and S. M. Tan, "Kindlin-3 mediates integrin α L β 2 outside-in signaling, and it interacts with scaffold protein receptor for activated-C kinase 1 (RACK1)," *Journal of Biological Chemistry*, vol. 287, no. 14, pp. 10714–10726, 2012.
- [236] G. E. Woodard, J. J. López, I. Jardín, G. M. Salido, and J. A. Rosado, "TRPC3 regulates agonist-stimulated Ca²⁺ mobilization by mediating the interaction between type I inositol 1,4,5-trisphosphate receptor, RACK1, and Orai1," *Journal of Biological Chemistry*, vol. 285, no. 11, pp. 8045–8053, 2010.
- [237] A. J. Clark and H. R. Petty, "Observation of calcium microdomains at the uropod of living morphologically polarized human neutrophils using flash lamp-based fluorescence microscopy," *Cytometry Part A*, vol. 73, no. 7, pp. 673–678, 2008.
- [238] P. Stanley, A. Smith, A. McDowall, A. Nicol, D. Zicha, and N. Hogg, "Intermediate-affinity LFA-1 binds α -actinin-1 to control migration at the leading edge of the T cell," *EMBO Journal*, vol. 27, no. 1, pp. 62–75, 2008.
- [239] A. Becchetti, G. Petroni, and A. Arcangeli, "Ion Channel Conformations Regulate Integrin-Dependent Signaling," *Trends in Cell Biology*, vol. 29, no. 4, pp. 298–307, 2019.
- [240] V. V. Artym and H. R. Petty, "Molecular proximity of Kv1.3 voltage-gated potassium channels and beta(1)-integrins on the plasma membrane of melanoma cells: effects of cell adherence and channel blockers.," *The Journal of general physiology*, vol. 120, no. 1, pp. 29–37, 2002.

- [241] O. Lindemann, C. Strodtzoff, M. Horstmann, N. Nielsen, F. Jung, S. Schimmelpfennig, M. Heitzmann, and A. Schwab, "TRPC1 regulates fMLP-stimulated migration and chemotaxis of neutrophil granulocytes," *Biochimica et Biophysica Acta - Molecular Cell Research*, vol. 1853, no. 9, pp. 2122–2130, 2015.
- [242] N. Nutile-McMenemy, A. Elfenbein, and J. A. DeLeo, "Minocycline decreases in vitro microglial motility, β 1-integrin, and Kv1.3 channel expression," *Journal of Neurochemistry*, vol. 103, no. 5, pp. 2035–2046, 2007.
- [243] M. P. Matheu, C. Beeton, A. Garcia, V. Chi, S. Rangaraju, O. Safrina, K. Monaghan, M. I. Uemura, D. Li, S. Pal, L. M. de la Maza, E. Monuki, A. Flügel, M. W. Pennington, I. Parker, K. G. Chandy, and M. D. Cahalan, "Imaging of Effector Memory T Cells during a Delayed-Type Hypersensitivity Reaction and Suppression by Kv1.3 Channel Block," *Immunity*, vol. 29, no. 4, pp. 602–614, 2008.
- [244] H. E. Gendelman, S. Ding, N. Gong, J. Liu, S. H. Ramirez, Y. Persidsky, R. Lee Mosley, T. Wang, D. J. Volsky, and H. Xiong, "Monocyte chemotactic protein-1 regulates voltage-gated K⁺ channels and macrophage transmigration," *Journal of Neuroimmune Pharmacology*, vol. 4, no. 1, pp. 47–59, 2009.
- [245] T. Németh, A. Mócsai, and C. A. Lowell, "Neutrophils in animal models of autoimmune disease," *Seminars in Immunology*, vol. 28, no. 2, pp. 174–186, 2016.
- [246] C. Nathan, "Neutrophils and immunity: challenges and opportunities," *Nature reviews. Immunology*, vol. 6, no. 3, pp. 173–182, 2006.
- [247] J. Reutershan and K. Ley, "Bench-to-bedside review: Acute respiratory distress syndrome - How neutrophils migrate into the lung," *Critical Care*, vol. 8, no. 6, pp. 453–461, 2004.
- [248] E. Abraham, A. Carmody, R. Shenkar, and J. Arcaroli, "Neutrophils as early immunologic effectors in hemorrhage- or endotoxemia-induced acute lung injury," *American Journal of Physiology-Lung Cellular and Molecular Physiology*, vol. 279, pp. L1137–L1145, 2000.
- [249] A. D. Luster, R. Alon, and U. H. von Andrian, "Immune cell migration in inflammation: present and future therapeutic targets," *Nature Immunology*, vol. 6, pp. 1182–1190, dec 2005.
- [250] C. R. Mackay, "Moving targets: Cell migration inhibitors as new anti-inflammatory therapies," *Nature Immunology*, vol. 9, no. 9, pp. 988–998, 2008.
- [251] C. B. O'Brien, E. R. Barnea, P. Martin, C. Levy, E. Sharabi, K. R. Bhamidimarri, E. Martin, L. Arosemena, and E. R. Schiff, "Randomized, Double-Blind, Placebo-Controlled, Single Ascending Dose Trial of Synthetic Preimplantation Factor in Autoimmune Hepatitis," *Hepatology Communications*, vol. 2, no. 10, pp. 1235–1246, 2018.
- [252] H. Wulff, P. A. Calabresi, R. Allie, S. Yun, M. Pennington, C. Beeton, and K. G. Chandy, "The voltage-gated Kv1.3 K⁺ channel in effector memory T cells as new target for MS," *Journal of Clinical Investigation*, vol. 111, no. 2, pp. 1703–1713, 2003.

- [253] P. Devarajan and Z. Chen, "Autoimmune effector memory T cells: The bad and the good," *Immunologic Research*, vol. 57, no. 1-3, pp. 12–22, 2013.
- [254] C. Beeton, H. Wulff, J. Barbaria, O. Clot-Faybesse, M. Pennington, D. Bernard, M. D. Cahalan, K. G. Chandy, and E. Beraud, "Selective blockade of T lymphocyte K⁺ channels ameliorates experimental autoimmune encephalomyelitis, a model for multiple sclerosis," *Proceedings of the National Academy of Sciences*, vol. 98, no. 24, pp. 13942–13947, 2001.
- [255] C. Beeton, H. Wulff, N. E. Standifer, P. Azam, K. M. Mullen, M. W. Pennington, A. Kolski-Andreaco, E. Wei, A. Grino, D. R. Counts, P. H. Wang, C. J. LeeHealey, B. S. Andrews, A. Sankaranarayanan, D. Homerick, W. W. Roeck, J. Tehranzadeh, K. L. Stanhope, P. Zimin, P. J. Havel, S. Griffey, H.-G. Knaus, G. T. Nepom, G. A. Gutman, P. A. Calabresi, and K. G. Chandy, "Kv1.3 channels are a therapeutic target for T cell-mediated autoimmune diseases.," *Proceedings of the National Academy of Sciences of the United States of America*, vol. 103, no. 46, pp. 17414–17419, 2006.
- [256] S. Kundu-Raychaudhuri, Y. J. Chen, H. Wulff, and S. P. Raychaudhuri, "Kv1.3 in psoriatic disease: PAP-1, a small molecule inhibitor of Kv1.3 is effective in the SCID mouse psoriasis - Xenograft model," *Journal of Autoimmunity*, vol. 55, no. 1, pp. 63–72, 2015.
- [257] S. K. Upadhyay, K. L. Eckel-Mahan, M. R. Mirbolooki, I. Tjong, S. M. Griffey, G. Schmunk, A. Koehne, B. Halbout, S. Iadonato, B. Pedersen, E. Borrelli, P. H. Wang, J. Mukherjee, P. Sassone-Corsi, and K. G. Chandy, "Selective Kv1.3 channel blocker as therapeutic for obesity and insulin resistance.," *Proceedings of the National Academy of Sciences*, vol. 110, no. 24, pp. E2239–48, 2013.
- [258] N. Thieblemont, H. L. Wright, S. W. Edwards, and V. Witko-sarsat, "Human neutrophils in auto-immunity," *Seminars in Immunology*, vol. 28, no. 2, pp. 159–173, 2016.
- [259] H. Katayama, "Development of psoriasis by continuous neutrophil infiltration into the epidermis," *Experimental Dermatology*, vol. 27, no. 10, pp. 1084–1091, 2018.
- [260] I. V. Grishkan, D. M. Tosi, M. D. Bowman, M. Harary, P. A. Calabresi, and A. R. Gocke, "Antigenic Stimulation of Kv1.3-Deficient Th Cells Gives Rise to a Population of Foxp3-Independent T Cells with Suppressive Properties," *The Journal of Immunology*, vol. 195, no. 4, pp. 1399–1407, 2015.
- [261] R. Lampé, Á. Kövér, S. Szucs, L. Pál, E. Árnay, R. Ádány, and R. Póka, "Phagocytic index of neutrophil granulocytes and monocytes in healthy and preeclamptic pregnancy," *Journal of Reproductive Immunology*, vol. 107, pp. 26–30, 2015.
- [262] R. Lampé, S. Szucs, M. Ormos, R. Ádány, and R. Póka, "Effect of normal and preeclamptic plasma on superoxide-anion production of neutrophils from healthy non-pregnant women," *Journal of Reproductive Immunology*, vol. 79, no. 1, pp. 63–69, 2008.

- [263] R. Lampé, S. Szucs, R. Ádány, and R. Póka, "Granulocyte superoxide anion production and regulation by plasma factors in normal and preeclamptic pregnancy," *Journal of Reproductive Immunology*, vol. 89, no. 2, pp. 199–206, 2011.
- [264] A. Langer-Gould, H. Garren, A. Slansky, P. J. Ruiz, and L. Steinman, "Late pregnancy suppresses relapses in experimental autoimmune encephalomyelitis: Evidence for a suppressive pregnancy-related serum factor," *Journal of Immunology*, vol. 169, no. 2, pp. 1084–1091, 2002.
- [265] H. R. Petty, A. L. Kindzelskii, J. Espinoza, and R. Romero, "Trophoblast Contact Deactivates Human Neutrophils," *The Journal of Immunology*, vol. 176, no. 5, pp. 3205–3214, 2006.
- [266] G. Matute-Bello, G. Downey, B. B. Moore, S. D. Groshong, M. A. Matthay, A. S. Slutsky, and W. M. Kuebler, "An official american thoracic society workshop report: Features and measurements of experimental acute lung injury in animals," *American Journal of Respiratory Cell and Molecular Biology*, vol. 44, no. 5, pp. 725–738, 2011.

Part II.

Appendix

A. Results from collaboration partners

A.1. PIF reduces voltage-induced $K_V1.3$ currents in $K_V1.3$ -overexpressing HEK-293 cells

To test whether PIF modifies neutrophil function by inhibition of $K_V1.3$, whole cell patch clamp experiments were conducted using $K_V1.3$ -overexpressing HEK-293 cells (h $K_V1.3$ -HEK-293), incubated with 300 nM PIF or carrier substance (Ctrl). 13 consecutive 10 mV steps from -80 mV to $+40$ mV were applied for 200 ms in 30 s intervals in order to activate $K_V1.3$. h $K_V1.3$ -HEK-293 control cells developed characteristic voltage-dependent $K_V1.3$ -currents (Fig. A.1-A). Pre-treatment with PIF abolished current activation almost completely. Quantification of current densities at the different voltage steps demonstrated a significant inhibition of $K_V1.3$ by PIF (Fig. A.1-B). The use of different concentrations of PIF revealed that PIF inhibits $K_V1.3$ in a dose-dependent manner with an IC_{50} of 10.2 ± 5 nM (Fig. A.1-C and -D).

A.2. Inhibition of $K_V1.3$ by PIF impairs calcium signaling in human neutrophils

In lymphocytes, $K_V1.3$ was shown to be involved in the regulation of Ca^{2+} signaling by sustaining Ca^{2+} influx via SOCE¹⁵⁶. K^+ efflux via $K_V1.3$ maintains an electrical gradient over the cell membrane, enabling continuous Ca^{2+} influx into the cells¹⁸³. To elucidate the role of $K_V1.3$ in CRAC channel dependent Ca^{2+} influx in human neutrophils, isolated cells from healthy blood donors were loaded with the fluorometric Ca^{2+} -indicator Rhod-2 AM under Ca^{2+} -free conditions and incubated with Thapsigargin to deplete intracellular Ca^{2+} stores in the endoplasmic reticulum (ER). Addition of Ca^{2+} to the medium induced a rapid increase in $[Ca^{2+}]_i$ in vehicle treated control cells (Ctrl, Fig. A.2). Inhibition of $K_V1.3$ with 300 nM PIF or 10 nM PAP-1, respectively, significantly reduced $[Ca^{2+}]_i$, demonstrating a central role of $K_V1.3$ in SOCE in neutrophils.

To see whether overall Ca^{2+} flux is altered by $K_V1.3$ inhibition as well, isolated human neutrophils were again loaded with Rhod-2 AM in Ca^{2+} -free medium and incubated with 300 nM PIF, 10 nM PAP-1 or vehicle (Ctrl). Addition of Ca^{2+} to the medium resulted in an increase of $[Ca^{2+}]_i$ in control cells and ensuing stimulation with 10 nM CXCL8 induced a strong elevation of $[Ca^{2+}]_i$ (Fig. A.3-A). Inhibition of $K_V1.3$ using PIF and PAP-1 significantly decreased overall $[Ca^{2+}]_i$ after application of Ca^{2+} and of CXCL8 (Fig. A.3-B and -C) with PAP-1 exhibiting an even stronger inhibitory effect compared to PIF.

Sufficient Ca^{2+} influx in neutrophils is a prerequisite for successful transition from arrest to a migratory phenotype under shear stress conditions¹⁵⁸. During neutrophil adhesion

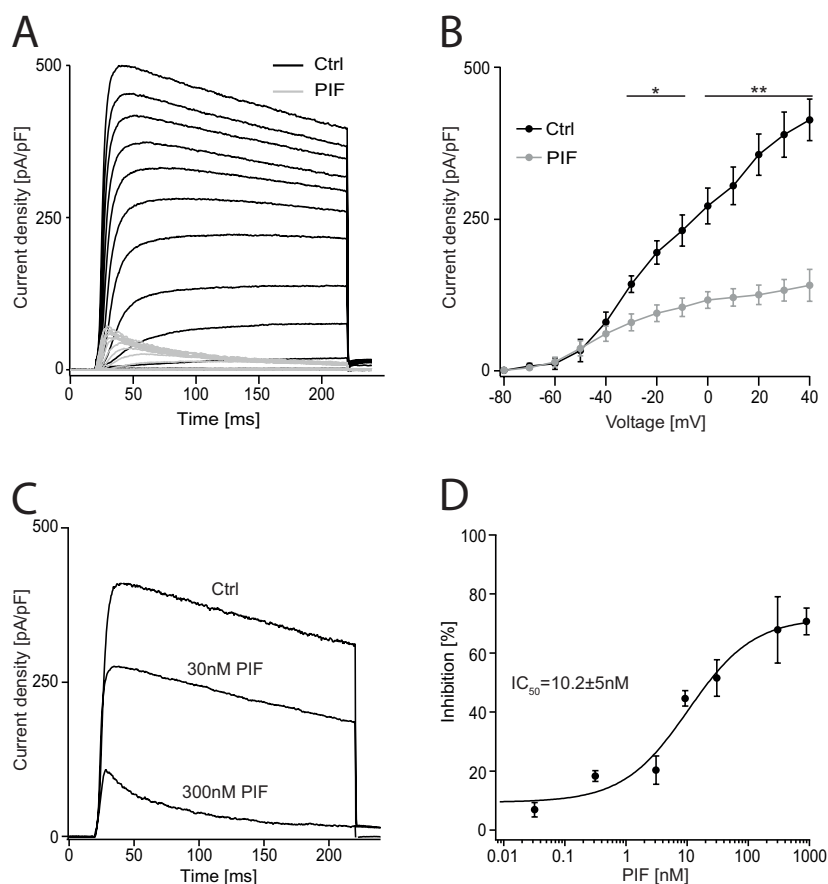


Figure A.1.: PIF reduces voltage-induced $K_V1.3$ currents in $K_V1.3$ -overexpressing HEK-293 cells. (A) HEK-293 cells, transiently overexpressing h $K_V1.3$ were incubated with PIF (gray, $n=4$ cells) or vehicle (Ctrl, black, $n=36$ cells) and activated by 13 consecutive 10 mV steps from -80 mV to $+40$ mV (all 13 traces of two representative cells). (B) Current-voltage relationship of Ctrl and PIF treated h $K_V1.3$ -HEK-293 cells (mean \pm SEM, repeated student's t-tests). (C) $K_V1.3$ -currents extracted at $+40$ mV in the absence and after pre-incubation with two different concentration of PIF (representative traces, $n=4-6$ cells per condition). (D) Dose-dependent inhibition of $K_V1.3$ -currents by increasing PIF concentrations (IC_{50} of 10.2 ± 5 nM, mean \pm SEM, $n=4-8$ cells per condition). The results were obtained in collaboration with S. Zierler and W. Nadolni from the Walther-Straub-Institut, LMU, Munich, Germany.

under flow, LFA-1/ICAM-1 bonds recruit Orai1 to LFA-1 containing focal adhesion spots, mediating local increase of $[Ca^{2+}]_i$ and subsequent remodeling of the actin cytoskeleton^{179,180}. To investigate the role of $K_V1.3$ on LFA-1 mediated mechano-signaling via SOCE, isolated human neutrophils, loaded with Rhod-2 AM and pre-treated with Thapsigargin under Ca^{2+} -free conditions, were perfused through microfluidic devices coated with LFA-1 high-affinity inducing antibodies (CBR LFA1/2) and ICAM-1¹⁰² at a constant shear rate level of 2 dyne/cm². Ca^{2+} was added to the medium and changes in $[Ca^{2+}]_i$ were monitored. Pre-incubation with 300 nM PIF or 10 nM PAP-1 significantly reduced Ca^{2+} influx compared to vehicle control (Ctrl), revealing a substantial contribution of $K_V1.3$ to LFA-1 dependent regulation of SOCE during post-arrest modification under flow (Fig. A.4).

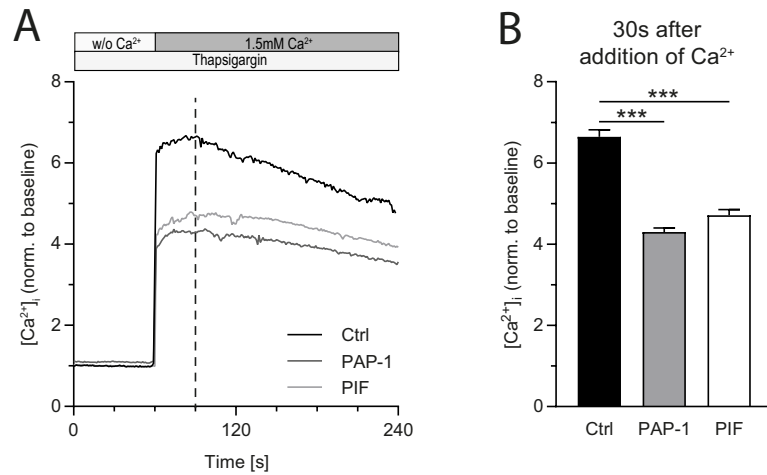


Figure A.2: $K_V1.3$ is involved in CRAC channel dependent Ca^{2+} influx in human neutrophils. Isolated human neutrophils were loaded with Rhod-2 AM, treated with Thapsigargin and subsequently incubated with PIF, PAP-1 or vehicle (Ctrl). (A) CRAC channel dependent changes in $[Ca^{2+}]_i$ were investigated before and after addition of Ca^{2+} to the medium (mean, n=57 (Ctrl), 60 (PAP-1), 88 (PIF) cells from 3 independent experiments) and (B) quantified 30s after application. (mean±SEM, 1-way ANOVA, Tukey's multiple comparison). The results were obtained in collaboration with S.I. Simon and V. Morikis, University of California, Davis, USA.

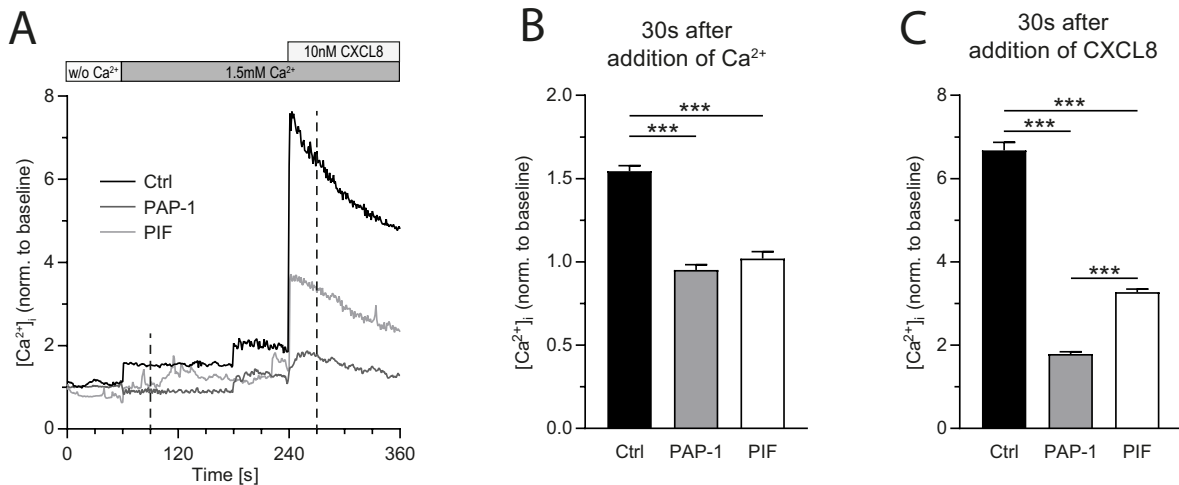


Figure A.3: $K_V1.3$ regulates total Ca^{2+} flux after CXCL8 stimulation in human neutrophils. Isolated human neutrophils were loaded with Rhod-2 AM and pre-treated with PIF, PAP-1 or vehicle (Ctrl). (A) Changes in overall $[Ca^{2+}]_i$ upon addition of Ca^{2+} and subsequent application of CXCL8 were investigated (mean) and quantified 30s after addition of either (B) Ca^{2+} (mean±SEM, n=115(Ctrl), 36 (PAP-1), 85 (PIF) cells) or (C) CXCL8, respectively. (mean±SEM, n=115(Ctrl), 69 (PAP-1), 114 (PIF) cells from 3 independent experiments, 1-way ANOVA, Tukey's multiple comparison). The results were obtained in collaboration with S.I. Simon and V. Morikis, University of California, Davis, USA.

A.3. PIF increases susceptibility to shear forces *in vitro*

To evaluate whether the disability of neutrophils to polarize and to switch to a migratory phenotype in the presence of PIF has implications on the resistance to shear forces, a detachment-assay was carried out. Isolated human neutrophils were incubated with

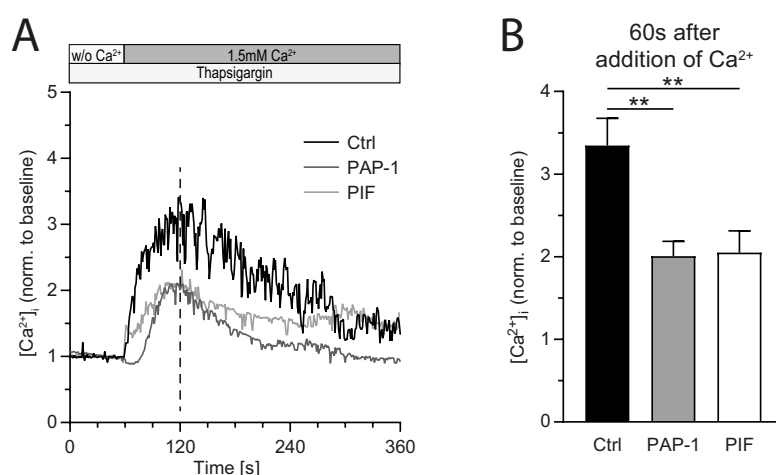


Figure A.4: $K_v1.3$ regulates intracellular Ca^{2+} concentrations under shear stress conditions. (A) Isolated human neutrophils were loaded with Rhod-2 AM and pre-treated with Thapsigargin to deplete intracellular ER Ca^{2+} stores. $K_v1.3$ was blocked with PIF, PAP-1 or vehicle (Ctrl) and cells were perfused through LFA-1 high-affinity inducing antibodies and ICAM-1 coated microfluidic devices (mean, $n=14$ (Ctrl), 38 (PAP-1), 27 (PIF) cells from 3 independent experiments) to measure $[Ca^{2+}]_i$ over time. (B) Quantification of $[Ca^{2+}]_i$ 60s after addition of Ca^{2+} to the medium (mean \pm SEM, 1-way ANOVA, Tukey's multiple comparison). The results were obtained in collaboration with S.I. Simon and V. Morikis, University of California, Davis, USA.

either 300 nM PIF, 10 nM PAP-1 or vehicle (Ctrl) and introduced into E-selectin, ICAM-1 and CXCL8 coated flow chambers. Cells were allowed to adhere for 3 min before shear was applied and increased every 30 s. Remaining cells at the end of each step were quantified. Incubation with PIF or PAP-1 resulted in a higher susceptibility of detachment to increasing shear forces compared to control (Fig. A.5).

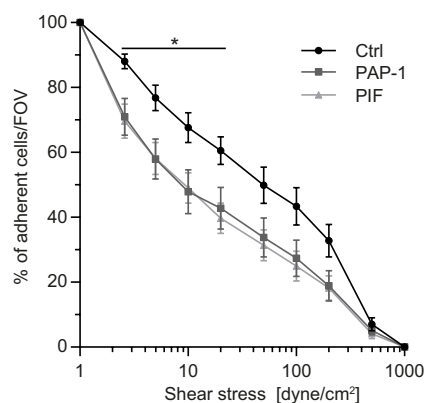


Figure A.5: PIF increases susceptibility to shear forces *in vitro*. Human neutrophils incubated with PIF, PAP-1 or vehicle (Ctrl) were introduced into E-selectin, ICAM-1 and CXCL8 coated flow chambers, exposed to increasing shear stress levels and remaining cells were quantified ($n=12-15$ flow chambers of 9-10 independent experiments one-way ANOVA, Dunnett's multiple comparison). The results were conducted by A. Yevtushenko under my supervision.

A.4. PIF impairs neutrophil recruitment in an animal model of acute lung injury after LPS stimulation

To investigate whether the inhibition of K_v1.3 by PIF might be a suitable therapeutic approach to treat overgrowing neutrophil infiltration in a clinically relevant setting, a model of acute lung injury (ALI) after LPS inhalation was performed²⁰⁸. Many severe airway diseases such as bronchitis, cystic fibrosis, chronic obstructive pulmonary disease (COPD) or ALI are characterized by substantial neutrophil infiltration^{206,207}. WT mice received an i.p. injection of 1 µg or 10 µg PIF or vehicle alone (Ctrl) 1 h prior to 30 min of exposure to LPS containing aerosol. One control group (w/o) did not receive any i.p. injection and was exposed to saline containing aerosol only. 4 h after inhalation, mice were sacrificed and recruitment of neutrophils to the lungs was analyzed by flow cytometry. In line with altered leukocyte adhesion in the mouse cremaster muscle (Fig. 4.1-A), i.p. application of both, 1 µg and 10 µg PIF prior to LPS inhalation completely impaired neutrophil recruitment to the pulmonary vasculature (Fig. A.6-A). Numbers of neutrophils in the lung interstitium (Fig. A.6-B) and in the broncho-alveolar lavage (BAL, Fig. A.6-C) were significantly reduced compared to control animals. Mice that were not exposed to LPS did not exhibit a noticeable amount of neutrophils in the interstitium and in the BAL. Finally, lung tissues of the mice were removed, fixed, stained with Mayer's hematoxylin and eosin (HE, Fig. A.6-D) and the sections were scored based on guidelines from the American Thoracic Society²⁶⁶. Quantification confirmed that both PIF concentrations significantly reduced the amount of invaded neutrophils into LPS stimulated lung tissue (Fig. A.6-E).

A.5. PIF reduces vascular leakage in a model of ALI

Massive infiltration of neutrophils into inflamed lungs is accompanied by an increase in permeability and by elevated protein content in the BAL, due to endothelial and epithelial injury²⁰⁷. Hence, in addition to the assessment of neutrophil recruitment to inflamed lungs in the ALI model, LPS induced vascular leakage was determined²⁰⁸. For that purpose, mice were injected with FITC-dextran 30 min prior to euthanasia and fluorescence of the BAL was measured and normalized to serum fluorescence levels. Albumin concentrations in the BAL were determined using ELISA. PIF treatment prior to LPS inhalation significantly reduced vascular leakage compared to control (Fig. A.7-A and -B) and reduced the fluorescence levels and albumin concentration in the BAL almost to basal levels (w/o group).

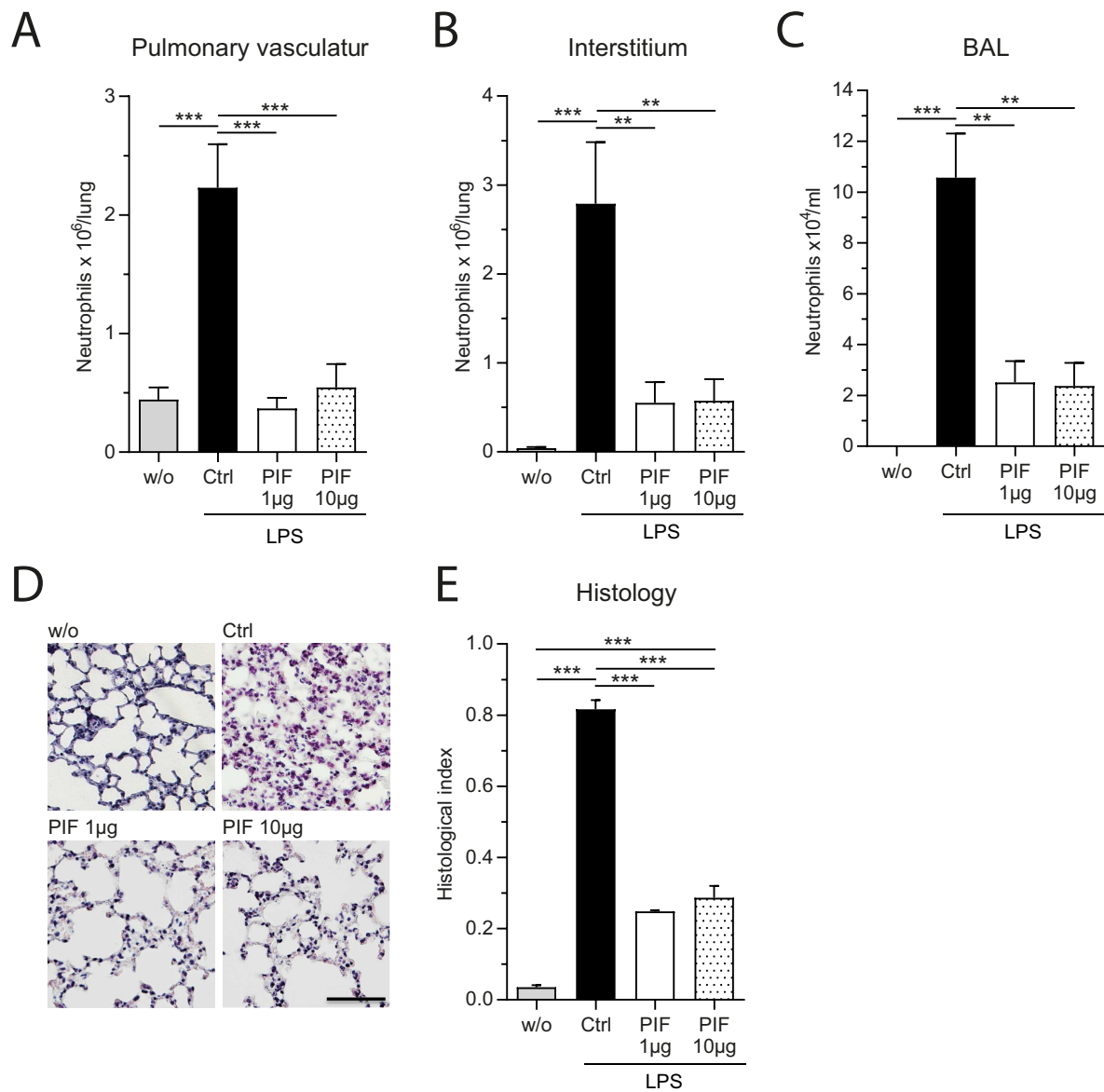


Figure A.6.: PIF impairs neutrophil recruitment in an animal model of acute lung injury. WT mice were i.p. injected with two different concentrations of PIF or with carrier substance (Ctrl) 1 h prior to LPS inhalation. 4 h later, neutrophil recruitment to (A) the pulmonary vasculature, (B) the lung interstitium and (C) into the broncho-alveolar space was analyzed. Animals from the w/o group did not receive an i.p. injection and were exposed to saline aerosol only (BAL: broncho-alveolar lavage, mean±SEM, n=7-9 mice per group, 1-way ANOVA, Tukey's multiple comparison). (D) Representative micrographs of lung sections, treated as indicated (scale bar: 250 µm) were (E) quantified according to²⁶⁶ (mean±SEM, n=3-4 mice per group, 1-way ANOVA, Tukey's multiple comparison).

The results were obtained in collaboration with O. Söhnlein, IPEK, LMU Munich, Munich, Germany, J. Grommes and J. Tilgner, RWTH Aachen, Aachen, Germany.

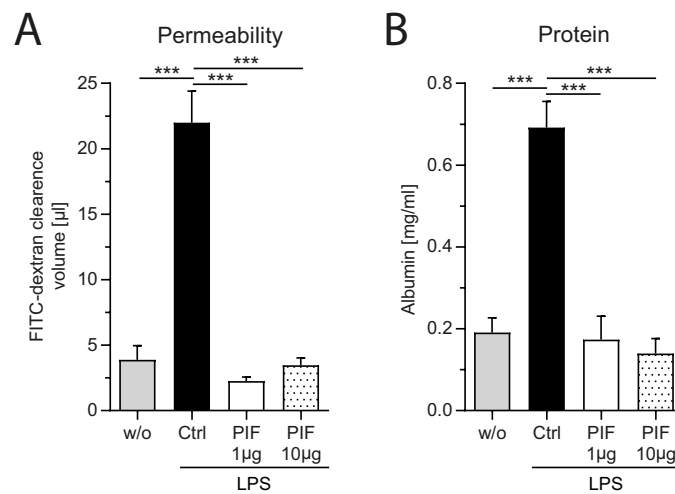


Figure A.7.: PIF reduces vascular leakage in a model of acute lung injury but does not alter integrity of cultured HUVEC cells upon TNF- α stimulation. Changes in vascular permeability were assessed by the measurement of FITC-dextran and albumin concentrations in the BAL of WT mice pre-treated i.p. with two different concentrations of PIF or carrier substance (Ctrl) 1 h prior to LPS exposure. One group did not receive an i.p. injection and was exposed to saline aerosol only (mean \pm SEM, n= n=7-9 mice, 1-way ANOVA, Tukey's multiple comparison).

Part IV.

Manuscript

1 Embryo-Derived Preimplantation Factor Disrupts Neutrophil Recruitment by
2 Reducing $K_v1.3$ -Regulated Sustained Store Operated Ca^{2+} Entry

3 Roland Immler¹, Wiebke Nadolni², Vasilios Morikis³, Ina Rohwedder¹, Jessica Tilgner⁴, Jochen
4 Grommes⁴, Anna Yevtushenko¹, Angela R M Kurz^{1,#}, Oliver Soehnlein^{5,6}, Markus Moser⁷, Thomas
5 Gudermann², Steffen Dietzel^{1,8}, Eytan Barnea⁹, Scott I Simon³, Susanna Zierler², Monika Pruenster^{1,†}
6 and Markus Sperandio^{1,†,*}

7
8 ¹ Walter Brendel Centre of Experimental Medicine, Biomedical Center, Institute of Cardiovascular
9 Physiology and Pathophysiology, Ludwig-Maximilians-Universität München, 82152 Planegg-
10 Martinsried, Germany

11 ² Walther-Straub Institute of Pharmacology and Toxicology, Ludwig-Maximilians-Universität
12 München, 80336 Munich, Germany

13 ³ Department of Biomedical Engineering, Graduate Group in Immunology, University of California,
14 Davis, CA 95616, USA

15 ⁴ Department of Vascular Surgery, RWTH Aachen, 52074 Aachen, Germany

16 ⁵ Institute for Cardiovascular Prevention (IPEK), Ludwig-Maximilians-Universität München, 80336
17 Munich, Germany

18 ⁶ Department of Physiology and Pharmacology (FyFa) and Department of Medicine, Karolinska
19 Institutet, 17177 Stockholm, Sweden

20 ⁷ Department of Molecular Medicine, Max Planck Institute of Biochemistry, 82152 Martinsried,
21 Germany

22 ⁸ Core Facility Bioimaging, Biomedical Center, Ludwig-Maximilians-Universität München, 82152
23 Planegg-Martinsried, Germany

24 ⁹ BioIncept LLC, New York, NY 10016, USA

25 # Current address: Centenary Institute, University of Sydney, New South Wales 2006, Australia

26 † These authors contributed equally to this work

27 * Corresponding author

28

29

30

31

32

33

34

35

36

37

38

39

40

41

42

43

44

45

Corresponding author:

Markus Sperandio, M.D.

Walter Brendel Center of Experimental Medicine

Biomedizinisches Centrum München

Ludwig-Maximilians-Universität

Großhaderner Str. 9

82152 Planegg-Martinsried

GERMANY

voice: +49 (0)89 2180 71513

Fax: +49 (0)89 2180 71511

Email: markus.sperandio@lmu.de

46 **Abstract**

47 Immune cells within the placenta exert essential functions throughout pregnancy but require tight
48 regulation in order to prevent recognition of the embryo as a 'semi-allograft'. Here, we report that
49 the embryonic derived peptide Preimplantation factor (PIF), which is secreted by trophoblast cells
50 and continuously released into maternal circulation, impairs neutrophil recruitment. PIF blocks $K_v1.3$
51 on neutrophils, a voltage gated potassium channel regulating membrane potential and sustained
52 store operated Ca^{2+} entry (SOCE) via K^+ efflux. Inhibition of $K_v1.3$ lowers intracellular Ca^{2+} signaling,
53 preventing post-arrest modifications by minimizing cell spreading and adhesion strengthening.
54 Consequently, PIF treatment inhibits neutrophil retention at sites of inflamed endothelium leading to
55 reduced neutrophil extravasation *in vivo*, a phenotype also observed in $K_v1.3$ deficient mice. We
56 conclude that PIF modulates neutrophil function and offers therapeutic capabilities beyond
57 pregnancy by potentially protecting patients from exuberant inflammation and excess neutrophil
58 recruitment.

59 141/150

60

61

62 **1. Introduction**

63 During pregnancy, pro- and anti-inflammatory states alternate in a finely orchestrated manner¹.
64 Successful pregnancy is initiated through infiltration of immune cells into the decidua to facilitate
65 blastocyst implantation, fetal growth and parturition¹. Imbalance in the composition of intrauterine
66 immune cell populations or of chemokine concentrations results in pregnancy complications
67 including spontaneous abortion², pre-eclampsia³ or preterm birth⁴. Trophoblast cells, which form the
68 cellular barrier between maternal and fetal tissue, play a dual role in the modulation of immune cell
69 function by secreting pro-inflammatory and homeostatic cytokines and growth factors¹. In addition,
70 they use the atypical chemokine receptor ACKR2 to scavenge pro-inflammatory chemokines at the
71 feto-maternal interface⁵, thereby reducing the chemokine gradient towards fetal tissue. Another
72 factor secreted by trophoblast cells is Preimplantation factor (PIF), which contributes to feto-
73 maternal crosstalk^{6,7}. PIF is a 15 amino acid secreted small peptide that can be detected in maternal
74 circulation at varying levels throughout pregnancy^{8,9}. It creates a pro-receptive milieu in the decidua
75 following conception¹⁰ and during trophoblast invasion¹¹. The peptide was shown to enhance local
76 progesterone activity, to increase steroid secretion and to enhance the expression of pro-tolerogenic
77 HLA molecules in cytotrophoblasts¹². Sufficient levels of PIF in the serum are required for embryo
78 development and successful birth^{9,13}. PIF also interacts with immune cells¹⁴ and attenuates the
79 severity of several T cell driven autoimmune diseases in animal models^{15,16}. However, the
80 mechanisms how PIF regulates immune responses and its role within the maternal circulation remain
81 elusive. Particularly, the action of PIF on innate immune cell function is largely unknown. Therefore,
82 we investigated the immune modulatory properties of PIF in neutrophil driven, acute inflammatory
83 scenarios outside the context of pregnancy.

84 Acute inflammatory processes involve the infiltration of innate immune cells into affected tissue¹⁷.
85 Neutrophils constitute the 'first line of defense'¹⁷ and their recruitment follows a sequence of well-
86 defined steps, starting with neutrophil tethering and rolling along the inflamed endothelium¹⁸.
87 Adhesion is followed by post-arrest modifications that strengthen the neutrophils' attachment to the
88 inflamed endothelium and guide the process of spreading, crawling and subsequent transmigration
89 through the endothelium. Once neutrophils arrive at the inflammatory site, they combat invading
90 pathogens and non-self-agents by generation of reactive oxygen species (ROS), release of granules,
91 phagocytosis and NETosis to immobilize and destroy microbes¹⁷. Besides their beneficial role in the
92 body's first line of defense against invading pathogens, neutrophils contribute to chronic
93 inflammatory disorders and autoimmune diseases¹⁷. Hence, therapeutic approaches targeting
94 neutrophil trafficking and functions are of particular interest to treat overwhelming innate immune
95 responses.

96 Using *in vivo* and *in vitro* mouse models, as well as electrophysiological techniques in primary human
97 neutrophils, we show that PIF inhibits the voltage-gated potassium channel $K_v1.3$ leading to
98 significant impairment of neutrophil recruitment. Thus, we identify PIF as a potent endogenous anti-
99 inflammatory agent and suggest a potential role of PIF as a therapeutic molecule beyond its function
100 during pregnancy.

101

102 **2. Results**

103 **PIF impairs leukocyte recruitment *in vivo* and *in vitro*.** To elucidate the influence of PIF on innate
104 immune cell functions, we studied leukocyte recruitment in an acute, predominantly neutrophil
105 driven, inflammatory setting¹⁹. Using intravital microscopy (IVM), leukocyte interactions with the
106 endothelium were assessed in postcapillary venules of TNF- α stimulated mouse cremaster muscles.
107 PIF was injected into the scrotum (intrascrotal; i.s.) of C57BL/6 wild-type (WT) mice 1h prior to i.s.
108 injection of TNF- α . As controls, either a scrambled version of the peptide (scrPIF) or the carrier
109 substance alone (Ctrl) was applied. The number of adherent cells on the inflamed endothelium was
110 significantly reduced in PIF-treated animals (Fig. 1a) compared to both control groups. In addition,
111 leukocytes in PIF treated mice displayed increased rolling velocities (Fig. 1b). Prior administration of
112 PIF further resulted in significantly reduced numbers of perivascular neutrophils compared to
113 controls (Fig. 1c, d). Application of PIF did not affect systemic white blood cell (WBC) and neutrophil
114 counts (Supplementary Tab. 1). In order to study whether PIF directly acts on leukocytes or mainly on
115 endothelial cells, we performed *in vitro* flow chamber assays. Glass capillaries were coated with
116 recombinant E-selectin, intracellular adhesion molecule-1 (ICAM-1) and CXCL1 to mimic inflamed
117 endothelium and murine whole blood was perfused through the chambers. Similar to the *in vivo*
118 observations, pre-incubation of murine whole blood with PIF resulted in significantly reduced
119 numbers of adherent leukocytes per field of view (FOV) (Fig. 1e) and in increased rolling velocities
120 (Fig. 1f) compared to controls. Overall surface expression of CD18, CD11a, CD11b, P-selectin
121 glycoprotein ligand-1 (PSGL-1), CD44, L-selectin, and CXCR2 on peripheral blood neutrophils was not
122 affected after i.s. injection of PIF compared to control as shown by flow cytometry (Supplementary
123 Fig.1a-g.). Taken together, in an animal model of acute inflammation, PIF alters leukocyte
124 recruitment by increasing rolling velocity of the cells, reducing transition to arrest on inflamed
125 endothelium and extravasation into inflamed tissue. This is predominately mediated by a direct
126 effect of PIF on leukocytes rather than on the endothelium, since an identical adhesion phenotype
127 was observed under defined *in vitro* flow chamber conditions.

128 **Functional K_v1.3 is expressed on human and murine neutrophils and is critical for leukocyte**
129 **recruitment *in vivo*.** Next, we tried to identify the molecular target of PIF. A mass spectrometry
130 analysis of decidual cells revealed a broad spectrum of putative interaction partners, including the
131 voltage gated potassium channel K_v1.3¹⁰. K_v1.3 has been reported to regulate cell adhesion and
132 integrin activation in lymphocytes²⁰. Since this channel has not been functionally identified on
133 neutrophils yet, we first analyzed expression of K_v1.3. Western blot analysis, with Jurkat cell lysates
134 as positive control, revealed expression of K_v1.3 in human and murine neutrophils (Fig. 2a).
135 Moreover, confocal microscopy (Fig. 2b) and flow cytometry (Supplementary Fig. 2) demonstrated

136 expression of $K_v1.3$ on the plasma membrane. To validate functionality of the channel on
137 neutrophils, we performed electrophysiological experiments using a whole-cell patch-clamp
138 approach. $K_v1.3$ channels on isolated human neutrophils were activated with a 10mV step protocol
139 from -80mV to +40mV at a holding potential of -80 mV with 30s intervals²¹. Neutrophils developed
140 typical voltage-activated potassium currents (Fig 2c), which were reduced by the addition of the
141 $K_v1.3$ -specific inhibitor 5-(4-Phenoxybutoxy)psoralen (PAP-1)²² (Fig. 2d). Local application of PAP-1
142 after current activation with a single voltage-step up to +40mV further demonstrated that these
143 potassium currents in neutrophils were sensitive to PAP-1-inhibition (Fig. 2e), indicating the
144 expression of functional $K_v1.3$ channels in primary human neutrophils.

145 To test whether inhibition of $K_v1.3$ with PAP-1 affects leukocyte recruitment *in vivo* similar to PIF
146 application, PAP-1 or vehicle alone (Ctrl) was injected i.s. into WT mice followed by application of
147 TNF- α to induce inflammation. The number of adherent leukocytes and rolling velocities were
148 determined. Inhibition of $K_v1.3$ via PAP-1 significantly reduced the number of adherent leukocytes
149 (Fig. 2f) in inflamed postcapillary venules compared to control. Notably, the level of inhibition was
150 equivalent to PIF-antagonized reduction of adhesion (Fig. 1a) and concomitant application of PAP-1
151 and PIF did not further reduce the number of adherent cells. Likewise, blockade of $K_v1.3$ by PAP-1
152 elevated leukocyte rolling velocities (Fig. 2g) compared to control. Again, simultaneous application of
153 PAP-1 and PIF did not further increase rolling velocities along inflamed endothelium. In a second set
154 of experiments, we examined leukocyte adhesion and rolling velocities after TNF- α stimulation in
155 mice lacking $K_v1.3$ ²³. In line with the previous results, loss of $K_v1.3$ resulted in a significant reduction
156 of adherent cells mm⁻² (Fig. 2h) and $K_v1.3$ ^{-/-}-leukocytes rolled significantly faster (Fig. 2i) compared to
157 controls. Moreover, injection of PIF into $K_v1.3$ deficient mice prior to TNF- α stimulation did not
158 further suppress leukocyte adhesion or alter rolling velocities. Overall leukocyte and neutrophil blood
159 counts did not differ among experimental groups in both experimental settings (Supplementary Tab.
160 2). Expression levels of CD18, CD11a, CD11b, PSGL-1, CD44, L-selectin, and CXCR2 on peripheral
161 blood neutrophils were similar between $K_v1.3$ ^{-/-} and WT mice (Supplementary Fig. 3a-g). Finally, we
162 quantified neutrophil extravasation in TNF- α stimulated cremaster muscles derived from PAP-1
163 treated WT, WT and $K_v1.3$ ^{-/-}-mice (Fig. 2j). A significant reduction of perivascular neutrophils was
164 observed with either inhibition or genetic deletion of $K_v1.3$ (Fig. 2k) compared to control. These data
165 demonstrate that $K_v1.3$ is crucial for neutrophil recruitment and transmigration *in vivo*.

166 **PIF reduces voltage-induced $K_v1.3$ currents in a $K_v1.3$ overexpressing cell line and in human**
167 **neutrophils.** Next, we aimed to clarify whether $K_v1.3$ channels were indeed molecular targets of PIF.
168 To do so, we expressed human $K_v1.3$ in HEK-293 cells and applied consecutive 10mV voltage-steps.
169 As expected, characteristic $K_v1.3$ currents developed in response to voltage-stimulation reaching

170 their maximum at +40mV (Fig. 3a). Application of PIF almost completely abolished current activation
171 in response to voltage-stimulation (Fig. 3a, 300nM). Quantification showed a characteristic increase
172 in current-voltage relationships in response to increasing membrane voltages, which was significantly
173 inhibited in the presence of PIF (Fig. 3b). Varying concentrations of PIF applied to active $K_v1.3$
174 currents revealed a dose-dependent inhibition of the channel with an IC_{50} of ~ 10.2 nM using Hill
175 equation (Fig. 3c,d). To verify its inhibitory properties on native neutrophil $K_v1.3$ channels, we applied
176 the same consecutive step-protocol to induce characteristic $K_v1.3$ currents, which were strongly
177 decreased by the application of PIF (Fig. 3e). Application of PIF on already active $K_v1.3$ currents
178 triggered via a single +40mV step showed an even stronger inhibition of current amplitudes (Fig.
179 3f,g), higher than the inhibition via PAP-1. Pre-incubation of human neutrophils with PIF and PAP-1 in
180 the extracellular bath solution confirmed our results observed via direct application (Supplementary
181 Fig. 4a-e). In contrast to PIF and PAP-1 treatment, 1-[(2-Chlorophenyl)diphenylmethyl]-1H-pyrazole
182 (TRAM-34), a specific inhibitor for the calcium activated potassium channel $K_{Ca}3.1$, which is also
183 expressed in neutrophils²⁴, did not show any significant inhibition of $K_v1.3$ currents. Our results
184 demonstrate that PIF specifically targets $K_v1.3$ channels and strongly inhibits the voltage-activated
185 potassium current in primary human neutrophils as well as in $K_v1.3$ overexpressing cell lines.

186 **$K_v1.3$ is involved in calcium signaling in human neutrophils.** In lymphocytes, $K_v1.3$ regulates Ca^{2+}
187 signaling by sustaining Ca^{2+} influx via store-operated Ca^{2+} entry (SOCE)²⁵. K^+ efflux via $K_v1.3$ affects the
188 membrane potential, maintaining a high driving-force for continuous Ca^{2+} influx²⁵. To determine the
189 contribution of $K_v1.3$ on SOCE in human neutrophils, we loaded neutrophils, isolated from healthy
190 donors, with the fluorometric Ca^{2+} -indicator Rhod-2 AM under Ca^{2+} -free conditions and pre-treated
191 them with Thapsigargin to deplete Ca^{2+} stores in the endoplasmic reticulum (ER). Subsequent
192 addition of Ca^{2+} to the medium increased intracellular Ca^{2+} concentrations ($[Ca^{2+}]_i$) via SOCE in vehicle
193 treated neutrophils (Ctrl), while presence of PIF or PAP-1 significantly reduced Ca^{2+} entry (Fig. 4a,b).
194 To study whether inhibition of $K_v1.3$ alters the overall Ca^{2+} flux in neutrophils, we measured changes
195 in $[Ca^{2+}]_i$ upon chemokine activation without prior ER Ca^{2+} store depletion. Rhod-2 AM loaded and
196 seeded neutrophils were exposed to Ca^{2+} which again induced an increase in $[Ca^{2+}]_i$. in control cells.
197 Ensuing application of CXCL8 resulted in a characteristic Ca^{2+} spike (Fig. 4c). Neutrophils pre-treated
198 with PIF or PAP-1 exhibited a significant drop in $[Ca^{2+}]_i$ in response to Ca^{2+} and to CXCL8 stimulation
199 (Fig. 4d,e). PAP-1-treatment reduced $[Ca^{2+}]_i$ to a higher extend compared to PIF treatment. Under
200 flow conditions, sufficient Ca^{2+} influx is a prerequisite for the transition from arrest to a migratory
201 phenotype in neutrophils²⁶. Under these conditions, high-affinity Leukocyte function antigen-1 (LFA-
202 1)/ICAM-1 bonds induce adhesion strengthening that resists fluid shear stress and supports
203 neutrophil arrest. Within membrane sites of focal adhesion, LFA-1 co-clusters with CRAC channels to
204 signal the influx in local cytosolic Ca^{2+} that activates neutrophil shape change and mobility²⁷. To

205 examine the role of $K_v1.3$ and PIF on LFA-1 mechano-signaling via SOCE, neutrophils were perfused
206 over glass substrates coated with high-affinity LFA-1 inducing antibody along with its endothelial
207 ligand ICAM-1 using a microfluidic device²⁸. Adherent cells were exposed to shear flow and the
208 addition of extracellular Ca^{2+} and ensuing changes in $[Ca^{2+}]_i$ were measured (Fig. 4f). Significant
209 inhibition of Ca^{2+} influx was observed in the presence of PIF or PAP-1 compared to control (Fig. 4g),
210 revealing a key role of $K_v1.3$ in LFA-1 dependent regulation of SOCE during post-arrest modification
211 steps. With these results, we demonstrate that $K_v1.3$ contributes substantially to sustained SOCE in
212 neutrophils and that an inhibition of K^+ efflux via $K_v1.3$ leads to reduced $[Ca^{2+}]_i$ under static and under
213 flow conditions.

214 **PIF impairs neutrophil post-arrest modifications.** To further delineate how reduced $[Ca^{2+}]_i$ in the
215 presence of PIF or PAP-1 exert functional defects on post-arrest modification under shear, we
216 performed spreading assays under appropriate shear flow conditions. For this, we isolated human
217 neutrophils from healthy donors, incubated the cells with PIF, PAP-1 or vehicle and introduced them
218 into microfluidic channels coated with E-selectin, ICAM-1 and CXCL8, simulating inflamed venules.
219 After a short period of interaction with the substrate, control neutrophils began to spread as
220 indicated by flattening of the cells and the appearance of a migratory phenotype with membrane
221 protrusions in the form of pseudopod formation (Fig. 5a). The cellular shape of neutrophils incubated
222 with PIF or PAP-1 remained smaller and rounder over time (Fig. 5b,c), displaying fewer protrusions
223 (Fig. 5d). To investigate whether reduced intracellular Ca^{2+} levels and impairment of spreading go
224 along with defective leukocyte adhesion strengthening, we performed an *in vitro*-detachment assay
225 by gradually increasing fluid shear forces. Isolated human neutrophils were incubated with PIF, PAP-1
226 or vehicle and introduced into E-selectin, ICAM-1 and CXCL8 coated flow chambers. After 3min of
227 settling and adhering, shear stress was applied and flow rate was incrementally increased.
228 Neutrophils, which were pre-incubated with PIF or PAP-1 were significantly more susceptible to
229 detachment at physiological shear stress levels (2-20 dyne cm^{-2}) compared to control cells (Fig. 5e).
230 These findings reveal that PIF and PAP-1 mediated inhibition of $K_v1.3$ and the resulting decrease in
231 $[Ca^{2+}]_i$ affect post-arrest modification steps, leading to defective cellular spreading and reduced cell
232 adhesion strengthening under physiological shear stress conditions.

233 **PIF impairs neutrophil recruitment in an animal model of acute lung injury after LPS stimulation.**
234 Many severe airway diseases like bronchitis, chronic obstructive pulmonary disease (COPD), cystic
235 fibrosis and acute lung injury (ALI), are characterized by massive neutrophil infiltration into the
236 lung²⁹. To evaluate whether $K_v1.3$ inhibition by PIF provides a potential therapeutic approach to
237 interfere with neutrophil recruitment in a clinically relevant setting, we performed a model of ALI
238 after LPS inhalation. To do so, we administered two different concentrations of PIF or carrier

239 substance intra-peritoneally (i.p.) to WT mice before exposing them to LPS containing aerosol.
240 Neutrophil counts in lung tissue (pulmonary vasculature and interstitium) and bronchoalveolar
241 lavage (BAL) were assessed by flow cytometry. In all three compartments, inhalation of LPS resulted
242 in significantly increased numbers of neutrophils compared to mice treated with saline aerosol alone
243 (w/o) (Fig. 6a-e). Injection of PIF prior to LPS exposure abolished neutrophil recruitment to the
244 pulmonary vasculature, the interstitium and the bronchoalveolar space almost completely. These
245 data clearly identify PIF as a strong immunomodulatory drug in an animal model of ALI and point out
246 its potential role for the treatment of acute inflammatory disorders.

247

248 3. Discussion

249 The maternal immune system plays a dual role during pregnancy. On the one hand, it remains
250 competent and active to successfully protect the organism from bacterial and viral infections. On the
251 other hand, it requires mechanisms for desensitization of immune responses to fetal tissue in order
252 not to recognize it as a 'semi-allogenic transplant'. Indeed, pregnant women are more susceptible to
253 bacterial infections^{30,31} and often appear clinically protected from pre-existing autoimmune
254 diseases^{32,33}. After parturition, the mother's immune system reverts to its previous state and
255 autoimmune diseases often relapse. These facts speak for the presence of a pregnancy specific
256 factor, sufficient to dampen immune cell functions within the maternal serum. Preimplantation
257 factor (PIF) is a pregnancy specific small peptide, secreted by trophoblast cells¹⁴ and present in
258 maternal serum throughout pregnancy⁸. In this study, we examined the role of PIF as a modulator of
259 inflammation. We show that PIF blocks the voltage gated potassium channel $K_v1.3$ on neutrophils,
260 thereby reducing SOCE and $[Ca^{2+}]_i$. Consequently, post-arrest modification is disturbed and
261 neutrophils are unable to spread and to withstand physiological shear forces, resulting in disrupted
262 leukocyte adhesion and extravasation into inflamed tissue.

263 Serum levels of PIF in maternal circulation range from ~50nM during the 1st to ~60nM during the 2nd
264 and 3rd trimester⁸. Given the fact that PIF inhibits $K_v1.3$ on peripheral blood neutrophils with an IC_{50}
265 of 10.2nM, we propose a role for PIF in actively desensitizing immune cells during pregnancy. In line,
266 sera of pregnant mice were shown to reduce T cell activation and cytokine production³⁴ and
267 neutrophils of pregnant women exhibit an overall diminished phagocytic capacity³⁵. ROS production
268 is lowered in neutrophils of pregnant women as well as in neutrophils of non-pregnant women
269 incubated with sera from pregnant women^{36,37}. Phagocytosis as well as ROS production strongly
270 depend on changes in intracellular Ca^{2+} levels²⁶. Therefore, interference of PIF with SOCE via
271 inhibition of $K_v1.3$ may constitute an effective mechanism to control neutrophil activity during
272 pregnancy with an increased susceptibility to infections. According to our findings, we suggest that
273 the reduced phagocytic activity together with lower ROS levels shown in previous studies, are
274 consequences of $K_v1.3$ inhibition by PIF. The observation that neutrophils change their Ca^{2+}
275 oscillations upon contact with trophoblast cells *in vitro*³⁸ further supports this hypothesis.

276 The functional role of $K_v1.3$ in immune cells has been investigated recently in T cells, showing that an
277 increase in $[Ca^{2+}]_i$ and concomitant depolarization of the cell membrane opens this voltage gated
278 channel, allowing potassium to leave the cell³⁹. K^+ efflux in turn hyperpolarizes the cellular
279 membrane leading to sustained Ca^{2+} influx via CRAC channels, thereby maintaining long lasting high
280 $[Ca^{2+}]_i$. In this study, we discovered surface expression of $K_v1.3$ on human and murine neutrophils by
281 western blot analysis, flow cytometry and confocal immunofluorescence microscopy. Using a whole-

282 cell patch-clamp approach, we show that depolarization of human neutrophils results in a
283 characteristic $K_v1.3$ outward current that was reduced by PAP-1, a specific $K_v1.3$ -inhibitor.
284 Additionally, we demonstrate that $K_v1.3$ directly affects Ca^{2+} signaling in neutrophils. Inhibition of
285 $K_v1.3$ by PAP-1 lowers CRAC channel dependent Ca^{2+} influx. As PIF reduces K^+ outward currents
286 similar to PAP-1, we provide evidence that PIF directly binds to and inhibits $K_v1.3$ as recently
287 assumed on the basis of mass spectrometry analysis¹⁰.

288 Fluid shear forces acting on LFA-1/ICAM-1 bonds amplify CRAC channel dependent Ca^{2+} influx in
289 neutrophils, enabling the cells to rearrange their cytoskeleton, a prerequisite for firm adhesion and
290 subsequent shape polarization and migration²⁷. Orai1 is the predominant CRAC channel in
291 neutrophils that cooperates with LFA-1 to regulate Ca^{2+} entry during recruitment²⁶. It is recruited to
292 focal adhesive sites, co-localizes with high affinity LFA-1 and facilitates F-actin polymerization²⁷. This
293 has led to the hypothesis that a molecular complex consisting of LFA-1, Kindlin3 and Orai1 mechano-
294 signals a local increase of intracellular Ca^{2+} and the creation of Ca^{2+} -rich microdomains, which enable
295 fast and efficient reorganization of the cytoskeleton to guide neutrophil emigration. We expand the
296 picture by showing that K^+ efflux through $K_v1.3$ is critical for maintaining membrane cation
297 equilibrium during LFA-1 mediated Ca^{2+} influx via SOCE. $K_v1.3$ may also be involved in the creation of
298 locally high Ca^{2+} concentrations within focal adhesions in T cells, as it physically interacts with β_1
299 integrins²⁰. Inhibition of $K_v1.3$ by PAP-1 or PIF resulted in a higher susceptibility of neutrophils to
300 increasing shear forces, suggesting that $K_v1.3$ is a central player in linking adhesion receptors to the
301 cytoskeleton in neutrophils. In line with these findings, application of PAP-1 or PIF, or genetic
302 deletion of $K_v1.3$ reduced the number of adherent cells in an acute inflammation model of the mouse
303 cremaster muscle *in vivo*. Consequently, extravasation of neutrophils in mice treated with PAP-1 or
304 PIF or within $K_v1.3$ knockout mice was severely reduced in this acute inflammation model.

305 Modulation of neutrophil recruitment by PIF dependent inhibition of $K_v1.3$ activity does not only
306 provide us with new insights into neutrophil biology, but also opens new therapeutic approaches in
307 the treatment of acute and chronic inflammatory conditions outside pregnancy. Autoimmune
308 arthritis, COPD or psoriasis are all characterized by massive infiltration of neutrophils^{29,40}. Here, we
309 show that PIF application disrupts neutrophil extravasation in an animal model of LPS induced acute
310 lung injury. Previous studies demonstrated that continuous PIF administration reduces the severity of
311 multiple sclerosis and type I diabetes mellitus in mouse models^{15,16}. In addition, PIF application
312 diminished Graft-versus-Host disease after bone marrow transplantation in mice⁴¹. Furthermore,
313 $K_v1.3$ has been suggested a promising pharmacological target to treat T cell mediated autoimmune
314 diseases, as it is highly upregulated on effector memory T (T_{EM}) but not on naïve T lymphocytes⁴².
315 Inhibition of $K_v1.3$ attenuates progression in multiple sclerosis⁴³, type I diabetes mellitus⁴⁴ or

316 psoriasis⁴⁵. As PIF directly acts on K_v1.3, blocks the channel and negatively regulates leukocyte
317 functions, we propose PIF as an interesting therapeutic compound in a whole variety of immune
318 disorders. In contrast to the large number of available K_v1.3 inhibitors⁴², PIF is an endogenous
319 peptide with an IC₅₀ of 10.2nM. Maternal serum levels during pregnancy are around 50-60nM,
320 implicating that systemic application of PIF as a therapeutic compound might exert minimal side
321 effects. A phase I safety study using PIF in patients with autoimmune hepatitis has shown positive
322 safety and tolerability⁴⁶. The proposed function of PIF on innate immune cells is furthermore of great
323 relevance, as there is increasing evidence that the innate immune system, especially neutrophils play
324 an important role in the appearance and maintenance of classical T cell driven diseases, such as
325 psoriasis, multiple sclerosis or type I diabetes mellitus^{40,47}.

326 In summary, we demonstrate that PIF suppresses neutrophil functions via its direct interaction with
327 the voltage-gated potassium channel K_v1.3 leading to impaired intracellular Ca²⁺ signaling and
328 reduced neutrophil recruitment into inflamed tissue. PIF may open a broad range of new therapeutic
329 opportunities in patients with unwanted excessive leukocyte recruitment including acute and chronic
330 inflammatory disorders, autoimmune disorders and graft-versus-host disease.

331

332 **Acknowledgements**

333 We thank Susanne Bierschenk and Nadine Schmidt for excellent technical assistance and Stephan
334 Grissmer for providing the hKv1.3 plasmid. We also thank Christoph Scheiermann for critically
335 reading the manuscript. Work was supported by the German Research Foundation (DFG)
336 collaborative research grant SFB914, projects A01 (to MM), B01 (to MS), the DFG TRR-152, projects
337 P14 (to SZ) and P15 (to TG) and the core facility bioimaging at the Biomedical Center, LMU, Planegg-
338 Martinsried, Germany.

339 **Authors contribution**

340 RI conceived and performed experiments, analyzed results and wrote the manuscript. WN, VM, IR,
341 JT, JG, AY, and ARMK performed experiments and analyzed data. OS, MM, TG, SD, EB provided their
342 expertise and critical reagents. SIS and SZ conceived experiments, analyzed results and provided their
343 expertise. MP and MS conceived experiments and wrote the manuscript.

344 **Competing Interests statement**

345 EB is chief scientist of BioIncept LLC (uncompensated). All other authors declare no competing
346 interests.

347

348 **Figure 1 PIF impairs leukocyte recruitment *in vivo* and *in vitro***

349 WT mice were pre-treated intrascrotally (i.s.) with PIF, scrPIF or vehicle (Ctrl) 1h prior to TNF- α
350 stimulation. **a**, Number of adherent leukocytes per vessel surface (n=25-30 vessels of 8-10 mice per
351 group, one-way ANOVA, Tukey's multiple comparison) and **b**, leukocyte rolling velocities (n=192
352 (Ctrl), 225 (scrPIF) and 222 (PIF) cells of 8-10 mice per group, one-way ANOVA, Tukey's multiple
353 comparison) were analyzed using intravital microscopy 2h after onset of inflammation. Cremaster
354 muscles were stained with Giemsa. **c**, Representative micrographs (scale bar: 30 μ m). **d**, Number of
355 perivascular neutrophils was quantified (n=49-51 vessels from 3 mice per group, one-way ANOVA,
356 Tukey's multiple comparison). **e,f**, E-selectin, ICAM-1 and CXCL1 coated flow chambers were
357 perfused with murine whole blood, incubated with PIF or vehicle (Ctrl) and number of adherent cells
358 FOV⁻¹ (n=7-9 flow chambers from 5 mice per group, unpaired student's t-test) and leukocyte rolling
359 velocities were assessed (n=78 (Ctrl) and 90 (PIF) cells from 5 mice per group, unpaired student's t-
360 test). *: p \leq 0.05 **: p \leq 0.01 ***: p \leq 0.001, data are represented as mean \pm s.d. or cumulative frequency.

361

362 **Figure 2 Functional K_v1.3 is expressed on human and murine neutrophils and plays a crucial role in**
363 **leukocyte recruitment *in vivo***

364 **a**, Total K_v1.3 protein levels of Jurkat cells (positive control), human (hPMN) and murine (mPMN)
365 neutrophils were analyzed by western blot. Detection of GAPDH served as loading control
366 (representative blot from n=3 independent experiments). **b**, Surface localization of K_v1.3 was
367 determined by confocal microscopy (representative images from n=3 independent experiments,
368 scale bar: 10 μ m). **c,d,e** Patch clamp was used to investigate functionality of K_v1.3 in primary human
369 neutrophils. **c**, Application of 13 consecutive 10mV steps from -80mV to +40mV induced the
370 development of voltage-activated potassium currents in control cells. **d**, Presence of PAP-1 reduced
371 voltage-activated potassium currents (representative traces no. 1, 4, 8, 13 of n=10 cells for each
372 treatment). **e**, Potassium currents measured in primary human neutrophils in absence (black) and
373 after direct application of PAP-1 (grey) after current activation with a single voltage-step from the
374 holding-potential of -80mV to +40mV (representative traces of n=4 cells). **f-i**, WT and K_v1.3^{-/-} mice
375 were pre-treated i.s. as indicated 1h prior to TNF- α stimulation. **f,h**, Number of adherent leukocyte
376 per vessel surface (n= 15-17 vessels of 4 mice per group and n=19 vessels of 5 mice per group,
377 respectively, one-way ANOVA, Tukey's multiple comparison) and **g,i**, leukocyte rolling velocities
378 (n=136 (Ctrl), 105 (PAP-1), 82 (PAP-1+PIF), one-way ANOVA, Tukey's multiple comparison) cells and
379 175 (WT), 123 (K_v1.3^{-/-}) and 124 (K_v1.3^{-/-}+PIF) cells, respectively) were assessed. **j,k**, Cremaster
380 muscles were stained with Giemsa. **j**, Representative micrographs (scale bar: 30 μ m). **k**, Number of
381 perivascular neutrophils was quantified (n=19-45 vessels of 3 mice per group, one-way ANOVA,
382 Tukey's multiple comparison). **: p \leq 0.01 ***: p \leq 0.001, data are represented as mean \pm s.d. or
383 cumulative frequency.

384

385 **Figure 3 PIF reduces voltage-induced K_v1.3 currents in a K_v1.3 overexpressing cell line and in**
386 **human neutrophils**

387 **a**, K_v1.3 currents were measured using patch clamp in HEK-293 cells transiently overexpressing hK_v1.3
388 channels (hK_v1.3-HEK-293) by the application of 13 consecutive 10mV steps from -80mV to +40mV
389 over 200ms in the absence (Ctrl, black, n=36 cells) and presence of PIF (grey, n=4 cells). All 13 traces
390 normalized to cell size as current density (pA/pF) of a representative cell are depicted. **b**, Current-

391 voltage relationship of control measurements (Ctrl, black) and PIF (grey) treated hK_v1.3-HEK-293 cells
392 (n=4 cells, repeated unpaired student's t-tests). **c**, K_v1.3 currents were extracted at +40mV in the
393 absence and after application of two different concentrations of PIF (n=4-6 cells). **d**, Dose-dependent
394 inhibition of K_v1.3 currents in hK_v1.3-HEK-293 cells by increasing concentrations of PIF application
395 was determined. Average peak current inhibition is shown in [%] plotted against increasing PIF
396 concentrations [nM] (n=4-8 cells, IC₅₀=10.2±5nM. Hill=0.8±0.4). **e**, K_v1.3 currents in primary human
397 neutrophils were induced by the application of consecutive voltage-steps as in **a**, before (Ctrl, black)
398 and after (grey) peptide application (representative traces no. 1, 4, 8, 13 from n=5 cells). **f**, K_v1.3
399 currents in primary human neutrophils were induced by the application of a single voltage-step to +
400 40mV, before (Ctrl, black) and after (PIF, grey) peptide application (representative traces of n=5
401 cells). **g**, Current inhibition [%] of K_v1.3 currents in primary human neutrophils after application of the
402 K_{Ca}3.1 blocker TRAM-34, PAP-1 and PIF (n=4-5 cells, one-way ANOVA, Tukey's multiple comparison).
403 *: p≤0.05; **: p≤0.01; ***: p≤0.001, data in **b,d,g** are represented as mean±SEM.

404

405 **Figure 4 K_v1.3 is involved in Ca²⁺ signaling in human neutrophils.**

406 Isolated human neutrophils were loaded with Rhod-2 AM and subsequently pretreated with PIF,
407 PAP-1 or vehicle (Ctrl). Changes in [Ca²⁺]_i were observed in Ca²⁺ free buffer and after the addition of
408 1.5mM Ca²⁺. **a**, CRAC channel dependent Ca²⁺ influx in human neutrophils pretreated with
409 Thapsigargin was determined under static conditions and **b**, [Ca²⁺]_i were quantified 30s after addition
410 of Ca²⁺ (n=57 (Ctrl) 60 (PAP-1) and 88 (PIF) cells from 3 independent experiments, one-way ANOVA,
411 Tukey's multiple comparison). **c**, Total Ca²⁺ flux was investigated after the addition of Ca²⁺ and after
412 stimulation with CXCL8 under static conditions. **d**, Total [Ca²⁺]_i relative to baseline was quantified 30s
413 after addition of Ca²⁺ (n=114 (Ctrl), 35 (PAP-1) and 80 (PIF) cells from 3 independent experiments,
414 one-way ANOVA, Tukey's multiple comparison) and **e**, 30s after stimulation with CXCL8 (n=115 (Ctrl),
415 69 (PAP-1) and 114 (PIF) cells from 3 independent experiments, one-way ANOVA, Tukey's multiple
416 comparison). **f**, Ca²⁺ flux of neutrophils pretreated with Thapsigargin perfused over a substrate of
417 ICAM-1 and CBR LFA1/2 LFA-1 antibody using microfluidic devices was measured and **g**, quantified
418 60s after addition of Ca²⁺ under shear conditions (n=14 (Ctrl), 36 (PAP-1) and 25 (PIF) cells from 3
419 independent experiments, one-way ANOVA, Tukey's multiple comparison). **: p≤0.01 ***: p≤0.001,
420 data in **a,c,f** are represented as mean and data in **b,d,e,g** are represented as mean±s.d. Dotted lines
421 in **a,c,f** represent the time points of quantification.

422 **Figure 5 PIF impairs neutrophil post-arrest modifications.**

423 Human neutrophils were pretreated with PIF, PAP-1 or vehicle (Ctrl), introduced into E-selectin,
424 ICAM-1 and CXCL8 coated flow chambers and monitored over time. **a**, Representative micrographs of
425 neutrophils 30s, 210s and 360s after attachment (scale bar: 10µm). **b**, Cell perimeter, **c**, cell
426 circularity and **d**, cell solidity were quantified over time (49 (Ctrl), 60 (PAP-1) and 42 (PIF) cells from
427 n=5 independent experiments, one-way ANOVA, Dunnett's multiple comparison). **e**, Human
428 neutrophils were exposed to stepwise increasing shear rates in E-selectin, ICAM-1 and CXCL8 coated
429 flow chambers and percentage of remaining neutrophils FOV⁻¹ was quantified after each step (n=12-
430 15 flow chambers of 9-10 independent experiments one-way ANOVA, Dunnett's multiple
431 comparison). *: p≤0.05 **: p≤0.01 ***: p≤0.001, data in **b, c, d, e** are presented as mean±SEM.

432

433 **Figure 6 PIF impairs neutrophil recruitment in an animal model of acute lung injury after LPS**
434 **stimulation.**

435 WT mice received an i.p. injection of two different concentrations of PIF or vehicle (Ctrl) 1h prior to
436 LPS inhalation and number of recruited neutrophils to **a**, pulmonary vasculature, **b**, lung interstitium
437 and **c**, in the bronchio-alveolar lavage (BAL) was analyzed. W/o-animals were exposed to saline
438 aerosol only (n=7-9 mice per group, one-way ANOVA, Tukey's multiple comparison). **d**,
439 Representative histological micrographs of lungs (scale bar: 250 μ m) and **e**, histological quantification
440 (n=3-4mice per group, one-way ANOVA, Tukey's multiple comparison). **: $p\leq 0.01$ ***: $p\leq 0.001$, data
441 are represented as mean \pm SEM.

442

443 **Methods**

444 **Mice:**

445 *Kcna3^{tm1lys}* (*Kv1.3^{-/-}*) mice²³ were purchased from Jackson Laboratories and backcrossed into C57BL/6
446 WT mice. WT mice were obtained from Charles River Laboratories (Sulzfeld, Germany). All mice were
447 maintained at the Walter Brendel Center for Experimental Medicine, LMU, Munich, at the Biomedical
448 Center, LMU, Planegg-Martinsried, Germany and at the Animal Facility of the University Hospital
449 Aachen. 8-25weeks old male and female mice were used for all experiments. Animal experiments
450 were approved by the government Oberbayern and government Nordrhein-Westfalen, Germany, AZ
451 55.2-1-54-2531-122/12, -229/15, ROB-55.2-2532.Vet_02-18-22 and 84-02.04.2013.A058.

452 **Animal models:**

453 Intravital microscopy (IVM) of the mouse cremaster muscle was performed as previously described⁴⁸.
454 Briefly, WT or *Kv1.3^{-/-}* mice received an intra scrotal (i.s.) injection of either PIF, scrambled PIF (scrPIF)
455 (both 1µg/mouse; BioSynthesis; provided by E. Barnea), 90µg of 5-(4-Phenoxybutoxy)psoralen (PAP-
456 1; Sigma-Aldrich), a combination of PIF and PAP-1, or vehicle (Ctrl; 0.25%DMSO/PBS) 1h prior to TNF-
457 α stimulation (i.s.; 500ng of recombinant murine (rm) TNF-α (R&D Systems)). 2h after induction of
458 inflammation, the carotid artery of anesthetized mice was cannulated for later blood sampling (using
459 a ProCyte Dx; IDEXX Laboratories) and the cremaster muscle was dissected. IVM was conducted on
460 an OlympusBX51 WI microscope, equipped with a 40x objective (Olympus, 0.8NA, water immersion
461 objective) and a CCD camera (KAPPA CF 8 HS). Postcapillary venules were recorded using VirtualDub
462 software for later off-line analysis. On the basis of the generated movies, leukocyte number of
463 adherent cells mm⁻² was counted and rolling velocities, vessel diameter and vessel length were
464 determined using FIJI software⁴⁹. During the entire observation, the muscle was superfused with
465 thermo-controlled bicarbonate buffer according to previous literature⁵⁰. Centerline velocity of each
466 venule was measured with a dual photodiode (Circusoft Instrumentation). After IVM, cremaster
467 muscles were removed, fixed with 4% paraformaldehyde (PFA), and stained with Giemsa (Merck,
468 Darmstadt, Germany) to calculate the number of perivascular neutrophils. Neutrophils were
469 discriminated from other leukocyte sub populations on the basis of the shape of cell nuclei and
470 granularity of the cytosol. The analysis of transmigrated leukocytes was carried out at the core facility
471 Bioimaging of the Biomedical Center with a Leica DM2500 microscope, equipped with a 100x
472 objective (Leica, 1.4NA, oil immersion) and a Leica DMC2900 CMOS camera.

473 The LPS induced acute lung injury (ALI) model was used as described elsewhere⁵¹. WT mice were
474 intra peritoneally (i.p.) injected with either 1µg, 10µg of PIF or vehicle (Ctrl) 1h prior to LPS
475 stimulation. Mice were exposed to aerosolized LPS (500µg ml⁻¹ in 0.9% saline) from *Salmonella*

476 *enteritidis* (Sigma-Aldrich) for 30min using a nebulizer (MicroAir, Omron Healthcare). Mice from the
477 w/o group did not receive any i.p. injection and were exposed to saline aerosol only. 4h after
478 inhalation, numbers of recruited neutrophils were assessed. 5 μ l of FITC conjugated anti-Ly6G
479 antibodies (eBioscience) were applied i.v. via tail injection 30min prior to killing the animals to label
480 intravascular neutrophils. After euthanasia, the trachea was cannulated and the lungs were flushed
481 5x with 0.5ml of PBS to obtain bronchoalveolar lavage (BAL). Afterwards, the pulmonary vasculature
482 was rinsed with 15ml of ice-cold PBS (with 0.5mM EDTA) before lungs were removed, digested with
483 Liberase (1:20; 25mg Liberase RI ml⁻¹ aqua; Roche) and passed through a cell strainer (70 μ m; Miltenyi
484 Biotec). Number of neutrophils was analyzed using a Canto II flow cytometer (Becton Dickinson) and
485 FlowJo software (Tree Star). Cells were labeled with PerCP-Fluor710 conjugated anti-Ly6G, PE-anti-
486 CD115, APC-eFluor780-anti-CD45 and APC-anti-F4/80 antibodies (all eBioscience). Neutrophils were
487 defined as CD45⁺, CD115⁻, Ly6G⁺ cells. Intravasal neutrophils were discriminated from interstitial
488 neutrophils according to their FITC-Ly6G⁺ signal. Part of the right lung was fixed in 4% PFA,
489 embedded in paraffin and stained with Mayer's hematoxylin and eosin (HE) and cut for histological
490 examination. Sections were scored based on guidelines from the American Thoracic Society⁵².

491 ***In vitro* flow chamber assays:**

492 To investigate leukocyte adhesion and leukocyte rolling velocity *in vitro*, flow chamber assays were
493 carried out as previously described⁴⁸. Shortly, rectangular borosilicate glass capillaries (0.04x0.4mm;
494 VitroCom) were coated with a combination of rmE-Selectin (CD62E Fc chimera; 20 μ g ml⁻¹; R&D
495 Systems), rmICAM-1 (ICAM-1 Fc chimera; 15 μ g ml⁻¹; R&D Systems) and rmCXCL1 (15 μ g ml⁻¹;
496 Peprotech) for 3h at room temperature (RT) and blocked with 5% casein (Sigma-Aldrich) over night
497 (ON) at 4°C. Whole blood was collected from anesthetized WT mice via the carotid catheter,
498 heparinized and incubated with either 300nM PIF or the carrier substance (Ctrl) for 10min at RT. The
499 incubated blood was then perfused through the flow chambers at a shear rate level of 2.7 dynes cm⁻²
500 using a high-precision syringe pump (Harvard Apparatus). Movies were recorded with an
501 OlympusBX51 WI microscope, equipped with a 20x objective (Olympus, 0.95NA, water immersion
502 objective) and a CCD camera (KAPPA CF 8 HS) and VirtualDub software. Number of adherent cells per
503 FOV was counted and rolling velocities were analyzed with FIJI.

504 **Neutrophil isolation:**

505 Murine bone marrow derived neutrophils were isolated with a neutrophil enrichment kit (STEMCELL
506 Technologies), whereas human neutrophils were extracted from whole blood of healthy volunteer
507 blood donors using Polymorphprep (AXIS-SHIELD PoC AS). Blood sampling was approved by the ethic
508 committee from the Ludwig-Maximilians-Universität München (Az. 611-15).

509 **Western blotting:**

510 Murine and human neutrophils (10^6 $100\mu\text{l}^{-1}$ lysis buffer) were lysed, homogenized with lysis buffer
511 (containing 150mM NaCl, 1% Triton X-100 (Applichem), 0.5% Sodium deoxycholate (Sigma-Aldrich),
512 50mM Tris-HCl pH 7.3 (Merck), 2mM EDTA (Merck) supplemented with protease (Roche),
513 phosphatase inhibitors (Sigma-Aldrich) and 1xLaemmli sample buffer) and boiled (95°C, 5min).
514 Proteins were resolved by SDS-PAGE and electrophoretically transferred onto PVDF membranes.
515 Rabbit anti-K_v1.3 (3 $\mu\text{g ml}^{-1}$, Alomone labs), mouse anti-GAPDH (1.5 $\mu\text{g ml}^{-1}$; clone 6C5; Calbiochem),
516 goat anti-rabbit-IRDye 800CW and goat anti-mouse-IRDye 680RD (both LI-COR Bioscience) were used
517 to detect the respective proteins on an Odyssey CLx (LI-COR Bioscience). Jurkat cells were used as
518 positive control.

519 **Confocal microscopy:**

520 Murine and human neutrophils were seeded on poly-L-lysine (0.1%; Sigma-Aldrich) coated object
521 slides (Ibidi), fixed with 2% PFA and blocked with 2% BSA (Capricorn Scientific) for 1h. Cells were
522 stained ON at 4°C using anti-K_v1.3 antibody (5 $\mu\text{g ml}^{-1}$, rabbit anti-K_v1.3; Alomone labs. Donkey anti-
523 rabbit-Alexa488 secondary antibody (5 $\mu\text{g ml}^{-1}$, Invitrogen) was then added for 1h at RT. Finally, cells
524 were stained with DAPI (Invitrogen) for 5min at RT before embedding them in ProLong Diamond
525 Antifade mounting medium (Invitrogen). Samples were imaged by confocal microscopy at the core
526 facility Bioimaging of the Biomedical Center with a Leica SP8X WLL microscope, equipped with a HC
527 PL APO 40x/1.30NA oil immersion objective. Images were processed (including removal of outliers
528 and background subtraction in the 488 channel) using FIJI software.

529 **Flow cytometry:**

530 Murine and human neutrophils cells were stained for 30min with rabbit anti-K_v1.3 (5 $\mu\text{g ml}^{-1}$,
531 Alomone Labs) followed by 30min incubation with secondary antibody (5 $\mu\text{g ml}^{-1}$, donkey anti-rabbit-
532 Alexa488; Invitrogen) at 4°C. Rat anti-Ly6G (clone 1A8; BioLegend) or anti-CD15 (clone W6D3;
533 BioLegend) together with anti-CD66b (clone G10M5; BioLegend) were used to define murine and
534 human neutrophil population, respectively. Flow cytometry data were acquired on a Beckman
535 Coulter Gallios flow cytometer and analyzed using Kaluza Flow Analysis Software (Beckman Coulter).

536 The expression patterns of surface molecules which are important in the context of leukocyte
537 recruitment were analyzed via flow cytometry. WT mice received either an i.s. injection of 1 μg PIF or
538 vehicle 2h prior to exsanguination. In a second set of experiments, non-treated WT and K_v1.3^{-/-} mice
539 were exsanguinated. Whole blood was stained with antibodies against CD18 (clone C71/16;
540 Pharmingen), CD11a (clone M17/4; eBioscience), CD11b, (clone M1/70; BioLegend), PSGL-1 (CD162;

541 clone 2PH1; Pharmingen), CD44 (clone IM7; BioLegend), L-selectin (CD62L; clone MEL-14;
542 BioLegend), and CXCR2 (CD182; clone 242216; R&D). Cells were fixed and erythrocytes were lysed
543 using FACS Lysing solution (BD Bioscience). Samples were analyzed using a Beckman Coulter Gallios
544 flow cytometer and Kaluza Flow analysis Software (Beckman Coulter). Anti-Ly6G (clone 1A8;
545 BioLegend) was used to define murine neutrophil population.

546 **Patch clamp of K_v1.3 overexpressing HEK-293 cells and isolated human neutrophils:**

547 HEK 293 cells were cultured in DMEM supplemented with 10% heat-inactivated FBS and 1%
548 penicillin/streptomycin at 37°C in humidified atmosphere (5% CO₂). The cells were transiently co-
549 transfected with cDNA plasmid encoding human K_v1.3 (kindly provided by Prof. Dr. Grissmer) and
550 Vivid Colors™ pcDNA™6.2/C-EmGFP-DEST Vector (Invitrogen) using Lipofectamine 3000 (Invitrogen).
551 Cells were used the day after transfection. Human neutrophils were isolated from whole blood of 5
552 different healthy volunteer donors using EasySep neutrophil enrichment kit (STEMCELL Technologies)
553 and resuspended in HBSS buffer (containing 0.1% of glucose, 1mM CaCl₂, 1mM MgCl₂, 0.25% BSA,
554 and 10mM HEPES (Sigma-Aldrich), pH7.4). Purity of isolated cells was determined by flow cytometry
555 (CD66b⁺/CD15⁺ population). Cells with a purity over 98±0.5% (mean±SEM) were used for
556 experiments. Cells were seeded on poly-D-lysine coated coverslips and subjected to patch-clamp
557 experiments in whole-cell configuration as follows: cells were clamped at a holding potential of -
558 80mV intermitted by repeated 200ms voltage steps from -80mV to +40mV using a 10mV interval
559 applied every 30s. Current maxima at +40mV were used for the calculation of K_v1.3 current
560 amplitudes. Currents were normalized to cell size as current densities in pA/pF. Capacitance was
561 measured using the automated capacitance cancellation function of the EPC-10 (HEKA, Harvard
562 Bioscience). Patch pipettes were made of borosilicate glass (Science Products) and had resistance 2–
563 3.5MΩ. K_v1.3 currents were inhibited with 10nM PAP-1 and K_{Ca}3.1 currents were blocked by 1μM
564 TRAM-34. Standard extracellular solution contained: 140mM NaCl, 2.8mM KCl, 2mM MgCl₂, 1mM
565 CaCl₂, 10mM HEPES, 11mM glucose (pH 7.2, 300mOsm). Intracellular solution contained: 134mM KF,
566 2mM MgCl₂, 1mM CaCl₂, 10mM HEPES, 10mM EGTA (pH 7.2, 300mOsm). Solutions were adjusted to
567 300mOsm using a Vapro 5520 osmometer (Wescor Inc). Channel blocker were either added to the
568 bath solution at least 15min prior to electrophysiological recordings or directly applied via an
569 application pipette using constant pressure. To determine IC₅₀ values for inhibitory effects of PIF on
570 K_v1.3 currents, data were fitted with the following equation:

$$571 \quad E(c) = E_{min} + (E_{max} - E_{min}) \times (1/(1 + (IC_{50}/c)^h));$$

572 with E being the effect (current inhibition) at a given concentration c of inhibitor, E_{min} the minimal
573 effect (current inhibition), E_{max} the maximally achievable effect, IC_{50} the half-maximal concentration
574 and h the Hill factor.

575 **Calcium signaling in human neutrophils:**

576 Human neutrophils were isolated from whole blood of healthy volunteers using EasySep neutrophil
577 enrichment kit (STEMCELL Technologies) in a manner approved by the institutional review board
578 protocol at the University of California, Davis (#235586-9). Isolated cells were suspended in HBSS
579 with 0.1% HSA at 10^6 cells ml^{-1} and treated with Mac-1 blocking antibody (clone M1/70; BioLegend)
580 prior to perfusion. Cells were then incubated with 1 μM Rhod-2 AM (ex/em: 552/581; Thermo Fisher
581 Scientific) with or without Thapsigargin (Thermo Fisher Scientific) for 20min at RT in the dark. For
582 static adhesion assays neutrophils were placed into a 48-well plate and allowed to settle for 60s prior
583 to addition of 1.5mM calcium containing media for 3min. Additionally, cells were stimulated by
584 addition of 10nM CXCL8 (Shenandoah) for 2min. For investigation of cellular Ca^{2+} signaling under flow
585 conditions microfluidic devices were designed to have four independent flow channels to analyze
586 multiple conditions per coverslip (dimensions: $60\mu m \times 2mm \times 8mm$, $h \times w \times l$). Circular glass coverslips
587 (35mm diameter) were treated with Piranha solution (one part concentrated sulfuric acid and 1 part
588 30% hydrogen peroxide) for 20min followed by treatment with acetone for 2min. Coverslips were
589 then dipped in 2% 3-aminopropyltriethoxysilane (Fisher Scientific) in acetone for 5min. Once dry,
590 Protein A/G (Fischer Scientific) was covalently attached to the aminosilinated surface using a
591 bis(sulfosuccinimidyl) substrate (BS3) crosslinker ON (Pierce Thermo Scientific). Afterwards,
592 coverslips were coated with recombinant human (rh)ICAM-1 (Fc chimera; $5 \mu g ml^{-1}$; R&D Systems),
593 CBR LFA1/2 LFA-1 antibody ($20 \mu g ml^{-1}$; BioLegend) for 1h, washed with PBS and blocked with 1%
594 Casein for 15min (Pierce Thermo Scientific). Neutrophils pre-treated with Rhod-2 AM and
595 Thapsigargin were perfused into the device at $0.1 dyne cm^{-2}$ and allowed to rest for 60s prior to shear
596 ramping up to $2 dyne cm^{-2}$ in 1.5mM calcium containing media via a syringe pump (Cellix Ltd). Images
597 were taken (1 fps) once neutrophils had settled in the 48 well plate or microfluidic device using a
598 Nikon Eclipse TE2000-S microscope (20x phase contrast air objective; 0.45NA) equipped with a 16-bit
599 digital CMOS camera (Andor ZYLA) with NIS Elements imaging software. All images were analyzed
600 using FIJI Software.

601 **Neutrophil spreading and detachment:**

602 To study neutrophil spreading, rectangular borosilicate glass capillaries ($0.2 \times 2.0mm$; CM Scientific)
603 were coated with rhE-Selectin (CD62E Fc chimera; $5 \mu g ml^{-1}$; R&D Systems), rhICAM-1 ($4 \mu g ml^{-1}$; R&D
604 Systems) and rhCXCL-8 ($10 \mu g ml^{-1}$; Peprotech) for 3h at RT and blocked with 5% casein ON at $4^\circ C$.

605 Isolated human neutrophils were applied into the flow chamber with a shear rate level of 1 dyne cm^{-2}
606 using a high-precision syringe pump (Harvard Apparatus). To avoid interaction of the cells with the Fc
607 part of the recombinant proteins, cells were incubated with hFc-block (human TruStain FcX;
608 BioLegend) for 5min at RT before being introduced into the chambers. Spreading behavior of the
609 cells was observed and recorded with a Zeiss Axioskop2 (provided with a 20x water objective, 0.5NA
610 and a Hitachi KP-M1AP camera) and VirtualDub. Cell shape changes were quantified using FIJI
611 software, analyzing cell perimeters, circularity ($4\pi \frac{[Area]}{[Perimeter]^2}$) and solidity ($\frac{[Area]}{[Convex Area]}$). To
612 investigate the resistance of neutrophils against increasing shear forces, μ -slides VI^{0.1} (Ibidi) were
613 coated with rhE-Selectin, rhICAM-1 and rhIL-8 as described above. Isolated human neutrophils were
614 resuspended in HBSS, blocked with hFc-block for 5min at RT and $10^6 \text{ cells ml}^{-1}$ were introduced into
615 the chamber and allowed to settle for 3min, before flow was started. First, 1 dyne cm^{-2} was applied
616 for 1min to remove non-attached cells and debris using HBSS and a high precision syringe pump.
617 Number of adherent cells FOV^{-1} was counted and set to 100%. Flow rates were then increased every
618 30s and the fraction of remaining cells was counted at the end of each time interval. Experiments
619 were conducted on a ZEISS, AXIOVERT 200 microscope, provided with a ZEISS 10x objective (NA:
620 0.25, and a SPOT RT ST Camera (Diagnostic Instruments, Inc.)) and MetaMorph software was used to
621 generate time laps movies for later on analysis.

622 **Statistics:**

623 Data are presented as mean \pm S.D. (Fig.1a, d, e; Fig.2f, h, k; Fig.3g; Fig.4b, d, 4e, g; Fig.6a, b, c, and 6e),
624 mean \pm SEM (Fig.3b, d; Fig.5b, c, d and e), as cumulative distribution, mean (Fig.4a, c and d), or
625 representative images/traces as depicted in the figure legends. Group sizes were selected based on
626 previous experiments. Data were analyzed and illustrated using GraphPad Prism 7 software
627 (GraphPad Software Inc.). Statistical tests were performed according to the number of groups being
628 compared. For pairwise comparison of experimental groups, an unpaired student's *t*-test and for
629 more than two groups, a 1-way or 2-way analysis of variance (ANOVA) with either Turkey's (to
630 compare all groups with each other) or Dunnett's (to compare experimental groups against control)
631 *post-hoc* test was carried out. P-values <0.05 were considered statistically significant and indicated as
632 follows: * $p < 0.05$; ** $p < 0.01$; *** $p < 0.001$.

633

634 **References**

- 635 1. Mor, G., Aldo, P. & Alvero, A. B. The unique immunological and microbial aspects of
636 pregnancy. *Nat. Rev. Immunol.* **17**, 469–482 (2017).
- 637 2. Sasaki, Y. *et al.* Decidual and peripheral blood CD4+CD25+regulatory T cells in early pregnancy
638 subjects and spontaneous abortion cases. *Mol. Hum. Reprod.* **10**, 347–353 (2004).
- 639 3. Sasaki, Y. *et al.* Proportion of peripheral blood and decidual CD4+CD25brightregulatory T cells
640 in pre-eclampsia. *Clin. Exp. Immunol.* **149**, 139–145 (2007).
- 641 4. Makhseed, M. *et al.* Pro-inflammatory maternal cytokine profile in preterm delivery. *Am. J.*
642 *Reprod. Immunol.* **49**, 308–318 (2003).
- 643 5. Teoh, P. J. *et al.* Atypical Chemokine Receptor ACKR2 Mediates Chemokine Scavenging by
644 Primary Human Trophoblasts and Can Regulate Fetal Growth, Placental Structure, and
645 Neonatal Mortality in Mice. *J. Immunol.* **193**, 5218–5228 (2014).
- 646 6. Barnea, E. R. Applying embryo-derived immune tolerance to the treatment of immune
647 disorders. *Ann. N. Y. Acad. Sci.* **1110**, 602–618 (2007).
- 648 7. Ramu, S. *et al.* PreImplantation factor (PIF) detection in maternal circulation in early
649 pregnancy correlates with live birth (bovine model). *Reprod. Biol. Endocrinol.* **11**, 105 (2013).
- 650 8. Tzonis, P. *et al.* Kinetics of circulating preimplantation factor (PIF) levels during pregnancy. *J.*
651 *Reprod. Immunol.* **86**, 42 (2010).
- 652 9. Stamatkin, C. W. *et al.* PreImplantation Factor (PIF) correlates with early mammalian embryo
653 development-bovine and murine models. *Reprod. Biol. Endocrinol.* **9**, 1–11 (2011).
- 654 10. Paidas, M. J. *et al.* A genomic and proteomic investigation of the impact of preimplantation
655 factor on human decidual cells. *Am. J. Obstet. Gynecol.* **202**, 459.e1-459.e8 (2010).
- 656 11. Moindjie, H. *et al.* Preimplantation Factor (PIF) Promotes Human Trophoblast Invasion1. *Biol.*
657 *Reprod.* **91**, 1–10 (2014).
- 658 12. Hakam, M. S. *et al.* Preimplantation Factor (PIF) Promotes HLA-G,-E,-F,-C Expression in JEG-3
659 Choriocarcinoma Cells and Endogenous Progesterone Activity. *Cell. Physiol. Biochem.* **43**,
660 2277–2296 (2017).
- 661 13. Stamatkin, C. W. *et al.* Preimplantation factor negates embryo toxicity and promotes embryo
662 development in culture. *Reprod. Biomed. Online* **23**, 517–524 (2011).
- 663 14. Barnea, E. R. *et al.* Immune regulatory and neuroprotective properties of preimplantation
664 factor: From newborn to adult. *Pharmacol. Ther.* **156**, 10–25 (2015).
- 665 15. Weiss, L. *et al.* Preimplantation factor (PIF) analog prevents type I diabetes mellitus (T1DM)
666 development by preserving pancreatic function in NOD mice. *Endocrine* **40**, 41–54 (2011).
- 667 16. Weiss, L. *et al.* Preimplantation factor (PIF*) reverses neuroinflammation while promoting
668 neural repair in EAE model. *J. Neurol. Sci.* **312**, 146–157 (2012).
- 669 17. Kolaczowska, E. & Kubes, P. Neutrophil recruitment and function in health and inflammation.
670 *Nat. Rev. Immunol.* **13**, 159–175 (2013).
- 671 18. Schmidt, S., Moser, M. & Sperandio, M. The molecular basis of leukocyte recruitment and its
672 deficiencies. *Mol. Immunol.* **55**, 49–58 (2013).

- 673 19. Sperandio, M., Pickard, J., Unnikrishnan, S., Acton, S. T. & Ley, K. Analysis of Leukocyte Rolling
674 In Vivo and In Vitro. *Methods Enzymol.* **416**, 346–371 (2006).
- 675 20. Levite, M. *et al.* Extracellular K⁺ and Opening of Voltage-gated Potassium Channels Activate T
676 Cell Integrin Function: Physical and Functional Association between Kv1.3 Channels and β 1
677 Integrins. *J. Exp. Med.* **191**, 1167–1176 (2000).
- 678 21. Grossinger, E. M. *et al.* Targeting proliferation of chronic lymphocytic leukemia (CLL) cells
679 through KCa3.1 blockade. *Leukemia* **28**, 954–958 (2014).
- 680 22. Schmitz, A. & Sankaranarayanan, A. Design of PAP-1, a selective small molecule Kv1.3 blocker,
681 for the suppression of effector memory T cells in autoimmune diseases. *Mol. Pharmacol.* **68**,
682 1254–1270 (2005).
- 683 23. Koni, P. A. *et al.* Compensatory anion currents in Kv1.3 channel-deficient thymocytes. *J. Biol.*
684 *Chem.* **278**, 39443–39451 (2003).
- 685 24. Henríquez, C. *et al.* The calcium-activated potassium channel KCa3.1 plays a central role in the
686 chemotactic response of mammalian neutrophils. *Acta Physiol.* **216**, 132–145 (2016).
- 687 25. Feske, S., Wulff, H. & Skolnik, E. Y. Ion channels in innate and adaptive immunity. *Annu. Rev.*
688 *Immunol.* **33**, 291–353 (2015).
- 689 26. Immler, R., Simon, S. I. & Sperandio, M. Calcium signalling and related ion channels in
690 neutrophil recruitment and function. *Eur. J. Clin. Invest.* **48**, e12964 (2018).
- 691 27. Morikis, V. A. & Simon, S. I. Neutrophil Mechanosignaling Promotes Integrin Engagement With
692 Endothelial Cells and Motility Within Inflamed Vessels. *Front. Immunol.* **9**, (2018).
- 693 28. Morikis, V. A. *et al.* Selectin catch-bonds mechanotransduce integrin activation and neutrophil
694 arrest on inflamed endothelium under shear flow. *Blood* **130**, 2101–2110 (2017).
- 695 29. Cowburn, A. S., Condliffe, A. M., Farahi, N., Summers, C. & Chilvers, E. R. Advances in
696 neutrophil biology: Clinical implications. *Chest* **134**, 606–612 (2008).
- 697 30. Priddy, K. D. Immunologic Adaptions During Pregnancy. *J. Obstet. Gynecol. Neonatal Nurs.* **26**,
698 388–394 (1997).
- 699 31. Kourtis, A. P., Read, J. S. & Jamieson, D. J. Infection and pregnancy. *N. Engl. J. Med.* **340**, 2211–
700 2218 (2014).
- 701 32. Gold, S. M. & Voskuhl, R. R. Pregnancy and multiple sclerosis: from molecular mechanisms to
702 clinical application. *Semin. Immunopathol.* **38**, 709–718 (2016).
- 703 33. Robijn, A. L., Murphy, V. E. & Gibson, P. G. Recent developments in asthma in pregnancy. *Curr.*
704 *Opin. Pulm. Med.* **25**, 11–17 (2019).
- 705 34. Langer-Gould, a, Garren, H., Slansky, A., Ruiz, P. J. & Steinman, L. Late pregnancy suppresses
706 relapses in experimental autoimmune encephalomyelitis: Evidence for a suppressive
707 pregnancy-related serum factor. *J. Immunol.* **169**, 1084–1091 (2002).
- 708 35. Lampé, R. *et al.* Phagocytic index of neutrophil granulocytes and monocytes in healthy and
709 preeclamptic pregnancy. *J. Reprod. Immunol.* **107**, 26–30 (2015).
- 710 36. Lampé, R., Szucs, S., Ormos, M., Ádány, R. & Póka, R. Effect of normal and preeclamptic
711 plasma on superoxide-anion production of neutrophils from healthy non-pregnant women. *J.*
712 *Reprod. Immunol.* **79**, 63–69 (2008).

- 713 37. Lampé, R., Szucs, S., Ádány, R. & Póka, R. Granulocyte superoxide anion production and
714 regulation by plasma factors in normal and preeclamptic pregnancy. *J. Reprod. Immunol.* **89**,
715 199–206 (2011).
- 716 38. Petty, H. R., Kindzelskii, A. L., Espinoza, J. & Romero, R. Trophoblast Contact Deactivates
717 Human Neutrophils. *J. Immunol.* **176**, 3205–3214 (2006).
- 718 39. Cahalan, M. D. & Chandy, K. G. The functional network of ion channels in T lymphocytes.
719 *Immunol Rev* **231**, 59–87 (2009).
- 720 40. Németh, T., Mócsai, A. & Lowell, C. A. Neutrophils in animal models of autoimmune disease.
721 *Semin. Immunol.* **28**, 174–186 (2016).
- 722 41. Azar, Y. *et al.* Preimplantation Factor (PIF*) Reduces Graft versus Host Disease (GVHD) by
723 Regulating Immune Response and Lowering Oxidative Stress. *Biol. Blood Marrow Transplant.*
724 **19**, 519–528 (2013).
- 725 42. Chandy, K. G. & Norton, R. S. Peptide blockers of Kv1.3 channels in T cells as therapeutics for
726 autoimmune disease. *Curr. Opin. Chem. Biol.* **38**, 97–107 (2017).
- 727 43. Beeton, C. *et al.* Selective blockade of T lymphocyte K⁺ channels ameliorates experimental
728 autoimmune encephalomyelitis, a model for multiple sclerosis. *Proc. Natl. Acad. Sci.* **98**,
729 13942–13947 (2001).
- 730 44. Beeton, C. *et al.* Kv1.3 channels are a therapeutic target for T cell-mediated autoimmune
731 diseases. *Proc. Natl. Acad. Sci. U. S. A.* **103**, 17414–17419 (2006).
- 732 45. Kundu-Raychaudhuri, S., Chen, Y. J., Wulff, H. & Raychaudhuri, S. P. Kv1.3 in psoriatic disease:
733 PAP-1, a small molecule inhibitor of Kv1.3 is effective in the SCID mouse psoriasis - Xenograft
734 model. *J. Autoimmun.* **55**, 63–72 (2015).
- 735 46. O’Brien, C. B. *et al.* Randomized, Double-Blind, Placebo-Controlled, Single Ascending Dose
736 Trial of Synthetic Preimplantation Factor in Autoimmune Hepatitis. *Hepatal. Commun.* **2**,
737 1235–1246 (2018).
- 738 47. Thieblemont, N., Wright, H. L., Edwards, S. W. & Witko-sarsat, V. Human neutrophils in auto-
739 immunity. *Semin. Immunol.* **28**, 159–173 (2016).
- 740 48. Pruenster, M. *et al.* Extracellular MRP8/14 is a regulator of β 2 integrin-dependent neutrophil
741 slow rolling and adhesion. *Nat. Commun.* **6**, 6915 (2015).
- 742 49. Schindelin, J. *et al.* Fiji: an open-source platform for biological-image analysis. *Nat. Methods* **9**,
743 676–682 (2012).
- 744 50. Ley, K. & Gaehtgens, P. Endothelial, not hemodynamic, differences are responsible for
745 preferential leukocyte rolling in rat mesenteric venules. *Circ. Res.* **69**, 1034–1041 (1991).
- 746 51. Grommes, J. *et al.* Simvastatin reduces endotoxin-induced acute lung injury by decreasing
747 neutrophil recruitment and radical formation. *PLoS One* **7**, 1–10 (2012).
- 748 52. Matute-Bello, G. *et al.* An official american thoracic society workshop report: Features and
749 measurements of experimental acute lung injury in animals. *Am. J. Respir. Cell Mol. Biol.* **44**,
750 725–738 (2011).
- 751

Figure 1 PIF impairs leukocyte recruitment *in vivo* and *in vitro*

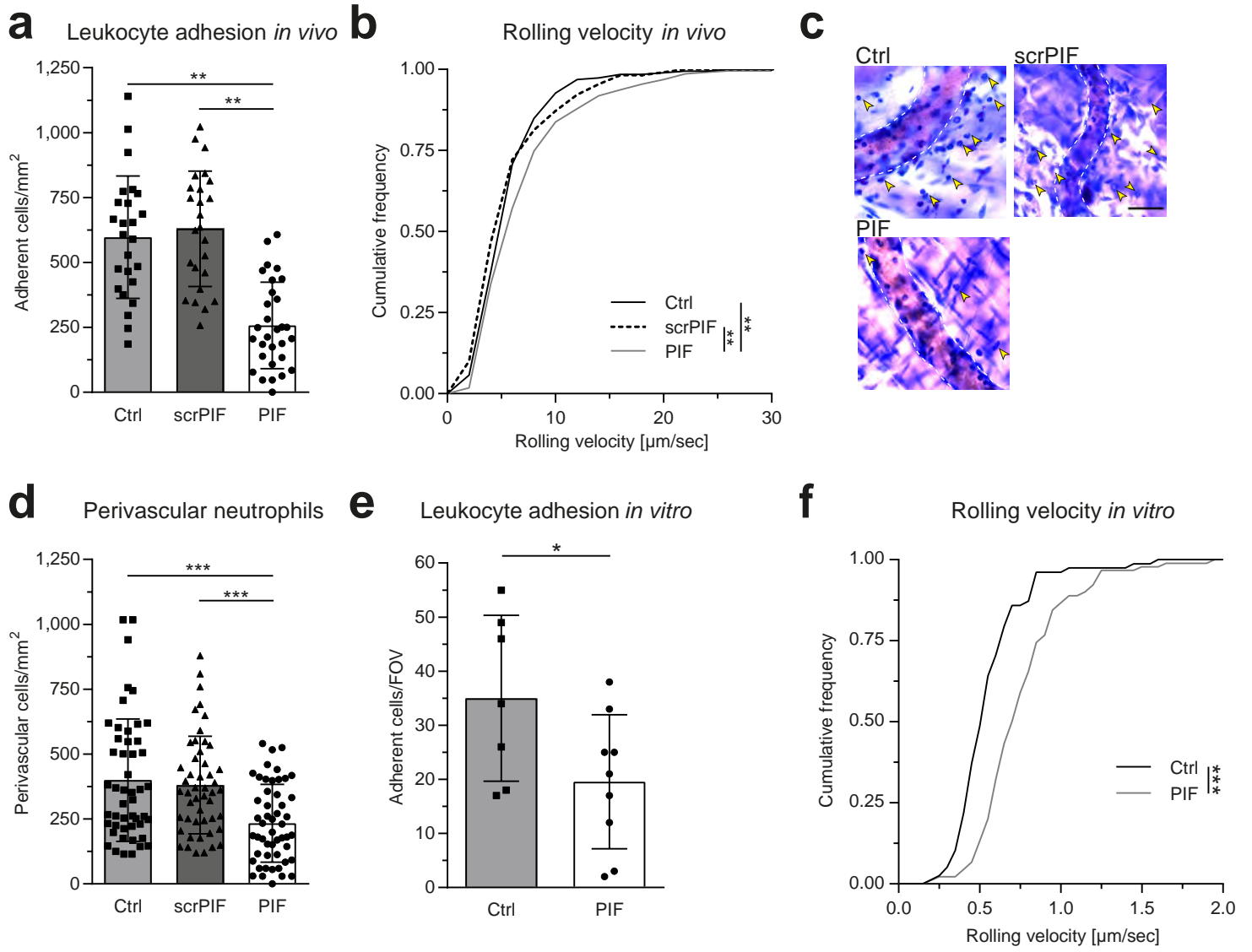


Figure 2 Functional $K_V1.3$ is expressed on human and murine neutrophils and plays a crucial role in leukocyte recruitment *in vivo*

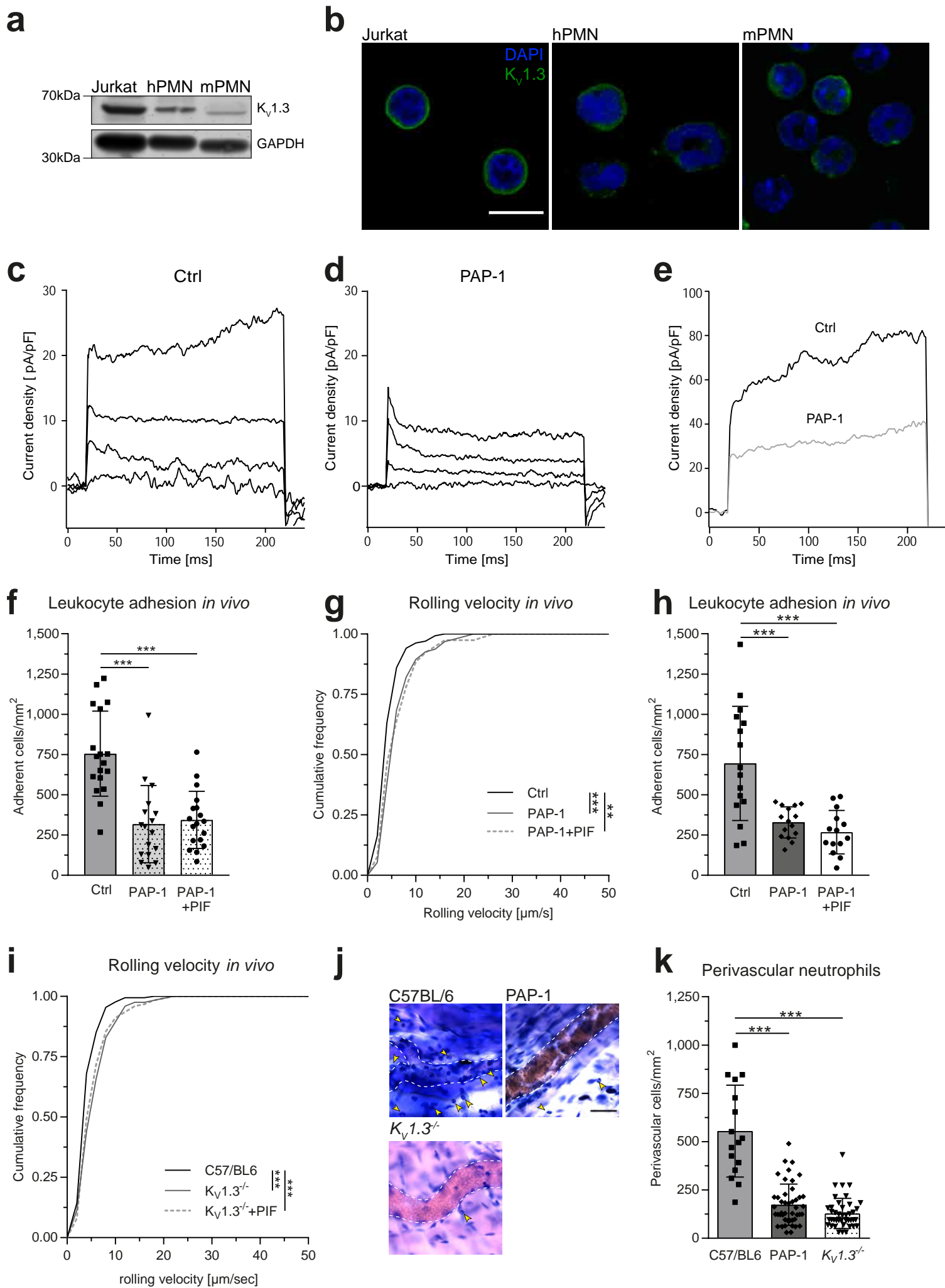


Figure 3 PIF reduces voltage-induced $K_v1.3$ currents in a $K_v1.3$ overexpressing cell line and in human neutrophils

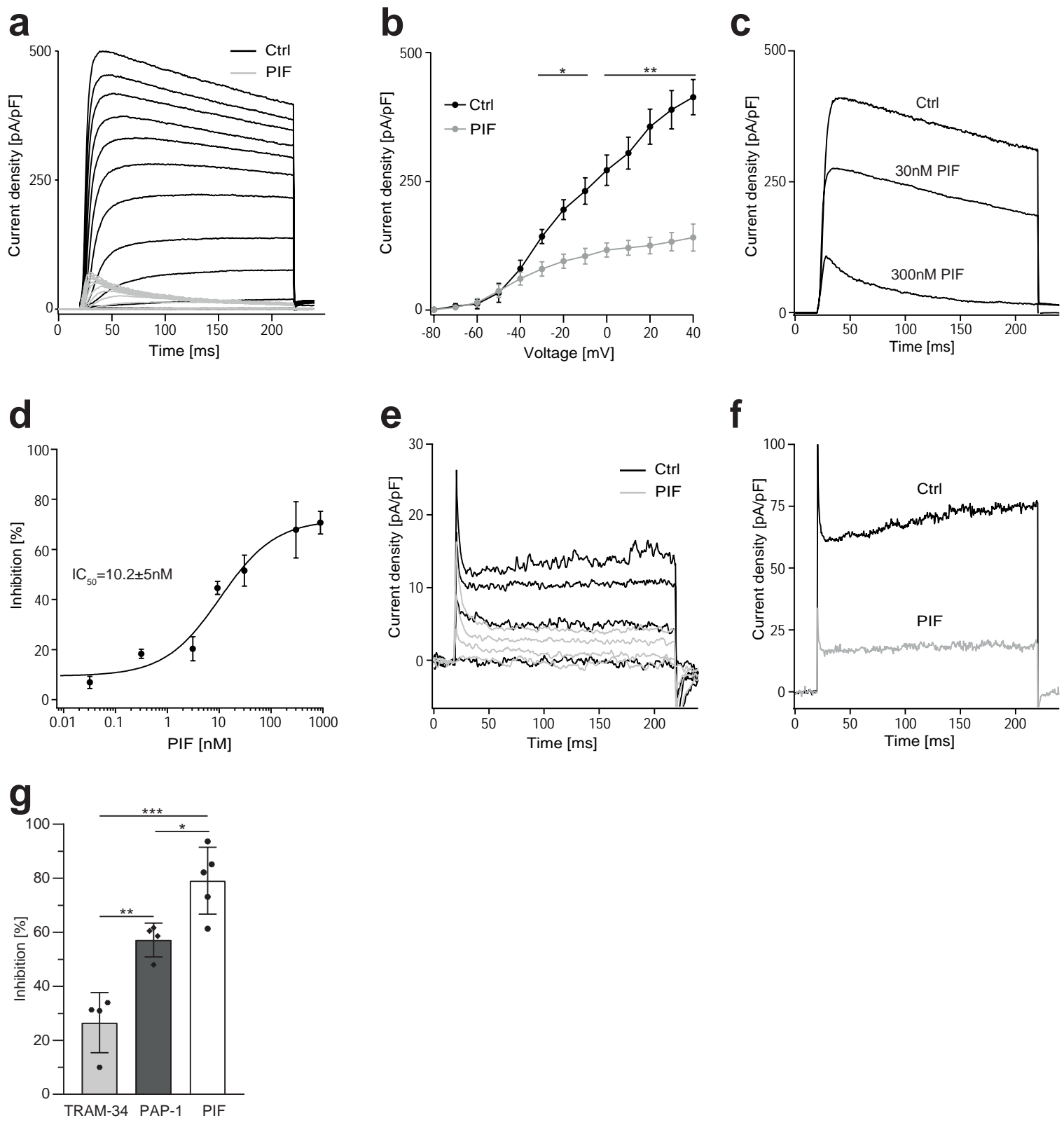


Figure 4 $K_V1.3$ is involved in Ca^{2+} signaling in human neutrophils

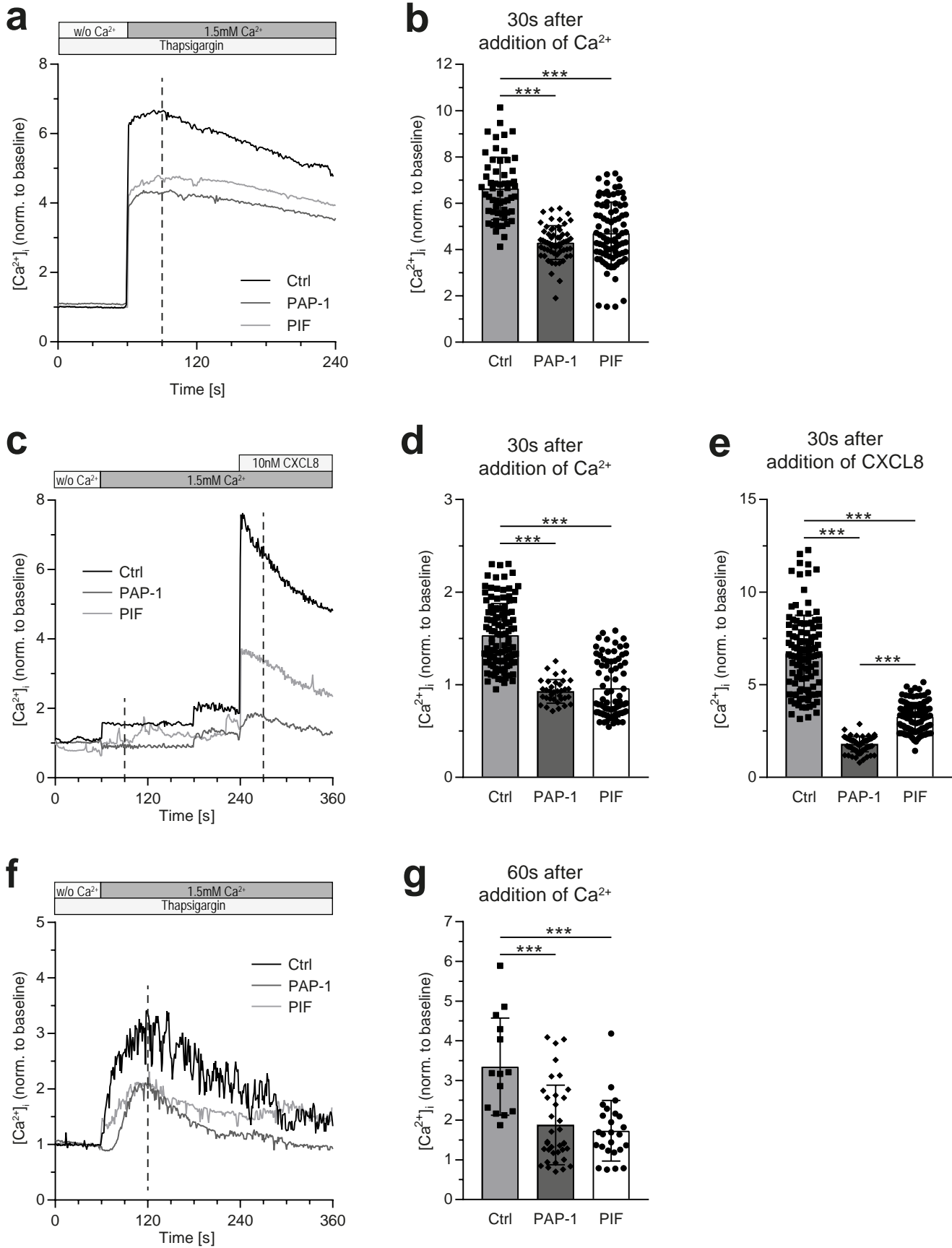
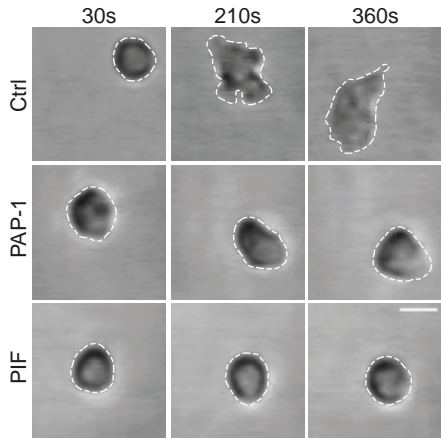
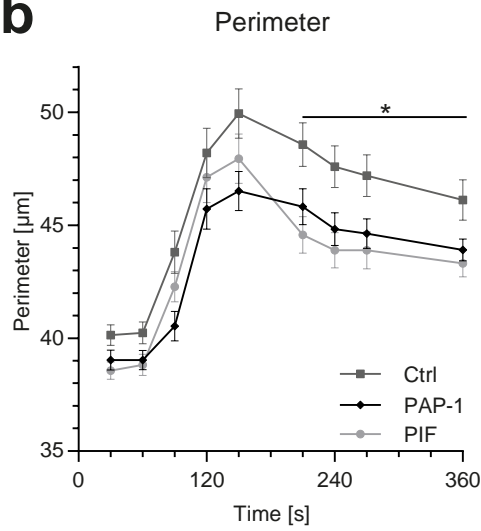


Figure 5 PIF impairs neutrophil post-arrest modifications

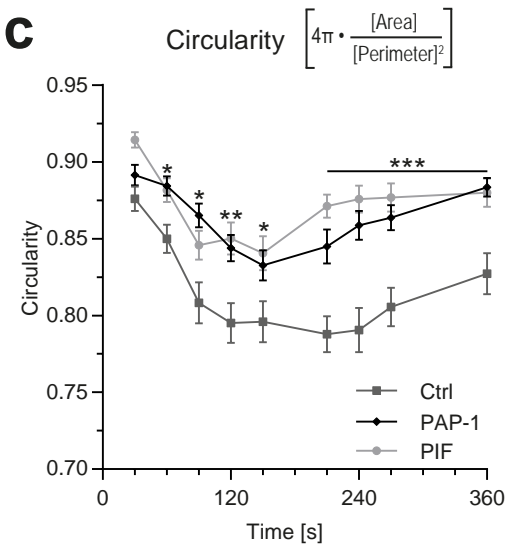
a



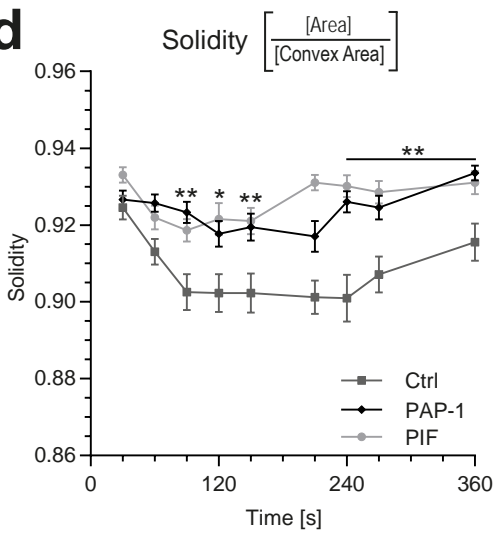
b



c



d



e

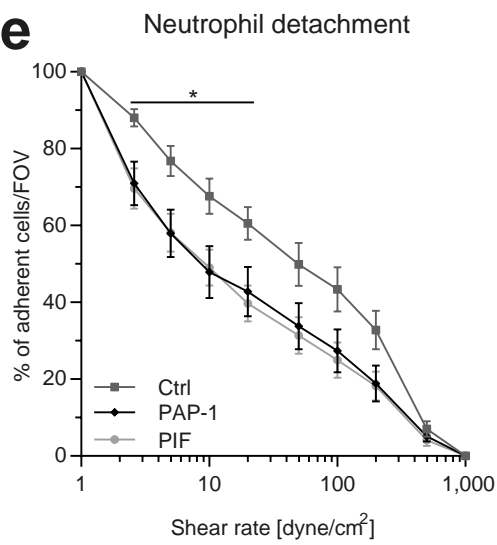
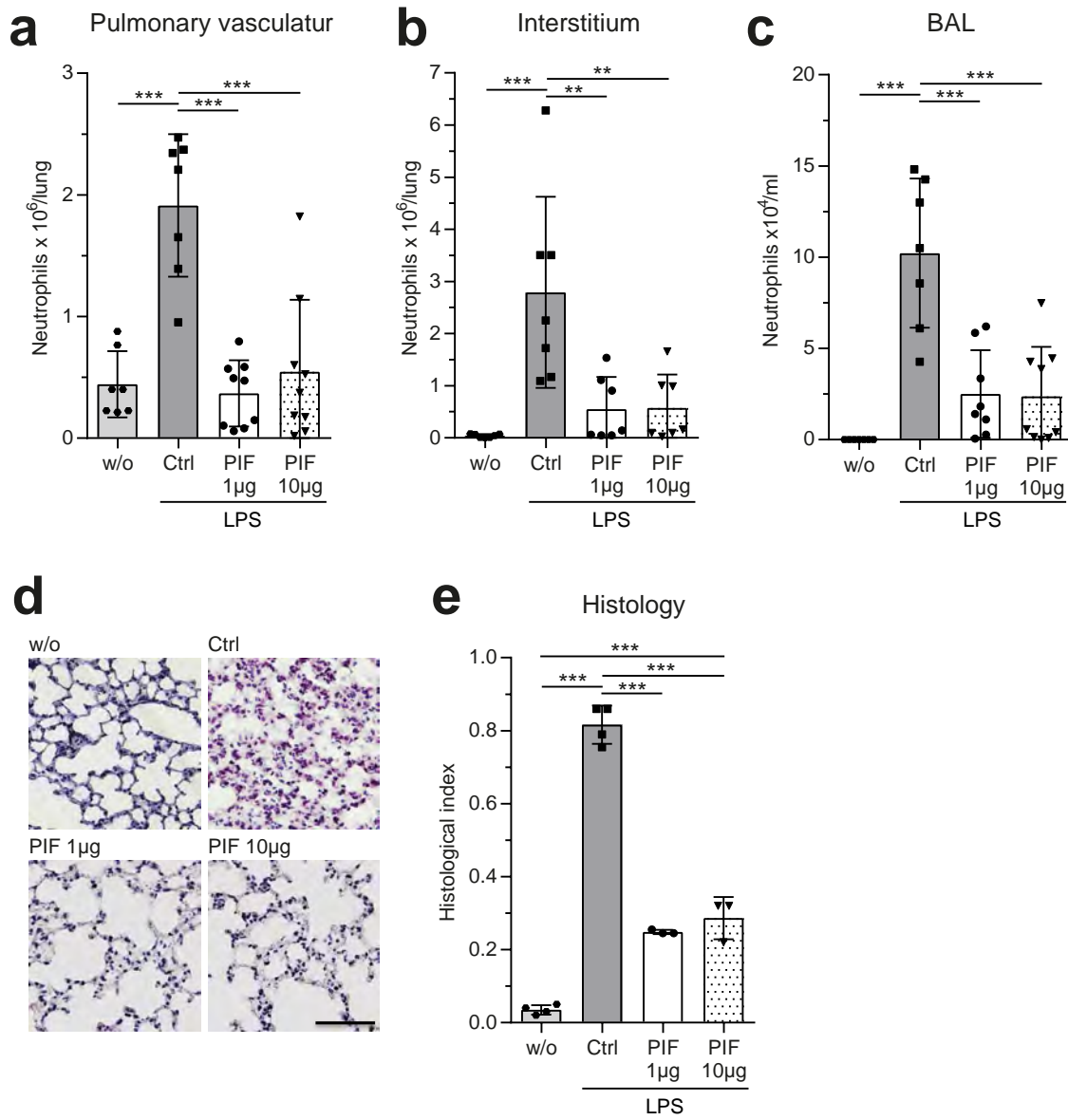
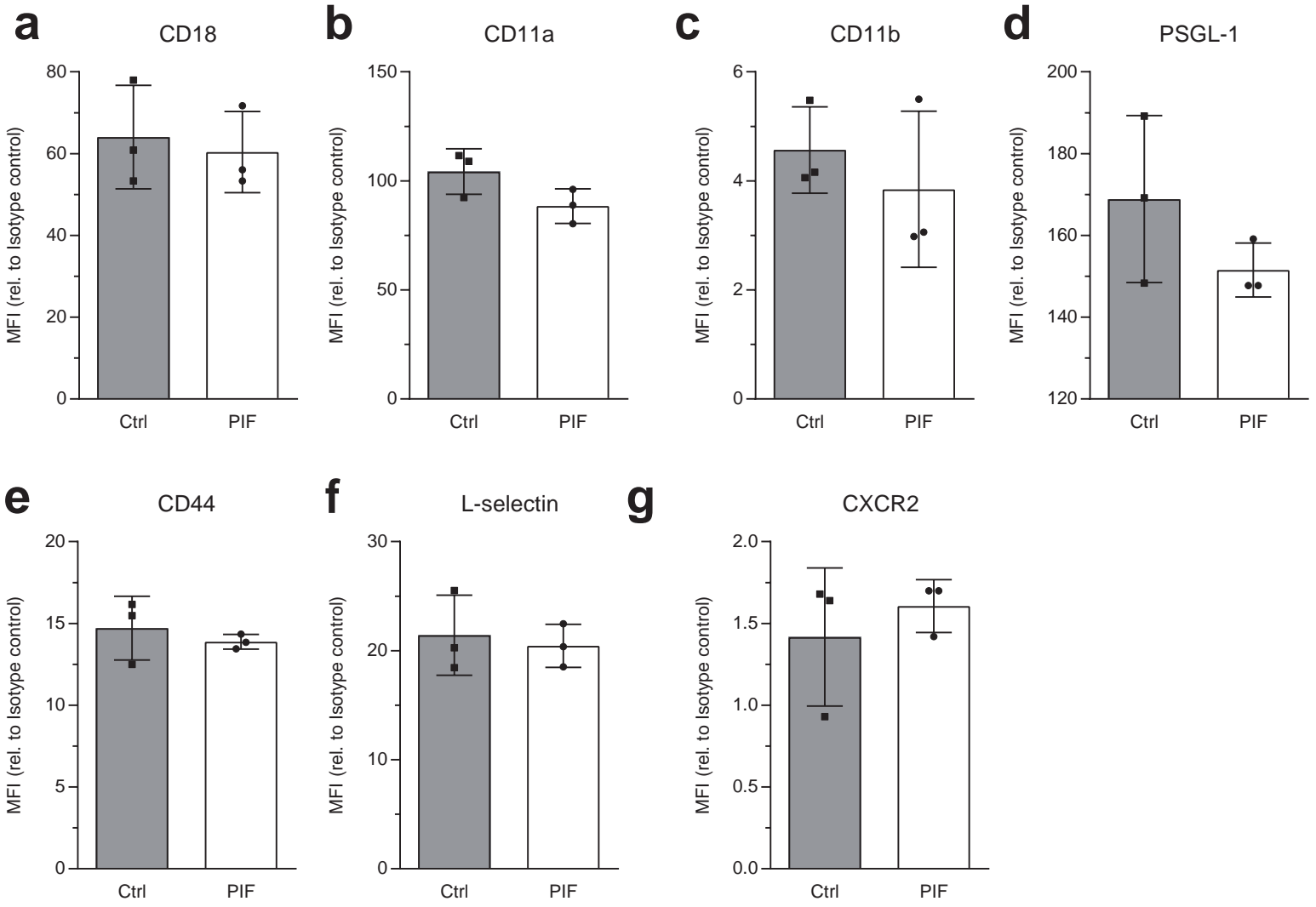


Figure 6 PIF impairs neutrophil recruitment in an animal model of acute lung injury after LPS stimulation



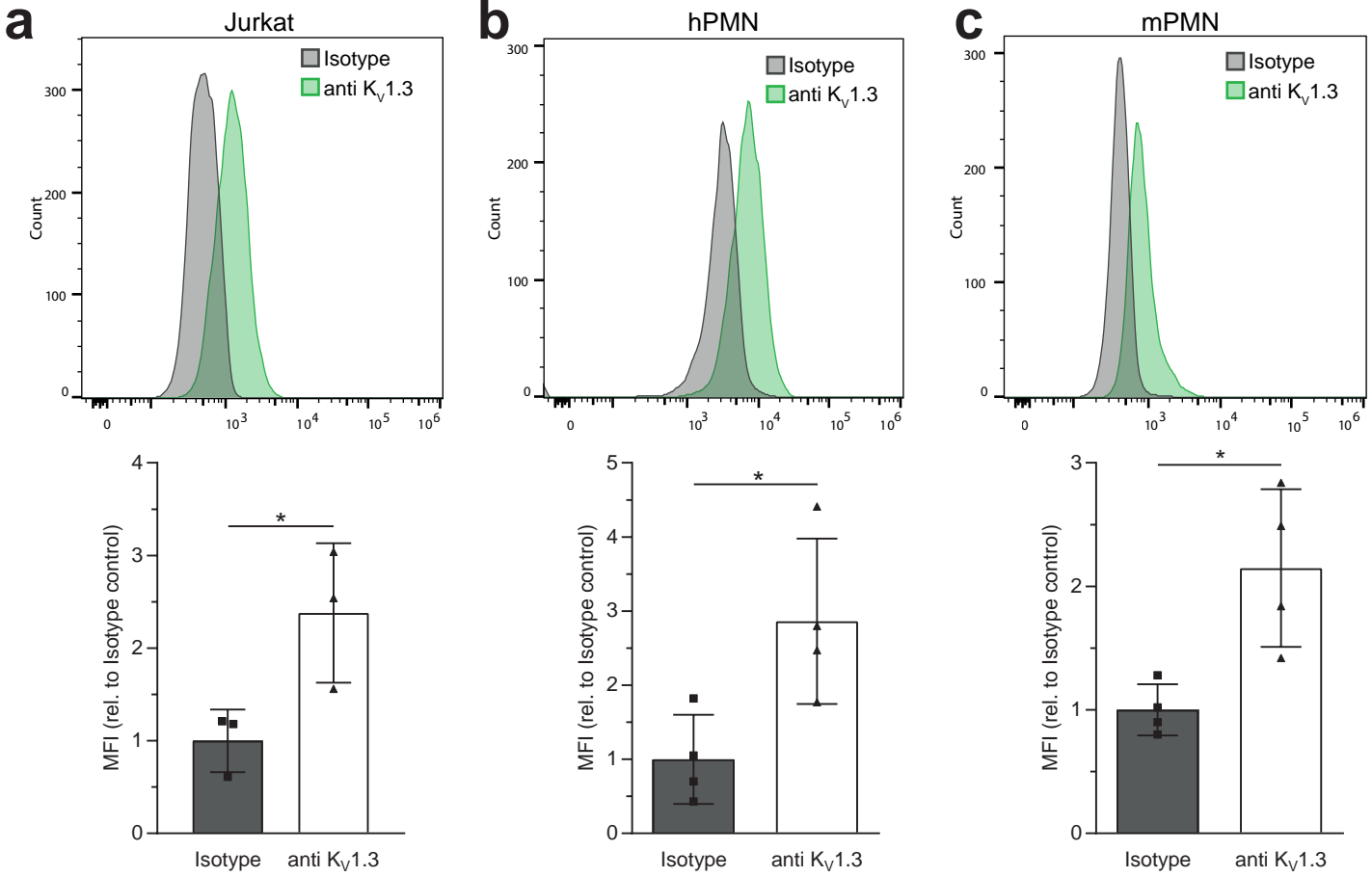
Supplementary Figure 1

PIF does not alter expression pattern of surface molecules important for neutrophil recruitment



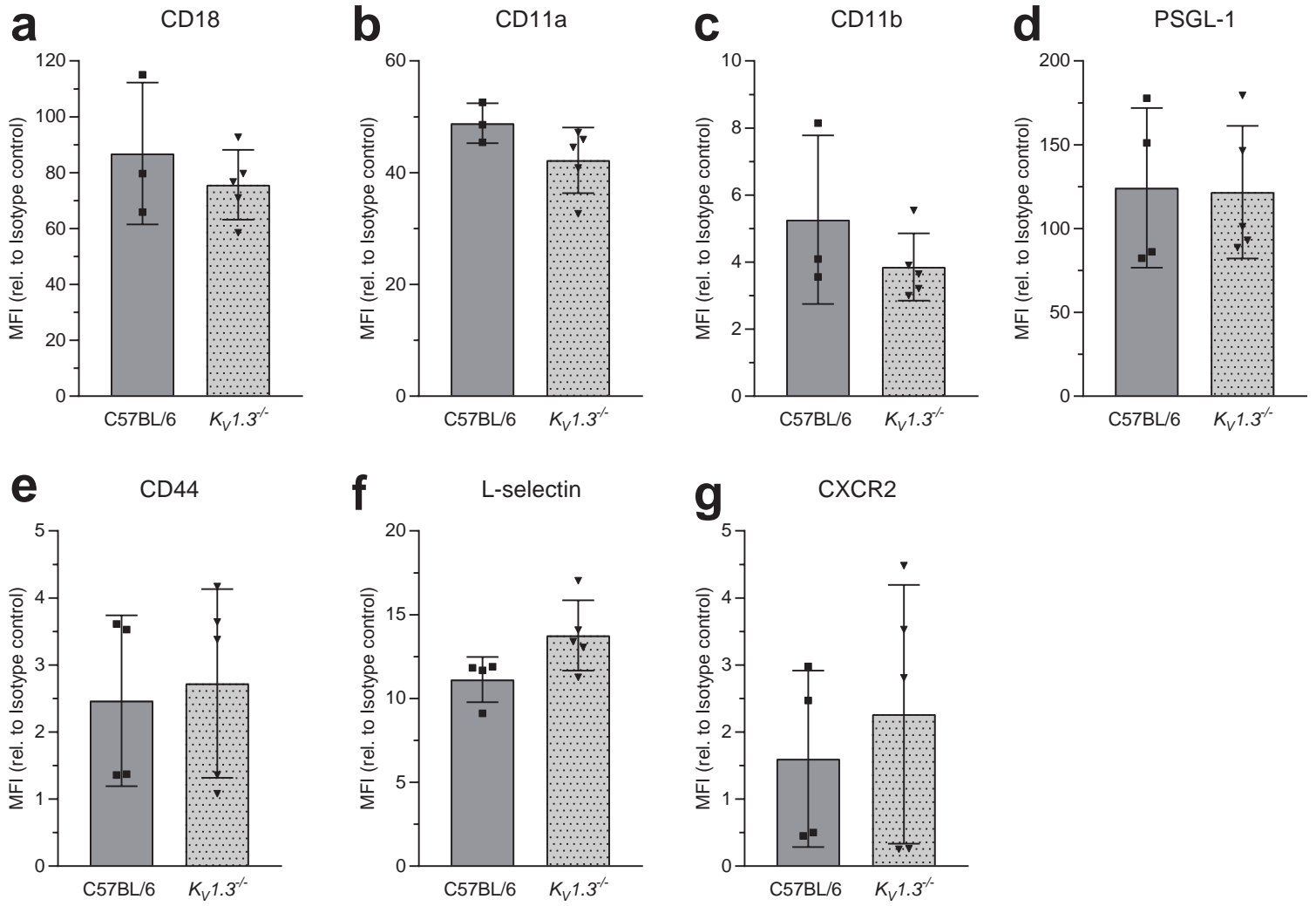
Supplementary Figure 2

K_V1.3 is expressed on human and murine neutrophils



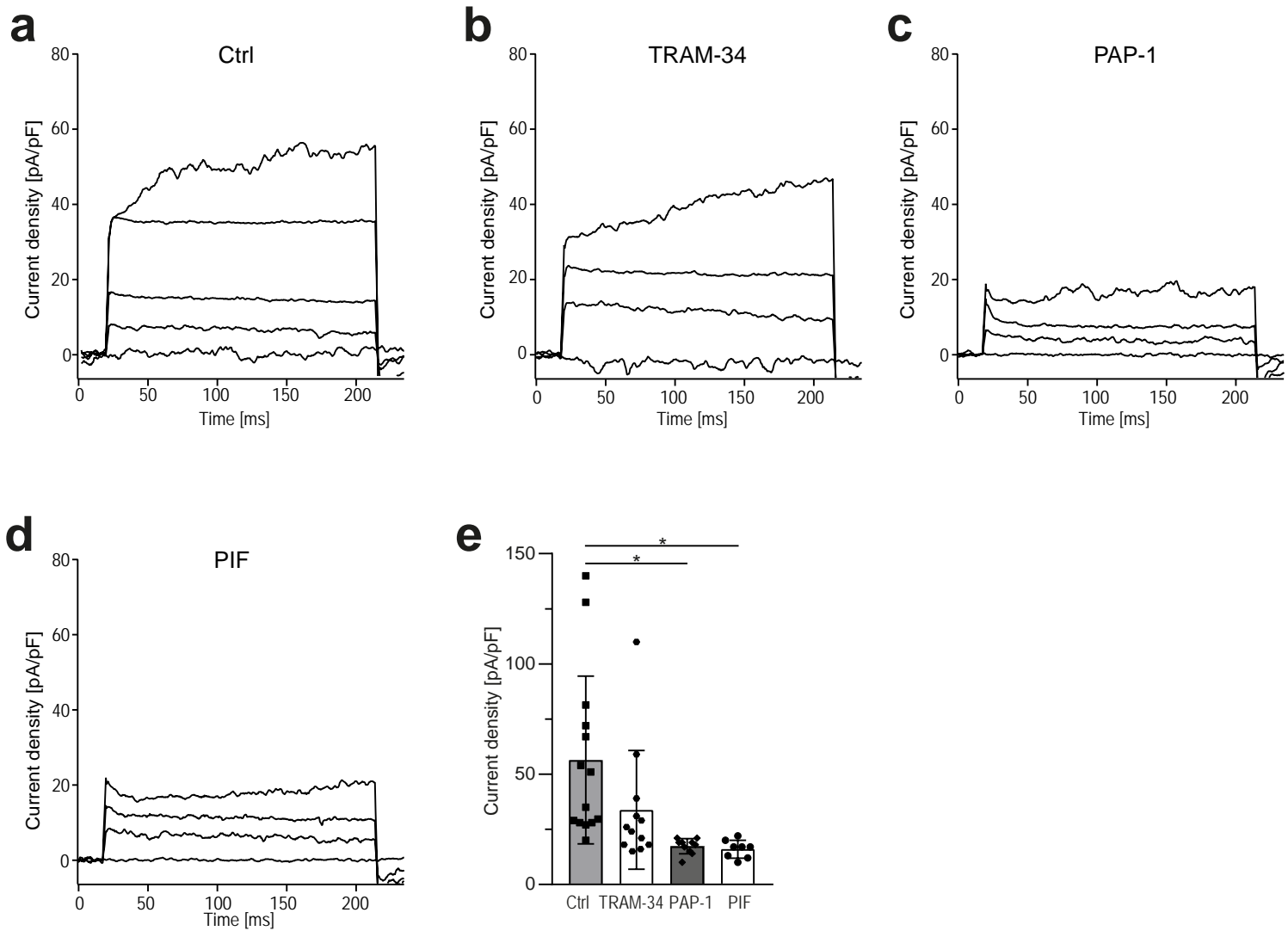
Supplementary Figure 3

$K_{\nu}1.3^{-/-}$ neutrophils share a normal expression pattern of surface molecules important for neutrophil recruitment



Supplementary Figure 4

PIF reduces $K_v1.3$ currents in isolated human neutrophils



Supplementary Figure 1 PIF does not alter expression pattern of surface molecules important for neutrophil recruitment.

a-g, Surface expression of CD18, CD11a, CD11b, PSGL-1, CD44, L-selectin, and CXCR2 on peripheral blood neutrophil from WT mice i.p. injected with PIF or vehicle 2h prior to blood harvesting was determined by flow cytometry (MFI= Mean fluorescence intensity, n=3 animals per group, unpaired student's t-test). Data are represented as mean±s.d.

Supplementary Figure 2 $K_v1.3^{-/-}$ is expressed on human and murine neutrophils.

Surface expression of $K_v1.3^{-/-}$ on **a**, Jurkat cells (positive control) isolated **b**, human and **c**, murine neutrophils was analyzed by flow cytometry (MFI= Mean fluorescence intensity, n=3-5 independent experiments, unpaired student's t-test). Data are presented as representative overlays and mean±s.d.

Supplementary Figure 3 $K_v1.3^{-/-}$ neutrophils share a normal expression pattern of surface molecules important for neutrophil recruitment.

a-g, Surface expression levels of CD18, CD11a, CD11b, PSGL-1, CD44, L-selectin, and CXCR2 on peripheral blood neutrophils from $K_v1.3^{-/-}$ and WT mice (MFI= Mean fluorescence intensity, n=3-5 mice per group, unpaired student's t-test). Data are presented as mean±s.d.

Supplementary Figure 4 PIF reduces $K_v1.3$ currents in isolated human neutrophils.

$K_v1.3$ current densities in primary human neutrophils (calculated as pA/pF) were triggered by the application of 13 consecutive 10mV steps from -80mV to +40mV over 200ms. Cells were pre-treated with **a**, vehicle (Ctrl) (representative trace no. 1, 4, 8, 10, 13 of n=15 cells), **b**, TRAM-34 (representative trace no. 1, 4, 8, 12 of n=13 cells), **c**, PAP-1 (representative trace no. 1, 4, 8, 13 of n=10 cells), or **d**, PIF (representative trace no. 1, 4, 8, 13 of n=8 cells). **e**, Current densities extracted at 100ms were quantified (n=8-15 cells, one-way ANOVA, Tukey's multiple comparison). *: $p \leq 0.05$. Data in **e**, are represented as mean±s.d.

Supplementary Table 1 Microvascular parameters. Vessel diameter, centerline velocity, wall shear rate, white blood cell counts (WBC) and neutrophil (PMN) counts of TNF- α stimulated WT mice pretreated with either PIF, scrPIF or vehicle (Ctrl), respectively (mean \pm SEM; 1-way ANOVA, Tukey's multiple comparison).

	n (mice)	n (venules)	Diameter [μ m]	Centerline velocity [μ m s $^{-1}$]	Wall shear rate [s $^{-1}$]	WBC [μ l $^{-1}$]	PMN [μ l $^{-1}$]
Ctrl	9	25	33 \pm 1	1696 \pm 140	1280 \pm 107	3798 \pm 385	1650 \pm 233
scrPIF	8	25	33 \pm 1	11612 \pm 1137	1194 \pm 95	3983 \pm 501	1811 \pm 287
PIF	10	30	31 \pm 1	1677 \pm 154	1338 \pm 124	3969 \pm 339	1632 \pm 170
			ns. (p=0.2714)	ns. (p=0.9175)	ns. (p=0.6566)	ns. (p=0.9376)	ns. (p=0.8377)

Supplementary Table 2 Microvascular parameters. Vessel diameter, centerline velocity, wall shear rate, white blood cell counts (WBC) and neutrophil (PMN) counts of TNF- α stimulated WT or $K_v1.3^{-/-}$ mice pretreated with either PAP-1, PIF, a combination of both substances or vehicle (Ctrl), respectively (mean \pm SEM; 1-way ANOVA, Tukey's multiple comparison).

	n (mice)	n (venules)	Diameter [μ m]	Centerline velocity [μ m s $^{-1}$]	Wall shear rate [s $^{-1}$]	WBC [μ l $^{-1}$]	PMN [μ l $^{-1}$]
Ctrl	4	17	30 \pm 1	1753 \pm 172	1448 \pm 154	3818 \pm 189	1915 \pm 194
PAP-1	4	15	30 \pm 1	2047 \pm 294	1677 \pm 230	4085 \pm 406	1473 \pm 327
PAP-1+PIF	4	15	29 \pm 1	1513 \pm 157	1283 \pm 116	3393 \pm 495	1670 \pm 425
			ns. (p=0.4690)	ns. (p=0.3543)	ns. (p=0.4324)	ns. (p=0.2649)	ns. (p=0.6490)
C57BL/6	5	19	31 \pm 1	1737 \pm 151	1381 \pm 122	2064 \pm 234	982 \pm 228
$K_v1.3^{-/-}$	5	19	29 \pm 1	1742 \pm 150	1465 \pm 126	2516 \pm 456	860 \pm 339
$K_v1.3^{-/-}$ +PIF	5	19	31 \pm 1	1900 \pm 106	1541 \pm 106	2956 \pm 347	1386 \pm 161
			ns. (p=0.2633)	ns. (p=0.6358)	ns. (p=0.6350)	ns. (p=0.2509)	ns. (p=0.3407)

D. Affidavit

Immler Roland

.....
Surname, first name

...

.....
Street

...

.....
Zip code, town

.....
Deutschland

.....
Country

I hereby declare, that the submitted thesis entitled

The role of Preimplantation factor (PIF) on leukocyte recruitment *in vivo*

is my own work. I have only used the sources indicated and have not made unauthorized use of services of a third party. Where the work of others has been quoted or reproduced, the source is always given.

I further declare that the submitted thesis or parts thereof have not been presented as part of an examination degree to any other university.

Martinsried, 06/12/2019

.....
Place, date

Roland Immler

.....
Signature, doctoral candidate